



Strathclyde Institute of Pharmacy
and Biomedical Sciences, Glasgow, UK

**The role of a monomer/dimer equilibrium and
the C-terminal tail in regulating translocation of
sphingosine kinase 1 to the plasma membrane
of breast cancer cells**

Ryan Brown


A thesis submitted in fulfilment of the requirements for the degree of Doctor
of Philosophy

Supervisor: Professor Nigel Pyne and Professor Susan Pyne

Declaration

This thesis is the result of the author's original research. It has been composed by the author and has not been previously submitted for examination which has led to the award of a degree.

The copyright of this thesis belongs to the author under the terms of the United Kingdom Copyright Acts as qualified by University of Strathclyde Regulation 3.50. Due acknowledgement must always be made of the use of any material contained in, or derived from, this thesis.

Signed: 

Date: 27th November 2020

Acknowledgements

I would like to thank several people for their contributions during my PhD. First and foremost, I would like to thank my supervisors, Professor Nigel Pyne and Professor Susan Pyne for their continued inspiration, help, support during my project and encouragement to progress in the field. The experiences I have had here at the University of Strathclyde under their supervision have shaped me into the researcher I am today and have progressed me further than I ever thought was possible. I would also like to thank the members of the Pyne group over the years, including Mariam Alsanafi, Abir Mohammed and Ahmed Alfaqih who made me feel comfortable when joining and helped me through the difficult times.

I am very grateful for the help I have received from Dr. Rothwell Tate and Professor David Adams who have both helped me greatly in my project. In addition, I would like to extend my thanks to Margaret MacDonald and Graeme Mackenzie for their friendship and support. I would like to thank my Dad and Joshua for being there through some difficult times. None of this would have been possible without the love and support from my partner Megan Greaves. We have been able to share this great experience together and been able to help each other in the process. She has always believed in me and been able to pick me up again in the darker times.

For what has been the first place I have really been able to call home, I really will miss Scotland and all of the people mentioned above. I will never forget the memories and what I have learnt here over the years as I progress on to the next chapter of my life, in the United States of America.

Lastly, I truly wish that the research I have conducted here, which at times has been my life, will progress the field of lipid research. Specifically, the mechanisms governing the translocation of sphingosine kinase 1 to the plasma membrane, which may one day be used in cancer therapeutics.

Dedication

This thesis can only be dedicated to one person, my mum, Shaney Brown, who without instilling her belief in me, none of this would have been possible. Your passing before my GCSE exams gave me the drive and focus to succeed. That drive remains and it is with you by my side that I know I can do anything I put my mind to. With this in mind, I continue to aim high. I hope you are proud, mum.

I love you and miss you very much.

Table of contents

DECLARATION	1
ACKNOWLEDGEMENTS	2
DEDICATION	3
ABBREVIATIONS	6
PUBLICATIONS	8
ABSTRACT	8
1.0 GENERAL INTRODUCTION	11
1.1 Sphingolipid synthesis and metabolism	11
1.2 Molecular structure, catalytic function and the role of sphingosine kinase 1 and 2 in cancer	22
1.3 Dysregulation of sphingolipid metabolism in cancer.....	33
1.5 Aims	41
.....	43
2.0 MATERIALS AND METHODS	44
2.1 Materials.....	44
2.2 Methods	51
.....	66
3.0 THE IMPORTANCE OF G_Q, PHOSPHATIDIC ACID AND DIMERISATION FOR SK1 TRANSLOCATION	67

3.1 Introduction	67
3.2 Results	69
3.3 Discussion	109
3.4 Summary and future directions	118
.....	119
4.0 THE ROLE OF THE C-TERMINUS IN THE TRANSLOCATION OF SK1	
.....	120
4.1 Introduction	120
4.2 Results	122
4.3 Discussion	160
4.4 Summary and future directions	166
.....	168
6.0 GENERAL DISCUSSION AND FUTURE DIRECTIONS	169
6.1 General discussion	169
6.2 Conclusion and future directions	172
7.0 REFERENCES	174

Abbreviations

ACh: Acetylcholine

AChE: Acetylcholinesterase

AD: Alzheimer's disease

APS: Ammonium persulphate

ATP: Adenosine 5'-triphosphate

BAR: Bin/Amphiphysin/Rvs

DAPI: 4, 6-Diamidino-2-phenylindole

DES: Dihydroceramide desaturase

DMEM: Dulbecco's Modified Eagle's Medium

DMSO: Dimethylsulfoxide

DNA: Deoxyribonucleic acid

ECL: Enhanced chemiluminescence

EEA: Early endosomal antigen

ERK1: Extracellular-regulated protein kinase 1

FITC: Fluorescein isothiocyanate

GFP: Green fluorescent protein

GPCR: G-protein coupled receptor

HEK: Human embryonic kidney

LBL-1: Lipid binding loop-1

mAChR: Muscarinic acetylcholine receptor

MAPK: Mitogen-activated protein kinase

MEK: MAPK kinase

nAChR: Nicotinic acetylcholine receptor

NT: Neurotransmission

PA: Phosphatidic acid

PBS: Phosphate-buffered saline

PKC: Protein kinase C

PLD: Phospholipase D

PM: Plasma membrane

PMA: Phorbol 12-myristate 13-acetate

PMSF: Phenylmethylsulfonyl fluoride

PS: Phosphatidylserine

S1P: Sphingosine 1-phosphate

S1PR: Sphingosine 1-phosphate receptor

SDS PAGE: Sodium dodecyl sulphate-polyacrylamide gel electrophoresis

SK1: Sphingosine kinase-1

SM: Sphingomyelin

SPNS2: Sphingolipid transporter 2

SPH: Sphingosine

TBST: Tris-buffered saline/Tween 20

TEMED: Tetramethylethylenediamine

TRITC: Tetramethyl rhodamine isothiocyanate

Publications

Brown, R. D. R., Adams, D. R., Pyne, S. & Pyne, N. J. (2020). The role of a monomer/dimer equilibrium and the C-terminal tail in translocation of sphingosine kinase 1 to the plasma membrane of breast cancer cells. *Journal of Biological Chemistry*. (in revision).

Abstract

Sphingosine kinase-1 (SK1) is able to translocate from the cytoplasm to the plasma membrane (PM) to catalyse the formation of sphingosine 1-phosphate (S1P) from sphingosine and adenosine triphosphate (ATP). It is known that both the expression and activity of SK1 is increased in many tumour types leading to a poorer prognostic outcome in terms of disease-specific survival (Heffernan-Stroud et al., 2013). In addition, the translocation/activation of SK1 to the plasma membrane induces oncogenesis. However, the mechanism of translocation requires further investigation in order to identify new targets for potential therapeutic intervention in the treatment of cancer. Therefore, the aim of the current study was to further examine the molecular mechanisms regulating the translocation of SK1 from the cytoplasm to the PM in MCF-7L breast cancer cells.

Phorbol myristate acetate (PMA) induced the extracellular signal-regulated kinase (ERK)-dependent translocation of wild type (WT) mouse green fluorescent protein (GFP)-SK1 (*mGFP-SK1*) from the cytoplasm to lamellipodia in the PM of MCF-7L breast cancer cells. In addition, carbachol also induced translocation of WT*mGFP-SK1* to lamellipodia, albeit in an ERK-independent manner. In contrast, S1P induced the ERK-independent translocation of WT*mGFP-SK1* to filopodia. Treatment of cells with either the phospholipase D (PLD) inhibitor, 5-Fluoro-2-Indolyl des-chlorohalopemide (FIPI), or the G_q inhibitor, YM254890 reduced translocation in response to phorbol myristate acetate (PMA), carbachol or S1P, suggesting that phosphatidic acid (PA) formation and G_q activation are required for phosphorylation-dependent and -independent translocation of SK1 to the PM of breast cancer cells.

It has previously been proposed that SK1 might be able to exist as monomer and dimer in equilibrium. The dimeric structure would allow for a contiguous membrane engagement interface consisting of hydrophobic patches on the lipid binding loop (LBL)-1 loop and a cluster of positively charged residues at the dimeric interface. The possibility of a monomer/dimer equilibrium was investigated by generating a constitutively

monomeric *mGFP-SK1* mutant, *mGFP-SK1-K49E* by introducing charge opposition in dimer interface. We also created a stabilized dimer *mGFP-SK1* mutant, *mGFP-SK1-I51C* by engineering a disulphide bond in dimer interface. Carbachol and PMA promoted the translocation of *mGFP-SK1-K49E* to lamellipodia, whereas in contrast to WT *mGFP-SK1*, S1P also induced translocation of *mGFP-SK1-K49E* to lamellipodia. On the other hand, carbachol or PMA promoted the translocation of *mGFP-SK1-I51C* to filopodia in a manner similar to S1P. These novel findings suggest monomeric and dimeric SK1 translocate to different PM micro-domains and that the position of the monomer/dimer equilibrium is determined by the ligand.

We additionally investigated the regulatory role of the C-terminal tail of SK1 by creating mutants of *mGFP-SK1*, termed T1-T5 in which 5 amino acids were sequentially truncated with the exception of T4 in which 19 amino acids in total were removed. We identified that *mGFP-SK1* T1 in which 5 amino acids were removed exhibited markedly reduced translocation in response to carbachol and S1P. However, further truncation of the C-terminus restored the ability of SK1 to translocate to the PM. These results are consistent with molecular modelling studies in which displacement of the C-terminus 'locking motif' (C-terminal amino acids 6-10) might be achieved by the binding of a putative adapter protein to the 'displacement motif' (C-terminal amino acids 1-5). It is proposed that this displacement of the C-terminal tail enables NTD:CTD twisting around a 'connecting rod' to produce alignment of membrane engagement determinants; namely the positive charge cluster and LBL-1 to promote translocation of SK1. Moreover, molecular modelling studies also suggest that the ERK-catalysed Ser²²⁵ phosphorylation might destabilize the auto-inhibitory C-terminal folding independently of the binding of the adapter protein. These findings represent a unified mechanism of SK1 translocation to the PM, involving either ERK-mediated phosphorylation of Ser²²⁵ or displacement of the C-terminal tail by a putative adaptor protein.

These novel findings provide new information concerning the mechanism of SK1 translocation that might assist in the identification of novel therapeutics aimed at perturbing translocation of this enzyme in cancer and to therefore reduce its oncogenic potential.

Chapter 1

General Introduction

1.0 General Introduction

Cell signaling is needed for the survival of all cells; without cellular interaction the default state of cells is apoptosis, unless extracellular signals are received to maintain life of the cell (Elmore 2007). Cellular signaling comprises a complex inter- and extracellular network of highly regulated pathways, where many signaling molecules have been identified. One class of signaling molecules that play an important role in health and disease, are lysophospholipids, which form part of the cell membrane. In addition, the role of lysophospholipids as cell signaling molecules is becoming increasingly recognised with roles in cancer (Pyne et al., 2018), inflammation (Tsai et al., 2016), cardiovascular diseases (Brakch et al., 2010) and neurodegenerative disease (Di Paolo et al., 2011). The balance of bioactive lipids involved in proliferation and apoptosis are governed by a group of lipid kinases. These kinases catalyse the conversion of membrane lipids to bioactive lipid-signaling molecules, although the regulation of kinase activity is poorly understood. The major focus of this research project is to elucidate the mechanisms regulating translocation of SK1 from the cytoplasm to the plasma membrane (PM). It is this change in sub-cellular localisation that is required for the catalytic conversion of membrane-bound sphingosine (SPH) to sphingosine 1-phosphate (S1P) that ultimately drives oncogenesis (Pyne et al., 2010; Huang et al., 2011).

1.1 Sphingolipid synthesis and metabolism

1.1.1 Structure and function of sphingolipids

Eukaryotic cellular membranes are composed of sphingolipids, glycerolipids and sterols that function to separate the contents of the cell from the external environment. These components are integrated with globular proteins to form the phospholipid bilayer membrane encasing cellular components of eukaryotic cells (Singer et al., 1972). Sphingomyelin (SM), a primary lipid component of the membrane, was initially isolated and documented by J. L. W. Thudichum when defining the molecular composition of the brain in 1874, to which sphingosine (SPH) was described to be a 'genuine educt and immediate principle in the brain'. Although the exact function eluded Thudichum at the time, its presence was clear. Hence this molecule was called sphingosine after the sphinx in Greek mythology to define its enigmatic character (Chatagnon et al., 1958).

Sphingolipids share the general structure of an 18-carbon saturated acyl backbone connected by an amide bond to the C2 atom of the sphingoid base group situated at the head of the molecule and are synthesized in the endoplasmic reticulum. This structure provides a polarity and amphipathic properties to the molecule SPH: (2S, 3R, 4E)-2-aminooctadec-4-ene-1, 3-diol. SPH can then be chemically modified to produce an array of functionally different sphingolipids such as various molecular species of SM, dependent on the substituent group added to the sphingoid base head bound to C1 via oxygen (Merrill 2002).

As mentioned, a primary role of sphingolipids is maintaining structural integrity of the plasma membrane (PM) that accompanies essential membrane proteins to separate cellular constituents from the extracellular environment. In addition, membrane lipids can be separated out into their hydrophilic and hydrophobic moieties. SM has a hydrophilic phosphate group often referred to as the 'head' and a hydrophobic saturated acyl backbone chain often referred to as the 'tail'. These amphipathic properties allow polar membrane lipids along with integrated membrane proteins to self-assemble with the hydrophilic 'head' being attracted to the aqueous state of the cell cytoplasm and the extracellular fluid either side of the membrane. On the other hand the hydrophobic 'tail' prefers the lipid environment within the PM (Hubbard et al., 1998). The biophysical properties of sphingolipids allow the molecules to either have access to both sides of the membrane, access to only a single side of the bilayer, or diffuse freely from a membrane across the cytosol or into extracellular space.

Within the membrane there is an asymmetrical distribution of lipids, where SM aggregates in lipid rafts. Saturation of the acyl fatty acid chain (tail) at lipid rafts enables the phospholipids to pack more tightly together with cholesterol, serving as platforms for a number of other membrane proteins that are capable of signaling (Brown et al., 2000). This close association of proteins in lipid rafts allows for cross talk, thereby enabling integrated cell signaling (Simons et al., 1997) facilitated by the solvent nature of the lipids (Singer et al., 1972). This is important for the endocytic process and signal transduction.

1.1.2 Sphingolipid metabolism

For cellular signaling and maintenance of cell membranes, sphingolipids must be readily available in the body. Although sphingolipids are present in foods, *de novo* biosynthesis of these molecules is necessary due to their low bioavailability; a

consequence of their degradation in the intestines (Vesper et al., 1999). The *de novo* process begins in the endoplasmic reticulum with the condensation of palmitoyl-CoA and serine in the endoplasmic reticulum to form 3-ketosphinganine, catalysed by serine palmitoyl transferase. 3-ketosphinganine is subsequently reduced to sphinganine (the backbone of all sphingolipids) by 3-ketosphinganine reductase. Sphinganine is then transformed into ceramide via the action of ceramide synthase and successive desaturation by dihydroceramide desaturase (Merrill 2002).

The highly water-insoluble ceramide is transported from the endoplasmic reticulum to the Golgi apparatus via vesicular transport (Watson et al., 2005; Kajiwara et al., 2014) or ceramide transfer protein, where it is preferentially incorporated into sphingomyelins or glycosphingolipids (Hanada et al., 2003). Ceramide can then be converted to SM through the actions of sphingomyelin synthase. The enzyme ceramidase allows for the conversion of ceramide to SPH, with sphingosine kinase 1 and 2 (SK1 and SK2) catalysing phosphorylation of SPH to produce S1P (Merrill 2002). Once the SPH backbone has been constructed the only way it can be eliminated is by the action of S1P lyase, which catalyses the irreversible catabolism of S1P to produce ethanolamine-1-phosphate and hexadecenal (Chalfant et al., 2005).

Along with *de novo* synthesis, ceramide can also be produced via the salvage of SPH, hydrolysis of SM or recycling of endogenous ceramide. The salvage pathway involves regeneration of ceramide via the breakdown of complex sphingolipids, through the actions of sphingomyelinase, acid- β -glucosidase, ceramidase and dihydroceramide synthase. These enzymes facilitate the production of free sphingosine, that undergo re-acylation to reform ceramide (Kitatani et al., 2008). Reacylation of SPH is likely to shift the fate of the cell from anti-proliferative to a senescent/apoptotic state (Hannun 1996). Another method of forming ceramide is through the conversion of SM to ceramide, via the action of sphingomyelinase, originally reported in astrocytes (Riboni et al., 1994). This reaction involves cleavage of the SM head group through the hydrolytic action of sphingomyelinase via the activity of phospholipase C (Marchesini et al., 2004). The final method of obtaining ceramide is through recycling endogenous short-chain ceramide via ceramidase to initially produce SPH, which is then converted to ceramide with the aid of ceramide synthase catalysing this process (Kitatani et al., 2008). Through this process, studies have shown that the addition of exogenous

short-chain ceramide can subsequently increase the levels of long-chain endogenous ceramide levels (Ogretmen et al., 2002).

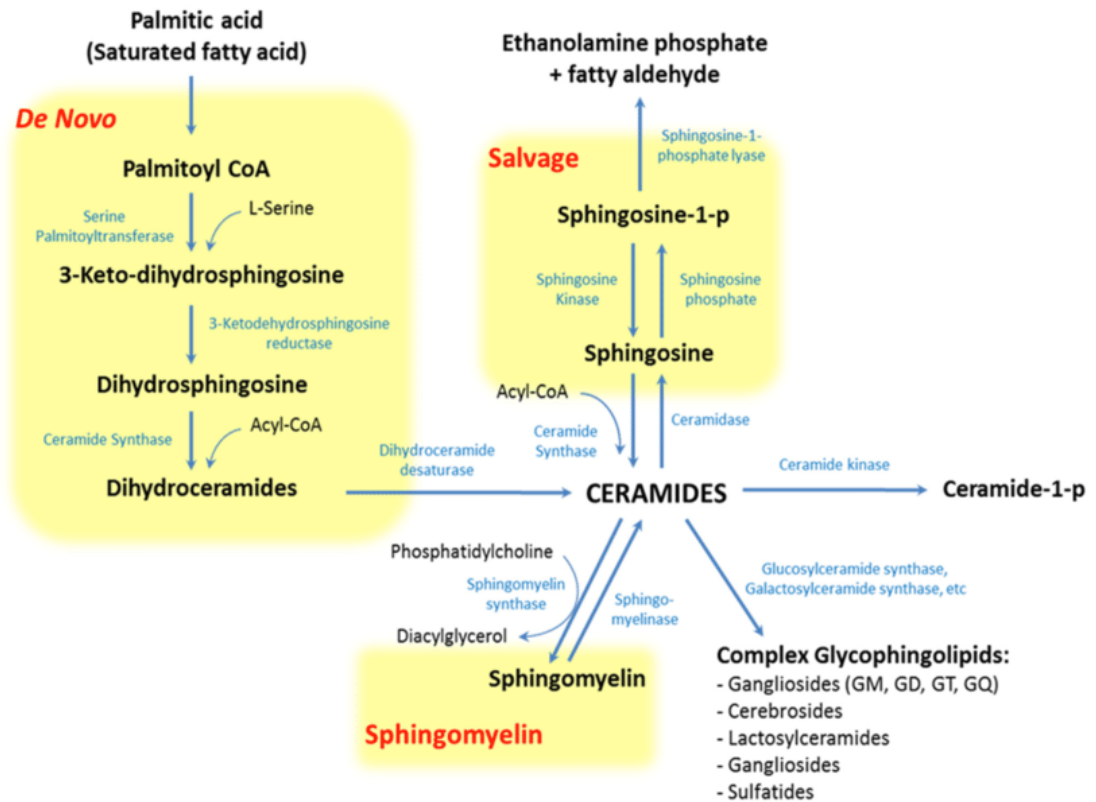


Figure 1.1 De novo synthesis of SPH and its bioactive metabolites (Castillo et al., 2016)

De novo synthesis of ceramide is the first step in the formation of sphingolipids. From here ceramide can interchangeably form SPH and SM, with SPH going on to subsequently produce sphingosine 1-phosphate (S1P). S1P can then be degraded via S1P lyase. Ceramide and SPH are associated with apoptosis, cell cycle arrest and cellular senescence (Pyne et al., 1996), where S1P promotes cell survival and cell proliferation (Chalfant et al., 2005).

With many routes of incorporating these bioactive lipids into the cell environment, tight regulation of *de novo* synthesis and the degradation of sphingolipids are required. Due to their somewhat opposing physiological effects; pro-apoptotic ceramide (Pyne et al., 1996) and pro-survival S1P (Chalfant et al., 2005) require tight regulation. It is understood therefore that interconversion between various sphingolipids has the ability to impact cell fate, originally demonstrated by S1P promoting the activation of ERK-1/2 in facilitating deoxyribonucleic acid (DNA) synthesis, whereas ceramides elicit activation of JNK and induce growth arrest (Gomez-Munoz et al., 1994; Pyne et al., 1996). Shortly after, this concept was coined the ‘sphingolipid rheostat’, describing the cellular balance between ceramide and S1P (Cuvillier et al., 1996). The concept

of sphingolipid rheostat was established after it was found that high cellular levels of ceramide induces growth arrest and apoptosis (Obeid et al., 1993), whereas high cellular S1P promotes proliferation (Olivera et al., 1993) whilst suppressing ceramide-mediated apoptosis (Cuvillier et al., 1996).

Even though many of these biosynthetic steps are physiologically important, it is the interconversion of SPH and S1P that has gained most attention due to their opposing physiological effects. This has placed both SK1, and SK2 at the forefront of interest in the sphingolipid rheostat and thus maintenance of correct cellular function (Wang et al., 2013). The balance of sphingolipids is therefore of great focus of many diseases including cancer (Newton et al., 2015). For this reason, the key regulatory enzymes are the target of many therapeutics, with the molecular regulatory mechanisms of SK1 being the focus of the current study.

1.1.3 Structure and function of bioactive sphingosine-1-phosphate in health and disease

S1P is a sphingolipid metabolite involved in sphingolipid rheostat by promoting growth, survival, angiogenesis, and metastasis, thereby regulating the fate of the cell. S1P is involved in disease pathogenesis of cancer (Pyne et al., 2010; Pyne et al., 2016), such as breast (Singh et al., 2020), ovarian (Hernandez-Coronado et al., 2019), hepatocellular carcinoma (Maceyka et al., 2020) and glioblastoma (Tea et al., 2020) to name a few. S1P has the ability to determine cell fate by acting as a ligand for the family of 5 G-protein coupled receptors (GPCR), S1P₁₋₅, in an autocrine or paracrine manner (Hobson et al., 2001), commonly known as 'inside-out' signaling (Takabe et al., 2014). S1P is generally considered to promote proliferation and survival, which are opposite to that of ceramide in a balance described as the 'sphingolipid rheostat' (Cuvillier et al., 1996; Pyne et al., 1996). It is not surprising therefore that an imbalance in these sphingolipids, namely an increase in S1P, can lead to disease pathologies, such as cancer (Pyne et al., 2010).

S1P cannot cross the PM lipid bilayer due to its polar nature and instead is synthesised intracellularly and actively transported across the PM by ATP-binding cassette transporters (ABC transporters) (Nagahashi et al., 2014). Evidence for this comes from the expulsion of S1P from mast cells via ABCC1 to promote inflammation (Mitra et al., 2006), from astrocytes via ABCA1 (Sato et al., 2007), from breast cancer cells via ABCC1 and ABCG2 (Takabe et al., 2010; Yamada et al., 2018) and from

thyroid carcinoma cells via ABCC1 (Bergelin et al., 2009). S1P is transported into the extracellular environment via MFSD2B in erythroid cells (Vu et al., 2017; Kobayashi et al., 2018). Alternatively, S1P can be transported via the sphingolipid transporter, SPNS2, which does not have an ATP binding motif and was originally discovered in zebrafish (Kawahara et al., 2009). Mutation of this transporter has been shown to cause cardia bifida (Osborne et al., 2008), which can be prevented by the application of exogenous S1P (Kawahara et al., 2009). However, unlike the ABC transporters (Lee et al., 2007; Hisano et al., 2011), SPNS2 is physiologically functional *in vivo*, with the cardia bifida phenotype being almost identical in *SPNS2* and *S1PR2* mutant zebrafish (Kupperman et al., 2000). Moreover, S1P can also be synthesised by exported SK1 in the extracellular environment (Ancellin et al., 2002). In a pathophysiological context, S1P is released into the tumour microenvironment via SPNS2, where it is able to bind to S1P receptors to promote inflammation, alter immune cell function and induce angiogenesis (Spiegel et al., 2019). Hence, S1P transporters may provide novel targets for cancer therapeutics.

Once synthesized, extracellular S1P is then able to exert differential effects depending on the sub-type of S1P receptor expressed on a particular cell type. For example, S1P₃ activation promotes the metastasis of triple negative breast cancer cells (Wang et al., 2018). Alternatively, S1P receptors can undergo vesicular expulsion from the membrane independent of S1P binding (Badawy et al., 2018; El Buri et al., 2018). This is demonstrated by α -Synuclein being able to drive the expulsion of S1P₁ from lipid rafts, leading to its uncoupling from G_i and thus impaired G_i signalling (Badawy et al., 2018). Furthermore, S1P₂ has also been shown to be released from breast cancer cells in exosomes where it is taken up by fibroblasts to promote proliferation through ERK-1/2 activation (El Buri et al., 2018).

In addition to binding to S1P₁₋₅, intracellular S1P has many roles in biology independent of S1P₁₋₅ binding. These targets differ depending on whether S1P is produced by SK1 or SK2 and which might be attributed to the different sub-cellular localisations of the two kinases. For example, S1P derived from SK1 binds to TNF receptor associated factor 2 (TRAF2) via its RING domain. This E3 ligase associates with SK1 and acts as a co-factor for TRAF2-catalysed Lys⁶³-polyubiquitination of RIP1, which is a protein kinase responsible for regulating cell survival and inflammation in the NF- κ B pathway (Alvarez et al., 2010). However, this remains controversial as more recent reports demonstrate no effect on the NF- κ B pathway

following the elimination of SK1. One other target of S1P is located on mitochondria, whereby SK2-produced S1P interacts with prohibitin 2 to facilitate cytochrome-c oxidase assembly and mitochondrial respiration (Strub et al., 2011). In contrast, SK2-derived S1P can cooperate with BAK to promote cytochrome-c release to impact mitochondrial outer-membrane potential and drive apoptosis (Chipuk et al., 2012). S1P can also bind directly to peroxisome proliferator-activated receptor-gamma (PPAR γ) His³²³ residue, thereby promoting the receptor to form a complex with proliferator-activated receptor-gamma coactivator 1 (PGC1 β) to promote neovascularisation (Parham et al., 2015).

Intracellular targets of S1P are also strongly associated with disease progression. In this regard, S1P produced by SK2 is able to bind with histone deacetylase-1 and -2 in the nucleus to sequester them from being enzymatically active, hence enhancing histone acetylation and gene expression (Hait et al., 2009). In support, increased nuclear S1P induced decreased histone deacetylase-1 and -2 activity and increased histone acetylation in *Drosophila* which have no S1P receptors (Nguyen-Tran et al., 2014). In addition, SK2-produced S1P can also bind human telomerase reverse transcriptase on the periphery of the nucleus. In this manner, S1P is able to mimic phosphorylation of human telomerase reverse transcriptase and promote cellular proliferation, linked to tumour growth (Panneer Selvam et al., 2015). Moreover, UVB irradiation and oxidative stressors can cause S1P to activate NF- κ B and bind the heat shock proteins, HSP90 α and GRP94, leading to increased cathelicidin anti-microbial peptide (CAMP) and thus enhanced inflammation and tumorigenesis (Park et al., 2016). Lastly, in neurons S1P is able to bind to β -site APP cleaving enzyme-1 to facilitate the production of A β , known to form plaques present in AD (Takasugi et al., 2011). In summary, S1P is a versatile lipid-signalling molecule that is able function within the cell or in the extracellular environment.

1.1.4 Structure and function of S1P₁₋₅ in health and disease

S1P is produced in close proximity to the PM, with the lipid subsequently able to traverse the membrane through the action of SPNS2 (Kawahara et al., 2009), via the energy-dependent ABC transporters (Nagahashi et al., 2014), or via MFSD2B in erythrocytes (Vu et al., 2017; Kobayashi et al., 2018). Once in the extracellular space, S1P can bind S1P₁₋₅ in an autocrine or paracrine manner. The formerly called endothelial differentiation gene receptors have 5 sub-types with variable expression

profiles, each bound to G-proteins. S1P₁ and S1P₅ receptors are coupled to G_i, while S1P₂ is coupled to G_i, G_q and G₁₃. S1P₃ can couple to G_i, G_q, or G_{12/13}, and S1P₄ is coupled to G_i and G₁₂. The S1P binding triggers activation of the G-protein complex, whereby the α subunit dissociates from the $\beta\gamma$ subunits, allowing the independent subunits to interact with their respective downstream effectors. With respect to cancer, S1P receptor expression often correlates with clinical prognosis (Watson et al., 2010). Indeed, targeting S1P receptors has proved successful in treating multiple sclerosis, with GilenyaTM (formulation of fingolimod/FTY720) leading to downregulation S1P₁ and thus S1P₁-mediated inflammatory T cell invasion to support remyelination (Brinkmann et al., 2004). That said, there remains no current treatments for cancer that target S1P receptors.

S1P₁ is ubiquitously expressed, although predominantly expressed within the heart and endothelial cells (Means et al., 2009) and has an important role in regulating angiogenesis and in maintaining the cardiovascular system. Moreover, an axis of SK1/S1P/S1P₁ connects NF- κ B and STAT3 signalling to IL-6 production. STAT3 is a transcription factor for the S1P₁ receptor gene, whereby activation of S1P₁ has also been shown to upregulate JAK2 tyrosine kinase and drive persistent STAT3 activation in a positive feedback loop in tumours, ultimately upregulating IL-6 production to promote tumour growth and metastasis (Lee et al., 2010; Liang et al., 2013). Furthermore, S1P₁ activation promotes cardiac hypertrophy, cardiac remodelling (Ohkura et al., 2017) and the enhancement of vascular barrier integrity (Allende et al., 2003); the latter of which is evidenced by studies using conditional knockout *S1PR1* mouse models that result in disrupted maturation of the vascular barrier, which produces an embryonically lethal phenotype (Allende et al., 2003). Moreover, *S1pr1*^{-/-} mice develop embryonically lethal haemorrhaging, indicating a critical role for S1P₁ in development (Liu et al., 2000). In myocytes, S1P₁ activation is linked to cardio-protection in ischemic conditions. In this case, heart myocytes are able to endure hypoxia for longer periods of time due to enhanced levels of S1P that acts on S1P₁ (Zhang et al., 2007). S1P₁ also has an important role in the lymphatic system, where it is the predominant receptor on T and B lymphocytes (Jeffery et al., 2011). More specifically S1P₁ has been shown to regulate the chemotaxis of macrophages, T and B lymphocytes, with low levels of S1P (~0.1-100 nM) reducing chemotaxis and high concentrations of S1P (~0.3-3 μ M) promoting chemotaxis (Graeler et al., 2002; Roviezzo et al., 2004; Allende et al., 2010; Messias et al., 2016).

S1P₁ is also suggested to have a role in cancer progression. This is evidenced by the overexpression of S1P₁ enhancing the progression of T-lymphoblastic lymphoma to T-lymphoblastic leukaemia, thereby driving intravasation (Feng et al., 2010). Another example is the overexpression of S1P₁ and IL-22R1 in invasive and bone metastatic cancer. In this context IL-22 promotes the expression of S1P₁ and IL-22R1 in MDA-MB-231 breast cancer cells, thus increasing SK1 expression and S1P in mesenchymal stem cells to drive metastasis and immune cell infiltration (Kim et al., 2020). On the contrary, S1P₁ being involved in neovascularisation is thought to hold therapeutic potential for improving the efficacy of anti-cancer therapies (Cartier et al., 2020). In this regard, activation of S1P₁ receptors on endothelial cells from S1P produced by tumours, upregulates VEGFR2-dependent c-Ab11 and Rac signalling and thus endothelial cell migration, accounting for enhanced tumour growth. This is further reinforced by deletion of the S1P₁ receptor gene from endothelial cells leading to a lower tumour vascularisation and growth (Balaji Ragunathrao et al., 2019). However, there is contrasting evidence for the role of S1P₁ in tumour progression, as others report that deletion of S1P₁ receptors from endothelial cells increases sprouting which equates to larger tumours and an increase in metastatic foci (Cartier et al., 2020). Conversely, S1P₁ has also been shown to prevent disease progression, with survival of glioblastoma patients positively correlating with high S1P₁ expression (Yoshida et al., 2010). In corroboration with S1P₁ displaying anti-tumour properties, over-expression of S1P₁ receptors in endothelial cells lead to the development of smaller tumours and an increased efficacy of anti-tumour therapies (Cartier et al., 2020). This signifies that S1P₁ function may be modulated in the tumour micro-environment to improve the response to anti-cancer therapies.

Even though S1P₂ shares ~50-60% homology with S1P₁, it is not ubiquitously expressed and is mainly expressed in the immune, cardiovascular and central nervous systems (Kluk et al., 2002). Evidence indicates this receptor is crucial in the development of the auditory system. In this regard, knockout of *S1pr2* renders mice deaf with abnormal head tilt, thus indicating vestibular defects along with anatomical abnormalities (MacLennan et al., 2006). Furthermore, S1P₂ is present in mast cells where it plays a crucial part in degranulation involved in inflammation and immune response (Jolly et al., 2004). S1P₂ has many opposing effects to that of S1P₁, for instance, S1P₂ inhibits migration and invasion (Arikawa et al., 2003; Lepley et al., 2005), whereas S1P₁ induces cell migration (Li et al., 2009). It is therefore believed that S1P₂ is protective against tumourigenesis in a cancer-specific context. In this

regard, *S1pr2^{-/-}* mice have been shown to develop clonal B-cell lymphoma, indicating a tumour suppressive role (Cattoretti et al., 2009). Furthermore, S1P₁ enhances the vascular barrier integrity in endothelial cells (Singleton et al., 2005), while S1P₂ activation disrupts the vascular barrier integrity (Sanchez et al., 2007). This disruptive role of S1P₂ reinforces the link between the receptor and its role in immune response involving degranulation of mast cells (Jolly et al., 2004) and increased vascular permeability. This is likely to enhance the infiltration of inflammatory cells into organ systems during inflammatory disease (Sanchez et al., 2007), indicating a role for in the epithelial defence against cancer involving epithelial cells and the elimination of neighbouring transformed epithelial cells. An example of this is S1P₂ activation leading to the Rho-kinase-mediated accumulation of filamin in healthy cells that neighbour RasV12-transformed cells, thereby promoting their apical extrusion (Yamamoto et al., 2016). S1P₂ has also been shown to be implicated in cancer cell migration, whereby activation of S1P₂ inhibits the migration of gastric cancer cells (Yamashita et al., 2006) and inhibition of which reduces the S1P-mediated inhibition of hepatocellular carcinoma cell migration (Matsushima-Nishiwaki et al., 2018). In addition, high expression correlating with improved prognosis in ER⁺ breast cancer patients (Ohotski et al., 2013). It should be noted, however, that some reports demonstrate that S1P₂ can promote the oncogenic transformation. In this case, SK1 activation leading to the production and expulsion of S1P, which activates S1P₂ promotes the upregulation of transferrin receptor 1 expression and hence the transformation into cancer cells (Pham et al., 2014). Moreover, MDA-MB-231 cells have been shown to shed S1P₂ in exosomes that can be taken up by fibroblasts and cleaved into a shorter form that is constitutively active, driving DNA synthesis (El Buri et al., 2018).

S1P₃ displays ~50% homology to S1P₁ and S1P₂ and is widely expressed in tissues such as the brain, lung, heart, liver, spleen, pancreas, kidney and thymus (Kluk et al., 2002). S1P₃ can couple to G_i and G_{12/13} to control regulation of Rac and thus cell migration (Sugimoto et al., 2003; Sensken et al., 2008), although the receptor is predominantly coupled to G_q (Chun et al., 2010) and S1P binding leads to internalisation of the receptor (ter Braak et al., 2009). In addition, this receptor holds relevance to the current study as M₃ acetylcholine receptors (M₃ AChR) (for which the ligand is carbachol) and S1P₃ are both G_q-coupled and highly likely to follow a conserved pattern of activation in terms of regulating SK1. In a physiological context S1P₃ appears to have an important role in regulating heart rate and cardio-protection

(Sanna et al., 2004). It has been shown that *S1pr3*^{-/-} mice do survive and therefore removal of this gene is not embryonically lethal. However, these mice have reduced litter sizes and cells are defective S1P signalling (Ishii et al., 2001). The viability of *S1pr3*^{-/-} offspring suggests compensatory roles for S1P₁ and S1P₂ in development, nevertheless triple mutations in *S1P1*^{-/-} *S1P2*^{-/-} *S1P3*^{-/-} produces more severe vascular defects than S1P₁ mutation alone (Kono et al., 2004). S1P₃ is the highest expressed of all the S1P receptors in breast cancer cells (Goetzl et al., 1999; Dolezalova et al., 2003), is greatly expressed in ependymomas (Magrassi et al., 2010) and is particularly elevated in human lung adenocarcinomas (Zhao et al., 2016). With regards to the latter, TGF-β promoted SMAD3 activation and the upregulation of S1P₃, leading to proliferation and metastasis, with knockdown of S1P₃ shown to block these effects (Zhao et al., 2016). S1P₃ activation is also believed to drive metastasis in thyroid carcinomas (Zhao et al., 2018). Moreover, activation of the receptor has been shown to modulate the blood brain barrier and to promote a leakier blood tumour barrier often seen in brain metastasis. S1P₃ is also upregulated on astrocytes, contributing to neuroinflammatory response in the tumour microenvironment and increased IL-6 and CCL-2 production, which drives enhanced blood tumour barrier permeability through relaxation of endothelial cell adhesion and may improve drug uptake in treating brain metastatic cancers (Gril et al., 2018).

Even though the majority of research has focussed on S1P₁₋₃, the S1P₄ and S1P₅ receptors are also biologically important. Both S1P₄ and S1P₅ couple to G_i and G_{12/13} (Ishii et al., 2001; Graler et al., 2003). S1P₄ is expressed predominantly within the hematopoietic system, more specifically in lymphoid tissue and leukocytes (Kluk et al., 2002), with activation leading to inhibition of cell proliferation and T-cell activation (Wang et al., 2005). This suggests roles for immune surveillance. In addition, S1P₄ activation leads to the rearrangement of the cytoskeleton required for cell motility in CHO-K1 cells (Graler et al., 2003). In relation to this, S1P₄ overexpression in erythroleukemia cells led to the formation of cytoplasmic extensions (Golfier et al., 2010). In a pathophysiological sense, expression of the S1P₄ correlates with a poorer prognosis and shorter survival times in patients with ER⁻ breast cancer (Ohotski et al., 2012). Moreover, S1P₄ interacts with human epidermal growth factor receptor 2 (HER2) to activate ERK-1/2 in MDA-MB-453 breast cancer cells (Long et al., 2010), indicating a role of S1P₄ in driving activation of the oncogene, HER2 and the growth of breast cancer cells (El Buri et al., 2018). Another tumour-promoting role of S1P₄ was demonstrated by ablation of the receptor, which reduced tumour growth of human

breast and colon cancers and increased the abundance of cytotoxic CD8⁺ T cells (Olesch et al., 2020)

S1P₅ was originally discovered in peripheral blood mononuclear cells from T-cell large granuloma lymphocyte leukaemia (Kothapalli et al., 2002), where it is shown to be upregulated in ~80% of T-cell large granuloma lymphocyte leukaemia patients (Shah et al., 2008). That being said, S1P₅ expression is mostly restricted to the brain (Im et al., 2000), more specifically on the surface of oligodendrocytes (Walzer et al., 2007) to mediate S1P-induced survival in a G_i-dependent manner (Jaillard et al., 2005). It is now known that S1P₅ is not exclusively expressed on oligodendrocytes and in fact displays two splice variants; a 5.4 kb form predominantly expressed in peripheral tissues and a 2.4 kb variant present on oligodendrocytes and leukemic large granuloma lymphocytes. In addition, S1P₅ are also expressed on natural killer cells, where perturbation of the activation of S1P₅ disrupts the ability of these cells to localise to inflamed tissue (Walzer et al., 2007). Furthermore, oligodendrocytes from *S1pr5*^{-/-} mice display migration defects (Novgorodov et al., 2007), albeit no significant impediment on myelination (Jaillard et al., 2005). More recently, S1P has been shown to drive mitosis by binding to S1P₅ and subsequent activation of phosphatidylinositol 3-kinase (PI3K) and AKT and thus may be druggable in terms of targeting the proliferation of cancer cells (Andrieu et al., 2017). The role of S1P₅ in cancer is less clear, with some reports indicating a tumour-suppressive role by promoting autophagy in serum-starved human prostate PC-3 cancer cells (Chang et al., 2009). More recently, high and low expression of S1P₅ respectively, knockdown of S1P₅ in SW620 and S1P₅ overexpression in SW480 cells demonstrate that receptor activation drives growth, migration and invasion of these cancer cells by activating NF- κ B/IDO1 signalling (Zhou et al., 2020).

S1PR₁₋₅ have variable levels of expression in the body, with each receptor subtype being accompanied with specific G-protein coupling in order to perform different cellular functions. The scope of the current study however will focus predominantly on S1PR₃ and G_q, and the interaction with SK1, with specific relevance to the role of this signaling interaction on cancer cell migration.

1.2 Molecular structure, catalytic function and the role of sphingosine kinase 1 and 2 in cancer

The *SPHK1* and *SPHK2* genes code for the two human sphingosine kinase isoforms,

SK1 and SK2; with three and two splice variants respectively (Kohama et al., 1998; Liu et al., 2000). Both isoforms are part of the DAG kinase family and catalyse the ATP-dependent phosphorylation of the C-1 hydroxy group on sphingosine, dihydrosphingosine, with SK2 also catalysing phosphorylation of phytosphingosine (Gault et al., 2010). All sphingosine kinases are composed of 5 conserved regions termed C1 through to C5, which constitute the sphingosine-binding site and the nucleotide-binding site (Adams et al., 2016). SK1a is 42.5 kDa in length, whereas SK1b is identical to SK1a, albeit with an 86 amino acid extension to the N-terminus and is 51 kDa in size. SK1c on the other hand is identical to SK1a but with a 14 amino acid N-terminal extension and is 43.9 kDa in size. Thus, the N-terminus region and hence amino acid length is not conserved, differentiating the isoforms. In comparison to SK1 isoforms all SK2 isoforms have additional N-terminus regions, with SK2b having an additional 36 amino acids compared with the SK2a isoform, albeit SK2a is still larger than all of the SK1 isoforms (Pitson 2011).

Sphingosine kinases contain N- and C-terminal domains encompassing the nucleotide- and lipid-binding sites respectively. In addition to their identification, crystallization has revealed that the nucleotide ligand, adenine, inserts between loops of the nucleotide binding site and the lipid, whilst SPH binds to the enzyme in the so-called 'J-channel' (Wang et al., 2013; Adams et al., 2016) (Fig. 1.2). The 'J-channel' of the enzyme is where SK1 and SK2 differ primarily; SK1 has the amino acids Ile¹⁷⁴, Met²⁷², Phe²⁸⁸ and Ala³³⁹, whereas in SK2 these are substituted with Val³⁰⁴, Leu⁵¹⁷, Cys⁵³³ and Thr⁵⁸⁴ respectively. The different amino acids within the 'J-channel' provide the two isozymes with slightly different biochemical properties (Adams et al., 2016). One other important region sandwiched in between the C- and N-terminal domains is where the hydrophobic tail of sphingosine is able to insert. Meanwhile the hydrophilic head of SPH forms hydrogen bonds with Asp⁸¹ of loop β 3- α 3, Asp¹⁷⁸ of helix α 7 and with Ser¹⁶⁸ of strand β 8 (Wang et al., 2013). These interactions within the SPH tail and head regions enable conformational changes to occur within loops of the enzyme in order to facilitate catalysis. In doing so, the 1-hydroxyl polar head group of SPH is able to reside close to the β -phosphate group of ATP, allowing SPH to undergo nucleophilic attack required for phosphorylation. Furthermore the Asp⁸¹ of loop β 3- α 3 acts as a base catalyst to enhance nucleophilicity of the 1-hydroxyl SPH head group, hence enabling a more efficient phosphoryl transfer to produce S1P (Wang et al., 2013).

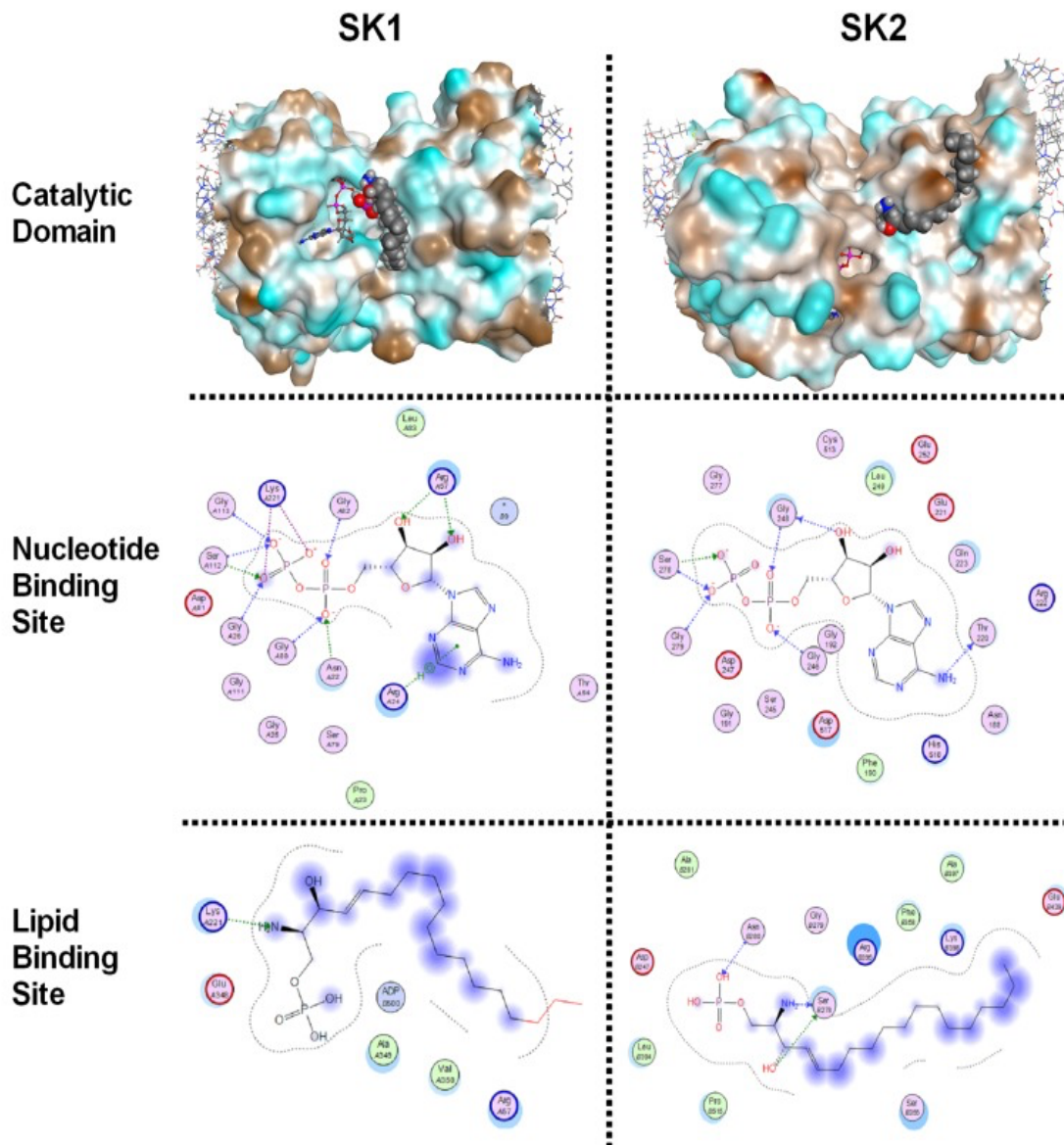


Figure 1.2 Domains and binding sites of SK1 and SK2 (Gao et al., 2012)

Graphic depiction of SK1 and SK2 indicating how SPH is able to bind to the enzyme between helices $\alpha 7$ and $\alpha 9$. There is significant variation within the lipid binding site (also known as the J-channel) of the two kinases, providing functionally different isozymes (Gao et al., 2012; Adams et al., 2016). Although key residues remain conserved between SK1 and SK2, plasticity in the J-channel is a major distinctive feature between the two isozymes (Adams et al., 2016). To illustrate, SK1 has an expanded heel region and a constricted toe, whereas SK2 has a narrow heel region and an enlarged toe, as a result the enzymes are able to have different functions and isozymes specific inhibitors exist (Chan et al., 2012; Pyne et al., 2018). Also shown are the residues in which the nucleotide is able to interact with in the respective kinases. Within SK1 the adenine is able to insert between the $\beta 1$ - $\alpha 1$ and $\beta 2$ - $\alpha 2$ loops, although with no crystal structure for SK2 it is not clear as to how the nucleotide interacts with the enzyme precisely (Chan et al., 2012; Adams et al., 2016).

Sphingosine kinase activity can be regulated by changes in transcription of other proteins, including PKC (Buehrer et al., 1996), tissue inhibitor of metalloproteinase-1 (Yamanaka et al., 2004) and activator protein-2 (Nakade et al., 2003). However, both SK1 and SK2 isoforms reside predominantly in the cytosol and exert their function by changing sub-cellular localization in a process known as translocation. This change in localization to areas where the substrate SPH is present is understood to be the primary regulatory mode of sphingolipid metabolism (Johnson et al., 2002; Pitson et al., 2003), with cell stimulation leading to modest, 1.5-4 fold increases in kinase activity (Rius et al., 1997; Yamanaka et al., 2004; Hengst et al., 2010). With both isoforms catalysing the same reaction, it is differences in sub-cellular localization of the two isoforms that defines them and determines their effects.

SK2 is located predominantly in the nucleus and perinuclear regions (Igarashi et al., 2003) and exerts mainly nuclear effects (Hait et al., 2009; Panneer Selvam et al., 2015). The enzyme can transit the nucleus because it contains both a nuclear export signal sequence and a nuclear localisation sequence (Ding et al., 2007). Unlike SK1 that has long been accepted to promote cell survival (Olivera et al., 1999), the functions of SK2 are still being unravelled. SK2 is thought to be pro-apoptotic, with overexpression inducing growth arrest and apoptosis (Beyer et al., 2018). Furthermore, mitochondrial localization of SK2 is thought to promote mitochondrial outer membrane permeabilization, cytochrome c release and subsequent apoptosis (Chipuk et al., 2012). In addition, SK2 has been reported to promote apoptosis through inhibition of DNA synthesis (Igarashi et al., 2003) and suppression of cell proliferation (Gao et al., 2012) due to the inclusion of a BH3 domain, which sequesters Bcl2 to promote apoptosis (Liu et al., 2003). However, it should be noted that SK2 has also been shown to exhibit anti-apoptotic functions dependent on the level of SK2 expression in the cells (Neubauer et al., 2016). In this regard, SK2 is also considered to promote cancer, whereby knockdown of SK2 has been shown to inhibit cell proliferation (Van Brocklyn et al., 2005; Gao et al., 2011) and cancer cell migration (Gao et al., 2011; Adada et al., 2015). Furthermore, SK2 overexpression has been shown to drive neoplastic transformation, proliferation and tumorigenesis of NIH3T3 cells (Neubauer et al., 2016). Increased expression of SK2 also correlates with poorer prognosis of non-small cell lung cancer (Wang et al., 2014). In addition, SK2 activity is thought to drive chemotherapeutic resistance, whereby knockdown of SK2 is able to chemosensitise cancer cells (Nemoto et al., 2009; Schnitzer et al., 2009). Interestingly, SK2 inhibits DNA synthesis under conditions of serum deprivation,

which drives the nuclear SK2 accumulation and promotes cycle arrest and apoptosis (Okada et al., 2005). The contrasting reports concerning the role of SK2 in cancer may be due to the different levels of SK2 expression within tumours. By comparing low and high overexpression of SK2 in tumours, Neubauer et al., (2016) demonstrated that high levels of SK2 reduced cell proliferation and survival that coincided with elevated cellular ceramide, whilst low levels of SK2 promoted the nuclear to PM translocation and increased extracellular S1P and thus neoplastic conversion (Neubauer et al., 2016). This could perhaps explain the conflicting reports on the role of SK2, whereby at low levels SK2 might form complexes with other proteins that drive its translocation to the PM (combinatorial signaling), and at high levels SK2 may form incompetent complexes due to the lack of availability of proteins to form competent complexes. Therefore, SK2 may exert a dominant negative effect by forming incompetent and competent complexes that compete for the same effector, whereby more incompetent complexes are formed at high levels of SK2, leading to increased apoptosis.

In contrast to SK2, SK1 is localized in the cytoplasm with a small proportion residing at the PM (Kohama et al., 1998; Delon et al., 2004). It should be noted however that SK1 can also be found in the nucleus. Even though it is unclear as to how SK1 enters the nucleus and this might be through the inclusion of nuclear localisation sequence, the kinase possesses a nuclear export sequences and deletion of these motifs leads to nuclear accumulation of SK1 (Inagaki et al., 2003). SK1 is understood to have a pivotal role in regulating bioactive lipid homeostasis and is therefore an attractive target for drug discovery. The separate knockout of *SPHK1* or *SPHK2* produces viable offspring (Allende et al., 2004), while the double knockout leads to abnormal cardiovascular development and produces a lethal phenotype. Thus, SK1 and SK2 show some redundancy in their function (Mizugishi et al., 2005). These results suggest the two isoforms may regulate the same sub-cellular pools of S1P. However, discrete function has been attributed to each isoform and therefore they are also capable of regulating non-overlapping functional intracellular S1P pools, whereby SK2 is able to compensate for the loss of SK1, but SK1 is not able to compensate for the loss of SK2 and produce S1P in the nuclear pool (Gao et al., 2011).

Regarding the more commonly associated functions of SK1, GPCR stimulation via extracellular ligands such as S1P or carbachol, or direct activation of PKC in response to PMA leads to the translocation of SK1 to the PM (Pitson et al., 2005; ter Braak et

al., 2009). Translocation enables SK1 to bind to membrane-bound acidic phospholipids such as phosphatidic acid (PA) (Delon et al., 2004) and phosphatidylserine (PS) (Stahelin et al., 2005) on the inner leaflet of the PM. PA is provided through activation of phospholipase D (Delon et al., 2004). SK1 is thought to be able to translocate using 2 mechanisms. The first is dependent on ERK-1/2, which catalyses the phosphorylation of Ser²²⁵ on SK1 to promote movement of the enzyme from the cytoplasm to the PM (Pitson et al., 2003). This was initially discovered through observing a 14-fold increase in SK1 catalytic activity following activation of ERK-1/2, with subsequent phosphorylation of Ser²²⁵ (Pitson et al., 2003), which is able to modulate the Thr⁵⁴ and Asn⁸⁹ interactions of SK1 with membrane-incorporated PS (Stahelin et al., 2005). More recently, it has now been shown that these residues are involved in ATP binding and in fact membrane binding is by hydrophobic patches on the LBL-1 of SK1 (Adams et al., 2016; Pulkoski-Gross et al., 2018). One other component involved in SK1 translocation is calcium and integrin-binding protein (CIB), which interacts with the calmodulin-binding site in order to shepherd SK1 from the cytoplasm to the PM (Sutherland et al., 2006; Jarman et al., 2010). Via a Ca²⁺-myristoyl switch, CIB1 is able to drive the translocation of SK1 to the PM and thus oncogenic signalling and neoplastic transformation by Ras (Zhu et al., 2017). On the other hand, CIB2 plays an opposing role to that of CIB1, blocking the translocation of SK1 to the PM and is downregulated in ovarian cancer that correlates with poorer prognosis (Zhu et al., 2017).

Later it was discovered that even after replacing Ser²²⁵ (with Ala), SK1 was still able to translocate to the plasma membrane in response to M₃ AChR stimulation (ter Braak et al., 2009). These findings indicated the presence of another mechanism of SK1 translocation that is independent of Ser²²⁵ phosphorylation and which occurred under a G_q drive. Therefore, the second mechanism involves G_q-dependent signalling and which is independent of phosphorylation state of the enzyme (ter Braak et al., 2009). Following this study Adams et al. 2016 hypothesised an alternative mechanism of SK1 translocation, independent of Ser²²⁵ phosphorylation, based upon crystallographic evidence and biochemical studies demonstrating that SK1 has a dimeric quaternary organisation (Lim et al., 2011). This organisation allows a concave region to form within the dimer that is host to a region of positive charged situated between two LBL-1 present within each monomer that contains hydrophobic residues on the outer surface (Fig. 1.3). This configuration allows the formation of a contiguous membrane engagement interface, acquiring electrostatic potential from the positively

charged residues at the dimer interface and hydrophobic patches on the LBL-1 to enable simultaneous embedding into the membrane and encapsulation of SPH (Adams et al., 2016; Pulkoski-Gross et al., 2018). Once at the PM the LBL-1 domains are able to insert into the bilayer to extract sphingosine. This involves a gating mechanism in LBL-1 (which forms the back wall of the catalytic site) that allows sphingosine to be pulled into the catalytic site followed by closure of LBL-1 to encapsulate the lipid in the catalytic site, where it is then converted to S1P (Adams et al., 2016). The proposal made here is that translocation of SK1 under G_q drive involves the alignment/misalignment of the membrane engagement interface, of which is governed by C-terminal tail orientation.

Ultimately, it is translocation of SK1 to the PM and the subsequent production of S1P that plays an important role in cell survival, proliferation and resistance to chemotherapy (Olivera et al., 1999). Moreover, high levels of SK1 is associated with oxaliplatin resistance and correlates with poor prognosis in hepatocellular carcinoma (Wang et al., 2018). In addition, ER⁺ breast cancer patients express high levels of SK1 that is associated with increased tamoxifen resistance and reduced survival time (Long et al., 2010; Watson et al., 2010). Furthermore, a role for SK1 in metastasis is evident. SK1 mRNA and protein expression is elevated in triple negative breast cancer cells. This is understood to drive metastasis of MDA-MB-231 cells to the lungs, dependent on the upregulation of *FSCN1*. Conversely SK1 knockdown in MDA-MB-453 cells decreased the invasiveness of these cells (Acharya et al., 2019).

The importance of SK1 for cell survival is also evidenced by the consequential effects of SK1 inhibitors that induce the ubiquitin-proteasomal degradation of SK1 (Loveridge et al., 2010). In this sense, fingolimod has been shown to induce proteasomal degradation of SK1 in breast cancer, human pulmonary artery smooth muscle and prostate cancer cells that induces growth arrest and apoptosis (Tonelli et al., 2010; McNaughton et al., 2016). In addition, TNF- α treatment has also been shown to induce apoptosis and is associated with the degradation of SK1 through cathepsin-B activation (Taha et al., 2005). In this regard, some SK1 inhibitors such as SKI-II have been observed to downregulate protein, albeit not mRNA expression of SK1, therefore utilising a lysosomal pathway thought to involve cathepsin B (Ren et al., 2010). Indeed, the development of isoform selective inhibitors with nanomolar potency would allow the specific therapeutic targeting of cancers, where one or the other isoform displays a predominant role in driving a particular disease pathology.

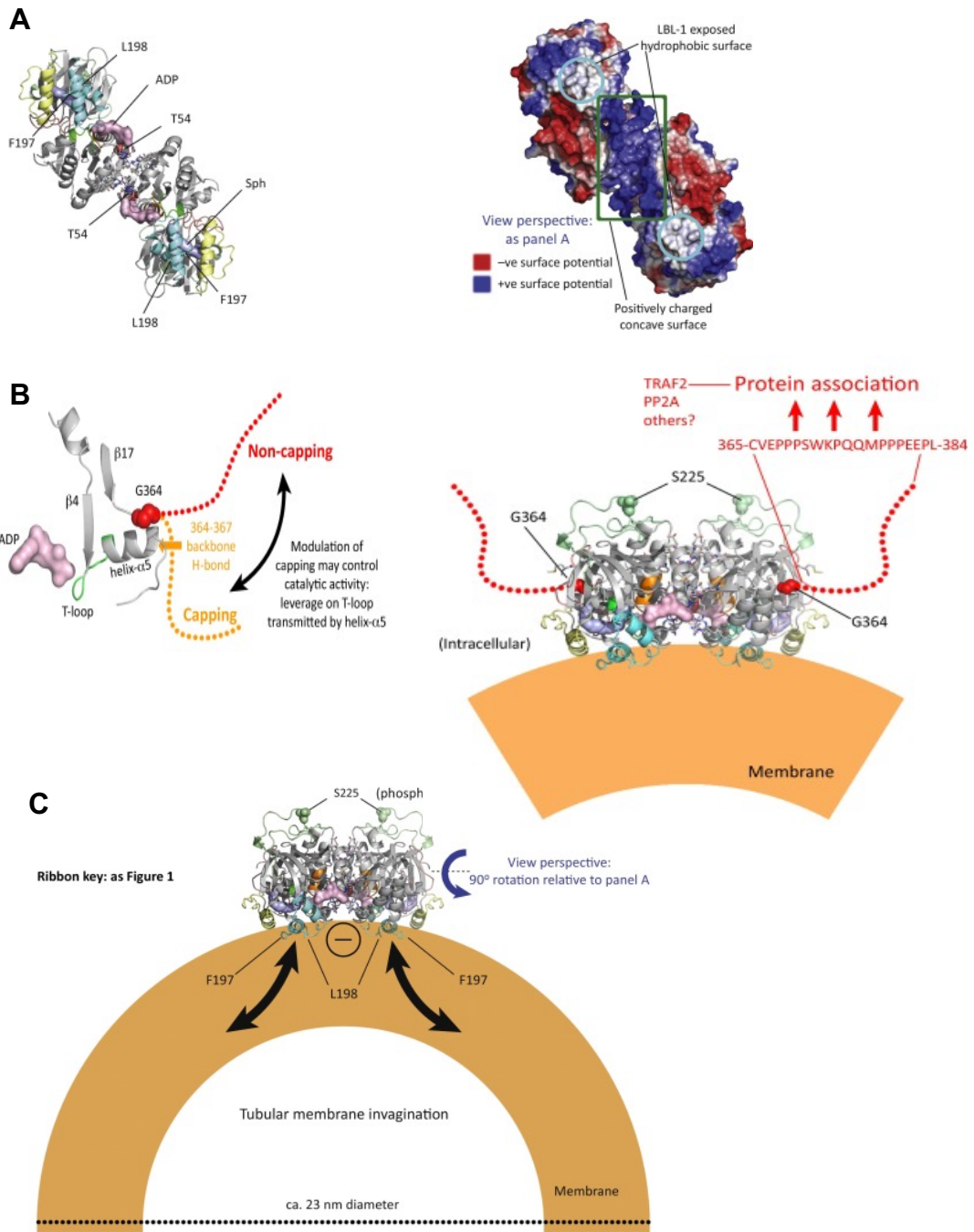


Figure 1.3 Mechanism of SK1 membrane targeting (Adams et al., 2016)

SK1 is able to dimerise providing a region of high positive charge (blue region) and exposure of hydrophobic patches (blue circles) to drive translocation of the kinase to the negatively charged PM (A). Alignment/misalignment of the hydrophobic patches and the positively charged residues is hypothesised to be governed by orientation of the C-terminus tail about Gly³⁶⁴ (B). With the 'cap' displaced, SK1 can bind to narrow tubular invaginations, characteristic of early endocytic events of filopodia (C) (Adams et al., 2016).

1.2.1 Dimerisation of SK1

Originally SK1 was believed to be a catalytically active monomeric protein (Olivera et al., 1998). This was based on experimental findings from gel filtration, however the emergence of 5 SK1 crystal structures indicated that SK1 is dimer (Adams et al., 2016). Comparative analysis with other DAGK_cat crystal structures indicates a common NTD-NTD formation displaying C₂-symmetry (Wang et al., 2013; Wang et al., 2014; Adams et al., 2016). The existence of dimeric SK1 is reinforced experimentally using immunoprecipitation analysis which showed that SK1 can form a minimal dimeric organisation (Lim et al., 2011; Liu et al., 2013). The ability of SK1 to become of dimeric does not eliminate the possibility of catalytically active monomeric SK1. Interestingly crystal structure analysis of *h*SK1 indicates a relatively modest interfacial surface contact (*ca.* 780 Å² buried solvent accessible surface area on each protomer), suggesting the possibility of a dynamic monomer/dimer SK1 equilibrium. This would allow for potentially additional regulation over the production of S1P and maybe different mechanisms of translocation. In this regard, it may be that the enzyme has the potential to dimerise, possibly increasing the repertoire of functions of the kinase, thereby explaining, in part, the pleiotropic effects of S1P. The monomer and dimer will be subject to an equilibrium transition.

SK1 is understood to dimerise in a similar manner to other kinases of the DAGK_cat family (Adams et al., 2016). Interestingly, in all cases there is a degree of annealing of the exposed β2 strands of protomers, and interactions of α1/α2 helices and their connecting loops. Therefore, SK1 is thought to dimerise through antiparallel partial annealing of exposed β2 strands on the NTD, leading to NTD-NTD engagement displaying C₂-symmetry about the x-axis (Adams et al., 2016). Furthermore, there is the potential for phosphorylation state of the R-loop to impact on dimerisation (Adams et al., 2016). In addition, in the current study we also provide evidence of a polar network to form a cross-dimer salt bridge. It should be noted however that residues involved in the dimerization interface are not conserved between SK1 and SK2. Therefore, the dimerisation interface of SK2 would differ from SK1 and further investigation would be needed to confirm the dimerisation capability of SK2.

Importantly, dimerisation would allow the formation of a contiguous membrane engagement interface across both protomers that incorporate positively charged residues and exposed hydrophobic patches (Adams et al., 2016; Bayraktar et al.,

2017) . Moreover, the increased density of positive charge at the dimerization groove would increase the binding affinity SK1 for the PM. The functional importance of dimerization and a contiguous membrane engagement interface has been demonstrated both through crystallographic analysis (Adams et al., 2016) and experimentally through mutagenesis of key residues (Shen et al., 2014; Pulkoski-Gross et al., 2018). Using *in silico* surface binding analysis, Pulkoski-Gross et al., (2018) demonstrated that 3 highly positively charged residues, namely Lys²⁷, Lys²⁹ and Arg¹⁸⁶ adjacent to the active site and substrate binding site are responsible for allowing SK1 to bind to membranes *in vitro* and in cells (Pulkoski-Gross et al., 2018). In addition, replacing key residues in the hydrophobic patch leads to ablation of SK1 membrane targeting required to target convex tubular membrane invaginations (Shen et al., 2014), indicating a requirement for both positively charged residues and the hydrophobic patch present on LBL-1. Once at the PM, SK1 can bind to PA and PS and extract SPH to disrupt membrane rigidity and facilitate endocytosis (Delon et al., 2004). Indeed, there is evidence that membrane targeting of SK1 is involved in key biological processes such as neurotransmission. In *Caenorhabditis Elegans* the knockdown of SK1 resulted in defective neurotransmission, which was rescued by over-expression of WT SK1 but not LBL-1 (V268Q-SK1) mutated SK1 (Shen et al., 2014). This reinforces the importance of the LBL-1 domains that mediate curvature-sensing interaction of SK1. In spite of these mechanistic studies, it is yet to be identified as to how specifically this mechanism functions to translocate SK1 to the PM, and what role a potential monomer/dimer SK1 equilibrium may play in cellular function.

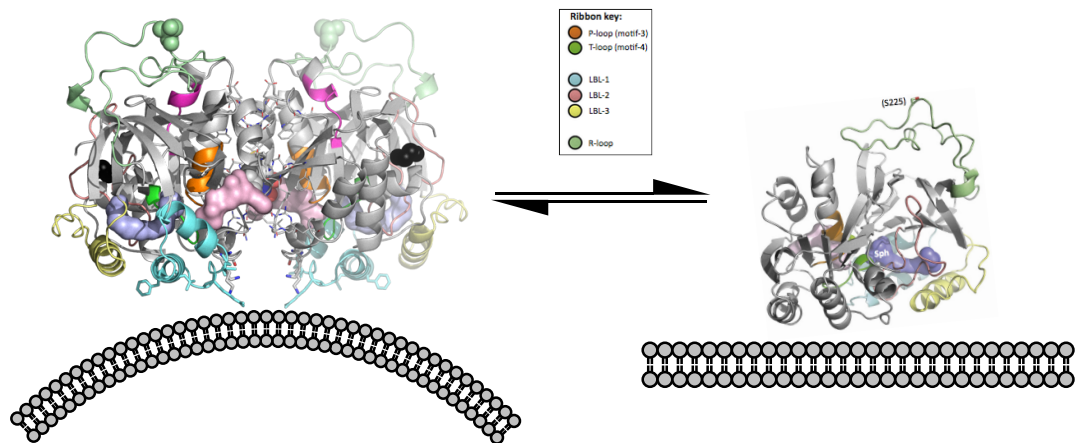


Figure 1.4 Binding of monomeric and dimeric SK1

The potential binding conformation of SK1 in a monomeric or dimeric configuration, utilising hydrophobic patches and positively charged residues. It is suggested that dimerization may allow SK1 to sense high membrane curvature, such as endocytic invaginations. SK1 may also be able to translocate to areas of the PM lacking high curvature, suggesting a role for monomeric SK1 (Adams et al., 2016).

1.2.2 C-terminal regulation of SK1

One other debate is how exactly the SK1 C-terminus is involved in regulating the association of SK1 with the PM. It has been suggested by Adams et al., (2016) that the C-terminus can perform 2 functions (Adams et al., 2016). Firstly, the C-terminus interacts with Gly³⁶⁴ on the α 5 helix of SK1, a helix that is extended to form part of the ATP-binding site. Therefore, de-capping of the α 5 helix may allow flexibility in the ATP binding site (T-loop) that could lead to enzyme activation. Moreover, the α 5 helix and T-loop residues are the same in *mSK1* and *hSK1* and therefore there is an evolutionary conservation, which would suggest biological significance (Adams et al., 2016). Secondly the C-terminal tail might influence NTD:CTD arrangement and presentation of membrane engagement interface (LBL-1 and the positive charged cluster at the dimer interface). Evidence is indicated through deletion of the C-terminus tail, with complete truncation of the C-terminus (1-363 amino acids) leading to constitutive PM translocation and enhanced catalytic activity of SK1, independent of Ser²²⁵ phosphorylation (Hengst et al., 2010). Therefore, protein-protein interactions that displace the C-terminus might regulate membrane interacting site on SK1, thereby allowing binding of the SK1 to the plasma membrane and activation of catalytic activity (Adams et al., 2016). Indeed, SK1 activation results from the C-terminus binding tumour necrosis factor receptor-associated factor 2 (TRAF2) at the

PPEE motif in response to TNF- α (Xia et al., 2002). Conversely, SK1 is deactivated from PP2A binding to the proline-rich region of the C-terminus (Barr et al., 2008; Pitman et al., 2011). This said, there is still no evidence of protein-protein interactions leading to 'uncapping' of the C-terminus.

1.3 Dysregulation of sphingolipid metabolism in cancer

With the two most central bioactive lipids, ceramide and S1P having opposing roles in promoting apoptosis and proliferation respectively, it is not surprising that imbalances in the sphingolipid rheostat has been heavily linked to cancer progression (Pyne et al., 2010; Ogretmen 2018). The balance of sphingolipids is known to control many aspects of oncogenesis, for example, growth, proliferation, migration, autophagy, invasion, metastasis and angiogenesis (Pyne et al., 2010). Therefore, the metabolism of these lipids is tightly regulated, and it is the enzymes responsible for their production that have drawn the most attention regarding anticancer therapeutics.

Cellular stress resulting from SPH and ceramide accumulation results in cancer cell death. To counter this there is increased tumour expression of glucosylceramide synthase, ceramide kinase, sphingomyelin synthase, sphingosine kinase and acid ceramidase, all contributing to the increased production of sphingolipids that promote cell survival (Strelow et al., 2000; Liu et al., 2010; Barcelo-Coblijn et al., 2011; Payne et al., 2014; Li et al., 2019). It is therefore clear that for the vast majority of cases, the imbalance in sphingolipids driving oncogenic transformation arises from the dysregulation of sphingolipid enzymes.

One important enzyme in modulating the sphingolipid rheostat is dihydroceramide desaturase (DES), which catalyses desaturation of dihydroceramide to produce ceramide via the insertion of a double bond between C4 and C5 of the sphingosine long-chain base (Kravcka et al., 2007). However, the role of DES has been somewhat confusing, with reports of both pro-apoptotic (Siddique et al., 2013) and autophagy-mediated anti-apoptotic roles (Hernandez-Tiedra et al., 2016). Pharmacological inhibition of DES by fenretinide has been shown to increase dihydroceramide and induce neuroblastoma (Rahmaniyan et al., 2011) and prostate cancer growth arrest (McNaughton et al., 2016).

Another producer of ceramide are sphingomyelinases, which are considered to be tumour suppressing enzymes. These enzymes hydrolyse sphingomyelin, of which

there are three subtypes: neutral (NSMase), acid (ASMase) and alkaline (Alk-SMase) based on the pH at which optimal activity is achieved (Linardic et al., 1994; Nyberg et al., 1996). ASMase has been shown to increase ceramide production, thus resulting in cell death of lymphoblasts in mice (Santana et al., 1996). Interestingly, the blood and tumour microenvironment of patients with non-small cell lung carcinoma has elevated ASMase activity. Reducing the activity of ASMase elevates Th-1 mediated and cytotoxic T cell mediated anti-tumour immunity, thereby highlighting ASMase is used by tumours to drive immune evasion (Kachler et al., 2017). NSMase are involved in exosome release (Trajkovic et al., 2008) and has been shown to be downregulated with reduced exosome release in hepatocellular carcinoma, which leads to suppressed growth arrest and poor prognosis (Lin et al., 2018). Lastly, downregulation of Alkaline-SMase has been shown to result in the development of larger colon tumours, demonstrating a tumour suppressive role (Chen et al., 2015).

Ceramide can be phosphorylated to produce ceramide-1-phosphate (C1P), a process catalysed by ceramide kinase (CERK) (Bajjalieh et al., 1989). C1P production leads to the synthesis of pro-inflammatory eicosanoids (Pettus et al., 2003). Moreover, increased CERK activity is associated with cancer cell survival and tumour recurrence (Payne et al., 2014), whilst its inhibition leads to growth arrest and apoptosis (Pastukhov et al., 2014). More recently, CERK overexpression has been shown to increase the activation of protein kinase Akt and drive the migration of non-metastatic MCF7 cells (Schwalm et al., 2020).

Once the sphingolipid backbone is formed, the only way it can be removed is through the catabolic action of S1P lyase 1 (SPL) to hydrolyse S1P to ethanolamine-1-phosphate and hexadecanol (Serra et al., 2010). In this regard, the action of SPL is considered pro-apoptotic enabling the removal of S1P and therefore is an attractive anti-cancer therapeutic target. Moreover, the expression of SPL is downregulated in various tumours and supports resistance to radio- and chemotherapy (Colie et al., 2009; Brizuela et al., 2012) .

Perhaps most important in cancer transformation is the activity of sphingosine kinases that produce proliferative S1P, of which both SK1 and SK2 have been shown to be upregulated in tumours (Ruckhaberle et al., 2008; Neubauer et al., 2016). Controversially however, there are multiple studies demonstrating an opposing role of SK2 when compared to SK1 (Maceyka et al., 2005), by inhibiting DNA synthesis

(Igarashi et al., 2003) and promoting apoptosis (Liu et al., 2003; Okada et al., 2005). In addition, SK2 has been shown to act as an epigenetic regulator by inhibiting histone deacetylase 1/2 activity through the production of S1P (Hait et al., 2009). Despite these reports, similarly to SK1, SK2 is also considered an oncogene (Venkata et al., 2014; Wang et al., 2014), with low-level overexpression promoting neoplastic transformation (Neubauer et al., 2016). SK2 also promotes EGF-mediated invasion of cancer cells by driving the activation of ezrin-redaxin-moesin proteins (Adada et al., 2015).

Evidence for the oncogenic effects of SK1 originated from NIH3T3 fibroblasts overexpressing SK1 showing serum-independent proliferation and growth, characteristic of oncogenic transformation and subsequently forming fibrosarcomas in mice (Xia et al., 2000). These effects were shown to be dependent on the catalytic activity of SK1, thereby defining SK1 as an oncogene. Surprisingly however, there are currently no known cancerous mutations associated with SK1 and it is the reliance that cancer cells have for SK1 that suggest that the enzyme is in fact involved in non-oncogene addiction of cancer cells (Vadas et al., 2008). Nevertheless, there is a vast array of evidence supporting a role for SK1 in cancer. The knockdown of SK1 has shown to prevent transformation (Dayon et al., 2009) and results in reduced proliferation (Brizuela et al., 2010), enhanced apoptosis (Gomez-Brouchet et al., 2007), reduced migration (Guo et al., 2006) and enhanced sensitisation to chemotherapy (Marfe et al., 2011). Conversely, studies overexpressing SK1 have been shown to transform healthy cells (Xia et al., 2000), increase proliferation and survival (Li et al., 2007), promote intravasation (Pan et al., 2011) and enhance chemoresistance (Marfe et al., 2011; Song et al., 2011). Indeed, many of these effects are observed without the need for overexpression, for example, prolactin is able to activate SK1 in MCF-7 cells to drive proliferation and migration (Doll et al., 2007)

1.3.1 Oncogenic mechanisms related to sphingolipids

With sphingolipid imbalance attributing to disease progression, it is not surprising therefore that the alterations in sphingolipid metabolism led to a vast array of cellular dysfunctions that promote oncogenesis. These changes in sphingolipid metabolism leads to dysfunctions regarding necroptosis and thus inflammation, autophagy, angiogenesis, ER stress, migration, apoptosis and proliferation of which the latter two were also discussed in 1.3.

Along with being the major driver of apoptosis, ceramide is also understood to induce necroptosis. This form of necrosis is programmed, which involves initiation via the activation of the death receptors such as tumour necrosis factor-1 (TNF1) (Vanlangenakker et al., 2011) and toll-like receptors (TLR) (Kim et al., 2013) along with activation of receptor-interacting protein-1/3 (RIPK1/3) (Cho et al., 2009). More recently, downstream of (RIPK1/3), mixed lineage kinase-domain like protein (MLKL) is thought to be phosphorylated and oligomerise (Weber et al., 2018) to ultimately cause necroptosis (Sun et al., 2012). The necrosome then forms pores in membranes enables the breakdown of mitochondrial, lysosomal and plasma membranes (Vandenabeele et al., 2010). It is now believed that ceramide is able to form a complex with RIPK1, coined the ceramidosome that forms large membrane pores in a similar manner to the necrosome to facilitate necroptosis (Nganga et al., 2019). Simply, the accumulation of endogenous ceramide has been shown to drive necroptotic cancer cell death (Bagnjuk et al., 2019). C₁₆-ceramide more specifically triggers mitophagy-induced necroptosis (Mizumura et al., 2018) and when caspase-8 is inhibited this form of ceramide promotes necroptotic trophoblast cell death (Bailey et al., 2017). Furthermore, interaction of ceramide with phosphatase 2A inhibitor (I2PP2A) activates PP2A to induce necroptosis and suppress tumour growth in lung tumour xenograft models (Saddoughi et al., 2013). From a therapeutic perspective, the delivery of liposomal ceramide initiates the oligomerization of MLKL and necroptosis, suppressing metastatic growth in an ovarian cancer xenograft model and is currently in clinical trials (Zhang et al., 2018).

Autophagy is stress response leading to the engulfing of proteins, lipids and organelles into membrane vesicles called autophagosomes. These are then sent for lysosomal degradation, which can induce autophagy-dependent cell death. Additionally, ER stress can induce autophagy-mediated cell death (Salazar et al., 2009). This evolutionary conserved stress response is considered pro-survival, however excessive autophagy induces cell death. Autophagy has multiple roles in cancer; promoting cell survival and inducing apoptosis and is considered a hallmark of cancer (Young et al., 2018). In the context of sphingolipids, dihydroceramide and ceramide induce autophagy. Tetrahydrocannabinol triggers accumulation of dihydroceramide in the ER of glioma cells that results in autophagy and apoptosis in a cytoprotective role (Hernandez-Tiedra et al., 2016), however conflictingly, DES1 inhibitors have also been shown to induce autophagy (Casasampere et al., 2017). This might be explained by the differential effects of native and polyubiquitination

forms of DES1, whereby polyubiquitination shifts the function of the enzyme from proapoptotic/autophagy to pro-survival (Alsanafi et al., 2018). Ceramide-induced stress via chemotherapy or exogenous ceramide promotes the accumulation of C₁₈-ceramide at the outer membrane of mitochondria in head and neck cancers. Here C₁₈-ceramide interacts with LC3B-II formed by the lipidation of microtubule-associated protein 1 light chain 3 β that ultimately leads to the recruitment of the autophagosome for mitochondrial disassembly/mitophagy in head and neck cancer (Sentelle et al., 2012) and myeloid leukaemia (Dany et al., 2016). Sphingolipids can also promote the degradation of specific proteins in order to promote oncogenesis. In this regard, SK1 has been shown to drive epithelial-mesenchymal transition in hepatoma cells by forming S1P to activate TRAF2/Beclin 1 and promote the specific lysosomal degradation of E-cadherin (Liu et al., 2017).

The actions of sphingosine kinases to produce S1P can lead to cell migration and intravasation that ultimately leads to metastasis of cancer (Hobson et al., 2001; Pyne et al., 2010). S1P plays a somewhat pleotropic role in cancer cell migration. As a general principle, S1P primarily acts by binding to S1P₃ (Filipenko et al., 2016) or S1P₁ (coupled to RAC/CDC42) (Li et al., 2009) to stimulate cancer cell motility. Initial studies showed S1P had an inhibitory role in cancer cell migration, independent of receptor binding (Sadahira et al., 1992; Yamamura et al., 1997; Wang et al., 1999). This can be explained by the concentrations of S1P used in these earlier studies. S1P was used in the micromolar range, although we now know that S1P₁₋₅ have an affinity for S1P in the nanomolar range, with S1P having a bell-shaped dose-response with regards to migration (Wang et al., 1999; Van Brocklyn et al., 2003). Moreover, more recent studies have demonstrated that low concentrations of S1P enhances motility, whilst high concentrations attenuate migration via the activity of regulator of G-protein signalling-2 (RGS2), independent of receptor internalization (Kohno et al., 2008).

In contrast, S1P₂ activation leads to the joint activation of Rho and inhibition of Rac to attenuate migration (Arikawa et al., 2003; Malchinkhuu et al., 2008). It should be noted however, that this mechanism is not universal to all cancers, with S1P₂ activation attenuating migration independent of Rac activity in glioma cells (Lepley et al., 2005). Nevertheless, there is a wealth of evidence indicating the anti-migratory effects of S1P₂. Therefore, the effect of S1P on migration is largely determined by the receptor sub-type present on the cell surface. For example, on gastric tumour cells that predominantly express S1P₃, S1P has a pro-migratory effect, whereas AZ-521

duodenum carcinoma cells that exclusively express S1P₂, S1P attenuated migration (Yamashita et al., 2006). This demonstrates the differential response based on receptor expression and highlights the importance of personalized cancer treatment in order to bring about the desired response with regards to minimizing disease progression.

Lastly, tumour neovascularization involves the diversion of endothelial cells in neighbouring, pre-existing vessels towards the tumour where they are able to proliferate and form new, functional, albeit morphologically abnormal networks to provide the tumour with nutrients and oxygen (Warren et al., 1978; Konerding et al., 1999). In doing so the tumour is able to grow and simultaneously starve surrounding tissues of oxygen and nutrients. This event is driven predominantly by hypoxia (Muz et al., 2015) leading to the induction of chronic stimulation of growth factors such as vascular endothelial growth factor (VEGF) (Goel et al., 2013), basic fibroblast growth factor (bFGF) (Korc et al., 2009) and platelet derived endothelial growth factor (Zhang et al., 2005). With that being said, sphingolipid signaling clearly has a role to play in tumour neovascularization (Takuwa et al., 2010). S1P signaling in this context is mediated primarily through the activation of S1P₁, which is highly expressed in tumour vessels and the importance of which is evidenced by the knockdown of S1P₁ resulting in reduced angiogenesis and tumour suppression (Chae et al., 2004). By contrast, antagonism of S1P₁ by FTY720 inhibits angiogenesis (LaMontagne et al., 2006). Additionally, S1P₂ is also thought to be involved in tumour angiogenesis, although its role is not completely clear. Originally, S1P₂ was shown to drive pathological angiogenesis of the retina, with S1P₂^{-/-} mice showing reduced retinal angiogenesis (Skoura et al., 2007). Since then, findings from another demonstrate S1P₂^{-/-} mice have increased angiogenesis and micro-vessel density promoting 60-100% increase in tumour growth, conferring an anti-angiogenic role (Du et al., 2010). Therefore, there may be a pathological event in neoplastic conversion leading to a shift in function of S1P₂ from anti-angiogenic to pro-angiogenic, perhaps driven by hypoxia.

1.3.2 Sphingosine kinase inhibitors as cancer therapeutics

Ceramide and S1P are at the forefront of the sphingolipid rheostat, whereby sphingosine kinases control the production of S1P and thus have an important role in the balance between cell survival and apoptosis. It is not surprising therefore that there has been extensive research into the development of sphingosine kinase

inhibitors (Pitman et al., 2016; Bayraktar et al., 2017) and the identification of SK1 crystal structures with bound inhibitors (Wang et al., 2014). Importantly, these inhibitors are thought to exert their effects by reducing the formation of S1P, but also altering the balance of other sphingolipid metabolites such as sphingosine and ceramide (Ogretmen et al., 2004; Sordillo et al., 2016).

Along with differing in their sub-cellular localization and regulation, SK1 and SK2 are distinct in their selectivity towards ligands and therefore inhibitors. Selectivity of both kinases is demonstrated by the ability of SK2 to exclusively phosphorylate FTY720, whereas the compound is a selective inhibitor of SK1 (Tonelli et al., 2010; Lim et al., 2011). However recently, FTY720 has been shown to be phosphorylated in *Sphk2*^{-/-} mice and therefore FTY720 may be a very poor substrate for SK1 (Liang et al., 2013). This selectivity comes primarily from structural differences in the hydrophobic lipid-binding 'J-channel' that accommodates the SPH tail (Adams et al., 2019). The ligand contact surface is comprised of 20 residues in *hSK1*, of which Ile¹⁷⁴, Met²⁷² and Phe²⁸⁸ differs in *hSK2*. Moreover, it is the substitution of Phe²⁸⁸ for Cys⁵³³ that is believed to elongate the 'J-channel' toe region and account for the enhanced plasticity of SK2 (Adams et al., 2019). One other important region of the 'J-channel' is the heel, formed by Leu³⁰² in SK1 and Leu⁵⁴⁷ in SK2, whereby SK2 possesses a contracted heel compared to SK1 (Adams et al., 2019).

This region was shown to be particularly important for the selectivity of the SK1 selective inhibitor, PF-543 (Wang et al., 2014). Co-crystal analysis indicated that the sulfonyl tail of PF-543 sits adjacent of the 'J-channel' heel, whereas the expanded toe and contracted heel of SK2, at least in part, accounts for the reduced affinity of PF-543 for SK2 (Adams et al., 2019). Moreover, this inhibitor has been shown to exert anti-cancer effects on human colorectal cancer cells, inducing programmed necrosis (Ju et al., 2016).

Initial sphingosine kinase inhibitors such as *L-threo* dihydrosphingosine (DHS:Sfingol), N,N-dimethylsphingosine (DMS) and N,N,N-trimethylsphingosine (TMS) compete for the binding of SK1 and SK2 to block their activities. Although these agents have shown therapeutic value in reducing tumour growth (Endo et al., 1991) and metastasis (Okoshi et al., 1991), they are not isoform-specific and have low specificity with off-target effects on PKC (Igarashi et al., 1989) and ceramide synthase (Sugiura et al., 2002). Furthermore, these compounds induce haemolysis (Kedderis

et al., 1995; Pitman et al., 2010) and therefore it was clear that these inhibitors could not be used as an anticancer thereby. Hence in 2003 French et al., developed 4 sphingosine kinase inhibitors, SKI-I; SKI-II; SKI-III; SKI-IV, which proved selective and without cytotoxic effects, unlike earlier inhibitors (French et al., 2003). Since then, the first SK2 specific inhibitor, ABC294640 (French et al., 2010), and the first SK1 specific inhibitor, SK1-I have both been developed (Paugh et al., 2008). Of the developed sphingosine kinase inhibitors (Pyne et al., 2010), the one that has gained the most attention is perhaps SKi (SKI-II; 2-(*p*-hydroxyanilino)-4-(*p*-chlorophenyl) thiazole)). This compound was shown to reduce the formation of S1P, inhibited proliferation and induced apoptosis (French et al., 2003), having both anti-tumour (French et al., 2006) and anti-inflammatory activities following oral administration (Maines et al., 2008), which demonstrates high bioavailability.

Since their development, sphingosine kinase inhibitors have been widely used in research in attempts to develop novel anticancer strategies, with sphingosine kinase isoforms expressed 2-8-fold higher in breast, ovarian, colon, stomach and lung cancers to name a few (French et al., 2003; Johnson et al., 2005; Sobue et al., 2006). To understand the function of sphingosine kinase inhibitors, one must consider the two roles of sphingosine kinases in cancer: as an oncogene and the modulation of sphingolipid metabolites. With regards to the first function, Xia et al., was the first to demonstrate SK1 acted as an oncogene in activating the Ras pathway (Xia et al., 2000) and later SK1 was shown to drive EGF-mediated cancer cell migration and tumour angiogenesis (Sarkar et al., 2005). In this regard, direct inhibition of SK1 with PF-543 has been shown to lead to a 10-fold reduction in S1P and rise in SPH (Schnute et al., 2012; Wang et al., 2014) to induce apoptosis (Ju et al., 2016). The toe and heel region of the 'J-channel' is particularly important for the selectivity of the SK1 selective inhibitor, PF-543 (Wang et al., 2014). Co-crystal analysis indicated that the sulfonyl tail of PF-543 sits adjacent of the 'J-channel' heel, whereas the expanded toe and contracted heel of SK2, at least in part, accounts for the reduced affinity of PF-543 for SK2 (Adams et al., 2019).

Sphingosine kinase inhibitors can alternatively alter the balance of its metabolic products, notably S1P that progresses cancer. S1P has been shown to mediate TNF (Alvarez et al., 2010) and NF- κ B signalling (Liang et al., 2013), hence is considered an oncogenic switch. In this case, one example of a sphingosine kinase inhibitor reducing activity of the enzyme indirectly is phenoxodiol (Gamble et al., 2006). This

agent indirectly inhibits sphingosine kinase by changing the ubiquinone/ubiquinol/NADH ratio leading to the inhibition of NADH oxidase on the surface of cancer cells (De Luca et al., 2005) and apoptosis (De Luca et al., 2010). Furthermore, SK1 inhibitors such as SK1-I have been shown to inhibit ERK/Akt signalling in leukaemia (Paugh et al., 2008) and JNK/Atk downstream of SK1 activation in glioblastoma (Kapitonov et al., 2009), demonstrating the different effects of various sphingosine kinase inhibitors.

The therapeutic value of sphingosine kinase inhibitors is clear, with safingol (*L-threo*-dihydrosphingosine) progressing through clinical oncology trials that is a substrate for both SK1 (and possibly SK2), thereby reducing S1P levels (Dickson et al., 2011). For the vast majority of SK1 inhibitors that directly target the actions of SK1 as an oncogene, the main focus is to prevent the binding of SPH (Wang et al., 2014) and/or ATP (Pitman et al., 2015), and to induce proteasomal degradation of SK1 (Pitman et al., 2015). The action of these inhibitors blocks catalytic activity and hence function of the kinase in diseased cells. However, at least for SK1, the enzyme is thought to be active as a dimer (Lim et al., 2011; Liu et al., 2013) and thus an alternative therapeutic approach would be to block the translocation of SK1, if for example, translocation in a pathological sense concerned either monomeric or dimeric SK1, or to specific PM micro-domains (Bayraktar et al., 2017). Blocking translocation in such specific events would allow more targeted inhibition of pathologic SK1 activity, whilst retaining basal catalytic activity of SK1 in healthy cells. The main caveat is that the complete mechanism of SK1 translocation is not currently understood. By fully understanding the mechanism of SK1 translocation and how this differs in oncogenic transformation, reveals avenues for novel, more targeted therapeutics and is the main focus of the current study. One such function of SK1 translocation is endocytic processing that becomes deregulated in lysosomal storage diseases (Platt 2014), Alzheimer's disease (Cataldo et al., 2000) and cancer (Mosesson et al., 2008) to name a few, the latter of which is another focus of the study.

1.5 Aims

The aim of the research is to establish the role of the monomer-dimer equilibrium and the C-terminal tail of SK1 in the phosphorylation-dependent and -independent translocation of this enzyme from the cytoplasm to the PM in breast cancer cells. In determining the structural membrane determinants in SK1 governing its translocation

to the PM, a better understanding of its role in oncogenesis will be revealed and novel anti-cancer therapeutics might become evident.

Chapter 2

Materials and Methods

2.0 Materials and Methods

2.1 Materials

2.1.1 General reagents and materials

All biochemicals were from Sigma Chemical Company (Poole, UK) unless otherwise stated.

BioRad, Watford, UK

1mM Mini-Protean® integrated spacer plate (#165-3311)

Mini-Protean® short plate (#165-3308)

Christainsen Linhardt, Munich, Germany

CEA Rö Blaufilm (X-RAY film) (#C011824)

KODAK RP X-Omat EXII (developer) (#KK17E2)

KODAK RP X-Omat EXII (fixer) (#KK17F1)

GE Healthcare, Little Chalfont, UK

Nitrocellulose membrane (#10600007)

Seralab, West Sussex, UK

Fetal bovine serum (FBS) (#FBS-500ML)

Sigma-Aldrich, Poole, UK

Pre-stained molecular weight (MW) marker (α_2 -Macroglobulin 180kDa, β -Galactosidase 116kDa, Lactoferrin 90kDa, Pyruvate kinase 58kDa, Fumarase 48.5kDa, Lactic dehydrogenase 36.5kDa, Triosephosphate isomerase 26.6kDa) (#SDS7B2)

Protein G sepharose ®, fast flow (#P3296)

Protein A sepharose ®, fast flow (#P9424)

Thermo Fisher Scientific Ltd., Loughborough, UK

Bovine serum albumin (BSA) (#10450141)

Dulbecco's Modified Eagle's Medium (DMEM) (#10566016)

Geneticin G-418 sulphate (#10463982)

LipofectAMINE® 2000 (#11668019)

Penicillin (10000 U/ml) and streptomycin (10000 μ g/ml) (PenStrep) (#15140122)

Trypsin (0.025%)/EDTA (0.01%) solution (#R001100)

Vector laboratories INC, Peterborough, UK

VECTASHIELD hard-set anti-fade mounting medium containing DAPI (#H-1500)

2.1.2 Agonists and antagonists

Avanti Polar Lipids, Inc. Alabama, USA

Sphingosine-1-phosphate (#860492P)

Caltag Medsystems, Buckingham, UK

YM254890 (#AG-CN2-0509-MC05)

Cayman Chemical, Michigan, USA

FIPI (5-Fluoro-2-Indolyl des-Chlorohalopemide) (#13563)

Sigma-Aldrich, Poole, UK

Carbachol (#C4382)

Dimethyl Sulfoxide (DMSO) (*as control stimulation*) (#W387509)

Methyl- β -Cyclodextrin (M β CD) (#C4555)

PD98059 (#P215)

Phorbol 12-myristate 13-acetate (PMA) (#P1585)

SKi (2-(*p*-hydroxyanilino)-4-(*p*-chlorophenyl)thiazole) (#S5696)

2.1.3 Antibodies

Abcam, Cambridge, UK

Phalloidin-iFluor 594 (#ab176757)

Abgent Inc, San Diego, USA

SK1 N terminal (rabbit polyclonal) (#AP7237a) Note: The anti-SK1 antibody was custom synthesised by Abgent using the antigens NH₂-CPRGGKGGKALQLFRSH-CONH₂ and NH₂-CPRGGKGGKALQLFRSH-CONH₂ (Huwiler et al., 2006).

BD Transduction Laboratories, Berkshire, UK

ERK2 (mouse monoclonal) (#610104)

Cell Signalling Technology, London, UK

PARP (rabbit polyclonal) (#9542)

Santa Cruz, Heidelberg, Germany

Clathrin (goat polyclonal) (#sc6579)

GAPDH (mouse monoclonal) (#sc47724)

Green fluorescent protein (eGFP) (mouse monoclonal) (#sc9996)

p-ERK (mouse monoclonal) (#sc7383)

Sigma-Aldrich, Poole, UK

Actin (rabbit polyclonal) (#A2066)

Early endosomal antigen 1 (EEA1) (mouse monoclonal) (#E7659)

GAPDH (rabbit polyclonal) (#G8795)

IgG (mouse)-FITC-conjugated (goat polyclonal) (#F0257)

IgG (mouse)-HRP-conjugated (goat polyclonal) (#A9169)

IgG (mouse)-TRITC-conjugated (goat polyclonal) IgG (#T5393)

IgG (rabbit)-FITC-conjugated (goat polyclonal) (#F0382)

IgG (rabbit)-HRP-conjugated (goat polyclonal) (#A0545)

IgG (rabbit)-TRITC-conjugated (goat polyclonal) IgG (#T6778)

2.1.4 Cell lines

All cell culture materials and reagents were purchased from *Thermo Fisher Scientific Ltd.*, (*Loughborough, UK*) unless otherwise stated. HEK293 cells were purchased (European Collection of Animal Cell Cultures, Salisbury, UK) and MCF7L cells were a kind gift from Rachel Schiff (Baylor College of Medicine, Houston). HEK293 cells stably over-expressing WTmGFP-SK1 were a kind gift from Nicholas Ktistakis (Babraham Institute, Cambridge).

Seralab, West Sussex, UK

Fetal bovine serum (FBS) (#FBS-500ML)

2.1.5 Primers

All primers were designed using Gene Runner (*Hastings software, USA*); optimum conditions are ~15 bases either side of the desired mutated site with a region of high GC content at either end (GC clamp), a GC content of ~60 % and a $T_m \geq 78$ °C. Primers were synthesised by Integrated DNA technologies (*Leuven, Belgium*) detailed in the table below. Primers were supplied at 25 nM, lyophilised and then stored at -20 °C. Prior to their use in PCR primers were diluted to 10 pM/ μ L.

Table 1 Forward and Reverse primers for the creation of mutant mGFP-SK1

Primer	Primer Sequence (5'-3')	T_m (°C)	GC (%)
GFP-mSK1-T1 Forward	ACTCCCGCGGGGGCCATAACCAGAAGAACCATAATC	69.2	56.8
GFP-mSK1-T1 Reverse	GATTATGGTTCTTCTGGTTATGGCCCCGCGGGGAGT	69.2	56.8
GFP-mSK1-T2 Forward	CATCCGGCCGGGACTAACGGCGGGGGCCACCT	75.9	75
GFP-mSK1-T2 Reverse	AGGTGGCCCCCGCGTTAGTCCCGGCCGGATG	75.9	75
GFP-mSK1-T3 Forward	TGGCAGCAGAGATGCCTAATCCGGCCGGGACTCCCG	73.2	66.7

GFP-mSK1- T3 Reverse	AGTCCCGGCCGGATTAGGCATCTCTGCTGCCA	71	62.5
GFP-mSK1- T4 Forward	CCTTTGGATGGTCTGTGGCTGAAGAGATGCCCCATCCGG	70	59
GFP-mSK1- T4 Reverse	CCGGATGGGGCATCTCTTCAGCCACAGACCATCCAAAGG	70	59
GFP-mSK1- T5 Forward	CAAGTGCACCCAACTACTAATGGATGGTCTGTGGCAG	65.9	50
GFP-mSK1- T5 Reverse	CTGCCACAGACCATCCATTAGTAGTTTGGGTGCACTTG	65.9	50
GFP-mSK1 R-loop forward	CACCTTGTTCTCTGGCGGCCAGTGCCTTCTC	71.1	64.7
GFP-mSK1 R-loop reverse	GAGAAGGCACTGGCGCCGCCAGGAACAAGGTG	71.1	64.7
GFP-mSK1- K49E Forward	GCAGAGATAACCTTTGAACTGATACTCACCGAAC	65.2	47.5
GFP-mSK1- K49E Reverse	GTTCGGTGAGTATCAGTTCAAAGTTATCTCTGC	65.2	47.5
GFP-mSK1- I51C Forward	GAGATAACCTTTAAACTGTGCCTCACCGAACGGAAGAACC	71.1	64.7
GFP-mSK1- I51C Reverse	GGTTCTTCCGTTCCGGTGAGGCACAGTTTAAAGTTATCTC	71.1	64.7

2.1.6 Molecular biology

Agilent, California, USA

pFuUltra II fusion Hotstart high fidelity DNA polymerase (includes 10x reaction buffer)
(#600670)

BD Biosciences, California, USA

LB-broth (#244620)

LB-agar (#281230)

Clontech, Göteborg, Sweden

eGFP-*mSK1* (gift from Nicholas Ktistakis) (contains kanamycin resistance gene, see appendix for plasmid map) (Delon et al., 2004) (discontinued)

New England Biolabs, Hitchin, UK

Deoxynucleotide (dNTP) solution mix (#N0447S)

Dpn1 (#R0176S)

NEB® 10-beta competent *E. coli* (high efficiency) (includes SOC-outgrowth media) (#C3019H)

Qiagen, Hilden, Germany

Plasmid maxi-prep kit (#12162)

Sigma-Aldrich, Poole, UK

Kanamycin (#K0254)

Thermo Fisher Scientific Ltd., Loughborough, UK

NanoDrop™ 2000/2000c Spectrophotometer (#ND-2000)

2.1.7 Radioactivity

Perkin Elmer, Beaconsfield, UK

ATP [γ - ^{32}P] (#BLU002A250UC)

Optiphase HiSafe 3 (#1200.437)

Thymidine [Methyl- ^3H] (#NET027L001MC)

2.2 Methods

2.2.1 Cell culture

All cell culture work was carried out in a class II biological safety cabinet under aseptic conditions. MCF-7L cells were maintained in a humidified incubator at 37°C, with CO₂ (5% (v/v)) in 75 cm² flasks using Dulbecco's Modified Eagle's Medium (DMEM) (10 mL) supplemented with foetal calf serum (FCS) (10% (v/v)), penicillin (100 U/mL) and streptomycin (100 µg/mL) (PenStrep) (complete DMEM media). Media was replaced every 3-4 days until the cells were ~70% confluent.

2.2.1.1 Maintenance of MCF-7L and HEK293 cell lines

Once ~70% confluence was achieved, cells were passaged by rinsing the cell monolayer with serum free DMEM media before incubation with trypsin (0.025%)/EDTA (0.01%) solution (1 mL) for 3 minutes to detach the cells. Detached cells were resuspended by adding complete DMEM media (9 mL) and passaged (typically at 1:10 dilution). Alternatively, cells were plated for experiments on to 6-well, 12-well, or 24-well plates (with the addition of sterile glass coverslips in the 12-well or 24-well plates when required for immunofluorescence experiments). For experiments, adherent cells were incubated with serum free DMEM media for 24 hours prior to the required treatments and processed for experimentation (see figure legends). The cells in this study were passaged no more than 20 times before returning to the base passage stored in liquid nitrogen (~passage 25).

2.2.3 Polymerase chain reaction using WT GFP-mSK1 as a template to create C-terminally truncated mSK1 and dimer mutant mSK1 (site directed mutagenesis)

All primers were designed using Gene Runner (*Hastings software, USA*) and synthesised by Integrated DNA technologies (*Leuven, Belgium*) (detailed in 2.1.5). PCR reaction mixtures contained 10x reaction buffer (5 μ l), dsDNA template (WTmGFP-SK1) (5 μ l (10 ng/ μ L)), both forward and reverse primer (1.5 μ l of 10 pM each), dNTP mix (1 μ l (contained 10 mM each NT), *pFuUltra II* fusion Hotstart high fidelity DNA polymerase (1 μ l (2.5 U/ μ L)) and ddH₂O (35 μ L) (50 μ L reaction total). The PCR reaction was heated to 95 °C for 2 minutes to activate the polymerase, followed by thermal cycling of 95 °C for 20 seconds, 60 °C for 20 seconds, 72 °C for 105 seconds, and cycled for 20 cycles. The parent DNA (WT GFP-mSK1) was then digested by incubating the PCR reaction with Dpn1 (methylation sensitive restriction enzyme) (1 μ l (20 U/ μ L)) for 2 hours at 37 °C.

2.2.4 Purification of plasmid constructs

2.2.4.1 Preparation of agar plates

LB-agar (15 g) was added to LB-broth (1 L) as per manufacturer's instructions and autoclaved before use. Once autoclaved, the LB-agar solution was heated until a fully liquid state and cooled until hand-hot. Antibiotic (kanamycin as required) (100 μ g/mL) was added under aseptic conditions and gently mixed before being poured into sterile petri dishes and left to solidify. Kanamycin was used for preparations of the eGFP-mSK1 plasmid construct.

2.2.4.2 *Escherichia coli* transformation

One vial of NEB® 10-beta competent *E. coli* (high efficiency) (50 μ L) was used for each transformation. The *E. coli* was initially thawed on ice for 10 minutes and then the PCR product (2 μ L) was added and left to incubate for 30 minutes (on ice). The bacteria were then heat shocked at 42 °C for 30 seconds and subsequently placed back on ice for 5 minutes. SOC-outgrowth media (vegetable peptone (2 %), yeast extract (0.5 %), NaCl (10 mM), KCl (2.5 mM), MgCl₂ (10 mM), MgSO₄ (10 mM),

glucose (20 mM)) (250 μ L) was then added and the culture placed in an orbital shaker (225 rpm) for 60 minutes at 37 °C. The culture was then plated at various dilutions (20 μ L – 200 μ L per petri dish) on to LB-agar selection plates containing the relevant antibiotic (100 μ g/mL) overnight at 37 °C.

2.2.4.3 Selection of *Escherichia coli* colonies and preparation of overnight cultures for maxi-prep

Individual colonies were selected from plates and grown in LB-broth culture (10 mL) containing antibiotic (kanamycin as required) (100 μ g/mL) for ~16 hours. Colonies were selected and grown in a starter culture containing LB broth (10 mL) and antibiotic (kanamycin) (100 μ g/mL) for ~8 hours in an orbital shaker (225 rpm) at 37 °C. The starter culture was then added to a larger volume of LB broth (100 mL) containing antibiotic (kanamycin as required) (100 μ g/mL) overnight (~16 hours) in an orbital shaker (225 rpm) at 37 °C.

2.2.4.4 Preparation and maintenance of glycerol stocks

Overnight culture (200 μ L) was added to autoclaved glycerol (800 μ L) in sterile microcentrifuge tubes and stored at -80 °C. Multiple glycerol stocks were maintained (fresh stocks each time a prep was completed), never being completely thawed.

2.2.4.5 Plasmid purification

The overnight culture (110 mL) was pelleted at 6000 x g, 4 °C for 15 minutes, with the pellet being resuspended in buffer P1 (10 mL) containing RNase A (100 μ g/ μ L). Buffer P2 (10 mL) was then added to the mixture and inverted 6 times before being incubated at room temperature (23 °C) for 5 minutes. Chilled buffer P3 (10 mL) was then added and the mixture inverted 6 times before being transferred into the barrel of the QIAfilter cartridge and incubated at room temperature (23 °C) for 10 minutes. The lysate was then filtered into a fresh 50 mL falcon tube and buffer ER (2.5 mL) added, inverted 10 times and incubated on ice for 30 minutes. Meanwhile buffer QBT (10 mL) was added to the QIAGEN-tip 500 and left to flow through by gravity. After incubation, the filtered

lysate was transferred to the QIAGEN-tip 500 and left to flow through by gravity. The QIAGEN-tip 500 containing the captured plasmid was washed with buffer QC (2 x 30 mL). The DNA was eluted into a fresh 50 mL falcon tube by adding buffer QN (15 mL) to the QIAGEN-tip 500. DNA was subsequently precipitated by adding isopropanol (10.5 mL) followed by centrifugation at 15000 x g, 4 °C for 30 minutes and the supernatant discarded. The plasmid pellet was washed using endotoxin-free ethanol (5 mL, (70 %)) followed by further centrifugation 15000 x g, 4 °C for 10 minutes. The plasmid DNA was then left to air-dry at room temperature (23 °C) for 5 minutes and redissolved in buffer TE (200 µL). The concentration (µg/µL) and quality of plasmid (260 nm/ 280 nm ratio, 1.8-1.9 is classed as 'pure') was determined using a NanoDrop™.

2.2.4.6 Confirmation of truncation and site directed mutagenesis

Plasmid constructs were sequenced by Eurofins (*Wolverhampton, UK*) using standard GATC forward and reverse primers (detailed below) in order to sequence the entire construct and confirm both the retention of the GFP-tag and incorporation of the desired site-directed mutagenesis.

Table 2 *mGFP-mSK1* constructs

Construct	Feature	Mutation
GFP	eGFP Vector (kanamycin resistant)	NA
WT <i>mGFP-SK1</i>	N-terminal GFP-tagged wild type (kanamycin resistant)	NA
GFP- <i>mSK1-T1</i>	N-terminal GFP-tagged mutant SK1 (kanamycin resistant)	5 amino acid C-terminal truncation
GFP- <i>mSK1-T2</i>	N-terminal GFP-tagged mutant SK1 (kanamycin resistant)	10 amino acid C-terminal truncation
GFP- <i>mSK1-T3</i>	N-terminal GFP-tagged mutant SK1 (kanamycin resistant)	15 amino acid C-terminal truncation
GFP- <i>mSK1-T4</i>	N-terminal GFP-tagged mutant SK1 (kanamycin resistant)	19 amino acid C-terminal truncation
GFP- <i>mSK1-T5</i>	N-terminal GFP-tagged mutant SK1 (kanamycin resistant)	25 amino acid C-terminal truncation

GFP- <i>mSK1-K49E</i>	N-terminal GFP-tagged mutant SK1 (kanamycin resistant)	Predicted forced monomer mutant
GFP- <i>mSK1-I51C</i>	N-terminal GFP-tagged mutant SK1 (kanamycin resistant)	Predicted forced dimer mutant

Table 3: Forward and Reverse primer used to sequence mGFP-SK1

Table 3 Forward and Reverse primer used to sequence mGFP-SK1

Primer	Primer Sequence (5'-3')
CMV-F (forward)	CGCAAATGGGCGGTAGGCGTG
pEGFP_C2-RP (reverse)	TTTAAAGCAAGTAAACCTC

2.2.5 Plasmid transfections

MCF-7L cells were plated on 12-well plates in complete DMEM media (1 mL) and left to adhere for at least 24 hours or until ~70% confluent. Following this, cells were transfected with of DNA (1 µg) (either mock transfection (no DNA), GFP, WTmGFP-SK1, GFP-*mSK1-T1*, GFP-*mSK1-T2*, GFP-*mSK1-T3*, GFP-*mSK1-T4*, GFP-*mSK1-T5*, GFP-*mSK1-K49E* or GFP-*mSK1-I51C*) which was diluted in DMEM media (without antibiotics) (50 µL) for each well to be transfected. LipofectAMINE® 2000 (3 µL) was diluted in separate DMEM media (without antibiotics) (50 µL) for every DNA construct (1 µg) to be transfected. The two separate components were incubated separately at room temperature (23 °C) for 5 minutes before being combined, gently mixed by pipetting and incubated at room temperature (23 °C) for a further 30 minutes. Meanwhile media in each well was replaced with DMEM media (900 µL) containing FCS (1% (v/v)) (without antibiotics). The DNA mixture was subsequently added drop wise to the wells and incubated for 24 hours prior to being used for further experimentation. For MCF-7L cells plated in 24-well plates the methodology remained the same, with the amount of DNA and all volumes being halved.

2.2.6 Cell Treatments

Agonists and inhibitors were reconstituted (typically at 1000 times the required final concentration) in either DMSO or dH₂O (as recommended by the manufacturer) and stored in aliquots at -20 °C. Where relevant, DMSO or dH₂O was used as a vehicle

control and the final concentration did not exceed 0.1% (v/v) in the media of cells being used in experimentation. Cells were plated in triplicate from 3 individual flasks (3 biological replicates) on 12-well plates or 24-well plates, as required, and grown to ~70% confluent (unless otherwise stated) before transfection (if required) for 24 hours. The media was replaced with serum free DMEM media (1 mL for 12-well and 24-well plates) for a further 24 hours and cells pre-treated or treated as described in figure legends. Cells were treated with vehicle (dH₂O/DMSO (1% (v/v))), carbachol (100 μM final), S1P (5 μM final) or PMA (1 μM final) for 10 minutes. Where indicated (see figure legends), cells were pre-incubated with MβCD (100 μM final) for 10 minutes, PD98059 (50 μM final) (inhibitor of MEK1 and MAP kinase cascade) for 1 hour, SKI (2-(*p*-hydroxyanilino)-4-(*p*-chlorophenyl)thiazole) (SK1/2 inhibitor) (10 μM final) for 24 hours, YM254890 (G_q/G₁₁ inhibitor) (10 μM final) for 30 minutes or FIPI (N-[2-[4-(2,3-Dihydro-2-oxo-1*H*-benzimidazol-1-yl)-1-piperidinyl]ethyl]-5-fluoro-1*H*-indole-2-carboxamide hydrochloride) (PLD-1/2 inhibitor) (100 nM final) for 1 hour. Cells were harvested for SDS-PAGE/western blotting or cover slips removed and processed for immunofluorescence microscopy.

2.2.7 Harvesting cell lysates

2.2.7.1 Harvesting whole cell lysate in Laemmli buffer

Media was aspirated from the wells of a 12 well plate prior to the addition of Laemmli sample buffer (200 μL per well) containing sodium dodecyl sulphate (SDS) (0.5% (w/v)), Tris base (125 mM, pH 6.7), ethylenediaminetetraacetic acid (1.25 mM), sodium pyrophosphate (0.5 mM), dithiothreitol (50 mM; added immediately before use), bromophenol blue (0.06% (w/v)) and glycerol (12.5% (v/v)). The lysed cells and buffer were etched/mixed within the well using a 1 mL pipette tip. The whole-cell lysate was then pushed through a 23-gauge hypodermic needle fitted to a 1 mL syringe, 8 times and placed into labelled microcentrifuge tubes. The samples were stored at -20 °C until used in SDS-PAGE/western blotting. Similar protein loading between samples was later determined by re-probing nitrocellulose membrane for cytosolic markers (actin/GAPDH) (see 2.2.9.3).

2.2.7.2 Harvesting whole cell lysate and cell fractions in isotonic sucrose buffer

Media was aspirated from the wells before washing each well with ice-cold phosphate buffered saline (PBS) (250 μ L) containing phosphate buffer (10 mM), KCl (2.7 mM) and NaCl (137 mM). This was removed and the cells from each well harvested in ice-cold isotonic sucrose buffer (200 μ L per well), containing Tris-HCl (10 mM; pH 7.4), ethylenediaminetetraacetic acid (1 mM), sucrose (0.25 M), Na_3VO_4 (0.5 mM), PMSF (0.2 mM), leupeptin (10 μ g/mL) and aprotinin (10 μ g/mL). Cells were disrupted, on ice, using a 1 mL pipette tip and 3 wells of a 12-well plate with the same treatment combined (600 μ L total). The cell lysate was pushed through a 25-gauge hypodermic needle fitted to a 1 mL syringe, 8 times and placed into labelled microcentrifuge tubes. Samples were processed further depending upon their use (see figure legends). For harvesting cytosolic (supernatant) and membrane fractions (pellet), samples were centrifuged at 4 °C for 60 minutes at 22,000 x g. After centrifugation, the supernatant (600 μ L) was transferred to a separate microcentrifuge tube and concentrated (4X) Laemmli sample buffer (200 μ L) was added. To the residual pellet, Laemmli sample buffer (1X) (800 μ L) was added. Both cellular fractions were resuspended using a 25-gauge hypodermic needle fitted to a 1 mL syringe 8 times and stored at -20°C until used in SDS-PAGE/western blotting. Similar protein loading between samples was later determined by re-probing the nitrocellulose membrane for cytosolic markers (actin/GAPDH).

2.2.8 SDS-PAGE

2.2.8.1 Preparation of polyacrylamide gels

The bottom (resolving) layer of the gel was made by combining acrylamide:bis-acrylamide (29:1) (10% (v/v)), Tris-Base (375 mM; pH 8.8), SDS (0.1% (w/v)), ammonium persulphate (APS) (0.05% (w/v)), and tetramethylethylenediamine (TEMED) (0.025% (w/v)). This was loaded between Mini-Protean® plates (1 mm spacer) and left to polymerise before the upper (stacking) layer of the gel was added. The upper (stacking) layer of the gel was made by combining acrylamide:bis-acrylamide (29:1) (4.5% (v/v)), Tris-Base (125 mM; pH 6.7), SDS (0.1% (w/v)), APS (0.05% (w/v)), and TEMED (0.1% (w/v)) before the insertion of a 10 or 15 well comb, as appropriate. Proteins were separated according to molecular weight (M_r) in the

resolving phase using this two-phase polyacrylamide gel. The stacking phase allows for the loading and condensation of proteins before entering the resolving phase.

2.2.8.2 Polyacrylamide gel electrophoresis

Following harvesting, equal sample volumes (15 μ L for 15-well or 20 μ L for 10-well gels) were loaded using a Hamilton syringe. On each gel, one well was allocated for loading of the pre-stained molecular weight markers (α_2 -Macroglobulin 180kDa, β -Galactosidase 116kDa, Lactoferrin 90kDa, Pyruvate kinase 58kDa, Fumarase 48.5kDa, Lactic dehydrogenase 36.5kDa, Triosephosphate isomerase 26.6kDa) (5 μ L). Proteins were separated using the Bio-Rad Mini-Protean® II electrophoresis kit at a voltage of 120 V and a current limit of 0.6 A for typically 1 hour, or until sample reached the end of the gel. Gels were submerged during electrophoresis in running buffer containing Tris-Base (25 mM), glycine (190 mM) and SDS (0.1% (w/v)) dissolved in dH₂O.

2.2.8.3 Protein transfer to nitrocellulose membrane

Subsequently the separated proteins were transferred from the gel to nitrocellulose membrane by their assembly between filter paper in a transfer cassette that was submerged in transfer buffer containing glycine (190 mM), Tris-Base (25 mM), dissolved in dH₂O along with methanol (20% (v/v)) for 60 minutes, at 100 V and a current limit of 0.6 A. The procedure was carried out in the Bio-Rad Mini- Trans-Blot kit.

2.2.9 Western blotting

2.2.9.1 Blocking of nitrocellulose membrane

Nitrocellulose membranes were blocked for 1 hour at ambient room temperature by incubation, with agitation, in blocking solution (bovine serum albumin (BSA) (3% (w/v)) in Tris buffered saline with Tween 20 (TBST) buffer containing Tween 20 (0.1% (v/v)), NaCl (100 mM) and Tris-Base (10 mM; pH 7.5)).

2.2.9.2 Protein detection with antibody

Nitrocellulose membranes were incubated overnight at 4 °C with constant rotation in an antibody solution. Primary antibodies were diluted in TBST (1:1000) containing BSA ((1% (w/v)) for commercial antibodies, or BSA (3% (w/v)) for the SK1 custom synthesised antibody). Following overnight incubation, membranes were washed 3 times for 7 minutes each in TBST, with constant agitation. The relevant horse radish peroxidase (HRP)-conjugated anti-mouse IgG or HRP-conjugated anti-rabbit IgG secondary antibody were diluted in TBST (1:20000) containing BSA (1% (w/v)) and incubated for 1 hour at ambient room temperature with constant agitation. Subsequently, membranes were washed for a further 3 times for 7 minutes each in TBST, with constant agitation.

Immunoreactive proteins were visualised through enhanced chemiluminescence (ECL) by incubating the membrane for 2 minutes in a mixture of equal parts of ECL solution 1 (containing luminol (2.5 mM), *p*-Coumaric acid (1.1 mM), Tris-Base (100 mM; pH 8.5)) and ECL solution 2 (containing H₂O₂ (30% (v/v)), 5.82 mM) in Tris-Base (100 mM; pH 8.5)). The two solutions were prepared separately and combined approximately 20 minutes in advance of incubation. Membranes were drained of residual ECL reagent and placed under a plastic film in an X-RAY developing cassette with X-RAY film and developed using a JP-33 automatic X-RAY film processor using developer, water and fixer (see 2.1.1). Immunoreactive proteins were presented as dark bands on the film. Relevant bands were identified by comparing their position on the film in comparison to the pre-stained molecular weight markers.

2.2.9.3 Stripping and re-probing of nitrocellulose membrane

The bound antibody complex was removed by incubating the membrane in stripping buffer containing Tris-HCl (62 mM; pH 6.7), β-mercaptoethanol (100 mM) and SDS (2% (w/v)) all dissolved in dH₂O, at 60°C for 40 minutes with constant agitation. Once complete, the membranes were washed 3 times for 7 minutes each in TBST with constant agitation, before being re-probed for a second protein of interest (e.g. a protein used to estimate of the level of total protein loaded in to each well as an

internal control (actin/GAPDH)). Membranes were similarly incubated and processed as described in 2.2.9.2.

2.2.10 Immunoprecipitation

2.2.10.1 Preparation of cell lysate

Media was aspirated from the wells and each well washed with of ice-cold phosphate buffered saline (PBS) (250 μ L). This was removed and, working on ice, the contents from 3 wells of a 12-well plate were harvested together in ice-cold lysis buffer (500 μ L) containing NaCl (137 mM), KCl (2.7 mM), MgCl₂ (1 mM), CaCl₂ (1 mM), NP-40 (1% (w/v)), glycerol (10% (v/v)), Tris-Base (20 mM; pH 8.0), BSA (1 mg/mL), Na₃VO₄ (0.5 mM), PMSF (0.2 mM), leupeptin (10 μ g/mL) and aprotinin (10 μ g/mL). The lysate was homogenised using a 25-gauge hypodermic needle fitted to a 1 mL syringe, 8 times and transferred to a microcentrifuge tube before rotating at 4 °C for 1 hour.

2.2.10.2 Protein Capture

The lysed cellular material was centrifuged at 22,000 x g, 4 °C for 10 minutes to remove cell debris. A small volume of the supernatant (50 μ L) retained as 'whole cell lysate' was added to concentrated (4x) Laemmli buffer (17 μ L) containing Tris-Base (238 mM; pH 6.5), glycerol (19.1% (v/v)), SDS (5.7% (w/v)) and bromophenol blue (0.024% (w/v)) (2-mercaptoethanol (10% (v/v)) added immediately prior to use). The remaining supernatant (~350 μ L) was transferred to a new microcentrifuge tube and pre-cleared using either protein A or G sepharose fast flow beads (20 μ L) (1 part immunoprecipitation lysis buffer:1 part protein A or G sepharose fast flow beads) by rotation at 4 °C for 20 minutes, Protein A sepharose was employed if using anti-rabbit IgG; protein G sepharose for anti-mouse IgG antibodies. The beads were pelleted by centrifugation at 22,000 x g, 4 °C for 1 minute, and the supernatant split into samples for immunoprecipitation and internal control (no primary antibody added) (~160 μ L each) which were transferred to new microcentrifuge tubes. The sample to be used for immunoprecipitation (~160 μ L) was incubated with primary antibody (2 μ L) and protein A or G sepharose fast flow beads (20 μ L) with rotation at 4 °C for 60 minutes. The internal control had protein A or G sepharose fast flow beads (20 μ L) added and was processed in parallel with no addition of primary

antibody. The immunoprecipitated protein complex and internal control samples were collected by centrifugation at 22,000 x g, 4 °C for 1 minute. The pellet was then washed by brief agitation with buffer A containing HEPES (10 mM; pH 7.0), NaCl (100 mM), PMSF (0.2 mM), NP-40 (0.5% (v/v)), and sedimented by centrifugation at 22,000 x g, 4 °C for 1 minute. The pellet was then washed by brief agitation with buffer A without NP-40 and sedimented again by centrifugation at 22,000 xg, 4 °C for 1 minute. The resulting supernatant was discarded and the beads from both protein capture and internal control were re-suspended in concentrated (4x) Laemmli buffer (20 µL). The beads were then heated to 100 °C for 3 minutes to disassociate the bound protein complexes.

2.2.10.3 SDS-PAGE/western blotting of immunoprecipitated proteins

The immunoprecipitates (and no antibody controls) were analysed by SDS-PAGE/western blotting (see 2.2.8 and 2.2.9) in parallel with a sample of whole cell lysate. Successful protein capture was identified through probing with a primary antibody corresponding to that used in the protein capture stage. Protein-protein interactions were sought by probing with an additional primary antibody by stripping/re-probing as previously described (2.2.9.3).

2.2.11 Immunofluorescence microscopy

2.2.11.1 Preparation of cells mounted on to microscope slides

Cells were plated in triplicate from 3 individual flasks (3 biological replicates) on 13 mm autoclaved glass cover slips in 12-well plates and incubated overnight to adhere before being transfected if required (see 2.2.5). The media was replaced with serum free DMEM media for 24 hours prior to treatment (see 2.2.6) (see figure legends). Following treatments, each well of cells was fixed with formaldehyde (3.7% (v/v)) in PBS) (1 mL), for 15 minutes at room temperature (23 °C). Cells were permeabilised by adding Triton X-100 (0.1% (v/v) in PBS) (1 mL) for 2 minutes.

For samples with cells overexpressing forms of GFP-*mSK1*, each cover slip was washed 3 times by immersion in PBS and directly mounted cell-side down onto a glass microscope slide with VECTASHIELD hard-set anti-fade mounting medium

containing DAPI (5 μ L). Following a brief 15-minute setting period, each cover slip was sealed using nail polish around the circumference of the cover slip. Prepared samples were stored (minimum overnight to completely set prior to imaging) at 4 °C until examined under the epifluorescence microscope.

For samples where endogenous protein was to be detected, non-specific binding was blocked by incubating the permeabilised cells on coverslips with blocking solution (FCS (5% (v/v)) and BSA (1% (w/v)) in PBS) (1 mL) for 30 minutes at room temperature (23 °C). Subsequently, samples were washed 3 times by immersion in PBS and transferred cell-side down to a humid, parafilm lined, light-proofed box where primary antibody (1:50) in blocking solution was spotted (20 μ L per cover slip) and incubated overnight at 4 °C. The cover slips were then briefly submersed in PBS and transferred to a fresh 12-well plate filled with PBS; the PBS was then aspirated off and gently refilled a further 2 times. The cover slips were placed face down in a humid, parafilm lined, light-proofed box with the relevant FITC- or TRITC-conjugated anti-mouse IgG or anti-rabbit IgG secondary antibody (20 μ L per coverslip) diluted (1:50) in blocking solution (FCS (5% (v/v)) and BSA (1% (w/v)) in PBS), and incubated at room temperature (23 °C) for 1 hour. Following incubation, the cover slips were washed again 3 times by immersion in PBS and mounted cell-side down onto a glass microscope slide with VECTASHIELD hard-set anti-fade mounting medium containing DAPI (5 μ L). After a brief 15-minute setting period, each cover slip was sealed using nail polish. Prepared samples were stored (minimum overnight to fully set prior to imaging) at 4 °C until examined under the epifluorescence microscope.

2.2.11.2 Image acquisition

The cover slips were imaged using an epifluorescent upright microscope (Nikon, Eclipse E600) with either 100X oil, 60X oil, 40X oil or 10X air lens (see figure legends). Images were captured using WinFluor imaging software (© University of Strathclyde, John Dempster, 2015). The exposure interval, gain and laser intensity were adjusted to enable image capture; these settings were kept constant throughout imaging a sample set. Dapi images were captures using an excitation wavelength of 405 nm, FITC using an excitation wavelength of 495 nm and TRITC using an excitation wavelength of 570 nm. The raw images were captured as tiff files which were analysed and made composite using ImageJ (Scion Corporation, Frederick, MD). All

analysis was performed in triplicate experiments with results representative of 15 cells on 3 separate cover slips per experiment.

2.2.11.3 Quantification of translocation of GFP-mSK1 variants

Cells were plated in triplicate from 3 individual flasks (3 biological replicates), transfected, quiesced and treated where required (see 2.2.1, 2.2.5, 2.2.6) (see figure legends). Images were acquired (see figure legends), analysed and made composite using ImageJ (see 2.2.11). For quantification of % of cells displaying lamellipodia or filopodia localisation of GFP-SK1, immunofluorescence images of 15 cells (randomly chosen) were acquired from triplicate experiments (45 cells in total). These were assessed (non-blinded) for evidence of GFP-SK1 translocation to the plasma membrane and whether this was predominantly 'spread' (lamellipodia) or localised to filopodia. Comparison was made with the relevant control cells (e.g. unstimulated vs stimulated or WT transfected vs mutant transfected) (see figure legends).

ImageJ (Scion Corporation, Frederick, MD) analysis of 5 raw images (n=5) acquired for GFP alone (no DAPI signal) was also used to additionally quantify plasma membrane translocated GFP-SK1 (5 cells from 3 individual cover slips). The segmented line tool was used to measure the pixel intensity (on a scale of 0-256 (black-white), corresponding to increasing amounts of GFP-SK1) for a distance of 500 pixels at the plasma membrane. Data from 5 cells were combined in series (distance of 2500 pixels). The average pixel intensity of 5 control cells (2500 pixels in total) was subtracted as background fluorescence for each experiment (mean centring). This was used to define baseline intensity (no/ little GFP-mSK1 translocation) within an experiment (treated cells membrane intensity – control cells membrane intensity = GFP-mSK1 translocation in response to treatment). All images were of similar brightness and contrast. The area under the curve (AUC) of a point-to-point plot of the 5 cells was calculated as a quantitative measure of GFP-*mSK1* translocation for a given treatment or SK1 mutant. Additionally, comparing the patterns and distributions of the intensity graphs was used to qualitatively assess phenotypes of GFP-mSK1 translocation.

2.2.11.4 Quantitative analysis of transfection efficiency

To determine the transfection efficiency of the various GFP-*mSK1* constructs used, cells were transfected on coverslips, processed and imaged using a 10X air lens accompanied with WinFluor imaging software (© University of Strathclyde, John Dempster, 2015). The raw images, captured as tiff files, were then made into composite images using ImageJ. For each construct, the percentage of GFP positive cells was calculated in 3 random 100 pixel x 100 pixel regions across 3 separate coverslips (9 regions in total). The percentage of GFP positive cells for each construct was then compared with that of every other construct by one-way ANOVA (Graphpad Prism 7, California, USA).

2.2.13 Wound healing assay

Cells were plated in triplicate from 3 individual flasks (3 biological replicates) on 13 mm autoclaved glass cover slips on 24-well plates and incubated overnight to adhere before being transfected as previously described (see 2.2.5). Ensuring the cell monolayer was close to confluency (~90% confluent), the media was then replaced with serum free DMEM media for 24 hours. For each cover slip, 1 vertical wound was then scored through the cell monolayer using a 1 mL pipette tip (wound area approximately 1-1.5 mm) and treatments were applied (see figure legends). Coverslips were either processed at 0 hours or after 22 hours incubation. Each cover slip was removed, and the cells fixed with formaldehyde (3.7% (v/v)) (1 mL) in PBS for 15 minutes at room temperature (23 °C). Each well of cells was then permeabilised using Triton X-100 (0.1% (v/v) in PBS) (1 mL) for 2 minutes, before being washed with PBS (1 mL) and directly mounted cell-side down onto a glass microscope slide with VECTASHIELD hard-set anti-fade mounting medium containing DAPI (5 µL). Following a brief 15-minute setting period, each cover slip was sealed using nail polish around the circumference of the cover slip. Samples were then stored (minimum overnight to fully set prior to imaging) at 4 °C.

Cover slips were imaged for both DAPI and GFP (FITC settings) using an epifluorescent upright microscope (Nikon, Eclipse E600) with 10X air lens accompanied with WinFluor imaging software. For image acquisition, the wound was positioned horizontal to the centre of the field of view as to image all cells that have migrated into the previously wounded area. One image was taken per wound on each

coverslip and experiments were performed in triplicate. The raw images, captured as tiff files, were analysed and made composite using ImageJ. Transfection efficiency was assessed as per 2.2.11.4.

2.2.14 Statistical analysis

Graphpad Prism software was used throughout (Graphpad Prism 7, California, USA). Data is presented as mean \pm SEM and was statistically analysed using two-way ANOVA and Tukey's multiple comparison test or by unpaired two-tailed t test (see figure legends).

Chapter 3
**The importance of G_q,
phosphatidic acid and
dimerisation for SK1
translocation**

3.0 The importance of G_q, phosphatidic acid and dimerisation for SK1 translocation

3.1 Introduction

The *SPHK1* and *SPHK2* genes encode two human sphingosine kinase isoforms, SK1 and SK2 (Kohama et al., 1998; Liu et al., 2000). SK1 is highly expressed in many cancers conferring poor clinical prognosis (French et al., 2003; Watson et al., 2010). In this regard, SK1 overexpression promotes cell proliferation (Olivera et al., 1999) and chemoresistance (Wang et al., 2018), whereas knockdown of SK1 is seen to reduce cell proliferation (Van Brocklyn et al., 2005). SK2 also has a role in oncogenesis. Studies have shown that ablation of SK2 reduces proliferation and cancer cell migration, having stronger anti-cancer effects than suppression of SK1 (Van Brocklyn et al., 2005; Gao et al., 2011).

SK1 and SK2 have been shown to have independent, functionally different sub-cellular localisation. SK2 is understood to move between the cytoplasm and the nucleus (Neubauer et al., 2019), whereby S1P produced by SK2 is known to bind to and inhibit the action of histone deacetylases to regulate gene expression (Hait et al., 2009). On the other hand, SK1 is localized primarily in the cytoplasm with a small proportion residing at the PM (Kohama et al., 1998; Delon et al., 2004), whereby receptor stimulation via extracellular ligands such as S1P or carbachol leads to the translocation of SK1 from the cytoplasm to the PM (ter Braak et al., 2009). Here it is able to bind to anionic phospholipids such as phosphatidic acid (PA) generated through activation of phospholipase D (Delon et al., 2004) and phosphatidylserine (PS) (Stahelin et al., 2005) that interact with Thr⁵⁴ and Asn⁸⁹ in SK1 (Stahelin et al., 2005; Hengst et al., 2009). Both SK1 and SK2 produce S1P, but it is S1P produced at the PM by SK1 that is understood to have a pivotal role in driving neoplastic conversion. This is evidenced by the overexpression of kinase dead SK1 failing to induce oncogenic transformation (Xia et al., 2000), hence SK1 is considered an oncogene and thus an attractive target for drug discovery.

In order to study the role of SK1 in oncogenesis it is important to understand the molecular mechanisms involved in its translocation to the PM that regulates activity of the enzyme. SK1 is able to translocate to the PM by at least two different mechanisms. The first is dependent on ERK-1/2, which catalyses the phosphorylation of Ser²²⁵ on the R-loop of SK1 to promote movement of the enzyme from the

cytoplasm to the PM in a manner that is dependent on PKC (Pitson et al., 2003). Ser²²⁵ can be dephosphorylated by PP2A, thereby deactivating the enzyme (Barr et al., 2008). Taken together, there is compelling evidence for the regulation of SK1 translocation and hence activation through phosphorylation/dephosphorylation. The second mechanism involves ligand-induced activation of receptors by carbachol or S1P that are coupled to G_q (ter Braak et al., 2009), which lead to conformational changes in the enzyme and allow for hydrophobic and electrostatic membrane engagement (Adams et al., 2016). Furthermore, there is now evidence to suggest that levels of [Ca²⁺]_i can regulate SK1 translocation independently of Ser²²⁵ phosphorylation. Binding of CIB1 is thought to promote the translocation of SK1 via the Ras-ERK pathway (Jarman et al., 2010; Zhu et al., 2017), whilst binding of CIB2 negatively regulates translocation (Zhu et al., 2017). Taken together, the mechanisms discussed are thought to be mutually exclusive (ter Braak et al., 2009; Hengst et al., 2010), hence translocation can be either phosphorylation-dependent involving ERK-1/2 or phosphorylation-independent involving G_q.

Adams et al., 2016 proposed based on crystallographic analysis that SK1 translocation likely involves conformational changes in the enzyme. These conformational changes expose a positively charged cluster of amino acids on the surface of the enzyme that electrostatically interact with anionic membrane-bound phospholipids such as PA and PS. Most importantly, the lipid binding loop-1 (LBL-1) domains facilitate membrane anchoring adjacent to a cluster of positively charged residues. Such a conformation allows for a contiguous hydrophobic and electrostatic membrane-engagement interface that enables simultaneous embedding of the enzyme and access to the substrate SPH by a gating mechanism involving opening of the LBL-1 patch (Adams et al., 2016; Pulkoski-Gross et al., 2018).

A key question in regard to SK1 function is whether it is organised as a monomer or dimer. Original literature indicated SK1 to be monomeric (Olivera et al., 1998), however recent crystal structures of SK1 have been produced (Wang et al., 2013; Wang et al., 2014), indicating structural similarities between SK1 and other DAGK_cat that share similar N-terminal domain (NTD) and C-terminal domain (CTD) folds that form β-sandwiches (Bakali et al., 2007; Adams et al., 2016). Interestingly, these related diacylglycerol kinases have a common NTD-NTD dimeric assembly, displaying C₂-symmetry (Wang et al., 2013; Adams et al., 2016). This suggests that SK1, which has a similar tertiary structure, may equally adopt a similar dimeric

quaternary structure. Furthermore, there are multiple reports involving immunoprecipitation that indicate SK1 exhibits a minimal dimeric assembly (Lim et al., 2011; Liu et al., 2013). Moreover, crystallographic analysis has revealed that in a dimeric assembly, SK1 has a dense concave region of positively charged residues at the dimer interface, that is likely to facilitate membrane-curvature sensing and interaction with anionic PM phospholipids (Adams et al., 2016). In this regard, dimeric SK1 will have a much higher density of exposed positively charged residues than the monomer and hence a greatly increased binding affinity for anionic phospholipids compared to the monomer. Interestingly, the interfacial surface contact is modest (ca. 780 Å² buried solvent accessible surface area per protomer), which is consistent with an ability to dynamically shift between monomeric and dimeric assemblies. We therefore investigated the translocation and cellular functions of monomeric and dimeric SK1, whereby the presence of a monomer/dimer SK1 equilibrium may provide an explanation for the pleiotropic properties of S1P by virtue of localisation of each to different PM micro-domains.

In summary, sub-cellular localisation of SK1 ultimately controls the catalytic conversion of SPH to S1P and thus neoplastic conversion and formation of cancer cells. The current study aims to reveal key structural determinants of SK1 that are critical for regulating translocation of the enzyme to the PM and hence to define the key mechanisms by which SK1 can promote oncogenesis.

3.2 Results

3.2.1 SK1 translocation detected by epifluorescence microscopy

In order to study the structural determinants governing the translocation of SK1 within the cell, it was necessary to over-express the wild type (WT) recombinant SK1 in an appropriate cancer cell model system. For this purpose, transiently overexpressed WTmGFP-SK1 in MCF-7L cells was used. Comparison was made with endogenous SK1 expressed in MCF-7L cells in order to establish whether recombinant and endogenous SK1 are regulated in an identical manner.

Epifluorescence microscopy was used to monitor translocation of SK1 from the cytoplasm to the PM. MCF-7L cells were stained with anti-SK1 and FITC-conjugated secondary antibodies to detect endogenous SK1. WTmGFP-SK1 was separately detected in MCF-7L cells using GFP fluorescence. Both FITC and GFP have similar excitation wavelengths and emit wavelengths of light around 510 nm, visibly

detectable as a green fluorescence. Representative images were obtained based on 3 individual experiments. Translocation of SK1 to specific PM micro-domains was determined by staining WTmGFP-SK1 expressing cells with cortactin, fascin or paxillin. Translocation was quantified based on 15 cells counted from random fields of view on 3 separate cover slips and presented as the percentage of cells displaying translocation specific to a particular phenotype (lamellipodia *versus* filopodia *versus* foci), for a given treatment. Additional analysis of translocation focused on the pixel intensity at the PM that represented either translocated endogenous SK1 or WTmGFP-SK1. The intensity around the PM was plotted from 5 individual cells and the area under the curve (AUC) calculated for the individual cells, which represented total translocated SK1.

Expression of both endogenous (Fig. 3.1) and WTmGFP-SK1 (Fig. 3.4) was confirmed by western blot analysis. The detection of endogenous SK1 with the anti-SK1 antibody in immunofluorescence studies was established using the same antibody to detect endogenous SK1 (Mr=42 kDa) in cell lysates by western blot analysis. Cells were incubated with SKi (10 μ M, 24 hours), which has been shown to induce the ubiquitin-proteasomal degradation of SK1 (Loveridge et al., 2010). The treatment with SKi induced a reduction in the amount of the anti-SK1 immuno-reactive 42-51 kDa protein bands, corresponding to SK1a-c, in lysates from MCF-7L cells (Fig. 3.1). MCF-7L cells were also transiently transfected with WTmGFP-SK1 or GFP vector alone and probed with anti-GFP antibody. The expression of the recombinant protein was confirmed by detecting a band with an Mr=69 kDa corresponding to WTmGFP-SK1 in lysates from transfected cells (Fig. 3.4). A protein band with an Mr=27 kDa corresponding to GFP in lysates from eGFP-transfected cells was also detected, thereby confirming specificity of the anti-GFP antibody (Fig. 3.4).

Carbachol, S1P and PMA were used to investigate SK1 translocation. S1P binds to S1P₃ in MCF-7 cells that is coupled to G_q (Windh et al., 1999). Carbachol can bind to muscarinic receptor sub-types which are either coupled to G_i or G_q (Offermanns et al., 1994). PMA on the other hand directly activates protein kinase C (PKC), which can regulate ERK-1/2 via phosphorylation of c-Raf (Marquardt et al., 1994). All 3 agonists have been shown to promote SK1 translocation (Pitson et al., 2003; ter Braak et al., 2009; Long et al., 2010).

Representative images revealed MCF-7L cells expressing endogenous (Fig. 3.1) or transiently overexpressing WTmGFP-SK1 (Fig. 3.4) displayed a similar translocation response following treatment with S1P, PMA or carbachol. This was quantified by measuring membrane intensity, and cells expressing either endogenous SK1 (Fig. 3.2) or transiently overexpressing WTmGFP-SK1 (Fig. 3.11) displayed significant increases in AUC following stimulation. Therefore, the recombinant system was used as an experimental approach to investigate the mechanism of SK1 translocation.

In WTmGFP-SK1 transiently overexpressing MCF-7L cells there was very little SK1 associated with the PM in vehicle treated cells, with the majority of SK1 resident in the cytoplasm and perinuclear region (Fig. 3.4). Treatment of cells with S1P, PMA or carbachol stimulated translocation of WTmGFP-SK1 to the PM (Fig. 3.4). These responses were observed as a redistribution of SK1 from the cytoplasm/perinuclear regions to the PM at the periphery of the cell (Fig. 3.4). Observations revealed that cells produced different phenotypes of translocation in response to the different agonists. This was further investigated by measuring co-localisation of WTmGFP-SK1 with markers for lamellipodia, filopodia or foci formation. For this WTmGFP-SK1 expressing cells were stimulated and stained for cortactin, fascin or paxillin to detect the translocation of SK1 to lamellipodia, filopodia or foci, respectively. Results indicated that PMA or carbachol promoted the translocation of WTmGFP-SK1 to lamellipodia that were also strongly positive for cortactin. On the other hand, S1P promoted the translocation of WTmGFP-SK1 to filopodia that were positive for fascin. These data provide evidence that WTmGFP-SK1 is able to translocate to different PM micro-domains in an agonist-dependent manner. These mechanisms were therefore further investigated.

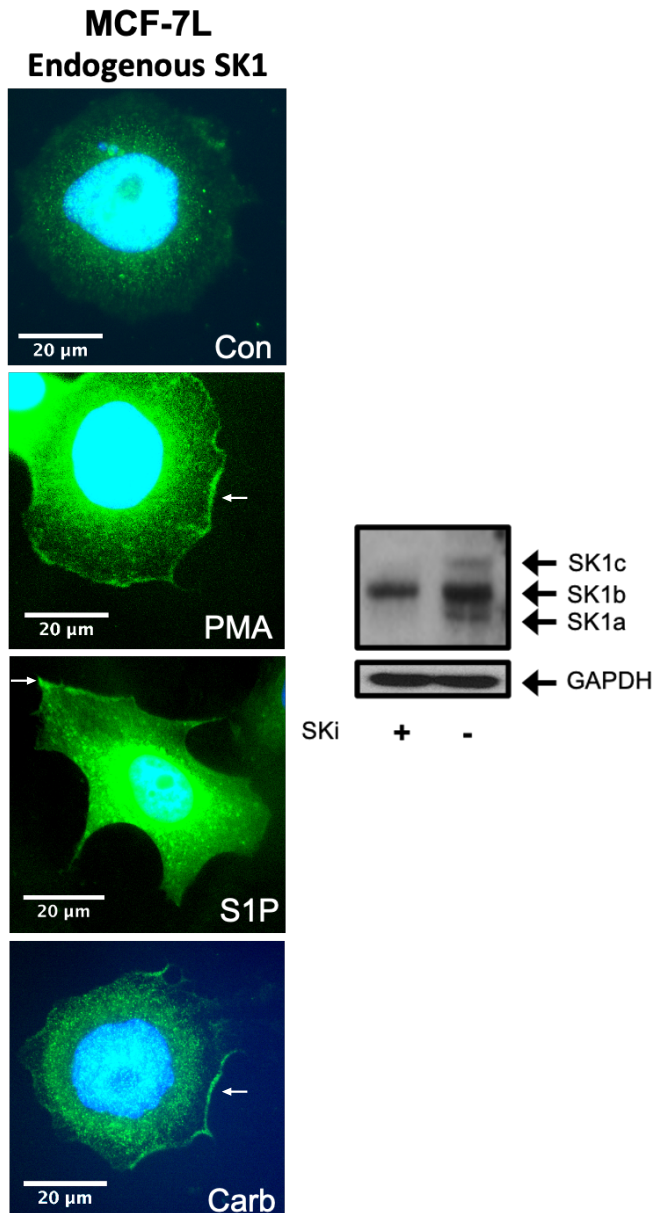


Figure 3.1 Stimulated MCF-7L cells expressing endogenous SK1

40x oil magnification photomicrographs of MCF-7L cells showing translocation of endogenous SK1 from the cytoplasm to the plasma membrane in response to S1P (5 μ M, 10 minutes), PMA (1 μ M, 10 minutes) or carbachol (100 μ M, 10 minutes) and compared with vehicle treated cells (Con, DMSO, 0.1% (v/v)). Cells were processed (see methods) and mounted with DAPI-containing mount to stain DNA (blue). SK1 was detected with an anti-SK1 antibody and FITC-conjugated secondary antibody (arrows show translocated SK1). Representative results are of 3 independent experiments. Inset is a western blot of lysate of cells treated with or without SKi (10 μ M, 24 hours) and probed with anti-SK1 antibody to confirm the identity of SK1.

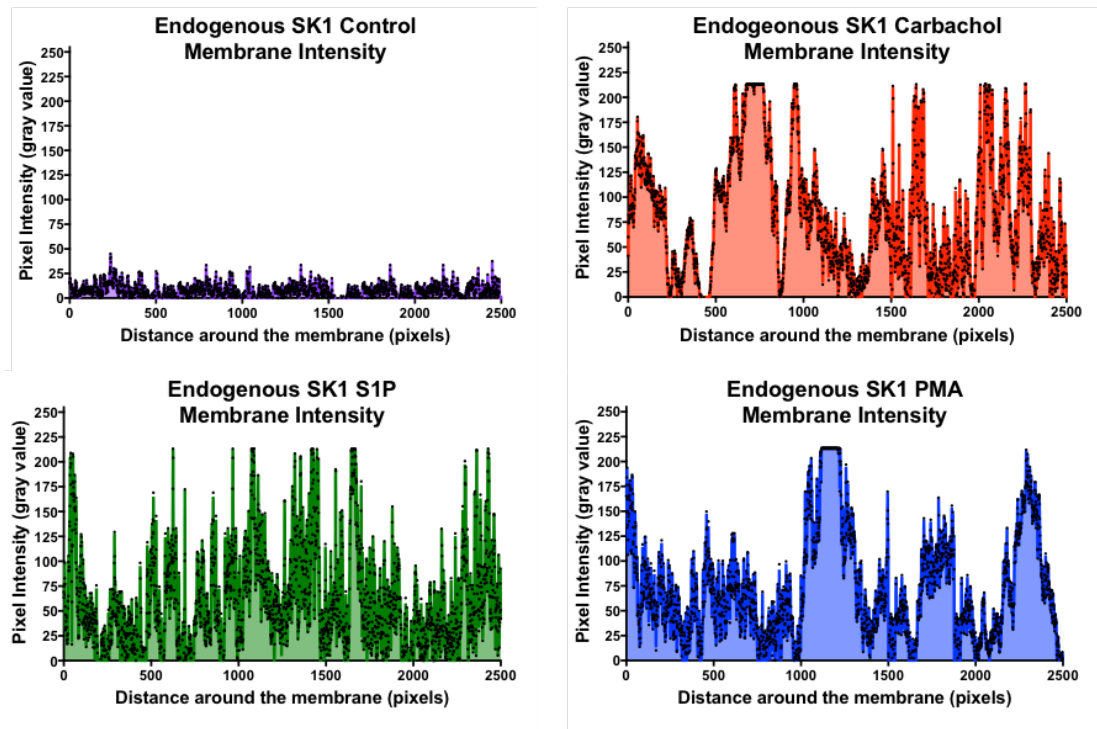


Figure 3.2 Membrane intensity recordings of endogenous SK1 in MCF-7L cells in response to various stimuli

Membrane intensity measurements of endogenous SK1 were made from 5 individual MCF-7L cells using an anti-SK1 antibody and FITC-conjugated secondary antibody. Measurements from 5 individual MCF-7L cells were stitched together (see methods) ($n=5$). Cells were treated with S1P ($5 \mu\text{M}$, 10 mins), PMA ($1 \mu\text{M}$, 10 mins) or carbachol ($100 \mu\text{M}$, 10 mins) and compared with control cells (DMSO 1% (v/v)).

Endogenous SK1

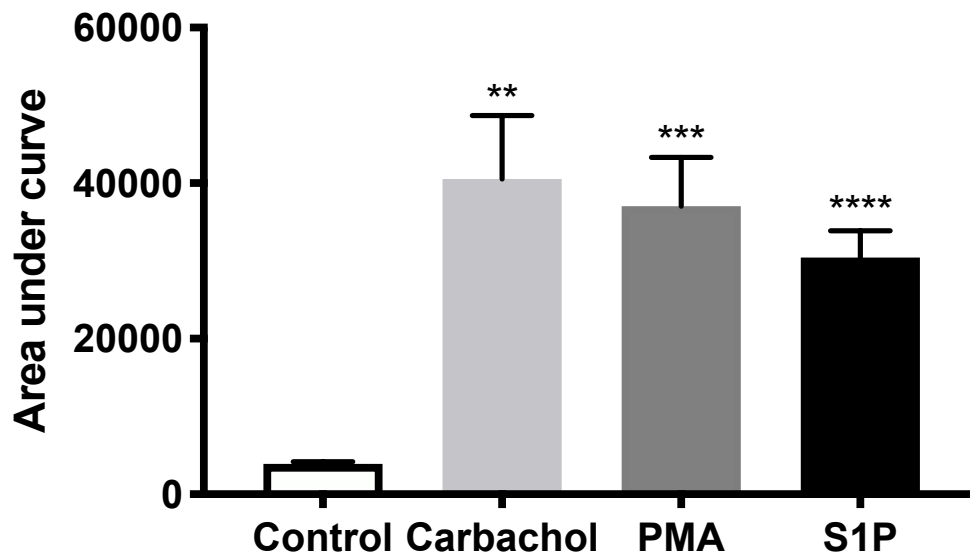


Figure 3.3 Area under curve analysis of endogenous SK1 translocation in MCF-7L cells in response to various stimuli

The bar graph represents the AUC of the total level of endogenous SK1 translocation in response to S1P (5 μ M, 10 mins), PMA (1 μ M, 10 mins) or carbachol (100 μ M, 10 mins) and compared with control cells (DMSO 1% (v/v)) (n=5); **p<0.01, ***p<0.001, ****p<0.0001 for stimulus *versus* control (unpaired, two-tailed t-test).

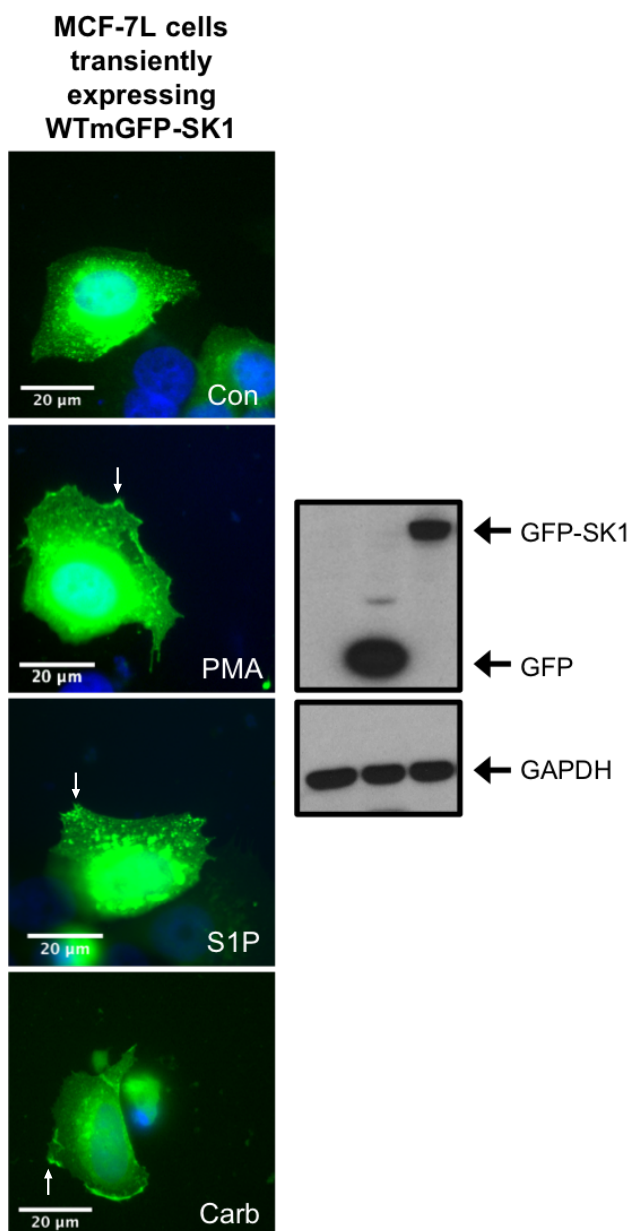


Figure 3.4 Stimulated MCF-7L cells transiently overexpressing WTmGFP-SK1

40x oil magnification photomicrographs of cells showing the translocation of transiently overexpressed WTmGFP-SK1 in response to S1P (5 μ M, 10 minutes), PMA (1 μ M, 10 minutes) or carbachol (100 μ M, 10 minutes) and compared with vehicle treated cells (Con, DMSO, 0.1% (v/v)). Cells were processed (see methods) and mounted with DAPI-containing mount to stain DNA (blue). WTmGFP-SK1 was detected by GFP (arrows show translocated mGFP-SK1). Representative results are of 3 independent experiments. Inset is a western blot confirming the successful expression of WTmGFP-SK1 using an anti-GFP antibody (lane 1: mock transfected cells; lane 2: transiently transfected GFP cells (27 kDa); lane 3: transiently transfected WTmGFP-SK1 cells (Mr = 69 kDa)).

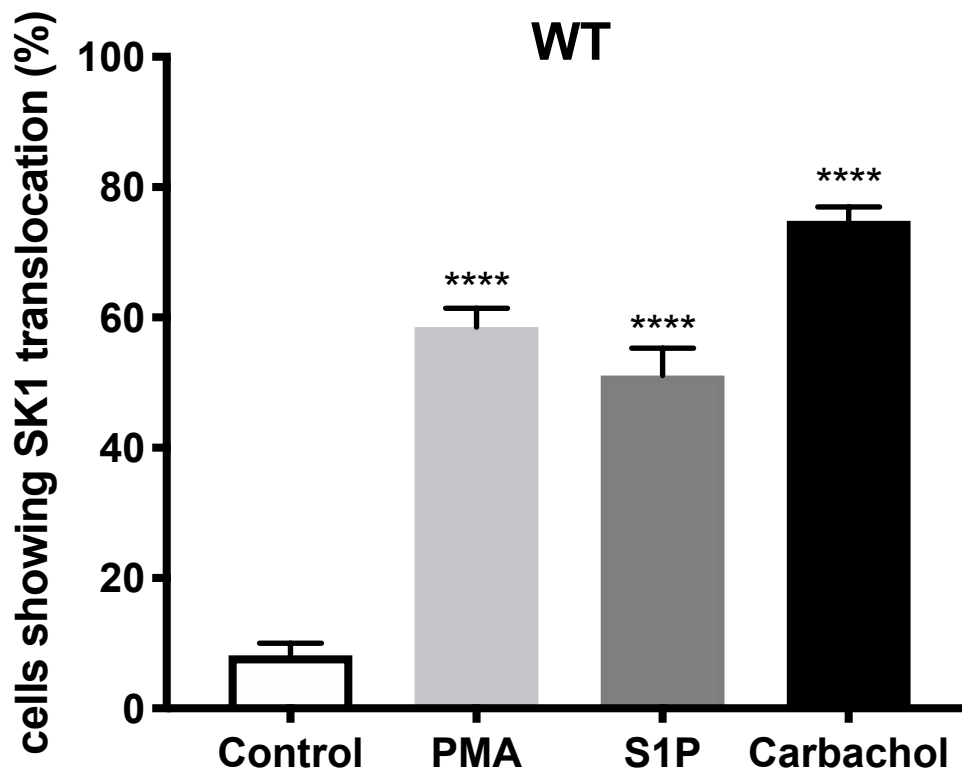


Figure 3.5 % of MCF-7L cells transiently overexpressing WTmGFP-SK1 showing translocation in response to various stimuli

The bar graph represents the % of MCF-7L cells transiently overexpressing WTmGFP-SK1 showing translocated WTmGFP-SK1 in response to S1P (5 μ M, 10 minutes), PMA (1 μ M, 10 minutes) or carbachol (100 μ M, 10 minutes) and compared to control cells (DMSO, 0.1% (v/v)). 15 random cells on 9 separate cover slips were analysed (n=9); ****p<0.0001 for stimulus *versus* control (unpaired, two-tailed t-test).

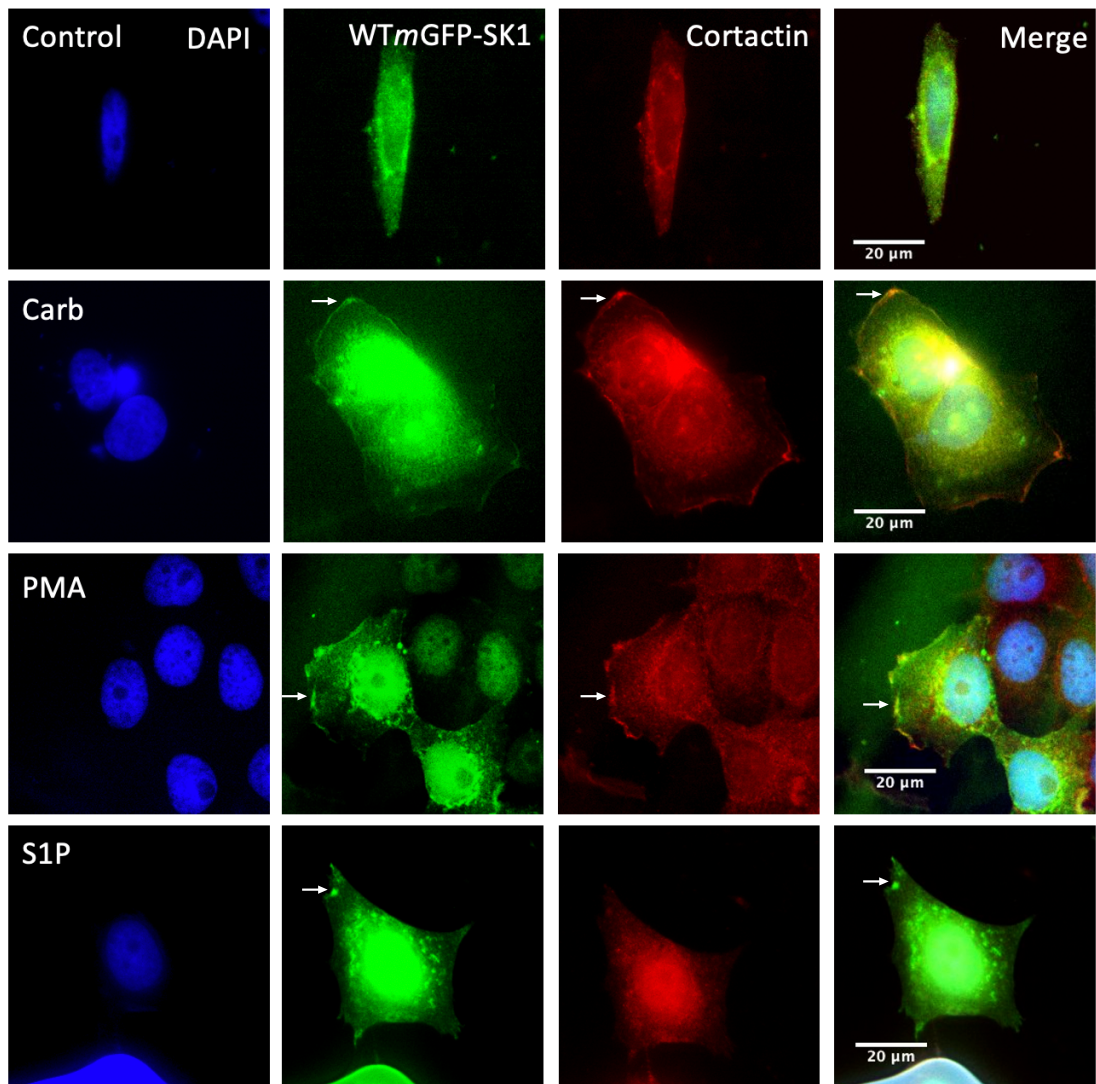


Figure 3.6 Stimulated MCF-7L cells transiently overexpressing WTmGFP-SK1 stained for cortactin

40x oil magnification photomicrographs of cells showing the translocation of transiently overexpressed WTmGFP-SK1 in response to S1P (5 μ M, 10 minutes), PMA (1 μ M, 10 minutes) or carbachol (100 μ M, 10 minutes) and compared with vehicle treated cells (Con, DMSO, 0.1% (v/v)). Cells were processed (see methods) and mounted with DAPI-containing mount to stain DNA (blue). WTmGFP-SK1 was detected by GFP (arrows show translocated mGFP-SK1). Lamellipodia were detected with an anti-cortactin antibody and a TRITC-conjugated secondary antibody. Representative results are of 3 independent experiments.

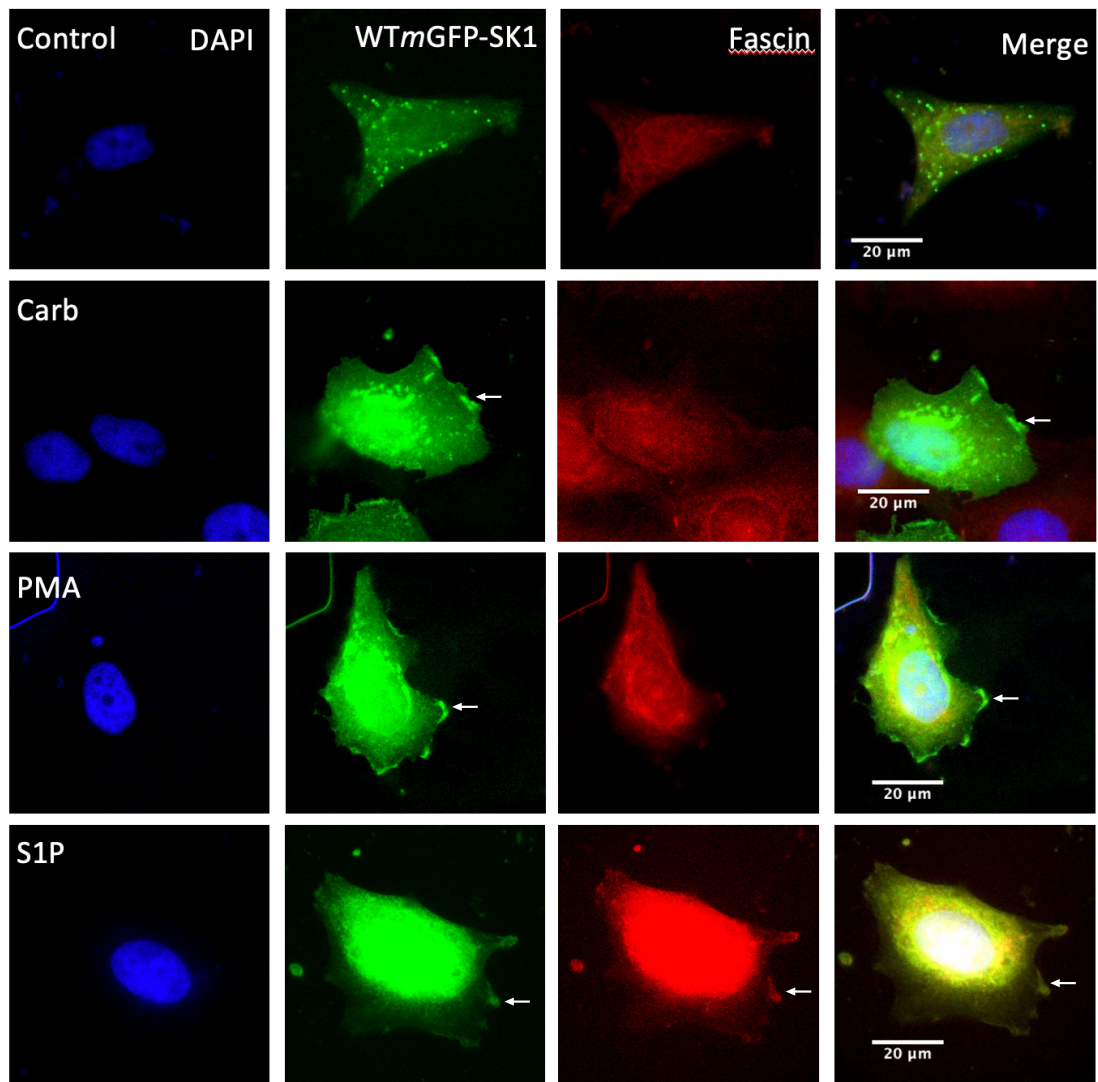


Figure 3.7 Stimulated MCF-7L cells transiently overexpressing WTmGFP-SK1 stained for Fascin

40x oil magnification photomicrographs of cells showing the translocation of transiently overexpressed WTmGFP-SK1 in response to S1P (5 μ M, 10 minutes), PMA (1 μ M, 10 minutes) or carbachol (100 μ M, 10 minutes) and compared with vehicle treated cells (Con, DMSO, 0.1% (v/v)). Cells were processed (see methods) and mounted with DAPI-containing mount to stain DNA (blue). WTmGFP-SK1 was detected by GFP (arrows show translocated mGFP-SK1). Filopodia were detected with an anti-fascin antibody and a TRITC-conjugated secondary antibody. Representative results are of 3 independent experiments.

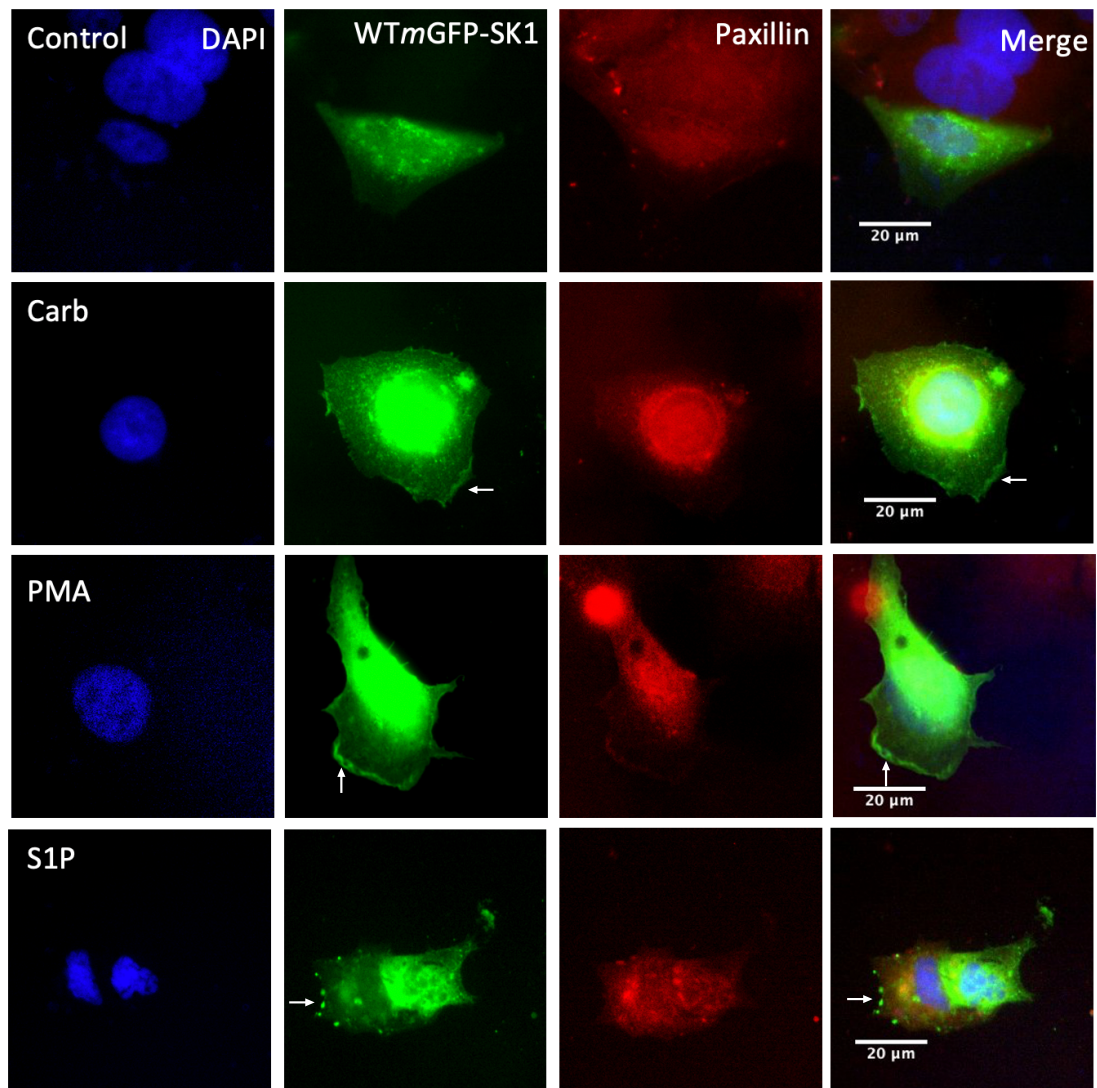


Figure 3.8 Stimulated MCF-7L cells transiently overexpressing WTmGFP-SK1 stained for Fascin

40x oil magnification photomicrographs of cells showing the translocation of transiently overexpressed WTmGFP-SK1 in response to S1P (5 μ M, 10 minutes), PMA (1 μ M, 10 minutes) or carbachol (100 μ M, 10 minutes) and compared with vehicle treated cells (Con, DMSO, 0.1% (v/v)). Cells were processed (see methods) and mounted with DAPI-containing mount to stain DNA (blue). WTmGFP-SK1 was detected by GFP (arrows show translocated mGFP-SK1). Foci were detected with an anti-paxillin antibody and a TRITC-conjugated secondary antibody. Representative results are of 3 independent experiments.

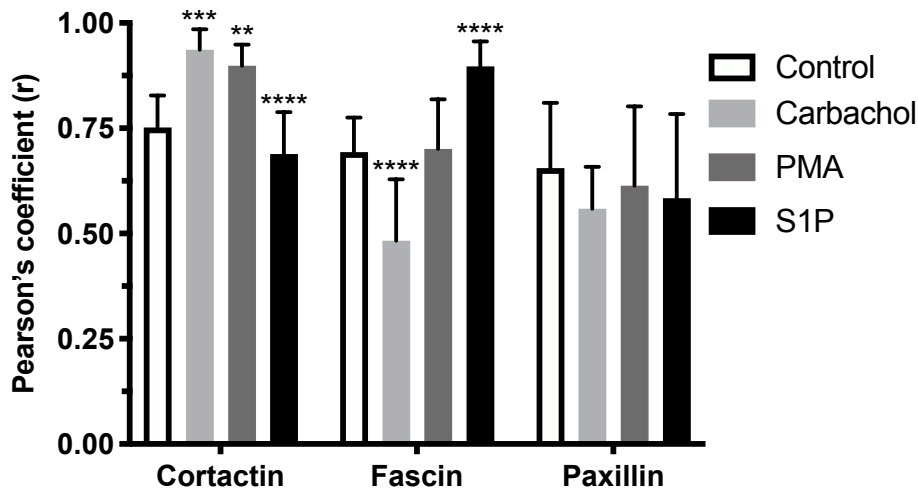


Figure 3.9 Quantification of co-localisation of MCF-7L cells transiently overexpressing WTmGFP-SK1 with cortactin, fascin or paxillin

The bar graph represents the Pearson's coefficient of cortactin, fascin or paxillin with WTmGFP-SK1 from transiently overexpressing MCF-7L cells in response to S1P (5 μ M, 10 minutes), PMA (1 μ M, 10 minutes) or carbachol (100 μ M, 10 minutes) and compared to control cells (DMSO, 0.1% (v/v)). 15 random cells on 3 separate cover slips were analysed (n=3); **p<0.01, ***p<0.001 and ****p<0.0001 for stimulus *versus* control for a given phenotype (two-way ANOVA with Tukey's multiple comparison test).

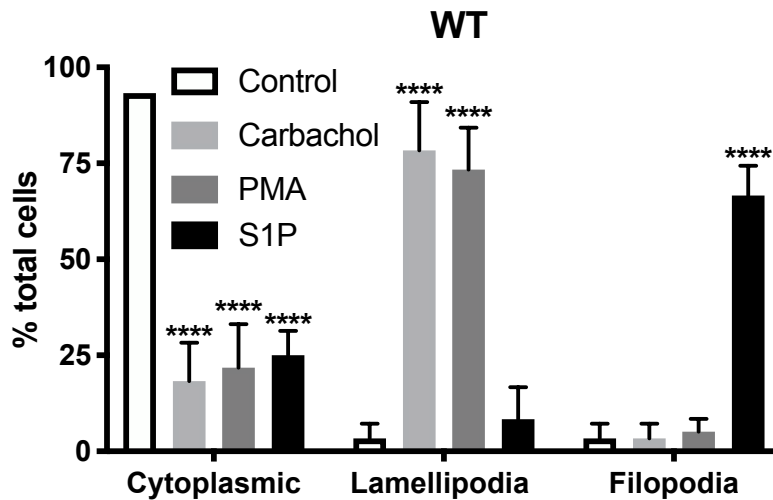


Figure 3.10 Phenotypic quantification of stimulated MCF-7L cells transiently overexpressing WTmGFP-SK1

The bar graph represents the % of MCF-7L cells transiently overexpressing WTmGFP-SK1 showing WTmGFP-SK1 in spread (lamellipodia) or filopodia micro-domains in response to S1P (5 μ M, 10 minutes), PMA (1 μ M, 10 minutes) or carbachol (100 μ M, 10 minutes) and compared to control cells (DMSO, 0.1% (v/v)). 15 random cells on 4 separate cover slips were analysed (n=4); ****p<0.0001 for stimulus *versus* control for a given phenotype (two-way ANOVA with Tukey's multiple comparison test).

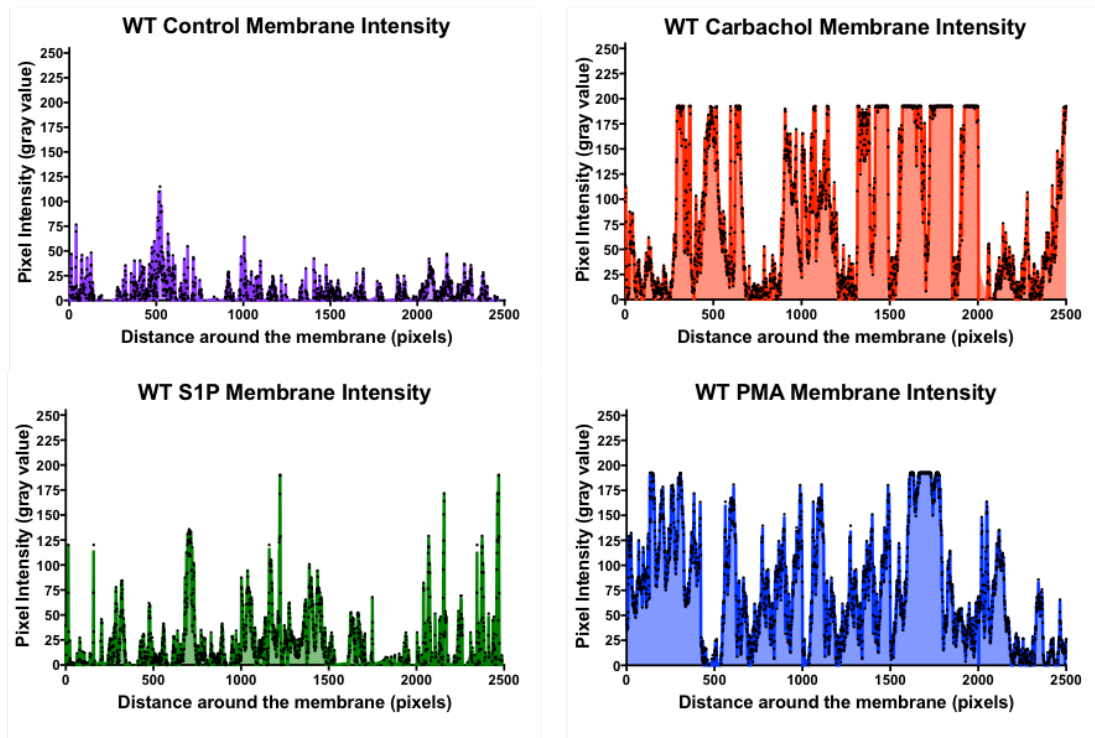


Figure 3.11 Membrane intensity recordings of MCF-7L cells transiently overexpressing WTmGFP-SK1 in response to various stimuli

Membrane intensity measurements of WTmGFP-SK1 were made from 5 individual MCF-7L cells transiently overexpressing WTmGFP-SK1 and stitched together (see methods) (n=5). Cells were treated with S1P (5 μ M, 10 mins), PMA (1 μ M, 10 mins) or carbachol (100 μ M, 10 mins) and compared with the control (DMSO 1% (v/v)).

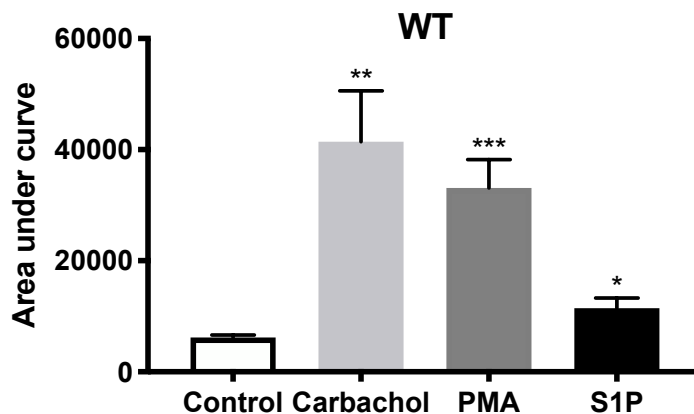


Figure 3.12 Area under curve analysis of MCF-7L cells transiently overexpressing WTmGFP-SK1 in response to various stimuli

The bar graph represents the AUC of the total level of WTmGFP-SK1 translocation in response to S1P (5 μ M, 10 mins), PMA (1 μ M, 10 mins) or carbachol (100 μ M, 10 mins) and compared with control cells (DMSO 1% (v/v)) (n=5); *p<0.05, **p<0.01, ***p<0.001 for stimulus *versus* control (unpaired, two-tailed t-test).

3.2.2 ERK-independent translocation of SK1 in response to S1P and carbachol

The signaling mechanism involved in regulating the translocation of SK1 was subsequently investigated. SK1 is able to translocate to the PM by at least two possible mechanisms as described in 3.1.

To discriminate between ERK-phosphorylation-dependent and -independent translocation of SK1, the MEK-1 inhibitor, PD98059 was used. First, we tested whether PD98059 blocked the activation of ERK-1/2 in response to PMA, S1P or carbachol. Pre-treatment of these cells with PD98059 reduced the activation of ERK-1/2 by PMA, S1P or carbachol (Fig. 3.13). In addition, endogenous SK1 and transiently overexpressed *WTmGFP-SK1* both retained the ability to translocate to the PM in response to S1P or carbachol following pre-treatment with PD98059 (Fig. 3.14). In contrast, there was negligible translocation of endogenous SK1 (Fig. 3.14) and *WTmGFP-SK1* (Fig. 3.16) in response to PMA, which was additionally quantified as a reduction in the membrane pixel intensity. These findings demonstrate that S1P and carbachol induce the translocation of SK1 from the cytoplasm to the PM via ERK-independent mechanisms.

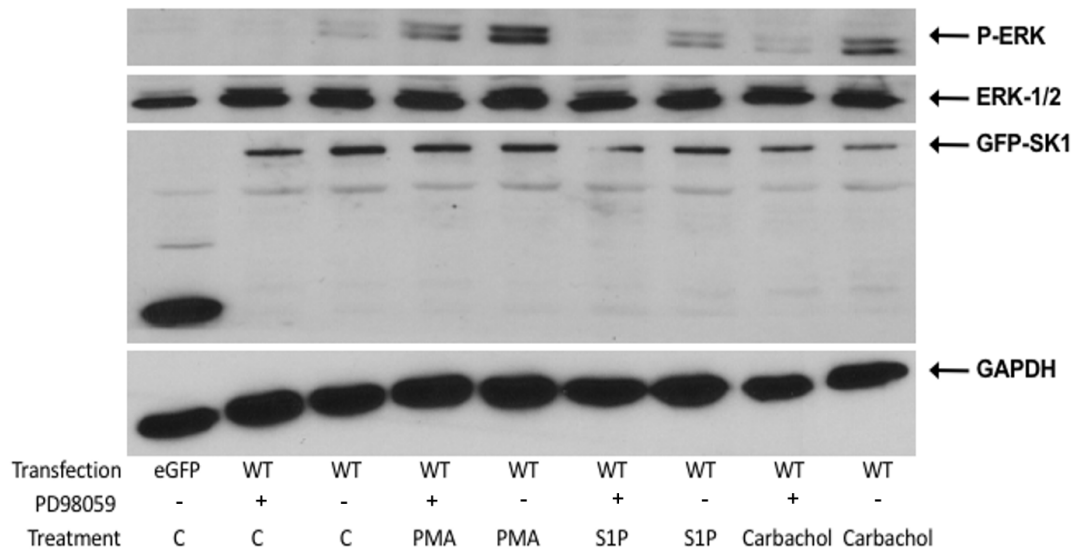
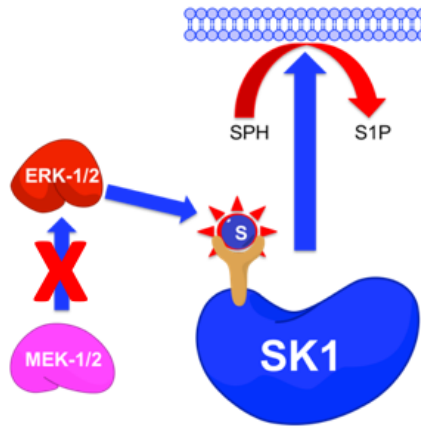


Figure 3.13 Stimulated MCF-7L cells transiently overexpressing WTmGFP-SK1 pre-treated with PD98059

Western blot showing the transient overexpression of eGFP or WTmGFP-SK1 and the inhibition of ERK-1/2 phosphorylation by PD98059 (50 μ M, 1 hour) (MEK-1/2 inhibitor) in response to S1P (5 μ M, 10 mins), PMA (1 μ M, 10 mins) or carbachol (100 μ M, 10 mins) and compared to the cells that were not pre-treated. Representative results are of 3 independent experiments.

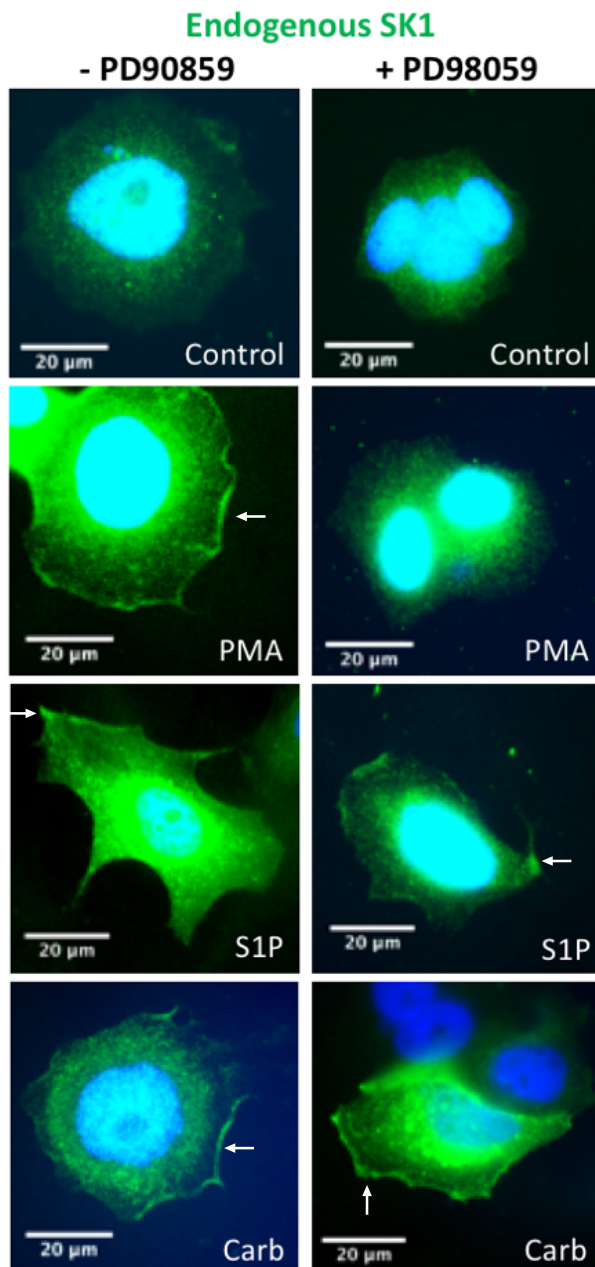


Figure 3.14 Stimulated MCF-7L cells pre-treated with PD98059

40x oil magnification photomicrographs of MCF-7L cells expressing endogenous SK1 pre-treated with PD98059 (50 μ M, 1 hour) and stimulated with S1P (5 μ M, 10 minutes), PMA (1 μ M, 10 minutes) carbachol (100 μ M, 10 minutes) or vehicle (Con, DMSO, 0.1% (v/v)) and compared to cells not re-treated. Cells were processed (see methods) and mounted with DAPI-containing mount to stain DNA (blue). SK1 was detected with an anti-SK1 antibody and a FITC-conjugated secondary antibody (arrows show translocated mGFP-SK1). Representative results is of 3 independent experiments.

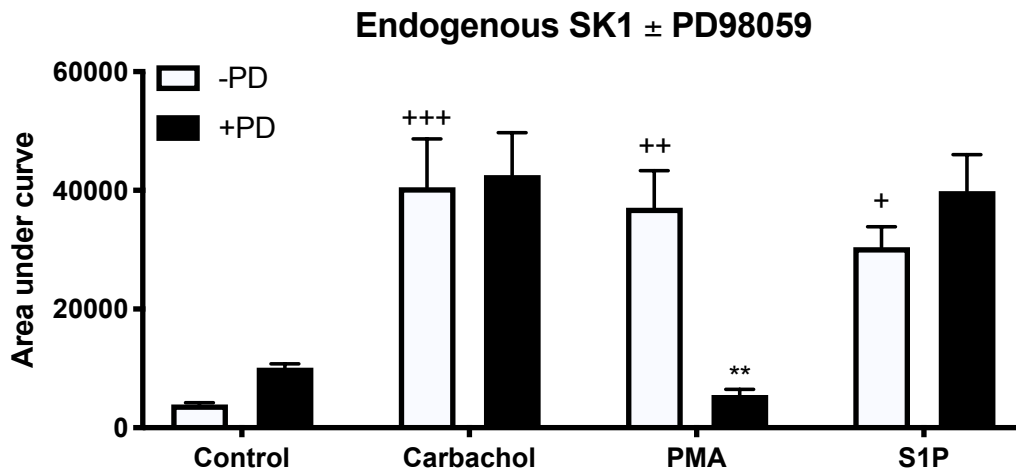


Figure 3.15 Area under curve analysis of stimulated MCF-7L cells pre-treated with PD98059

The bar graph represents the AUC of the total level of endogenous SK1 translocation in response to S1P (5 μ M, 10 mins), PMA (1 μ M, 10 mins), carbachol (100 μ M, 10 mins) or vehicle (Con, DMSO, 0.1% (v/v)), with and without pre-treatment of PD98059 (50 μ M, 1 hour) (n=5); **p<0.01 for PMA alone *versus* PMA with PD98059; +p<0.05, ++p<0.01 and +++p<0.001 for stimulus *versus* control (two-way ANOVA with Tukey's multiple comparison test).

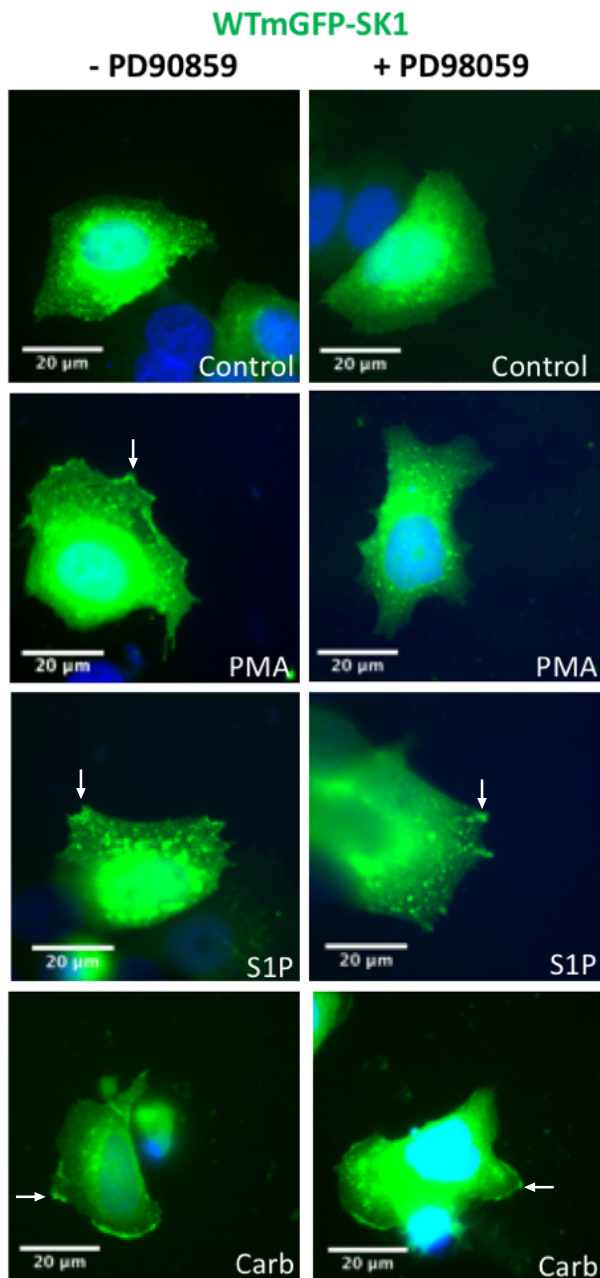


Figure 3.16 Stimulated MCF-7L cells transiently overexpressing WTmGFP-SK1 pre-treated with PD98059

40x oil magnification photomicrographs of MCF-7L cells transiently overexpressing WTmGFP-SK1 pre-treated with PD98059 (50 μ M, 1 hour) and stimulated with S1P (5 μ M, 10 minutes), PMA (1 μ M, 10 minutes) carbachol (100 μ M, 10 minutes) or vehicle (Con, DMSO, 0.1% (v/v)) and compared to cells not re-treated. Cells were processed (see methods) and mounted with DAPI-containing mount to stain DNA (blue). SK1 was detected with by GFP (arrows show translocated mGFP-SK1). Representative results is of 3 independent experiments.

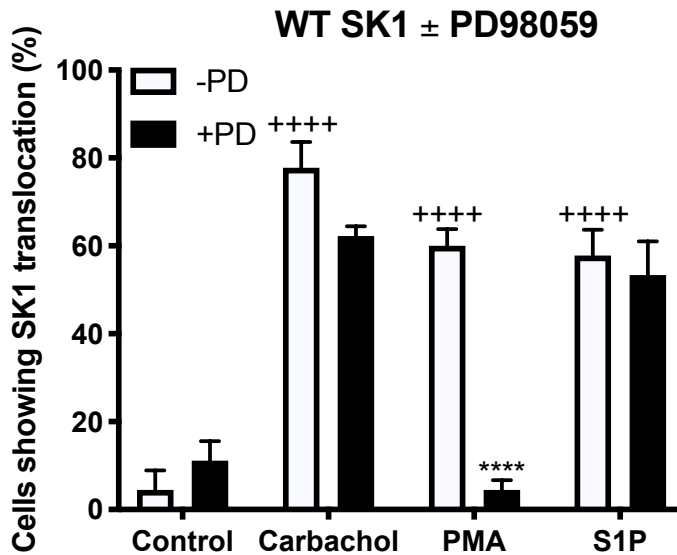


Figure 3.17 % of stimulated MCF-7L cells transiently overexpressing WTmGFP-SK1 showing translocation when pre-treated with PD98059

The bar graph represents the % of MCF-7L cells transiently overexpressing WTmGFP-SK1 showing translocated WTmGFP-SK1 in response to S1P (5 μ M, 10 mins), PMA (1 μ M, 10 mins), carbachol (100 μ M, 10 mins) or vehicle (Con, DMSO, 0.1% (v/v)), with and without pre-treatment of PD98059 (50 μ M, 1 hour). 15 random cells on 3 separate cover slips were analysed (n=3); ****p<0.0001 for PMA alone versus PMA with PD98059; ****p<0.0001 for stimulus versus control (two-way ANOVA with Tukey's multiple comparison test).

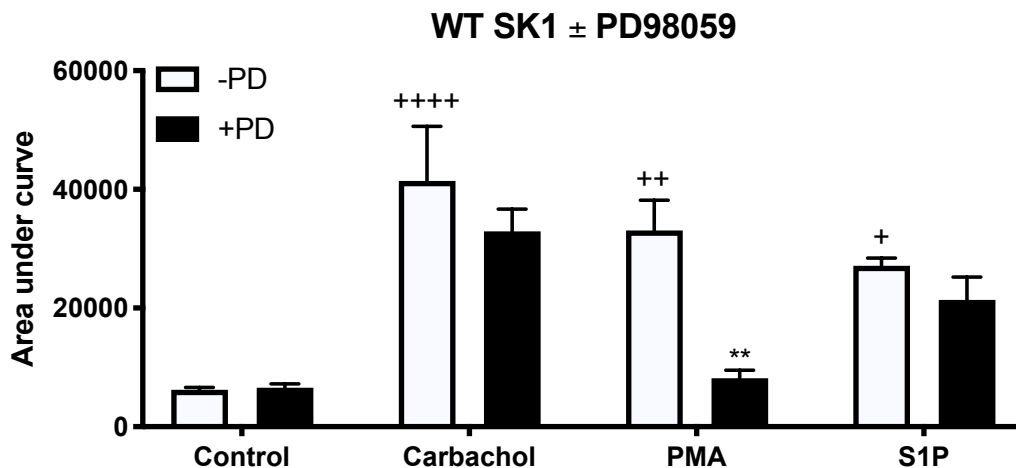


Figure 3.18 Area under curve analysis of transiently overexpressing WTmGFP-SK1 MCF-7L cells pre-treated with PD98059

The bar graph represents the AUC of the total level of WTmGFP-SK1 translocation in response to S1P (5 μ M, 10 mins), PMA (1 μ M, 10 mins), carbachol (100 μ M, 10 mins) or vehicle (Con, DMSO, 0.1% (v/v)), with and without pre-treatment of PD98059 (50 μ M, 1 hour) (n=5); **p<0.01 for PMA alone versus PMA with PD98059; *p<0.05, **p<0.01 and ****p<0.0001 for stimulus versus control (two-way ANOVA with Tukey's multiple comparison test).

3.2.3 G_q is required for the translocation of SK1

Previous literature indicates that constitutively active G_q drives translocation of SK1 to the PM (ter Braak et al., 2009). Therefore, the role of G_q in regulating the translocation in response to GPCR activation was investigated. For this purpose, MFC-7L cells transiently overexpressing WTmGFP-SK1 were used and SK1 tested for its ability to translocate in response to S1P, PMA or carbachol in the presence and absence of the G_q inhibitor YM254890, which blocks GDP-GTP exchange (Nishimura et al., 2010). YM254890 was shown to block the translocation of WTmGFP-SK1 in response to S1P, PMA or carbachol (Fig. 3.19), which was also detected as a loss in membrane pixel intensity (Fig. 3.21). These findings indicate that G_q activity is crucial for phosphorylation-dependent and phosphorylation-independent SK1 translocation. However, it remains to be investigated whether G_q binds directly or functions indirectly to regulate SK1.

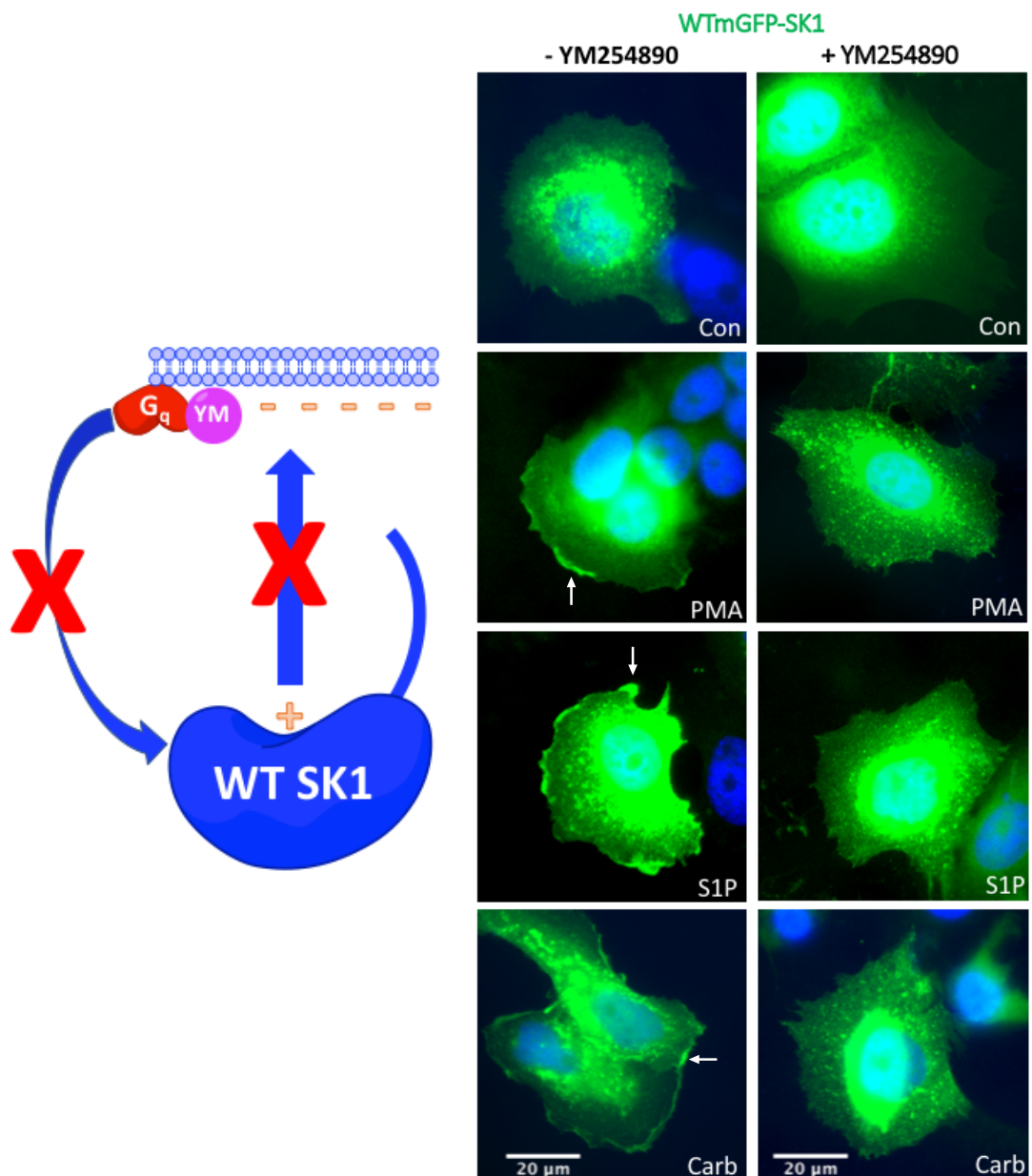


Figure 3.19 Stimulated MCF-7L transiently overexpressing WTmGFP-SK1 cells pre-treated with YM254890

40x oil magnification photomicrographs of MCF-7L cells transiently overexpressing WTmGFP-SK1 pre-treated with YM254890 (10 μ M, 30 minutes) and stimulated with S1P (5 μ M, 10 minutes), PMA (1 μ M, 10 minutes) carbachol (100 μ M, 10 minutes) or vehicle (Con, DMSO, 0.1% (v/v)) and compared to cells not re-treated. Cells were processed (see methods) and mounted with DAPI-containing mount to stain DNA (blue). SK1 was detected with by GFP (arrows show translocated mGFP-SK1). Representative results is of 3 independent experiments.

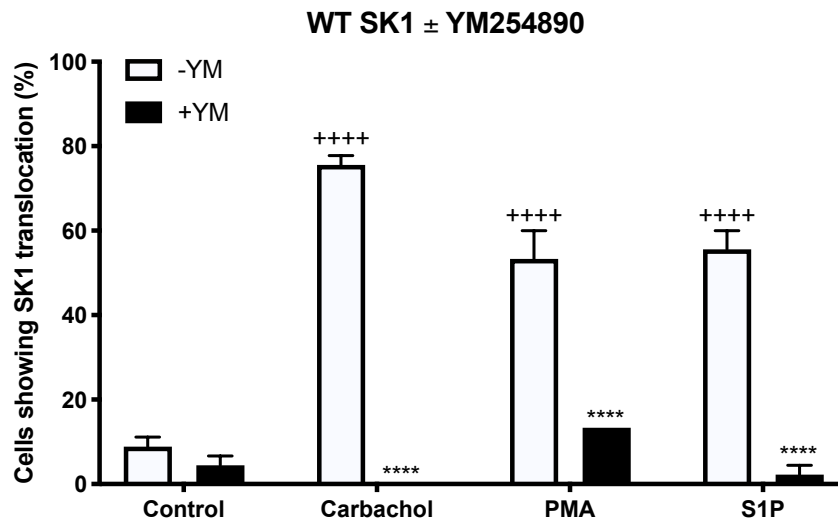


Figure 3.20 % of stimulated MCF-7L cells transiently overexpressing WTmGFP-SK1 showing translocation when pre-treated with YM254890

The bar graph represents the % of MCF-7L cells transiently overexpressing WTmGFP-SK1 showing translocated WTmGFP-SK1 in response to S1P (5 μ M, 10 mins), PMA (1 μ M, 10 mins), carbachol (100 μ M, 10 mins) or vehicle (Con, DMSO, 0.1% (v/v)), with and without pre-treatment of YM254890 (10 μ M, 30 mins). 15 random cells on 3 separate cover slips were analysed (n=3); ****p<0.0001 for stimulus alone *versus* stimulus with YM254890; ****p<0.0001 for stimulus *versus* control (two-way ANOVA with Tukey's multiple comparison test).

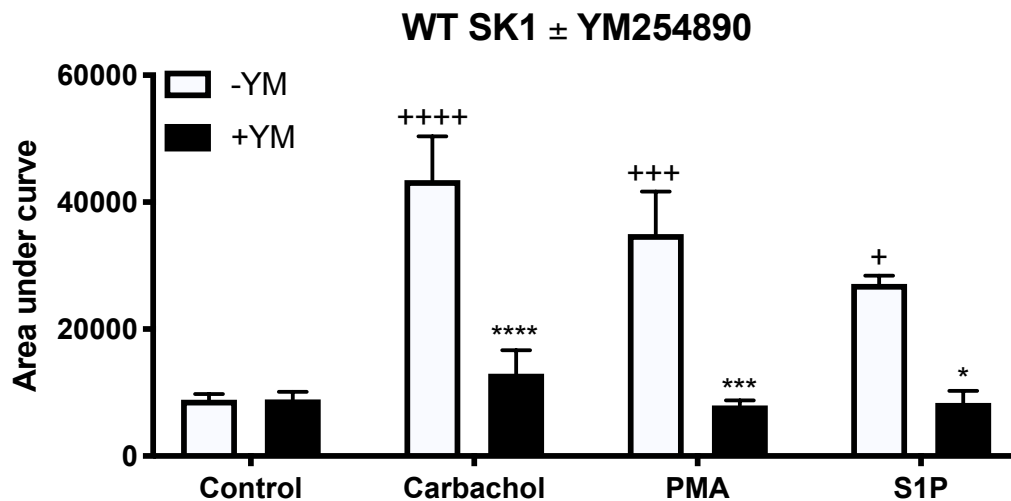


Figure 3.21 Area under curve analysis of transiently overexpressing WTmGFP-SK1 MCF-7L cells pre-treated with YM254890

The bar graph represents the AUC of the total level of WTmGFP-SK1 translocation in response to S1P (5 μ M, 10 mins), PMA (1 μ M, 10 mins), carbachol (100 μ M, 10 mins) or vehicle (Con, DMSO, 0.1% (v/v)), with and without pre-treatment of (YM254890 (10 μ M, 30 mins) (n=5); *p<0.05, ***p<0.001 and ****p<0.0001 for stimulus alone *versus* stimulus with YM254890; +p<0.05, +++p<0.001 and ****p<0.0001 for stimulus *versus* control (two-way ANOVA with Tukey's multiple comparison test).

3.2.4 Phosphatidic acid production is required for the translocation of SK1

SK1 displays preferential translocation to areas of the PM that are rich in PA (Delon et al., 2004), which is an anionic phospholipid produced by phospholipase D (PLD). Moreover, it is proposed that a positively charged cluster of amino acids residing at the dimerisation cleft interacts with membrane-bound acidic phospholipids (Adams et al., 2016). We therefore examined whether PLD activity and hence the formation of PA, was important for the translocation of SK1.

To investigate, the recombinant SK1 was tested for its ability to translocate to the PM following PMA, S1P or carbachol stimulation, in the presence or absence of the PLD inhibitor, FIPI. MCF-7L cells transiently overexpressing WTmGFP-SK1 displayed a reduction in translocation in response to PMA, S1P or carbachol when pre-treated with FIPI (Fig. 3.22). The inhibitor also led to a reduction in membrane pixel intensity following stimulation with all 3 agents (Fig. 3.24). These data indicate that GPCR-mediated translocation, but also ERK-1/2-dependent translocation requires newly formed membrane-bound PA.

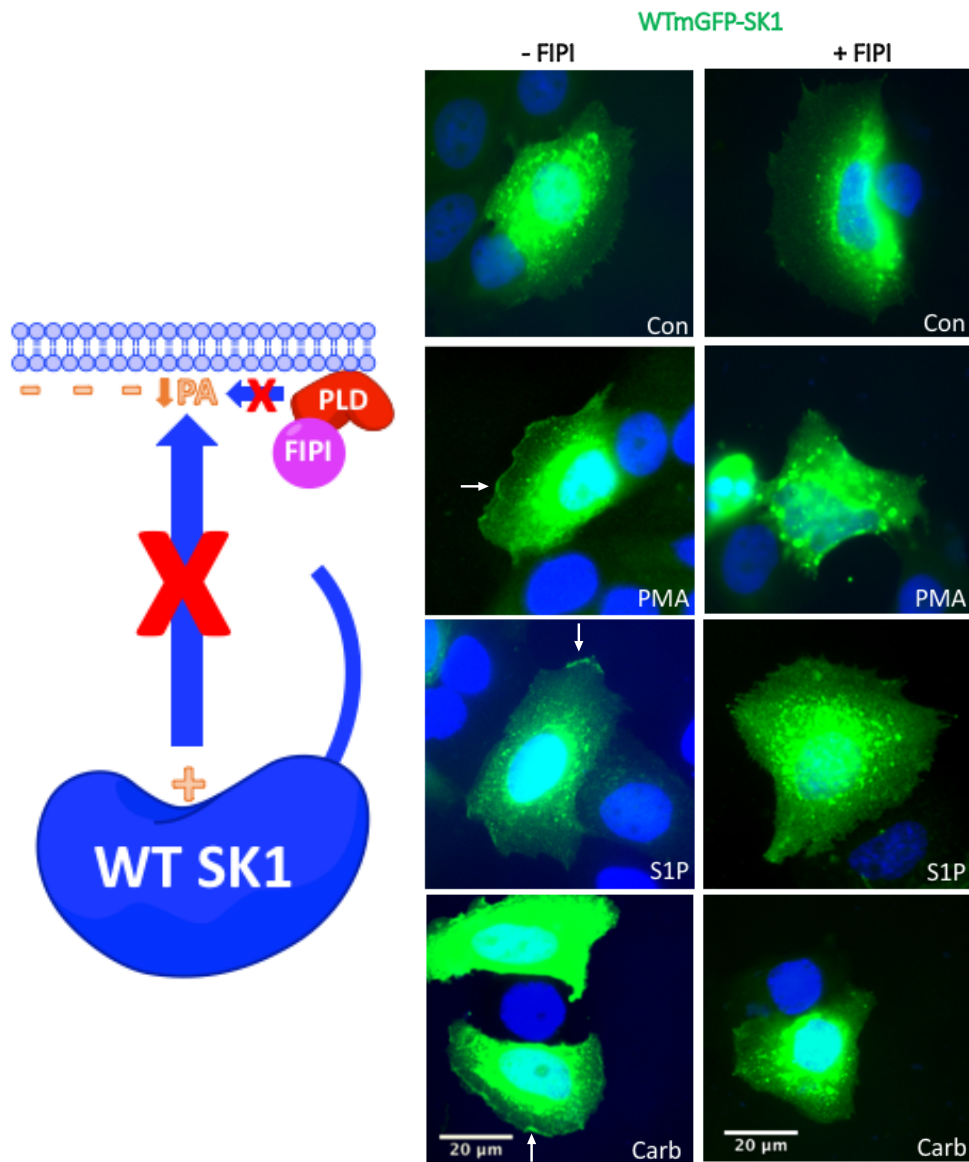


Figure 3.22 Stimulated MCF-7L cells transiently overexpressing WTmGFP-SK1 pre-treated with FIPI

40x oil magnification photomicrographs of MCF-7L cells transiently overexpressing WTmGFP-SK1 pre-treated with FIPI (PLD-1/2 inhibitor) (100 nM, 1 hour) and stimulated with S1P (5 μ M, 10 minutes), PMA (1 μ M, 10 minutes) carbachol (100 μ M, 10 minutes) or vehicle (Con, DMSO, 0.1% (v/v)) and compared to cells not re-treated. Cells were processed (see methods) and mounted with DAPI-containing mount to stain DNA (blue). SK1 was detected with by GFP (arrows show translocated mGFP-SK1). Representative results is of 3 independent experiments.

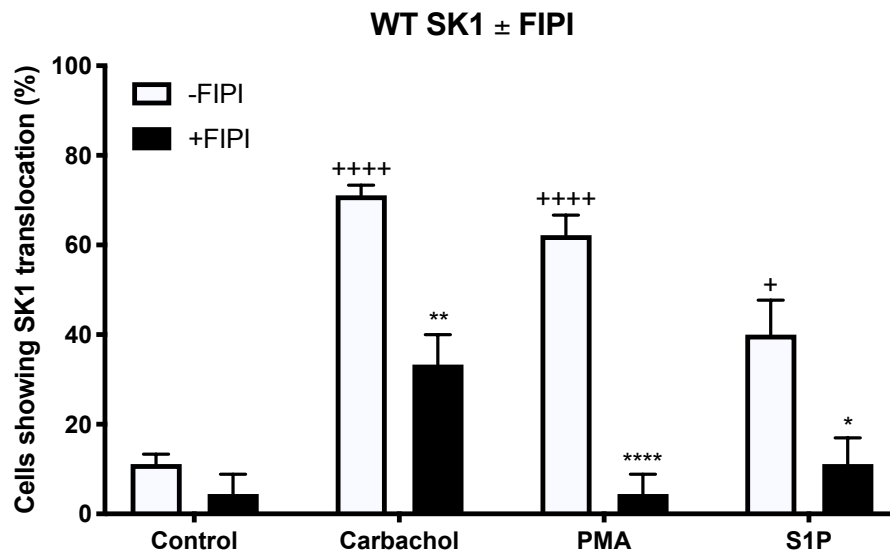


Figure 3.23 % of stimulated MCF-7L cells transiently overexpressing WTmGFP-SK1 showing translocation when pre-treated with FIPI

The bar graph represents the % of MCF-7L cells transiently overexpressing WTmGFP-SK1 showing translocated WTmGFP-SK1 in response to S1P (5 μ M, 10 mins), PMA (1 μ M, 10 mins), carbachol (100 μ M, 10 mins) or vehicle (Con, DMSO, 0.1% (v/v)), with and without pre-treatment of FIPI (100 nM, 1 hour). 15 random cells on 3 separate cover slips were analysed (n=3); *p<0.05, ***p<0.001 and ****p<0.0001 for stimulus alone *versus* stimulus with FIPI; +p<0.05 and ****p<0.0001 for stimulus *versus* control (two-way ANOVA with Tukey's multiple comparison test).

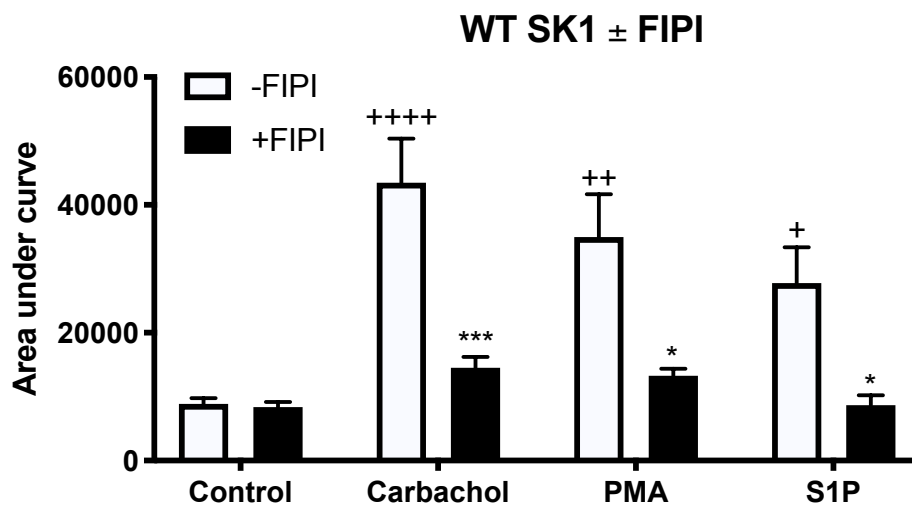


Figure 3.6 Area under curve analysis of transiently overexpressing WTmGFP-SK1 MCF-7L cells pre-treated with FIPI

The bar graph represents the AUC of the total level of WTmGFP-SK1 translocation in response to S1P (5 μ M, 10 mins), PMA (1 μ M, 10 mins), carbachol (100 μ M, 10 mins) or vehicle (Con, DMSO, 0.1% (v/v)), with and without pre-treatment of FIPI (100 nM, 1 hour) (n=5); *p<0.05 and ***p<0.001 for stimulus alone *versus* stimulus with FIPI; +p<0.05, **p<0.01 and ****p<0.0001 for stimulus *versus* control (two-way ANOVA with Tukey's multiple comparison test).

3.2.5 Creation of mGFP-SK1-K49E and mGFP-SK1-I51C dimerisation mutants

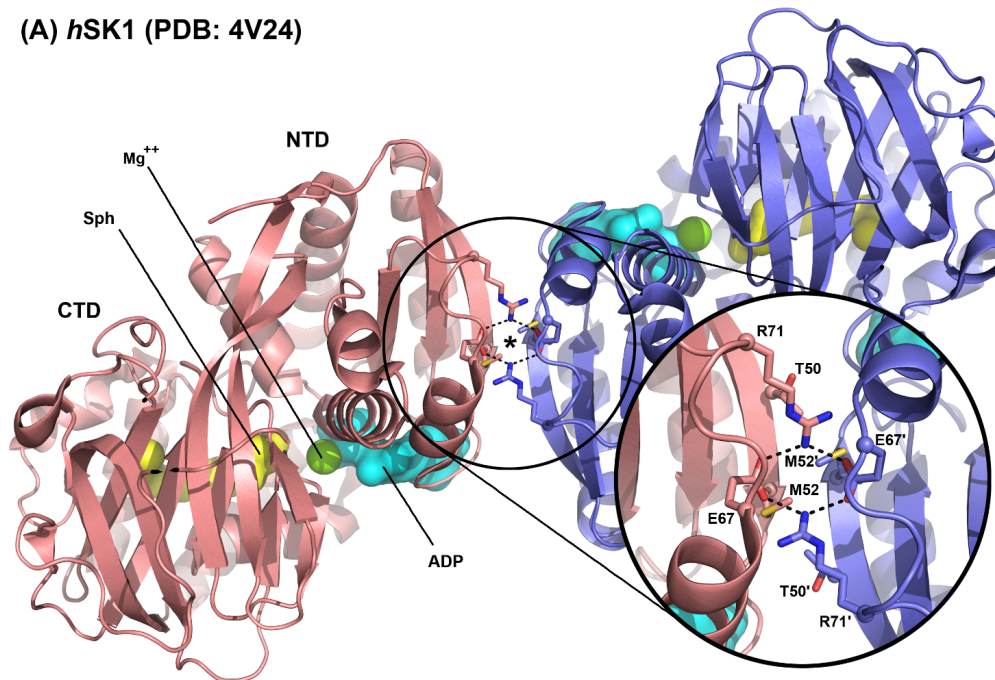
Positively charged amino acids situated at the core of SK1 form a contiguous membrane-engagement interface with hydrophobic patches present on LBL-1 in the dimeric SK1 (Adams et al., 2016; Pulkoski-Gross et al., 2018). Indeed, dimeric SK1 is likely to exhibit greater avidity for the PM compared with the monomer due to the higher density of positive charge present at the dimeric interface and the presence of two LBL-1 loops. Moreover, previous observations in the current study revealed that carbachol or PMA promoted the translocation of SK1 to lamellipodia, whereas S1P promoted translocation to filopodia. Therefore, the possibility that a monomer/dimer equilibrium exists and is responsible for regulating translocation of SK1 to different PM micro-domains was investigated.

In similar manner to related DAGK_cat proteins (Adams et al., 2016), SK1 exhibits head-to-head dimerization (NTD:NTD) with partial annealing of the exposed β 2 strand from each protomer displaying C_2 symmetry (180° around its X axis) (shown in Fig. 3.25 by asterisk). In addition, there is also packing of hydrophobic residues (51-LML-53 in *hSK1*) along the exposed β 2 strand that contributes to the dimerization interface (shown here by M52 in *hSK1*). Moreover, a salt bridge network forms at the dimerization interface involving E67/R71 in *hSK1* and E66/K49 in *mSK1* where arginine is replaced by a histidine. More specifically, in *mSK1* where T50 is replaced by K49, this allows for the existence of a surrogate E66:K49:E66':K49' polar network in order to maintain the dimerisation interface (Fig. 3.25).

To investigate the importance of SK1 dimerisation on translocation, two site-directed mutagenesis approaches was used, either attempting to force SK1 to become dimeric (mGFP-SK1-I51C, termed 'forced dimer') or proposed to destabilise the salt bridge through charge reversal to enhance formation of the monomeric protein (mGFP-SK1-K49E, termed 'forced monomer'). In this regard, the C_γ -centres for I51 and I51' in *mSK1* suggest the two isoleucine residues likely lie within van der Waals contact of one and other. Therefore, the dimer may be stabilised through an engineered disulphide bond by replacement with cysteine residues (Fig. 3.25). The forced dimer was generated using primers that encoded a triple base point mutation in WTmGFP-SK1 from ATA to TGC at the I51 position (Fig. 3.26). This was to change the residue to a cysteine and attempt to promote the formation of a disulphide bridge between two protomers. The forced monomer was generated using primers that encoded a single base point mutation in WTmGFP-SK1 from AAA to GAA at the K49 position

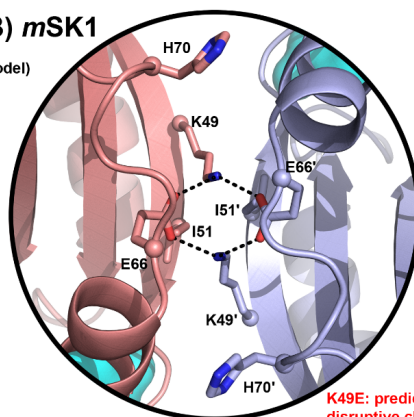
(3.26), thereby replacing the residue with glutamic acid and hence reversing the charge to attempt to destabilise dimer formation.

(A) *hSK1* (PDB: 4V24)



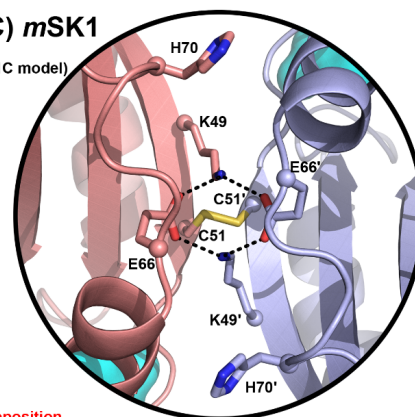
(B) *mSK1*

(model)



(C) *mSK1*

(I51C model)



K49E: predicted disruptive charge opposition

Figure 3.7 SK1 dimerisation interface and rationale for site-directed mutagenesis

(A) NTD:NTD dimerisation of *hSK1* is through E67:R71:E67':R71' salt bridge formation about a C₂-symmetry axis (asterisk between red and blue protomers) (1.8 Å resolution structure, 4V24) (Wang et al., 2014). Yellow surface represents bound SPH and green sphere/cyan surface represents Mg-ADP (4VZB/4VZD) (Wang et al., 2013). Packing of hydrophobic residues (M52 shown here) contributes to dimerization interface. (B) In *mSK1* dimerisation is maintained by a surrogate E66:K49:E66':K49' polar network (black dotted lines) and can be disrupted by a K49E charge reversal. (C) Dimerisation can be 'stabilised' by the incorporation of an engineered disulphide bond.

WTmGFP-SK1	301	KLILTERKNHARELVCAEELGHWDALAVMSGDGLMHEVVNGLMERPDWET	350
mGFP-SK1-K49E	301	ELILTERKNHARELVCAEELGHWDALAVMSGDGLMHEVVNGLMERPDWET	350
WTmGFP-SK1	301	KLILTERKNHARELVCAEELGHWDALAVMSGDGLMHEVVNGLMERPDWET	350
mGFP-SK1-I51C	301	KLCILTERKNHARELVCAEELGHWDALAVMSGDGLMHEVVNGLMERPDWET	350

Figure 3.8 Site-directed mutagenesis for mGFP-SK1-K49E and mGFP-SK1-I51C

To generate *mGFP-SK1-K49E* A single base point mutation in WTmGFP-SK1 at the K49 position from AAA to GAA changed the amino acid at position 49 to glutamic acid, thereby reversing the charge of the amino acid proposed to be important in formation of the salt bridge between protomers. To generate *mGFP-SK1-I51C* A triple base point mutation in WTmGFP-SK1 at the I51 position from ATA to TGC changed the amino acid at position 51 to cystine, thereby allowing the formation of a disulphide bridge between protomers.

3.2.6 Translocation of mGFP-SK1-K49E and mGFP-SK1-I51C in response to various agonists

It is proposed that a monomer/dimer SK1 equilibrium governs the translocation of SK1 to the different PM micro-domains e.g. lamellipodia and filopodia. This might occur through differences in binding affinity for other putative partner proteins that bind either the dimer or monomer. It is also hypothesized that dimeric SK1, by having a higher density of positively charged residues is able to translocate to regions on the PM that are lower in PA in filopodia *versus* lamellipodia.

To examine this, MCF-7L cells transiently overexpressing *mGFP-SK1-K49E* or *mGFP-SK1-I51C* were tested for their ability to translocate in response to S1P, PMA or carbachol. Successful overexpression of *mGFP-SK1-K49E* or *mGFP-SK1-I51C* was confirmed by western blot analysis using an anti-GFP antibody (Mr=69 kDa). Immunofluorescence microscopy revealed that S1P, PMA or carbachol promoted the translocation of *mGFP-SK1-K49E* or *mGFP-SK1-I51C* to the PM (Fig. 3.27). However, further investigation indicated that when compared to the number of WTmGFP-SK1 transiently overexpressing cells, *mGFP-SK1-K49E*, but not *mGFP-SK1-I51C* transiently overexpressing cells displayed a reduced translocation in response to all 3 agents (Fig. 3.28). Additional analysis revealed that there was reduced membrane pixel intensity of *mGFP-SK1-K49E* and *mGFP-SK1-I51C* in response to carbachol and PMA, but not S1P (Fig. 3.29). In this regard, *mGFP-SK1-K49E* displayed a reduced pixel intensity at the membrane in response to carbachol or PMA, whereas *mGFP-SK1-I51C* exhibited more localized regions of membrane pixel intensity. Furthermore, in response to S1P, *mGFP-SK1-K49E* displayed fewer

peaks in membrane pixel intensity that were broader in size, accounting for no overall change in AUC. The differences in distribution of membrane pixel intensity of mGFP-SK1-I51C and mGFP-SK1-K49E suggest phenotypic differences in translocation resulting from mutation and possible disruption to the monomer/dimer SK1 equilibrium.

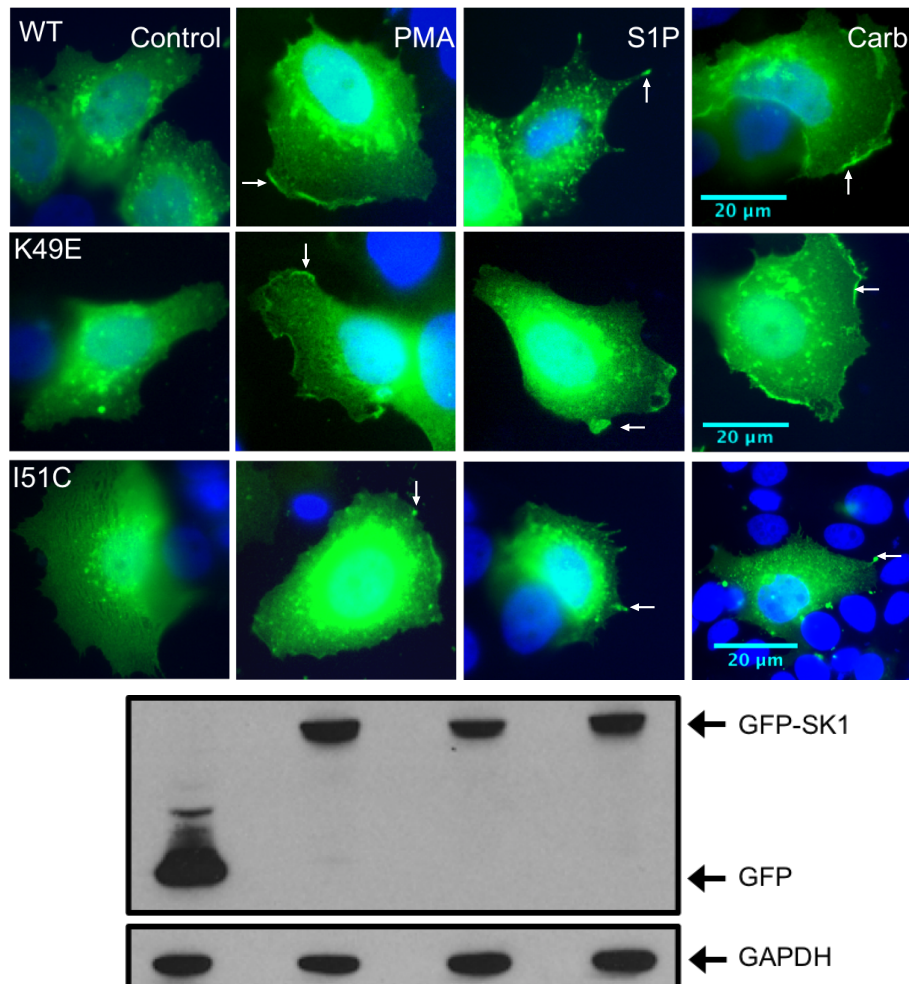


Figure 3.9 Stimulated MCF-7L cells transiently overexpressing WTmGFP-SK1, mGFP-SK1-K49E or mGFP-SK1-I51C

40x oil magnification photomicrographs of MCF-7L cells showing the translocation of WTmGFP-SK1, mGFP-SK1-K49E or mGFP-SK1-I51C in response to S1P (5 μM, 10 minutes), PMA (1 μM, 10 minutes), carbachol (100 μM, 10 minutes) or vehicle (DMSO, 0.1% (v/v)). Cells were processed (see methods) and mounted with DAPI-containing mount to stain DNA (blue). mGFP-SK1 forms were detected by GFP (arrows show translocated mGFP-SK1). Representative results is of 3 independent experiments. Inset is a western blot confirming the successful expression of WTmGFP-SK1, mGFP-SK1-K49E and mGFP-SK1-I51C using an anti-GFP antibody (lane 1: GFP vector transfected cells (27 kDa); lane 2: transiently transfected WTmGFP-SK1 cells (69 kDa); lane 3: transiently transfected mGFP-SK1-K49E cells (69 kDa); lane 4: transiently transfected mGFP-SK1-I51C cells (69 kDa)).

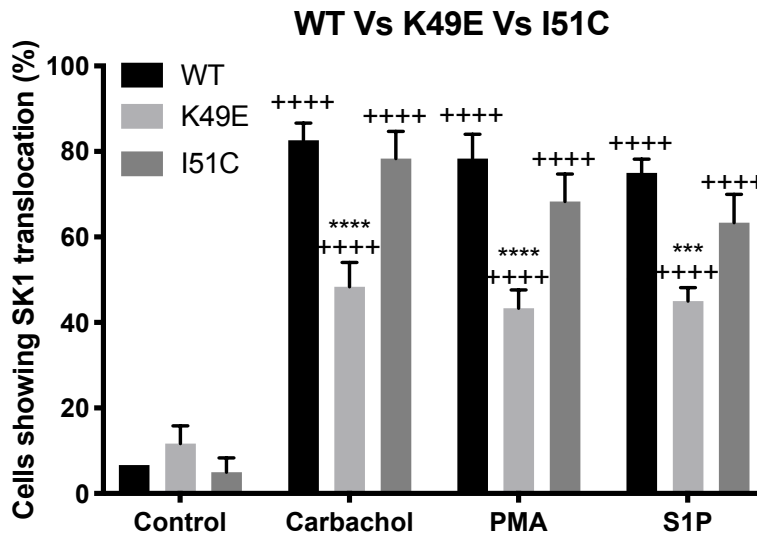


Figure 3.10 % of stimulated MCF-7L cells transiently overexpressing WTmGFP-SK1 mGFP-SK1-K49E or mGFP-SK1-I51C showing translocation

The bar graph represents the % of MCF-7L cells transiently overexpressing WTmGFP-SK1, mGFP-SK1-K49E or mGFP-SK1-I51C showing translocated mGFP-SK1 in response to S1P (5 μ M, 10 mins), PMA (1 μ M, 10 mins), carbachol (100 μ M, 10 mins) or vehicle (Con, DMSO, 0.1% (v/v)). 15 random cells on 3 separate cover slips were analysed (n=3); ***p<0.001 and ****p<0.0001 for K49E or I51C mutant versus WT; ****p<0.0001 for stimulus versus control for WT, K49E or I51C mutant (two-way ANOVA with Tukey's multiple comparison test).

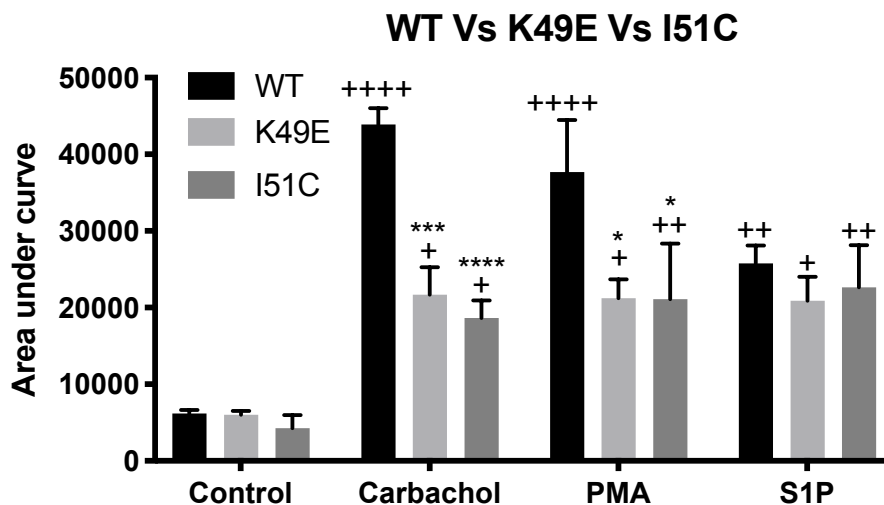


Figure 3.29 Area under curve analysis of stimulated MCF-7L cells transiently overexpressing WTmGFP-SK1, mGFP-SK1-K49E or mGFP-SK1-I51C

The bar graph represents the AUC of the total level of WTmGFP-SK1, mGFP-SK1-K49E or mGFP-SK1-I51C translocation in response to S1P (5 μ M, 10 mins), PMA (1 μ M, 10 mins), carbachol (100 μ M, 10 mins) or vehicle (Con, DMSO, 0.1% (v/v)) (n=5); *p<0.05, ***p<0.001 and ****p<0.0001 for K49E or I51C mutant versus WT for a given stimulus; *p<0.05, **p<0.01 and ****p<0.0001 for stimulus versus control for WT, K49E or I51C mutant (two-way ANOVA with Tukey's multiple comparison test).

3.2.7 Translocation phenotypes of mGFP-SK1-K49E and mGFP-SK1-I51C in response to various agonists

The next aim was to define the translocation phenotype of *mGFP-SK1-I51C* and *mGFP-SK1-K49E* in response to S1P, PMA or carbachol. Similar to previous observations, PMA or carbachol promoted the translocation of WT*mGFP-SK1* to lamellipodia, whereas S1P promoted translocation to filopodia. When compared to the phenotype displayed by WT*mGFP-SK1* in response to carbachol or PMA, *mGFP-SK1-K49E* and *mGFP-SK1-I51C* both displayed phenotypic shifts in translocation. Carbachol and PMA promoted the translocation of *mGFP-SK1-K49E* to lamellipodia, albeit to a lesser extent to what is displayed by WT*mGFP-SK1* (Fig. 3.32). In contrast to WT*mGFP-SK1*, S1P also promoted the translocation of *mGFP-SK1-K49E* to lamellipodia (Fig. 3.30). *mGFP-SK1-I51C* translocated to filopodia in response to carbachol, PMA or S1P, and therefore contrasts with WT*mGFP-SK1* with respect to carbachol and PMA (Fig. 3.30).

In summary, these data support the hypothesis that monomeric SK1 is able to translocate to lamellipodia, whereas a dimeric SK1 translocates to filopodia. Moreover, disruption to the salt bridge produces an enzyme with reduced capability to translocate to the PM in response to ligand. This may be due to the charge reversal leading to a reduction in the overall net charge of the positively charged dimeric interface important for translocation.

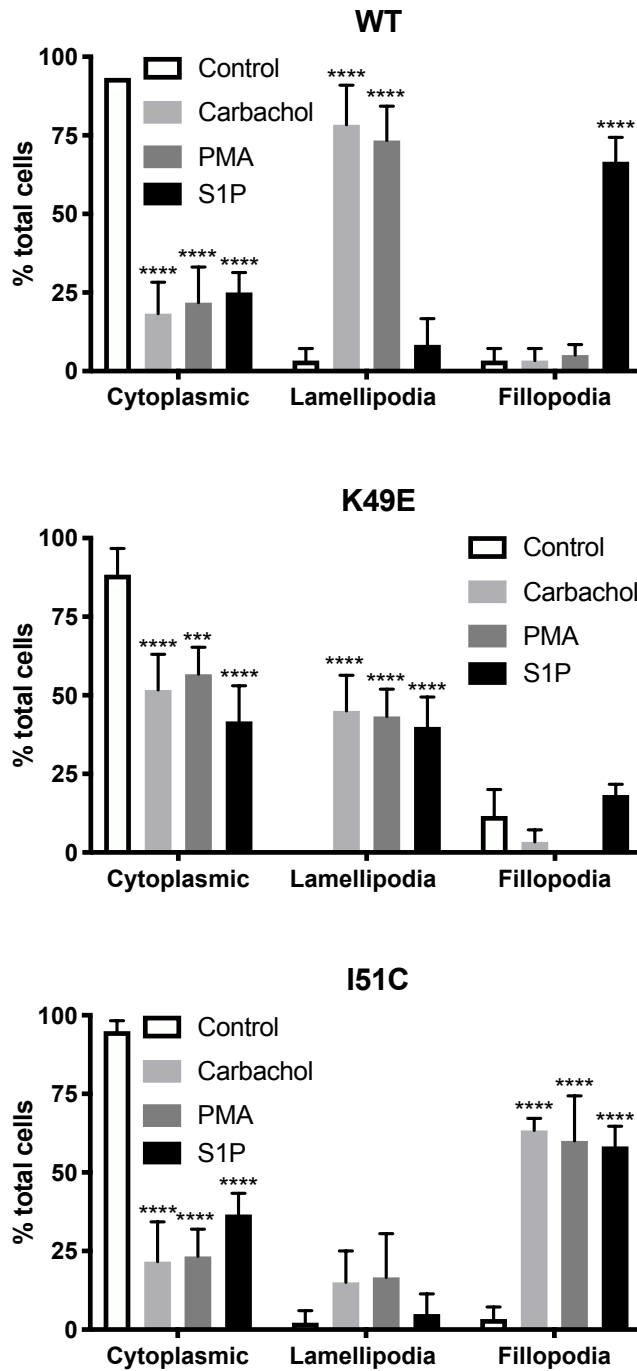


Figure 3.30 Phenotypic quantification of stimulated MCF-7L transiently overexpressing WTmGFP-SK1, mGFP-SK1-K49E or mGFP-SK1-I51C

The bar graphs represent the % of MCF-7L cells transiently overexpressing WTmGFP-SK1, mGFP-SK1-K49E or mGFP-SK1-I51C showing mGFP-SK1 in spread (lamellipodia) or fillopodia micro-domains in response to S1P (5 μ M, 10 minutes), PMA (1 μ M, 10 minutes) or carbachol (100 μ M, 10 minutes) and compared to control cells (DMSO, 0.1% (v/v)). 15 random cells on 4 separate cover slips were analysed (n=4); ***p<0.001 and ****p<0.0001 for stimulus versus control for a given phenotype (two-way ANOVA with Tukey's multiple comparison test).

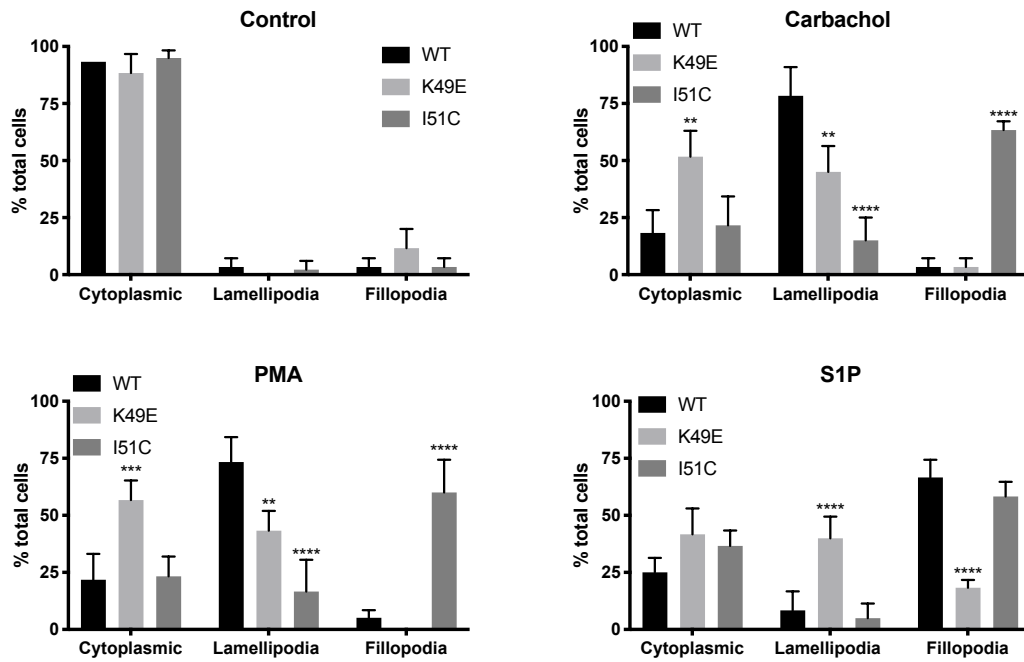


Figure 3.31 Phenotypic shift of stimulated MCF-7L transiently overexpressing mGFP-SK1-K49E or mGFP-SK1-I51C compared to WTmGFP-SK1

The bar graphs represent the % of MCF-7L cells transiently overexpressing mGFP-SK1-K49E or mGFP-SK1-I51C showing mGFP-SK1 in spread (lamellipodia) or filopodia micro-domains in response to S1P (5 μ M, 10 minutes), PMA (1 μ M, 10 minutes) or carbachol (100 μ M, 10 minutes) or vehicle (DMSO, 0.1% (v/v)) and compared to the phenotype displayed by WTmGFP-SK1. 15 random cells on 4 separate cover slips were analysed (n=4); **p<0.01, ***p<0.001 and ****p<0.0001 for K49E or I51C mutant versus WT for a given phenotype (two-way ANOVA with Tukey's multiple comparison test).

3.2.8 mGFP-SK1-K49E is functionally deficient in mobilising F-actin

Previous reports using MCF-7 Neo cells, indicate that SK1 mediates actin rearrangement into lamellipodia necessary for migration (Long et al., 2010; Lim et al., 2011). In addition, the data presented in 3.2.7 suggest mGFP-SK1-K49E has a reduced capability to translocate to lamellipodia. Therefore, whether the reduced ability to translocate to lamellipodia is associated with a reduction in F-actin mobilisation at the PM was investigated. MCF-7L cells transiently overexpressing WTmGFP-SK1, mGFP-SK1-K49E or mGFP-SK1-I51C were treated with carbachol and stained with phalloidin red to detect F-actin, before being mounted with DAPI-containing mount to stain DNA. Co-localisation of F-actin and mGFP-SK1 was detected as yellow staining.

Carbachol promoted the mobilisation of F-actin and WTmGFP-SK1 into lamellipodia, which was also shown in mGFP-SK1-K49E expressing cells, albeit to a lesser extent.

This was observed as more diffuse staining of both *mGFP-SK1-K49E* and F-actin at the PM when compared to *WTmGFP-SK1* transiently overexpressing cells (Fig. 3.34). Conversely, carbachol promoted the dense co-localization of *mGFP-SK1-I51C* and F-actin in filopodia (Fig. 3.34). These findings suggest that *mGFP-SK1-K49E* which is reduced in translocation to the PM in response to carbachol, also exhibits less mobilisation of F-actin necessary for migration.

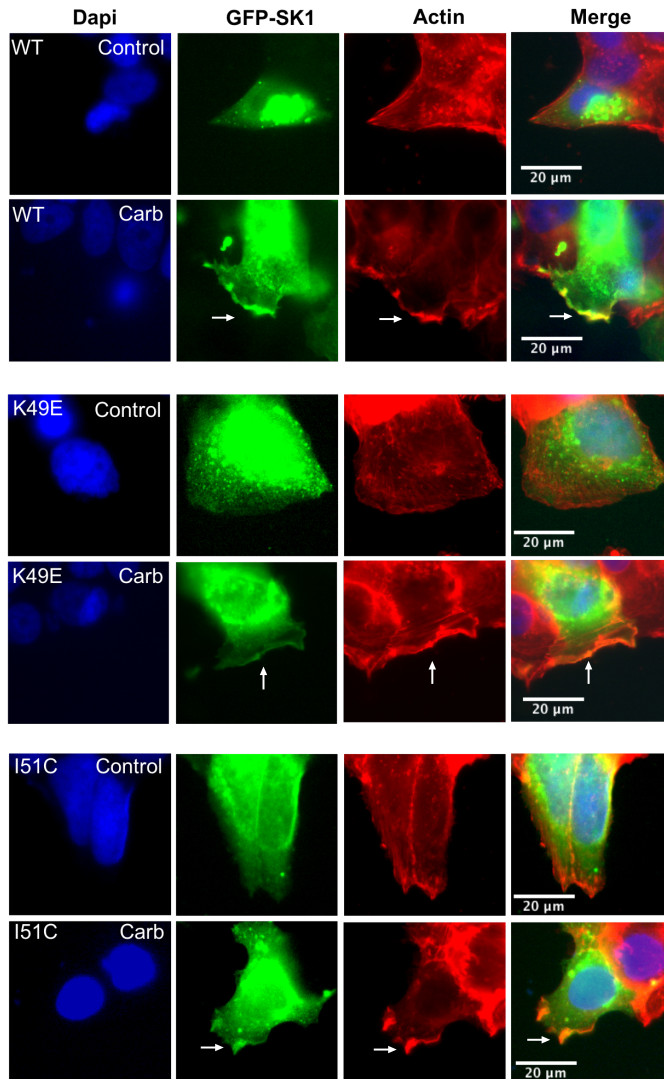


Figure 3.32 Stimulated MCF-7L cells transiently overexpressing WTmGFP-SK1, mGFP-SK1-K49E and mGFP-SK1-I51C stained for F-actin

40x oil magnification photomicrographs of MCF-7L cells showing the translocation of WTmGFP-SK1, *mGFP-SK1-K49E* or *mGFP-SK1-I51C* in response to S1P (5 μ M, 10 minutes), PMA (1 μ M, 10 minutes), carbachol (100 μ M, 10 minutes) or vehicle (DMSO, 0.1% (v/v)). Cells were processed (see methods) and were stained with phalloidin-red to observe F-actin (red) before being mounted with DAPI-containing mount to stain DNA (blue). *mGFP-SK1* forms were detected by GFP (arrows show translocated mGFP-SK1). Representative results is of 3 independent experiments.

3.2.9 mGFP-SK1-K49E is functionally deficient in promoting migration

SK1 translocation is understood to drive the migration of cancer cells (Sarkar et al., 2005; Doll et al., 2007). Therefore, we investigated whether these phenotypic differences in translocation altered the functional ability of MCF-7L cells to migrate. MCF-7L cells transiently overexpressing *mGFP-SK1-K49E* or *mGFP-SK1-I51C* were tested for their ability to migrate into a wounded area in response to carbachol (100 μ M, 22 hours) or S1P (5 μ M, 22 hours). Migration was assessed after 22 hours of treatment. The total number of cells and GFP-positive cells that had migrated into the wound were counted and subsequently displayed as a percentage of migrated cells that were expressing WT*mGFP-SK1*, *mGFP-SK1-K49E* or *mGFP-SK1-I51C*, which was compared to the level of migration of cells expressing solely GFP.

Importantly there was no difference in the transfection efficiency of the constructs used, hence differences in migration were due to mutations introduced into SK1 alone (Fig. 3.33). Migration was significantly increased in control cells transiently overexpressing *mGFP-SK1-I51C* (Fig. 3.36 & 3.39). Following 22 hours of carbachol or S1P treatment, cells transiently overexpressing WT*mGFP-SK1* displayed increased migration above cells overexpressing WT*mGFP-SK1* after 22 hours control treatment (Fig. 3.36 & 3.39). In addition, *mGFP-SK1-I51C* overexpressing cells stimulated with 22 hours of carbachol displayed no increase in migration when compared to vehicle treated *mGFP-SK1-I51C* overexpressing cells (Fig. 3.36 & 3.39). This is likely because there is maximum SK1-mediated migration with 22 hours of vehicle treatment. Notably, there was no increased migration of *mGFP-SK1-K49E* following 22 hours of carbachol or S1P treatment *versus* cells expressing this mutant after 22 hours control treatment (Fig. 3.36 & 3.39), suggesting a threshold requirement for translocated SK1 to elicit migration.

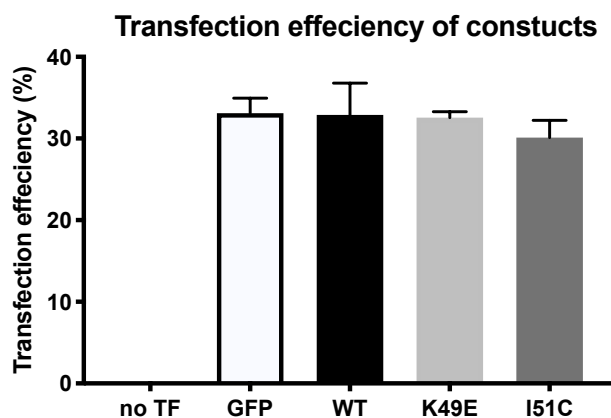


Figure 3.33 Transfection efficiency of GFP, WTmGFP-SK1, mGFP-SK1-K49E and mGFP-SK1-I51C

The bar graph represents the transfection efficiency of GFP, WTmGFP-SK1, mGFP-SK1-K49E and mGFP-SK1-I51C. Results are representative of 3 independent experiments (one-way ANOVA).

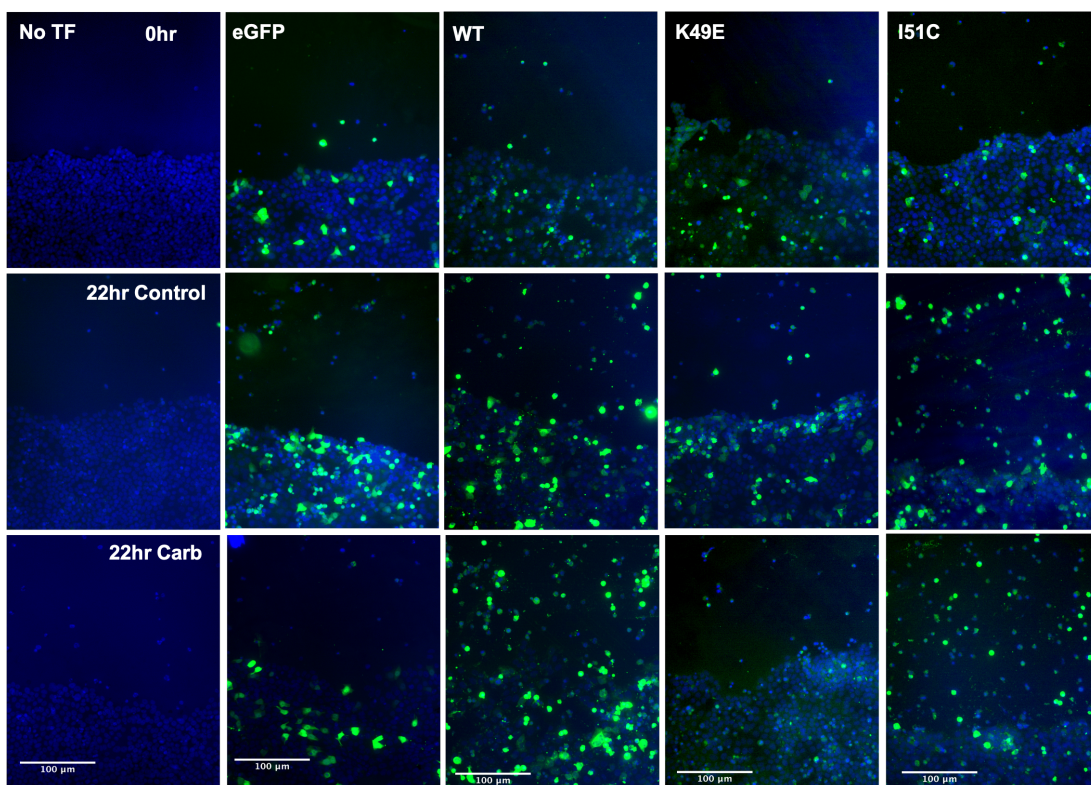


Figure 3.34 Migration assay of carbachol stimulated MCF-7L cells transiently overexpressing GFP, WTmGFP-SK1, mGFP-SK1-K49E or mGFP-SK1-I51C

MCF-7L cells transiently overexpressing GFP, WTmGFP-SK1, mGFP-SK1-K49E or mGFP-SK1-I51C were treated with carbachol (100 μ M, 22 hours) or as control (dH₂O, 1% (v/v), 22 hours) following the application of a wound to the cell monolayer. 10x oil magnification photomicrographs showing the migration of cells into the wounded area. Results are representative of 3 independent experiments.

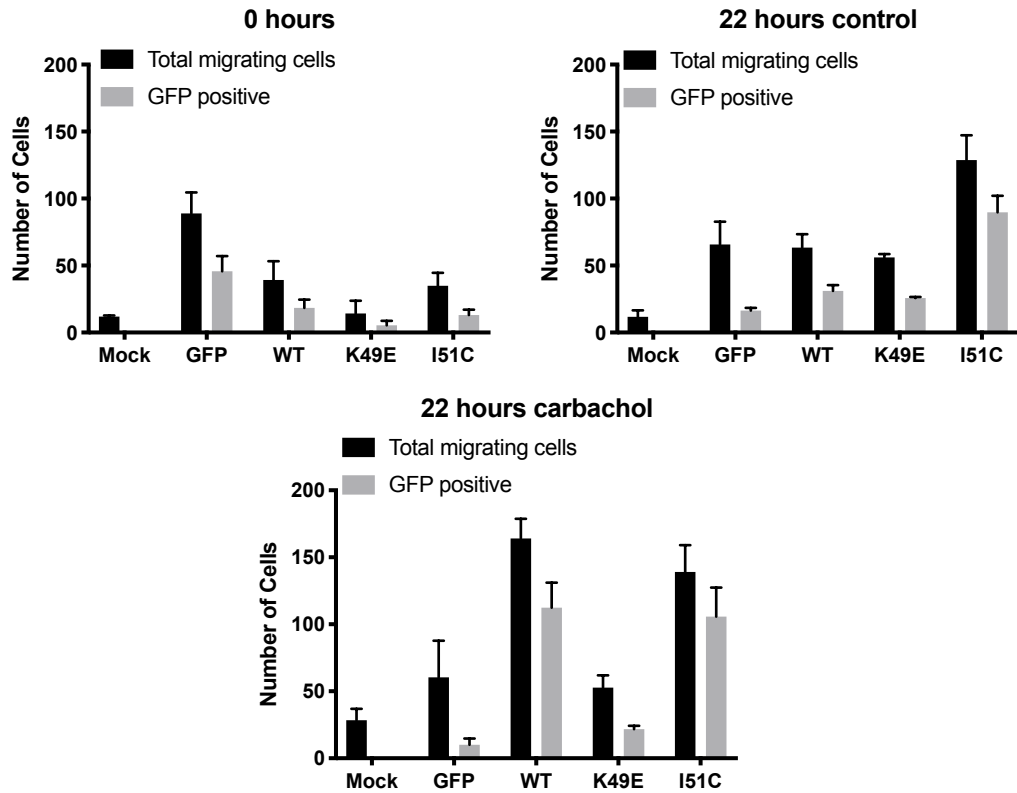


Figure 3.35 MCF-7L cells transiently overexpressing GFP, WTmGFP-SK1, mGFP-SK1-K49E or mGFP-SK1-I51C in response to carbachol in the wound after 22 hours control or carbachol treatment or immediately after scoring

The bar graphs represent the total number of cells in the wound either immediately after wounding (0 hours), or after carbachol (100 μ M, 22 hours) or control (dH₂O, 1% (v/v), 22 hours) treatment (n=3).

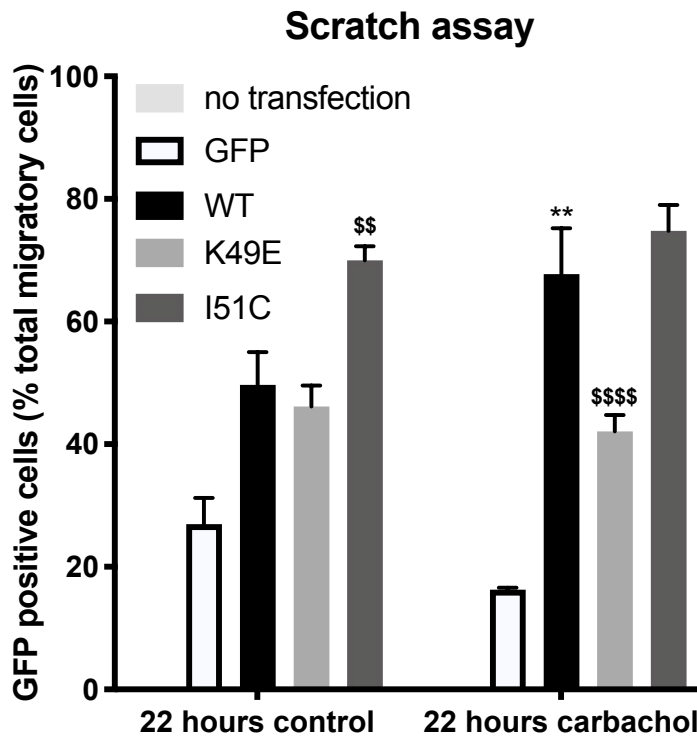


Figure 3.36 Quantification of the migration assay of MCF-7L cells transiently overexpressing GFP, WTmGFP-SK1, mGFP-SK1-K49E or mGFP-SK1-I51C in response to carbachol

The bar graph represents the % migration of GFP positive cells into the wound (n=3); **p<0.01 stimulated versus control for a given construct; \$p<0.01 for control mGFP-SK1-I51C versus control WTmGFP-SK1 and \$\$\$\$p<0.0001 for stimulated mGFP-SK1-K49E versus stimulated WTmGFP-SK1 (two-way ANOVA with Tukey post hoc test).

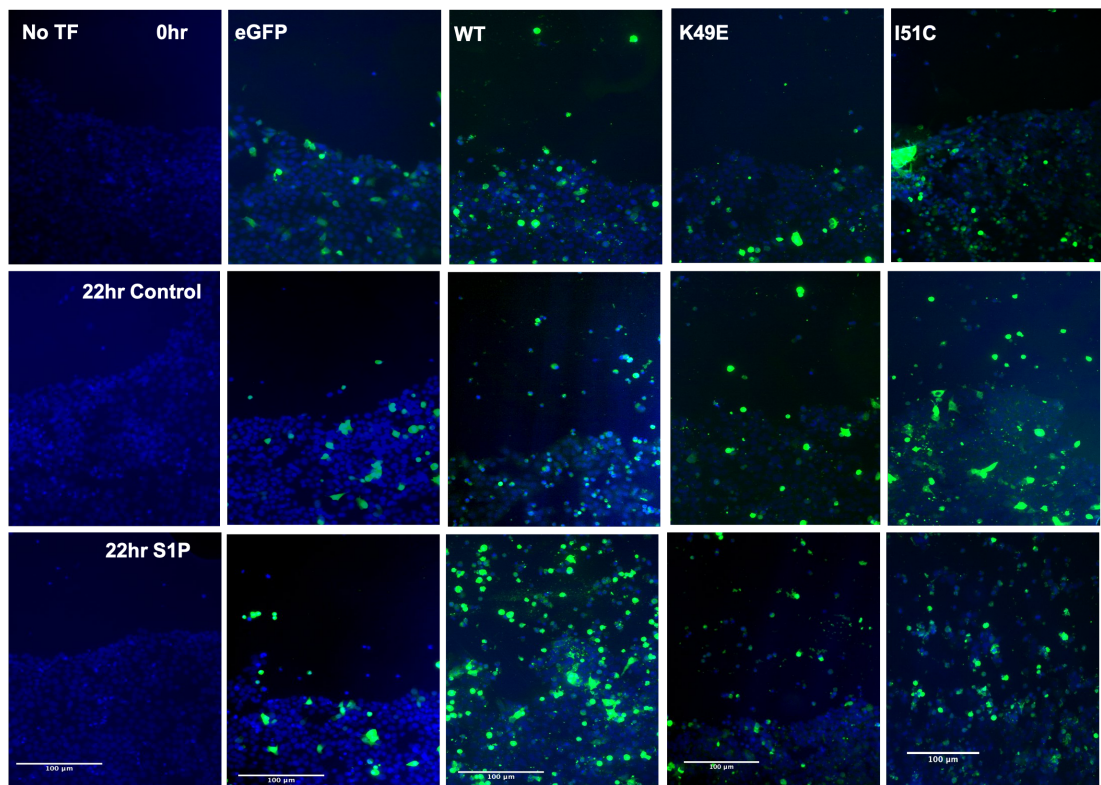


Figure 3.37 Migration assay of S1P stimulated MCF-7L cells transiently overexpressing GFP, WTmGFP-SK1, mGFP-SK1-K49E or mGFP-SK1-I51C

MCF-7L cells transiently overexpressing GFP, WTmGFP-SK1, mGFP-SK1-K49E or mGFP-SK1-I51C were treated with S1P (5 μM, 22 hours) or as control (dH₂O, 1% (v/v), 22 hours) following the application of a wound to the cell monolayer. 10x oil magnification photomicrographs showing the migration of cells into the wounded area. Results are representative of 3 independent experiments.

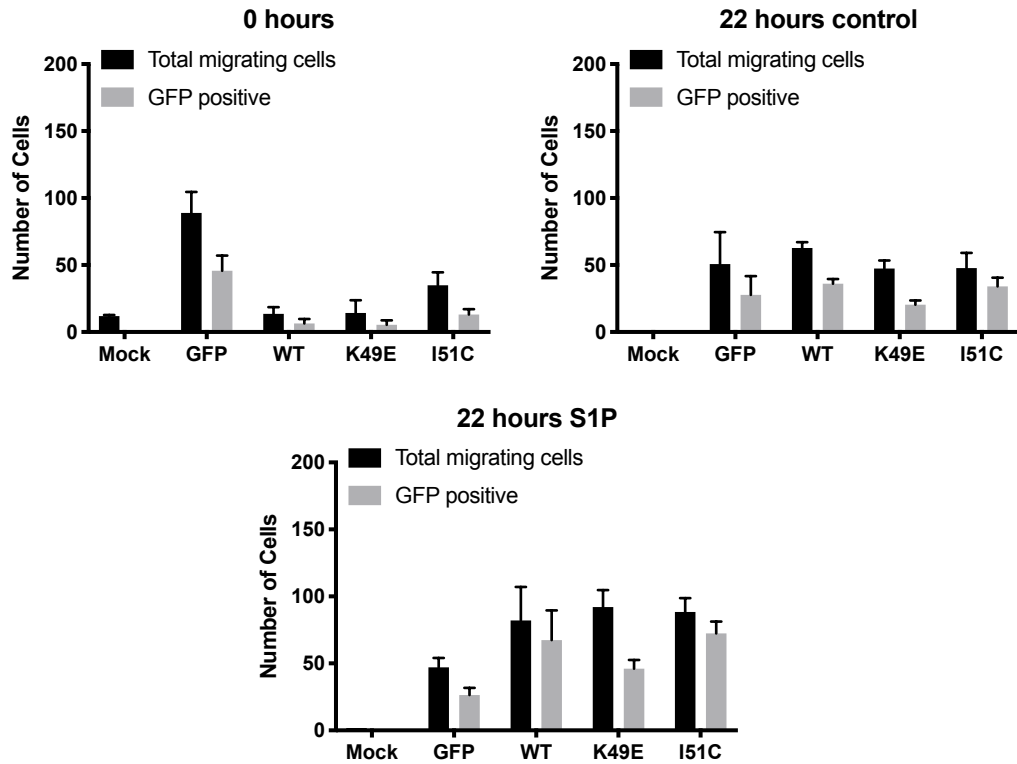


Figure 3.38 MCF-7L cells transiently overexpressing GFP, WTmGFP-SK1, mGFP-SK1-K49E or mGFP-SK1-I51C in response to S1P in the wound after 22 hours control or S1P treatment or immediately after scoring

The bar graphs represent the total number of cells in the wound either immediately after wounding (0 hours), or after S1P (5 μ M, 22 hours) or control (dH₂O, 1% (v/v), 22 hours) treatment (n=3).

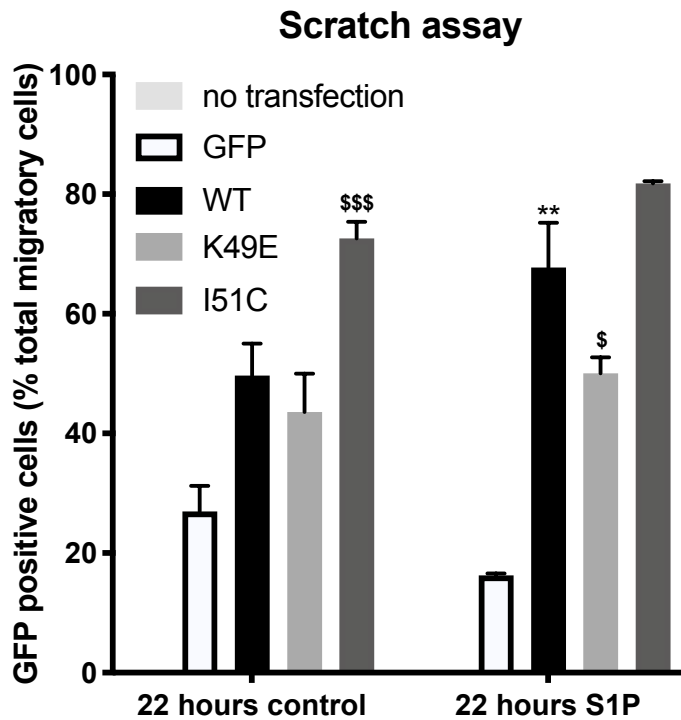


Figure 3.11 Quantification of the migration assay of MCF-7L cells transiently overexpressing GFP, WTmGFP-SK1, mGFP-SK1-K49E or mGFP-SK1-I51C in response to S1P

The bar graph represents the % migration of GFP positive cells into the wound (n=3); **p<0.01 for stimulated *versus* control for a given construct; \$\$\$p<0.001 for control WTmGFP-SK1 *versus* control mGFP-SK1-I51C and \$p<0.05 for stimulated WTmGFP-SK1 *versus* stimulated mGFP-SK1-K49E (two way ANOVA with Tukey post hoc test).

3.3 Discussion

The current study provides evidence for the translocation of SK1 from the cytoplasm to the PM in response to carbachol, S1P or PMA within MCF-7L cells. This movement is facilitated by the activation of G_q and PLD, with the latter possibly leading to acidic PA being formed at the PM to enable electrostatic interaction with the enzyme. In addition, the evidence also indicates that SK1 is subject to a monomer/dimer equilibrium that affects the translocation of SK1 to different PM micro-domains.

SK1 is able to translocate to the PM via Ser²²⁵ phosphorylation (Ser²²⁴ in *mSK1*) (Pitson et al., 2003), or alternatively in a phosphorylation-independent manner involving G_q-coupled GPCR activation (ter Braak et al., 2009). Although Ser²²⁵ phosphorylation was not measured directly, previous observations indicate that PMA is able to promote ERK-1/2 phosphorylation of *mSK1* but not *mSK1* with a Ser²²⁴ mutation (S224A) (Pitson et al., 2003). Therefore, it is highly likely that PMA is promoting SK1 translocation via ERK-1/2 phosphorylation and thus Ser²²⁴

phosphorylation in this cell system. In addition, crystallographic evidence indicates that conformation of SK1 is likely to play an important role in its translocation to the PM. Dimerisation of SK1 enables a contiguous hydrophobic and positively charged surface to form in the same plane that may be used in curvature sensing of the PM (Adams et al., 2016). It is unknown whether the monomer is able to translocate in a curvature sensing manner. In this regard, the membrane architecture may determine the translocation of SK1 to different PM micro-domains. For example, monomeric SK1 possibly lacking curvature sensing mechanisms may translocate to lamellipodia whereas dimeric SK1 may translocate to filopodia, where there might be a great degree of membrane curvature. This possibility requires further investigation.

3.3.1 SK1 translocates to plasma membrane micro-domains in a ligand-specific manner

Both endogenous SK1 and transiently overexpressed WT*mGFP*-SK1 translocate in response to S1P, PMA or carbachol in MCF-7L cells. Similarities in translocation between the endogenous and recombinant systems suggests conservation of the mechanisms involved and validating the use of *mGFP*-SK1 for investigation. It should be noted however, that in both the endogenous and overexpressed system there was cell to cell variation in both the staining of endogenous SK1 and expression of WT*mGFP*-SK1. In the endogenous system where the expression of SK1 is constant, what is observed is simply differences in the cell-to-cell binding affinity of the SK1 antibody and this is not likely to effect results. In the overexpressed system however, differences in expression may have the potential to impact what is observed in translocation. This impact is minimised by taking a large sample size which is likely to encompass cells with a range of WT*mGFP*-SK1 expression. In addition, for membrane intensity recordings, the brightness/contrast is adjusted to 'normalise' expression between cells and therefore allows comparisons to be made.

Observations of translocation in the current study were similar to those previously reported (Pitson et al., 2003; ter Braak et al., 2009), indicating that the model is robust. Further observations revealed that the phenotype of WT*mGFP*-SK1 translocation differed depending on the agonist stimulation. These PM micro-domains were subsequently defined by staining cells for cortactin, fascin and paxillin used to identify lamellipodia, filopodia and foci, respectively. Co-localisation of WT*mGFP*-SK1 with these markers was quantified using Pearson's correlation coefficient, whereby a Pearson's correlation coefficient of 1 represents perfect co-localisation (Akoglu 2018).

The formation of focal adhesions enables cells to anchor to the extracellular matrix via integrin binding and the mobilization of F-actin and is important for cancer cell invasiveness (Wehrle-Haller 2012). Furthermore, previous reports show that FTY720 S-phosphonate treatment (a sphingoid analogue of the S1P receptor agonist, FTY720) of pulmonary endothelial cells resulted in the activation of focal adhesion kinase and thus, the formation of focal adhesions (Wang et al., 2015). This may explain the formation of focal adhesions in the current study, whereby SK1 translocation that facilitates the production of S1P may also lead to the activation of focal adhesion kinase. Indeed, similar to the expression of SK1, other proteins involved in the focal adhesion kinase pathway also have increased expression in tumours. These include intracellular adhesion molecule-1 (Liu et al., 2013). Thus, the translocation of SK1 into focal adhesions in response to S1P may be important in metastasis of breast cancer cells; required to anchor cells to extracellular matrix. In the current study, none of the agonists used enhanced co-localisation of Paxillin with WTmGFP-SK1 and thus it was concluded that translocation was not to focal adhesions.

Notably, PMA or carbachol significantly increased Pearson's correlation coefficient of WTmGFP-SK1 with cortactin above control levels, inferring translocation to lamellipodia (Bryce et al., 2005). Moreover, the formation of lamellipodia has been shown to involve polarized membrane trafficking enabling protrusions into the extracellular space (Ridley et al., 1992), indicative of endocytosis (Romer et al., 2010) or migration (Veale et al., 2011); two key hallmarks of cancer (Sarkar et al., 2005; Mosesson et al., 2008). Importantly in the context of the oncogenic role of SK1, previous studies have shown that migration of cancer cells through lamellipodia formation drives metastasis (Kim et al., 2011).

Conversely, S1P significantly increased Pearson's correlation coefficient of WTmGFP-SK1 with Fascin above control levels, inferring filopodia formation (Zanet et al., 2012). These structures function differently to focal adhesions, although are similar in appearance (Wehrle-Haller 2012). Filopodia protrude from lamellipodia to provide the cell with chemosensory information as it migrates through the microenvironment of invading tissues (Pfisterer et al., 2020; Yoshihara et al., 2020). These S1P-induced filopodia are similar in appearance to those observed in previous reports, which also show that formation is dependent on the phosphorylation of ezrin, radixin and moesin via S1P₂ activation (Gandy et al., 2013).

Perhaps surprisingly was that the Pearson's correlation coefficient was still positive for that of control treated cells. This may be due to the relatively small level of re-localisation of SK1 from the cytoplasm/perinuclear regions to the PM. In addition, the majority of the staining of WT*m*GFP-SK1 and cortactin, fascin or paxillin was in perinuclear regions. This may be attributed to synthesis of both of the proteins and thus explains why Pearson's correlation coefficient remains high without stimulation. These results indicate that the different PM sub-structures for which WT*m*GFP-SK1 is able to translocate to in response to PMA or carbachol are lamellipodia, and filopodia in response to S1P. In summary, by understanding the signaling involved in the translocation of SK1 to specific PM micro-domains, this has the potential to provide novel, more targeted therapeutic targets for cancer metastasis.

3.3.2 SK1 translocates to the plasma membrane in an ERK-1/2-independent manner

The current study aimed to characterise the mechanisms through which SK1 is able to translocate to the PM in response to GPCR activation. In this respect, it is postulated that treatment with S1P (acting on S1P₃) or carbachol (acting on M₃ mAChR) impacts on the monomer/dimer equilibrium and thus translocation to different PM micro-domains.

Firstly, the presence of phosphorylation-dependent and phosphorylation-independent mechanisms of SK1 translocation was demonstrated. This was evidenced by the use of PD98059 that reduces ERK-1/2 phosphorylation and thus reduces proliferation (Shimo et al., 2007) and migration (Hao et al., 2007). The results demonstrated that PD98059 reduced the phosphorylation of ERK-1/2, thereby preventing the phosphorylation-dependent translocation previously identified to be via phosphorylation of Ser²²⁵ (Ser²²⁴ in *m*SK1). This was observed as a lack of translocation of endogenous SK1 and WT*m*GFP-SK1 in response to PMA, but not S1P or carbachol. These findings indicate that PMA promotes the translocation of SK1 in an ERK-1/2 dependent manner. Even though S1P and carbachol activate ERK-1/2, the findings with PD98059 demonstrate that translocation in response to S1P and carbachol is ERK-1/2 independent. This is likely due to the extent of ERK-1/2 activation, where PMA is most effective and activates ERK-1/2, possibly above a threshold level that is required to phosphorylate SK1. Moreover, the results also corroborate with previous reports demonstrating SK1 translocation in response to S1P or carbachol is independent of Ser²²⁵ (ter Braak et al., 2009) and having no

requirement for ERK-1/2. Thus, translocation of SK1 in response to S1P and carbachol is Ser²²⁵ phosphorylation-independent.

3.3.3 SK1 translocation requires G_q

PM localisation determinants involved in the translocation of SK1 were identified. SK1 is able to translocate from the cytoplasm to the PM following stimulation with platelet-derived growth factor, nerve growth factor, insulin-like growth factor or tumour necrosis factor- α (Alvarez et al., 2007). In addition, SK1 is also able to be activated by GPCRs such as S1P₁₋₅ (Pyne et al., 2010) and M₃ mAChR (ter Braak et al., 2009). More specifically, activation of G_q-coupled GPCRs via carbachol or S1P results in rapid, sustained translocation of SK1 to the PM (ter Braak et al., 2009; Long et al., 2010). It was therefore hypothesised that G_q is important in facilitating the translocation of WTmGFP-SK1 to the PM. To investigate this, YM254890 was used that specifically inhibits G_q/G₁₁ by preventing the exchange of GDP for GTP (Takasaki et al., 2004), whilst having no effect on the activity of other G-proteins (Nishimura et al., 2010). YM254890 blocked the translocation of WTmGFP-SK1 in response to S1P, carbachol and PMA. These observations are supported by similar reports in HEK293 cells, where constitutively active G_q alone is sufficient to drive the translocation of SK1 (ter Braak et al., 2009). Therefore, G_q is essential for the GPCR- and ERK-mediated translocation of SK1.

Perhaps surprisingly PMA-mediated translocation was inhibited. This may be explained by the activity of PMA on G_q. In this regard, it is known that palmitoylation is required for G_q membrane attachment and function (Wedegaertner et al., 1993). Moreover, PMA can activate G_q through rapid and dynamic palmitoylation of G α_q (Stanislaus et al., 1997). Therefore, PMA-stimulated translocation of SK1 might regulation involving palmitoylation of G α_q . It remains to be determined whether G_q binds directly or indirectly to SK1.

3.3.4 SK1 translocation requires PLD activation

To understand the importance of electrostatic potential between the PM and SK1 in facilitating its translocation FIPI was used, which is a compound that inhibits the PLD-1/2 activity and hence the production of PA (Su et al., 2009). FIPI was shown to block the translocation of WTmGFP-SK1 in response to S1P, carbachol and PMA. These observations are consistent with previous reports that demonstrate the translocation of SK1 to areas of the PM that are rich in PA. Here the authors demonstrate that SK1

is able to directly interact with the acidic phospholipid, independent of its catalytic activity (Delon et al., 2004), thereby suggesting PA generation alone is sufficient to drive translocation. In addition, phosphorylation-dependent translocation has been shown to promote the binding of SK1 to an additional acidic membrane-bound phospholipid, phosphatidylserine (Stahelin et al., 2005). This suggests that GPCR-mediated translocation and ERK-1/2-mediated translation is dependent on the production of membrane-bound PA or PS that may suggest potential mechanistic overlap. Importantly, PMA, S1P₃ and muscarinic receptors via PKC can activate PLD to induce formation of PA (Banno et al., 2001; Han et al., 2007; Hu et al., 2011), and this provides explanation for the translocation of SK1 to PM micro-domains (e.g. lamellipodia and filopodia).

Taken together, SK1 translocation is reduced by ablating possible PA production or G_q activation. This suggests neither PM localization determinant is able to compensate for the loss of the other. This can be explained by the fact that G_q is upstream of PKC and therefore PLD/PA formation e.g. they are in a sequential pathway. Inhibition of either G_q or PLD will therefore, not compensate for each other.

3.3.5 Monomeric and dimeric SK1 translocate to different PM micro-domains

Originally, chromatography and western blot analysis indicated SK1 to be a monomeric protein, with individual protomers being catalytically active (Olivera et al., 1998). Since then, multiple crystal structures have become available (Wang et al., 2013; Wang et al., 2014) that has provoked further investigation into the structure of SK1. Findings from these studies suggests that SK1 can exist as a dimer (Adams et al., 2016; Bayraktar et al., 2017). Importantly, dimerization enables contiguous hydrophobic and positively charged surfaces to align in the same plane, allowing for simultaneous PM embedding and access to SPH a curvature-sensitive manner (Adams et al., 2016). Therefore, it is proposed that monomeric and dimeric SK1 are able to translocate to distinct PM micro-domains based on their quaternary structure.

In this case, ligands might be able to alter the position of the SK1 monomer/dimer equilibrium to induce translocation to specific PM micro-domains. The consequence of the differential localization of SK1 to different PM micro-domains might be distinct signaling by the monomer *versus* dimer to thereby explain, in part, the pleiotropic properties of S1P. Previous literature suggests SK1 dimerisation occurs by either β 1- β 2 and β 2- β 2 interactions, or α 2- β 1 and α 2- β 2 interactions (Bayraktar et al., 2017).

However, herein it is proposed that dimerization occurs through packing of the $\beta 2$ strand NTD:NTD to enable the formation of a salt bridge. This modest interface would provide plasticity in dimerization, allowing the enzyme to dynamically shift between monomeric and dimeric states.

To investigate the presence of a monomer/dimer equilibrium two mutagenesis approaches were adopted to either to attempt to disrupt dimer formation by charge opposition or to 'stabilise' dimer formation by incorporating an engineered disulphide bridge. Overexpression of mutant *mGFP-SK1* indicated that *mGFP-SK1-K49E* localized to lamellipodia, albeit reduced when compared to *WTmGFP-SK1*, and *mGFP-SK1-I51C* localized to filopodia. The reduced translocation of *mGFP-SK1-K49E* when compared to the *WTmGFP-SK1* may be explained by the charge reversal on the surface of the enzyme. The substitution of a lysine for a glutamic acid residue will reduce the overall net positive charge present on the surface of SK1. This is likely to reduce the potential difference between SK1 and membrane-bound anionic phospholipids understood to be important for translocation (Adams et al., 2016).

Importantly, *mGFP-SK1-K49E* localized to lamellipodia and *mGFP-SK1-I51C* to filopodia, irrespective of the agonist used. This may be explained by disruption the monomer/dimer equilibrium by potentially having either solely monomeric or dimeric SK1. In this case, it is proposed that stimulation of *WTmGFP-SK1* leads to a shift in the monomer/dimer equilibrium that in turn determines whether the enzyme translocates to lamellipodia or filopodia. The agonists are unable to shift the equilibrium in the case of *mGFP-SK1-K49E* and *mGFP-SK1-I51C* due to the mutagenesis and potential disruption to the monomer/dimer equilibrium. This constrains translocation of the mutants to lamellipodia or filopodia. Taken together, the ligands do not appear influence the translocation of SK1 by regulating architecture of the PM *per se* because agonist specificity would still be retained by the mutants in terms of translocation to these structures if this was the case. Instead, the ligands influence the monomer/dimer equilibrium of the WT enzyme, which, in turn, determines the PM sub-structure localization of the enzyme.

Extrapolated to the *WTmGFP-SK1* system, these observations suggest that PMA and carbachol shift the equilibrium of SK1 in favour of the monomer, thereby promoting the translocation to lamellipodia. In contrast, S1P likely promotes dimeric assembly of the WT enzyme and translocation to filopodia. For this to happen, receptor ligands

may promote the association of different proteins located in lamellipodia *versus* filopodia with the monomer or dimer respectively. This may be achieved by ligand-specific association of the monomer or dimer with these proteins to establish a new equilibrium that could alter the position of the monomer/dimer equilibrium. Alternatively, the PM may function in an 'auto-catalytic' manner to influence oligomerization of SK1, dependent on the abundance of PA in certain PM micro-domains. For example, in lipid-rafts where GPCRs are more abundant, receptor activation may lead to a higher density of PA being formed in these areas in comparison to the rest of the PM. This may explain why *mGFP-SK1-I51C* that we predict is dimeric localized to filopodia, whereby the high density of positive charge at the dimerization groove provides a greatly increased affinity for PA, enabling the translocation to filopodia. Thus, it is speculated that filopodia contains less PA than lamellipodia that because of the possible increased avidity of the dimer *versus* the monomer for PA, would result in preferential translocation of the dimer to filopodia. Translocation to lamellipodia by the monomer might require higher PA. Alternatively, dimeric assembly and the presence of a concave positive charge may provide dimeric SK1 with additional curvature sensing properties over that of monomeric SK1. In this regard the dimer is likely to translocate to areas of the PM with higher degrees of membrane curvature, possibly explaining why dimeric SK1 is present in filopodia. Indeed, it is unclear whether the monomer is able to bind in a similar curvature-sensitive manner because of the lack of planarity between LBL-1 and the positive charged cluster. This represents a potential divergence point that would enable the monomer and dimer to bind to different PM micro-domains that exhibit different structural architecture. Furthermore, the increased avidity for PA of the dimer suggests that residency time in filopodia might be more sustained than the monomer in lamellipodia thereby leading to different kinetics of S1P formation that could result in different signaling pathways being activated by the dimer compared with the monomer. This possibility requires further study.

The presence of an SK1 monomer/dimer equilibrium might provide the cell with temporal and spatial regulation of S1P production, potentially regulating different cell functions or disease states (such as oncogenesis) and providing S1P with pleiotropic properties. Hence, the functional differences of *mGFP-SK1-K49E* and *mGFP-SK1-I51C* that we predict lead to the formation of solely monomeric and dimeric SK1, respectively, was investigated.

3.3.6 Monomeric and dimeric SK1 function differently

S1P-stimulated translocation of SK1 has been shown to mobilise actin into lamellipodia necessary for migration (Long et al., 2010; Lim et al., 2011). Moreover, SK1 has been reported to bind actin filaments in macrophages (Kusner et al., 2007). *mGFP-SK1-I51C* showed similar levels of co-localization with F-actin compared with the *WTmGFP-SK1* and, in contrast to *WTmGFP-SK1* this was in filopodia. On the other hand, *mGFP-SK1-K49E* displayed reduced, more diffuse co-localization. This is concurrent with observations whereby *mGFP-SK1-K49E* was less able to translocate to the PM in response to carbachol and which may be explained by the reduced avidity for the PM discussed in 3.3.5.. Previous studies have shown that SK1 can bind actin (Kusner et al., 2007). Therefore, the reduced co-localisation of *mGFP-SK1-K49E* with actin might simply reflect reduced translocation of actin-bound SK1.

S1P binding to S1P₃ has been shown to promote the migration of MCF-7L cells in a manner which is dependent on the translocation of SK1 (Long et al., 2010). Conversely, knockdown of SK1 has been reported to reduce the migration of MCF-7L cells (Sarkar et al., 2005; Doll et al., 2007). Therefore, the functional role of monomeric and dimeric SK1 was explored by investigating cell migration. It should be noted that even though the potential of measuring proliferating cells was minimised through quiescence, MCF-7L cells are cancer cells and hence serum-independent, therefore it is a possibility that some 'migrating' cells were actually proliferating cells. The results demonstrate that cells over-expressing *mGFP-SK1-K49E* were unable to migrate in response to carbachol or S1P. The translocation of *mGFP-SK1-K49E* to lamellipodia was reduced, but not abolished, in response to carbachol, suggesting that a threshold level of SK1 translocation to lamellipodia is required in order to promote migration. Moreover *WTmGFP-SK1* exhibits increased migration in response to carbachol or S1P, thereby suggesting that both lamellipodia and filopodia localization of SK1 can drive migration. These findings support a link between lamellipodia and filopodia localization of SK1 and migration. Interestingly, the *mGFP-SK1-I51C* mutant promoted migration in the absence of carbachol. The reason for this is unknown. One possibility is that the scratching and stress to cells promotes translocation of this mutant to the PM. Alternatively, the *mGFP-SK1-I51C* mutant might regulate intracellular signaling pathways that promote cell migration independent of its localization at the PM. These possibilities require further investigation.

3.4 Summary and future directions

In conclusion, this chapter provides evidence for the translocation of SK1 from the cytosol to the PM that is dependent on G_q activation and the generation of PLD-derived PA. In addition, evidence is presented for novel regulatory mechanisms of SK1 translocation, involving dimerisation of SK1. Results from mGFP-SK1-I51C and mGFP-SK1-K49E suggest that SK1 is subject to a monomer/dimer equilibrium enabling translocation to different PM micro-domains, which is influenced in a ligand-specific manner. Therefore, specifically preventing monomeric SK1 translocation to lamellipodia and reducing cancer cell migration may provide a novel therapeutic approach for inhibiting metastasis. Strategies to prevent dimerization might also be usefully exploited to prevent disease-forming mechanisms that are governed by the dimer and these need to be identified in the future. This latter approach has been demonstrated to inhibit the activity of other signaling proteins, such as RAF (Hu et al., 2013) and Ras (Nan et al., 2015).

The evidence herein suggests that PMA resulting in ERK-1/2 activation promotes monomeric SK1 translocation to lamellipodia. In addition, carbachol-stimulated translocation of SK1 to lamellipodia involves the monomer but occurs in a phosphorylation-independent manner. S1P on the other hand results in the translocation of dimeric SK1 to filopodia in a phosphorylation-independent manner. In agreement with these findings, vascular smooth muscle cells have been reported to retain the ability to form filopodia and migrate in the presence of PD98059 (Li et al., 2006), thereby further reinforcing the notion that translocation of dimeric SK1 to filopodia is phosphorylation-independent. The improved understanding of the monomer/dimer SK1 equilibrium might offer better therapeutic targeting to be achieved to inhibit neoplastic conversion and metastasis.

Future studies will involve investigating whether mGFP-SK1-I51C and mGFP-SK1-K49E are constitutively dimeric or monomeric proteins, respectively. This is important, to attribute the differences in translocation to imbalances to the monomer/dimer equilibrium. This will involve a proximity ligation assay whereby dimerization of the protein can be observed, thereby confirming that the changes in the amino acid sequence has led to the changes at a conformational level. Previous attempts to characterise these mutants have included the use of native SDS-PAGE, however these were unsuccessful and due to the COVID-19 pandemic experimentation was halted and thus characterisation was not achieved.

Chapter 4

**The role of the C-terminus in
the translocation of SK1**

4.0 The role of the C-terminus in the translocation of SK1

4.1 Introduction

Oncogenic transformation of cells involves the translocation of SK1 from the cytoplasm to the PM to allow access to the enzyme's substrate, SPH (Xia et al., 2000). Indeed, constitutive localisation of SK1 at the PM promotes neoplastic conversion, which is dependent upon the catalytic activity of SK1 and therefore, formation of S1P (Pitson et al., 2005). The CTD of SK1 hosts the SPH binding site (J-channel), whereas the NTD binds ATP, necessary for phosphorylation of SPH. Between the two domains resides the catalytic centre. PS and PA are integral in the binding of SK1 to the PM, whereby membrane engagement and curvature sensing involves the exposure of a hydrophobic patch on the overleaf of LBL-1 (Leu¹⁹⁴/ Phe¹⁹⁷/ Leu¹⁹⁸) and positive charged residues (Lys²⁷/ Lys²⁹/ Arg¹⁸⁶) (Shen et al., 2014; Pulkoski-Gross et al., 2018). In this sense, interdomain movement may allow for the alignment of a contiguous binding interface to ultimately facilitate the translocation of SK1.

The SK1 C-terminus binds various proteins, including multiple binding tumour necrosis factor receptor-associated factor 2 (TNF α 2) (Xia et al., 2002), and protein phosphatase 2A (PP2A) that is known to deactivate the enzyme (Barr et al., 2008; Pitman et al., 2011). It has previously been suggested that the C-terminal tail (365-CVEPPPSWKPQQMPPPEEPL-384) has an important role in regulating SK1 translocation (Adams et al., 2016), evidenced by the enzyme displaying constitutive activation and Ser²²⁵-independent PM localisation as a result of complete removal of the C-terminus alone (Hengst et al., 2010). Moreover, Gly³⁶⁴ is located adjacent to the C-terminus end of helix- α 5 that is conserved across *mSK1* and *hSK1* and which is involved in ATP binding and catalytic activity as part of the T-loop. Regulation of activity may therefore involve residues 364-367 that are well positioned to cap helix- α 5 via hydrogen donor interactions and movement of the cap might affect T-loop plasticity and hence catalytic turnover and SK1 translocation. It is therefore hypothesised that orientation of the C-terminus may control interdomain movement and thus the critical alignment of hydrophobic patches on LBL-1 and positively charged residues at the dimerization groove necessary to drive translocation of SK1. This said, the C-terminus is not present in the available crystal structures (Wang et al., 2013; Wang et al., 2014) and therefore how it regulates translocation is not fully understood. We therefore proposed that the C-terminal is paramount in controlling the

translocation of SK1 to the PM via interdomain movement and this is investigated by sequential truncation of the C-terminal tail.

Alternative mechanisms may involve the regulatory-loop (R-loop), which is situated between strands $\beta 9/ \beta 10$, opposite the membrane binding surface and hosts the solvent-exposed Ser²²⁵ phosphorylation site for ERK, which is conserved in *mSK1* and *hSK1*. The complete mechanisms regulating phosphorylation-dependent translocation are also not currently known, but are understood to involve Ser²²⁵ phosphorylation in *hSK1* (Pitson et al., 2003) and CIB1/2 (Jarman et al., 2010; Zhu et al., 2017) to promote and negate SK1 translocation respectively. It is possible, that interdomain movement via Ser²²⁵ phosphorylation, analogous to the C-terminal tail in phosphorylation-independent translocation, may also affect the presentation of the positive electrostatic potential surface of the NTD and LBL-1. In this sense, Ser²²⁵ phosphorylation may displace Asp²³⁵ on the R-loop tip from a basic pocket composed of His¹⁵⁶/Arg¹⁶²/His³⁵⁵ to present key basic residues (Adams et al., 2016). Moreover, Ser²²⁵ phosphorylation may also modulate dimerization of the enzyme and thus translocation potential of the enzyme (Adams et al., 2016).

Evidence for the phosphorylation-dependent and -independent translocation of SK1 to the PM raises the question as to whether any mechanistic overlap exists between what were originally considered mutually exclusive mechanisms (Pitson et al., 2003; ter Braak et al., 2009). Indeed, SK1 has been shown to translocate to the PM as a result of G_q activation; independent of Ser²²⁵ phosphorylation (ter Braak et al., 2009). However, it may be possible that Ser²²⁵ phosphorylation results in conformational changes within the enzyme to displace the C-terminus, thus enabling interdomain movement and facilitating the alignment of a contiguous membrane binding interface. This would provide structural basis for a unified mechanism of translocation that encompasses both translocation/activation via phosphorylation of Ser²²⁵ and translocation/activation independent of Ser²²⁵ phosphorylation. We therefore investigated the importance of the C-terminal tail and R-loop for the translocation of SK1 from the cytoplasm to the PM in MCF-7L cells. We also explored potential G_q and PA interactions with SK1 in terms of the functional role of the C-terminus. Specific focus concerned the translocation of SK1 to different PM micro-domains when the C-terminus or R-loop are disrupted.

4.2 Results

4.2.1 Generation of serially truncated C-terminal mutants of mGFP-SK1

The role of the C-terminus in terms of modulating inter-domain movement and thus alignment of a contiguous membrane-engagement surface was investigated. In order to study the importance of the length and specific regions of the C-terminus, site-directed mutagenesis was used to introduce premature stop codons to create C-terminally truncated mutants of *mGFP-SK1*. The C-terminus was truncated by 5, 10, 15, 19 and 25 amino acids to create the mutants T1, T2, T3, T4 and T5 respectively (Fig. 4.1). Moreover, T4 and T5 lack the putative α 5-cap (corresponding to *hSK1* 364-367), whereas this region is retained in T1 to T3. Furthermore, T4 retained Gly³⁶⁴ understood to act as a pivot for the cap (Adams et al., 2016), whereas T5 had the C-terminus completely removed. The rest of the *mGFP-SK1* T1/2/3/4/5 sequence remained unchanged.

	351	361	371	381
eGFP-WT mSK1	QVHPNYLWMV	CGSRDAPSGR	DSRRGPPPEE	P
eGFP-mSK1-T1	QVHPNYLWMV	CGSRDAPSGR	DSRRGP	
eGFP-mSK1-T2	QVHPNYLWMV	CGSRDAPSGR	D	
eGFP-mSK1-T3	QVHPNYLWMV	CGSRDA		
eGFP-mSK1-T4	QVHPNYLWMV	CG		
eGFP-mSK1-T5	QVHPNY			

Figure 4.1 Mutagenesis of mGFP-SK1 to create mGFP-SK1 T1-5

C-terminally truncated mutants of WT*mGFP-SK1* were created by sequentially reducing the length of the C-terminus. T1, T2, T3, T4 and T5 have 5, 10, 15, 19 and 25 amino acids removed respectively.

4.2.2 Translocation of C-terminally truncated mutants of mGFP-SK1

The importance of the length, or specific regions of the C-terminus for translocation was explored. For this, MCF-7L cells transiently overexpressing WT*mGFP-SK1* or *mGFP-SK1* T1-5 were tested for their ability to translocate in response to S1P, PMA or carbachol. Confirmation of expression of WT*mGFP-SK1* and *mGFP-SK1* T1-5 was by western blot analysis (Fig. 4.2).

Notably, compared with WT enzyme, *mGFP-SK1* T1 lacking the last 5 amino acids at the C-terminus (PPEEP) that are conserved in the *hSK1*, exhibited reduced translocation in response to carbachol or S1P, whilst translocation in response to PMA was unaffected (Fig. 4.3). Furthermore, it was shown that *mGFP-SK1* T1 did not translocate to the PM within a 10 minute stimulation period in response to S1P or carbachol, thereby suggesting that *mGFP-SK1* T1 does not bind and then dissociate

from the membrane at a rate that is faster than WT*mGFP-SK1* (Fig. 4.7). Interestingly, translocation in response to S1P or carbachol was restored following further truncation of the C-terminus (e.g. *mGFP-SK1* T2-5) (Fig. 4.3).

The reduced ability of the T1 mutant to translocate, and restoration of T2, suggests that last 10 amino acids of the C-terminus are important for GPCR-mediated translocation of SK1, although these do not appear to be crucial for phosphorylation-dependent translocation. These findings suggest the last 5 amino acids host a protein binding site that is required to bind the C-terminus and that amino acid residues 6-10 might function as a translocation brake.

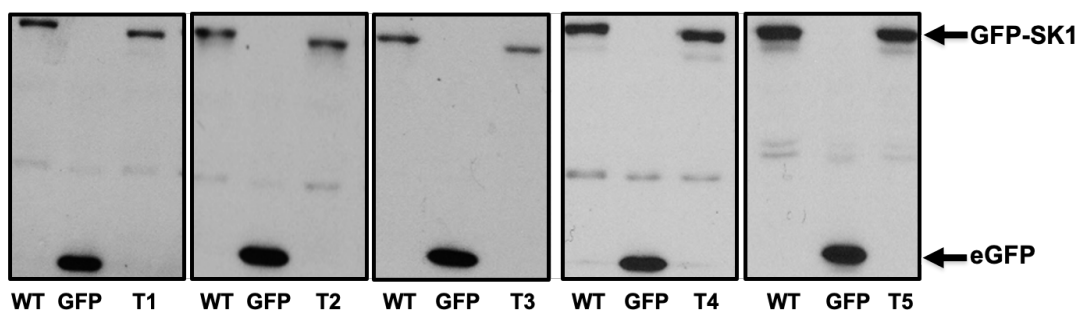


Figure 4.2 *mGFP-SK1* T1-5 expression in MCF-7L cells

Western blot showing whole cell lysates of MCF-7L transiently overexpressing truncated forms of *mGFP-SK1*. The western blot illustrates a mobility shift when compared to the WT*mGFP-SK1* following truncation of the C-terminal tail. Results are representative of 3 independent experiments.

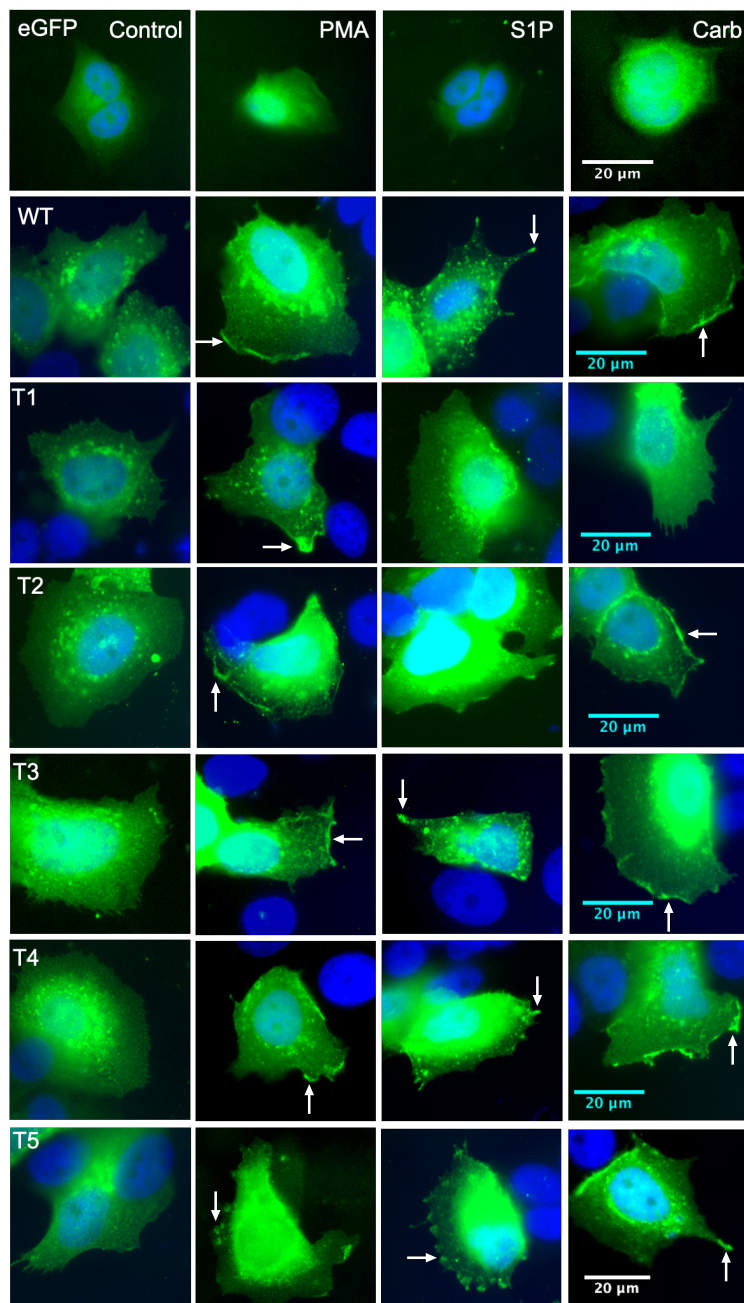


Figure 4.3 Stimulated MCF-7L cells transiently overexpressing eGFP, WTmGFP-SK1 or mGFP-SK1 T1-5

40x oil magnification photomicrographs of cells showing the translocation of transiently overexpressed WTmGFP-SK1 or mGFP-SK1 T1-5 in response to S1P (5 μ M, 10 mins), PMA (1 μ M, 10 mins) or carbachol (100 μ M, 10 mins) and compared with vehicle treated cells (Con, DMSO, 1% (v/v)). Cells were processed (see methods) and mounted with a DAPI-containing mount to stain DNA (blue). Forms of mGFP-SK1 were detected by GFP (arrows represent translocated SK1). Representative result is of three independent experiments.

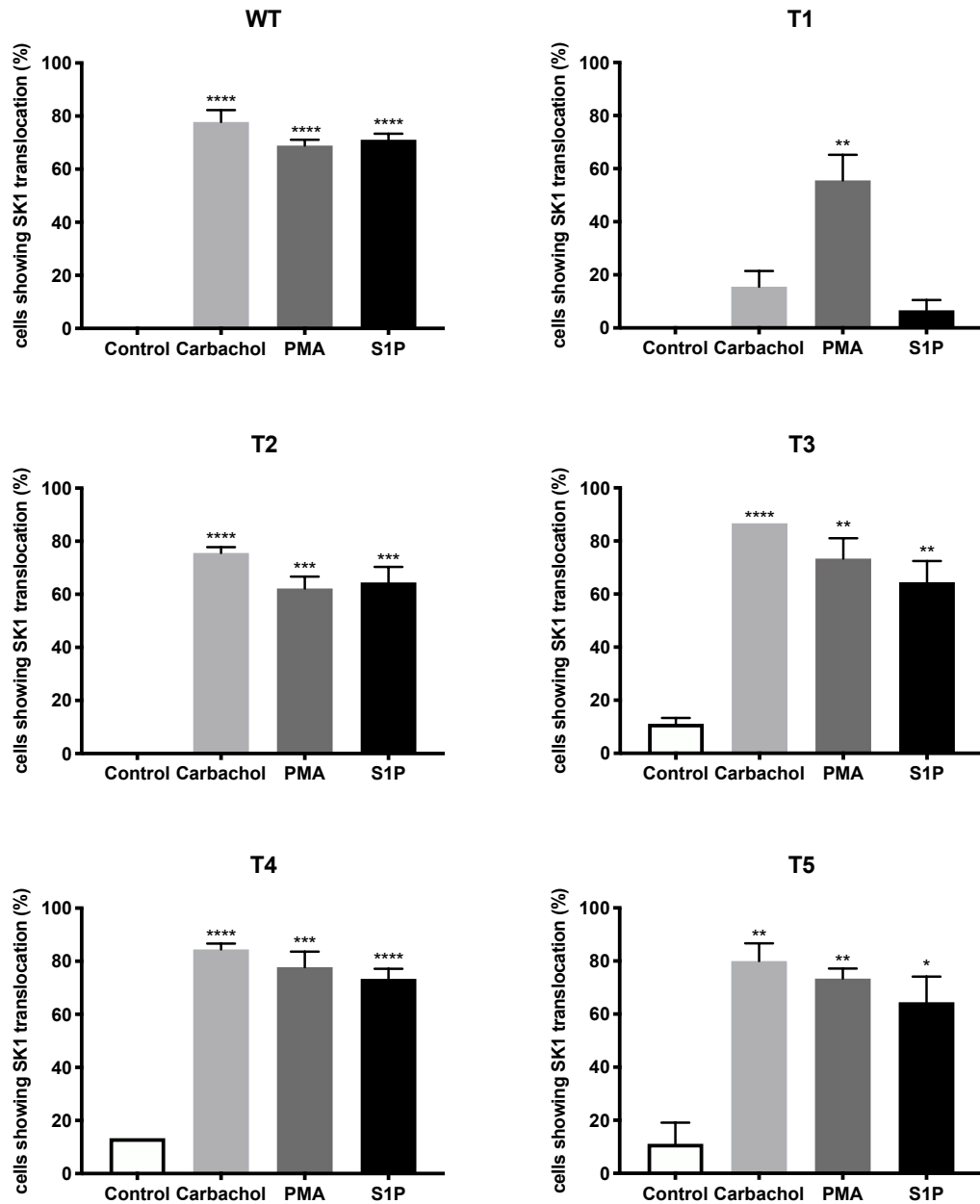


Figure 4.4 % of MCF-7L cells transiently overexpressing WTmGFP-SK1 or mGFP-SK1 T1-5 showing translocation in response to various stimuli

The bar graph represents the % of MCF-7L cells transiently overexpressing WTmGFP-SK1 showing translocated WTmGFP-SK1 in response to S1P (5 μ M, 10 minutes), PMA (1 μ M, 10 minutes) or carbachol (100 μ M, 10 minutes) and compared to control cells (DMSO, 0.1% (v/v)). 15 random cells on 3 separate cover slips were analysed (n=3); *p<0.05, **p<0.01, ***p<0.001, ****p<0.0001 for stimulus versus control (unpaired, two-tailed t-test).

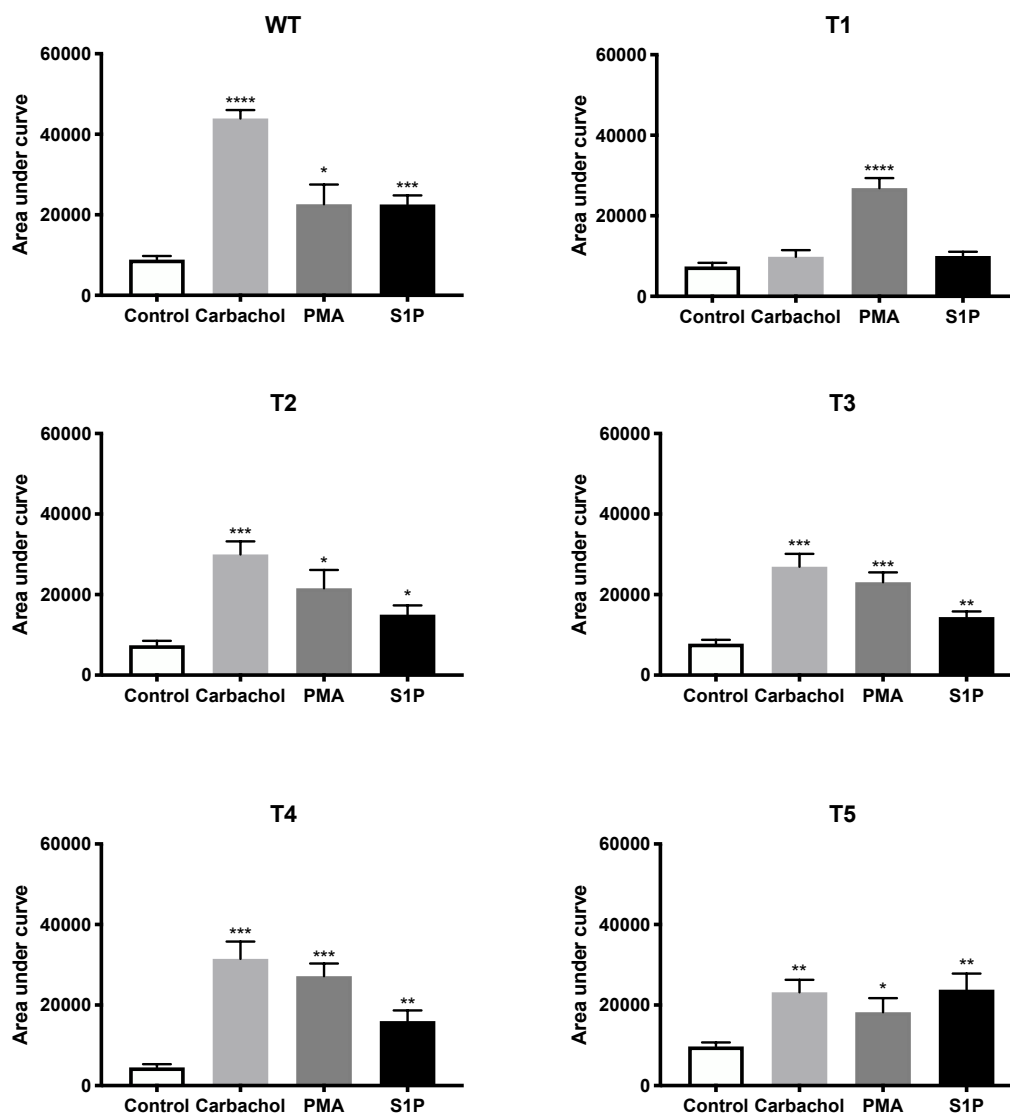


Figure 4.5 Area under curve analysis of MCF-7L cells transiently overexpressing WTmGFP-SK1 or mGFP-SK1 T1-5 in response to various stimuli

The bar graphs represent the AUC of the total level of WTmGFP-SK1 or mGFP-SK1 T1-5 translocation in response to S1P (5 μ M, 10 mins), PMA (1 μ M, 10 mins) or carbachol (100 μ M, 10 mins) and compared with control cells (DMSO 1% (v/v)) (n=5); *p<0.05, **p<0.01, ***p<0.001, ****p<0.0001 for stimulus versus control (unpaired, two-tailed t-test).

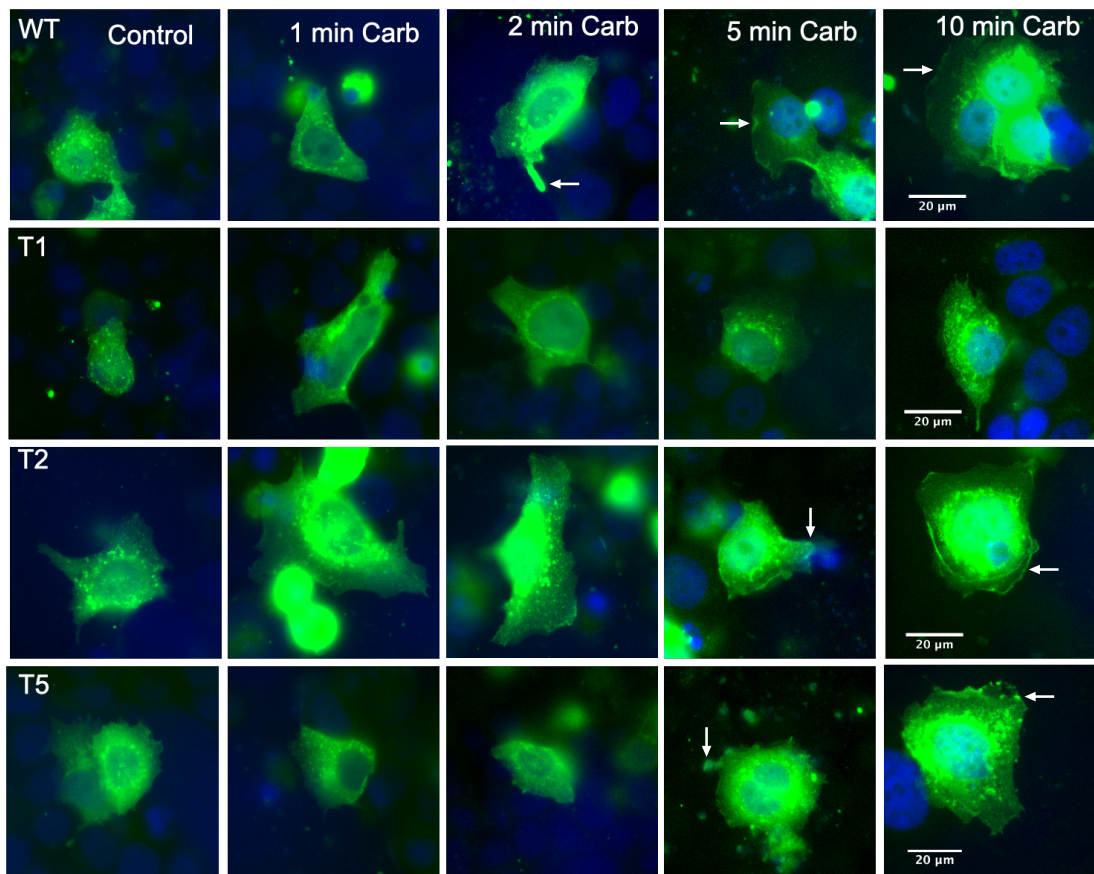


Figure 4.6 Time-course of WTmGFP-SK1 or mGFP-SK1 T1/2/5 translocation

40x oil magnification photomicrographs of MCF-7L cells transiently overexpressing WTmGFP-SK1 or mGFP-SK1 T1/2/5 were treated with carbachol (100 μ M; 1, 2, 5 or 10 mins) and compared to vehicle treated cells (DMSO, 1% (v/v)). Cells were processed and mounted with a DAPI-containing mount to stain DNA (blue). *m*GFP-SK1 forms were detected by GFP (arrows represent translocated SK1). Representative result is of three independent experiments.

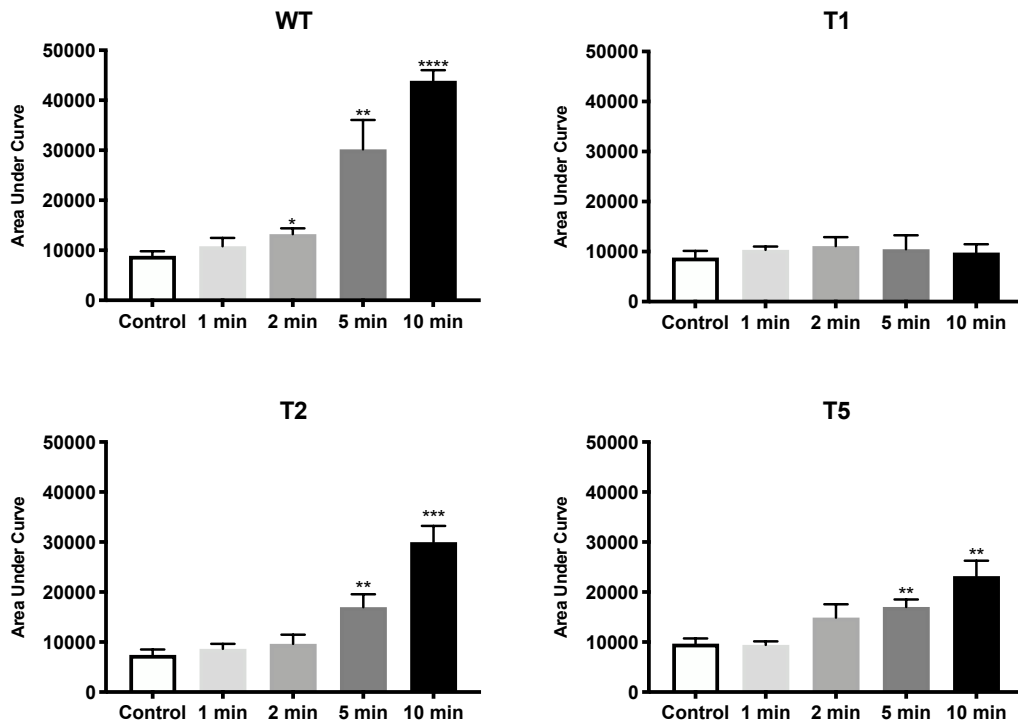


Figure 4.7 Area under curve analysis of time-course of stimulated MCF-7L cells transiently overexpressing WTmGFP-SK1 or mGFP-SK1 T1/2/5

The bar graph represents the AUC of the total level of WTmGFP-SK1 or mGFP-SK1 T1/2/5 translocation in response to carbachol (100 μ M; 1, 2, 5 or 10 mins) and compared with control cells (DMSO 1% (v/v)) (n=5); **p<0.01, ***p<0.001, ****p<0.0001 for stimulus versus control (unpaired, two-tailed t-test).

4.2.3 Phenotypes of translocation of mGFP-SK1 T1-5

Observations in 3.2.1 revealed that carbachol or PMA promoted the translocation of SK1 to lamellipodia, whereas treatment with S1P led to SK1 being localized to filopodia. In relation to this, the impact of the C-terminus length on the translocation to different PM micro-domains was explored.

mGFP-SK1 T1 produced a similar phenotype of translocation to that seen with WTmGFP-SK1 in response to PMA, whilst being unable to translocate following treatment with carbachol or S1P (Fig. 4.8). This suggests mGFP-SK1 T1 is able to translocate in a phosphorylation-dependent manner. Moreover, carbachol, S1P or PMA promoted the translocation of mGFP-SK1 T2-4 in a similar manner to WTmGFP-SK1 (Fig. 4.8). Although, mGFP-SK1 T5 translocated to filopodia irrespective of the agonist used, indicating a phenotypic shift from lamellipodia to filopodia in response to carbachol or PMA (Fig. 4.8).

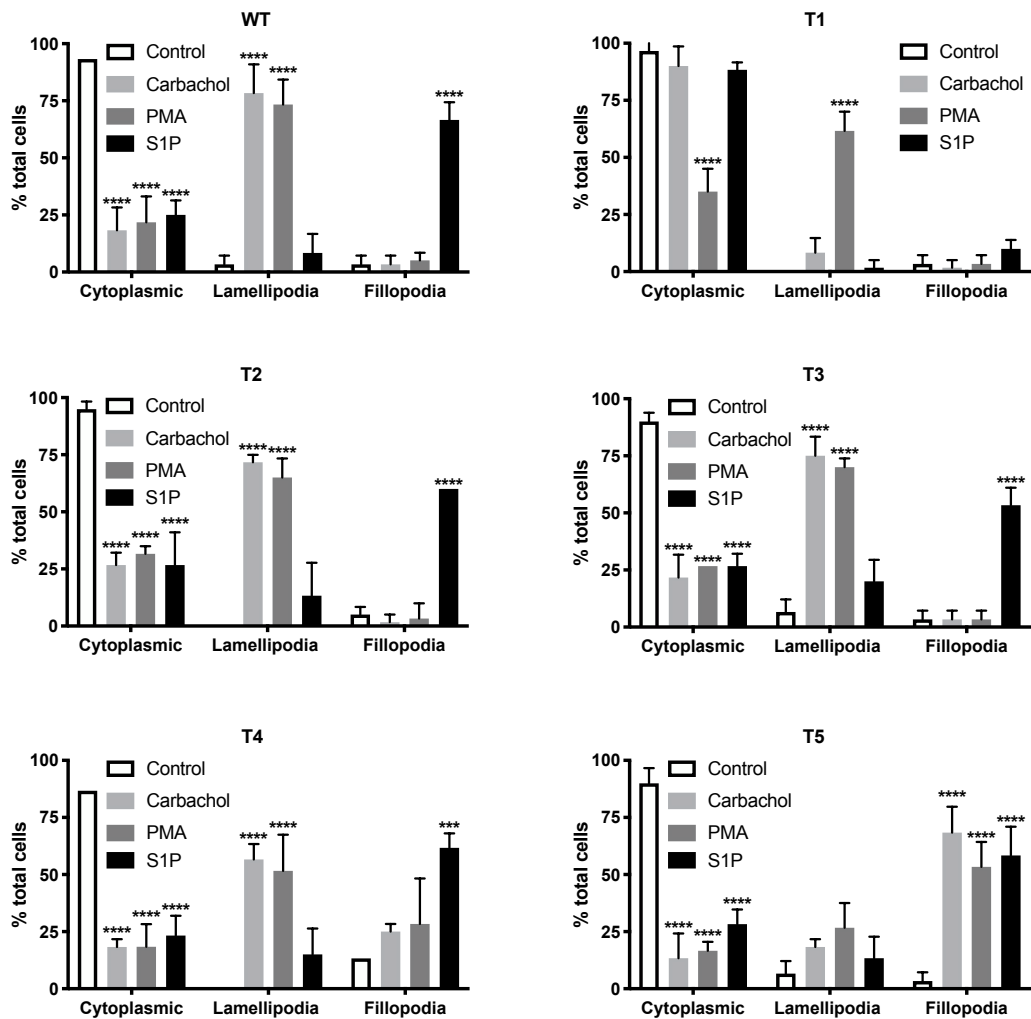


Figure 4.8 Phenotypic quantification of stimulated MCF-7L cells transiently overexpressing WTmGFP-SK1 or WTmGFP-SK1

The bar graph represents the % of MCF-7L cells transiently overexpressing WTmGFP-SK1 or mGFP-SK1 T1-5 showing mGFP-SK1 in spread (lamellipodia) or fillopodia micro-domains in response to S1P (5 μ M, 10 minutes), PMA (1 μ M, 10 minutes) or carbachol (100 μ M, 10 minutes) and compared to control cells (DMSO, 0.1% (v/v)). 15 random cells on 4 separate cover slips were analysed (n=4); ***p<0.001, ****p<0.0001 for stimulus versus control for a given phenotype (two-way ANOVA with Tukey's multiple comparison test).

4.2.4 mGFP-SK1-T1 is functionally deficient in wound healing

The functional impact of the inability of mGFP-SK1 T1 to translocate in response to GPCR stimulation was further investigated. SK1 translocation to the PM and the subsequent production of S1P induces cell migration (Sarkar et al., 2005; Doll et al., 2007) via S1P₃ activation (Long et al., 2010). Therefore, we measured the ability of

MCF-7L cells transiently overexpressing truncated forms of *mGFP-SK1* to migrate in response to S1P or carbachol.

Firstly, the transfection and over-expression of WT and T1-5 mutants established to exhibit similar efficiency (Fig. 4.9). Following 22 hours of vehicle treatment, there was no difference in the migration of WT*mGFP-SK1* or *mGFP-SK1* T1/2/5 expressing cells (Fig. 4.12 & 4.15). Carbachol (Fig. 4.12) or S1P (Fig. 4.15) promoted the migration of cells transiently overexpressing WT*mGFP-SK1*, *mGFP-SK1* T2 and *mGFP-SK1* T5. Migration was not increased above control for S1P or carbachol treated cells transiently overexpressing *mGFP-SK1* T1 and this was reduced compared to migration of stimulated WT*mGFP-SK1* overexpressing cells (Fig. 4.12 & 4.15). These data indicate that the last 5 amino acids of the C-terminus are required to translocate to the PM in response to GPCR activation, which is subsequently crucial for cell functions such as migration.

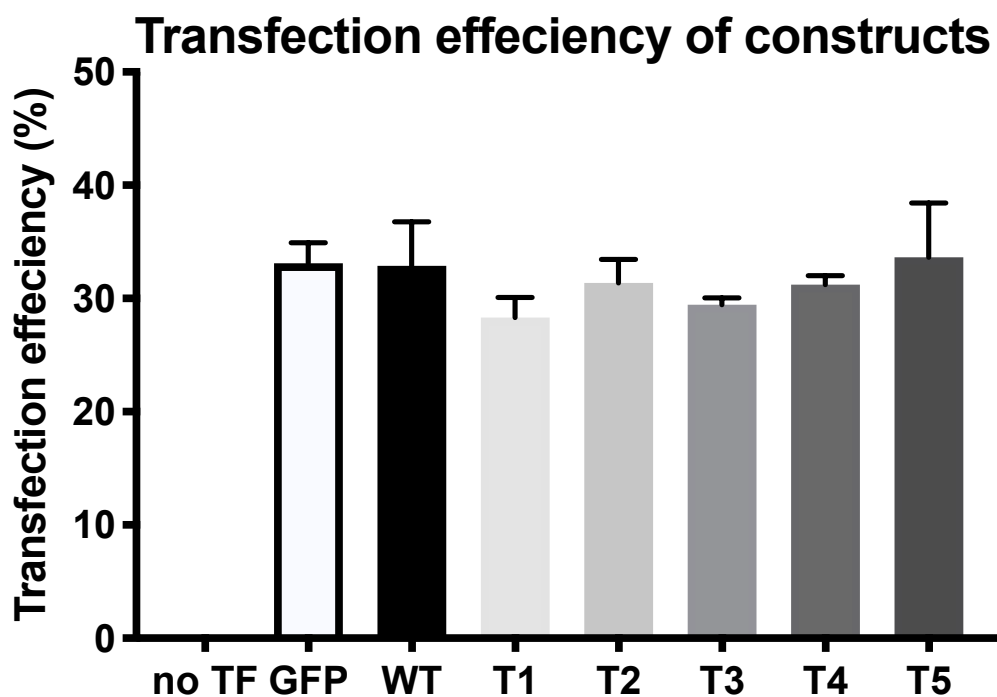


Figure 4.9 Transfection efficiency of GFP, WT*mGFP-SK1* and *mGFP-SK1* T1-5

The bar graph represents the transfection efficiency of GFP, WT*mGFP-SK1* and *mGFP-SK1* T1-5. Results are representative of 3 independent experiments (one-way ANOVA).

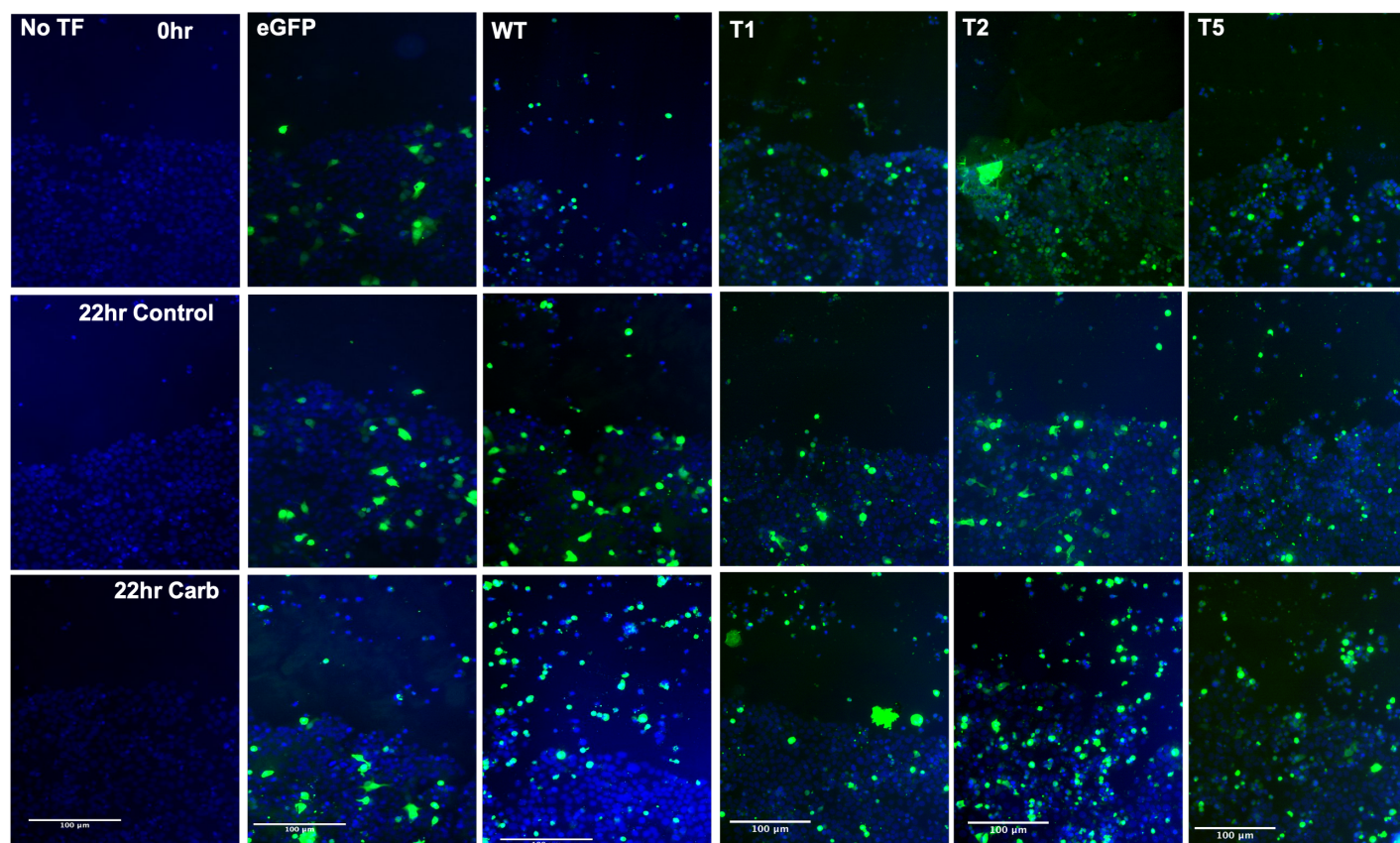


Figure 4.10 Migration assay of carbachol stimulated MCF-7L cells transiently overexpressing GFP, WTmGFP-SK1 or mGFP-SK1 T1-5

MCF-7L cells transiently overexpressing GFP, WTmGFP-SK1 or mGFP-SK1 T1-5 were treated with carbachol (100 μ M, 22 hours) or as control (dH₂O, 1% (v/v), 22 hours) following the application of a wound to the cell monolayer. 10x oil magnification photomicrographs showing the migration of cells into the wounded area. Cells were processed and mounted with a DAPI-containing mount to stain DNA (blue). mGFP-SK1 forms were detected by GFP. Results are representative of 3 independent experiments.

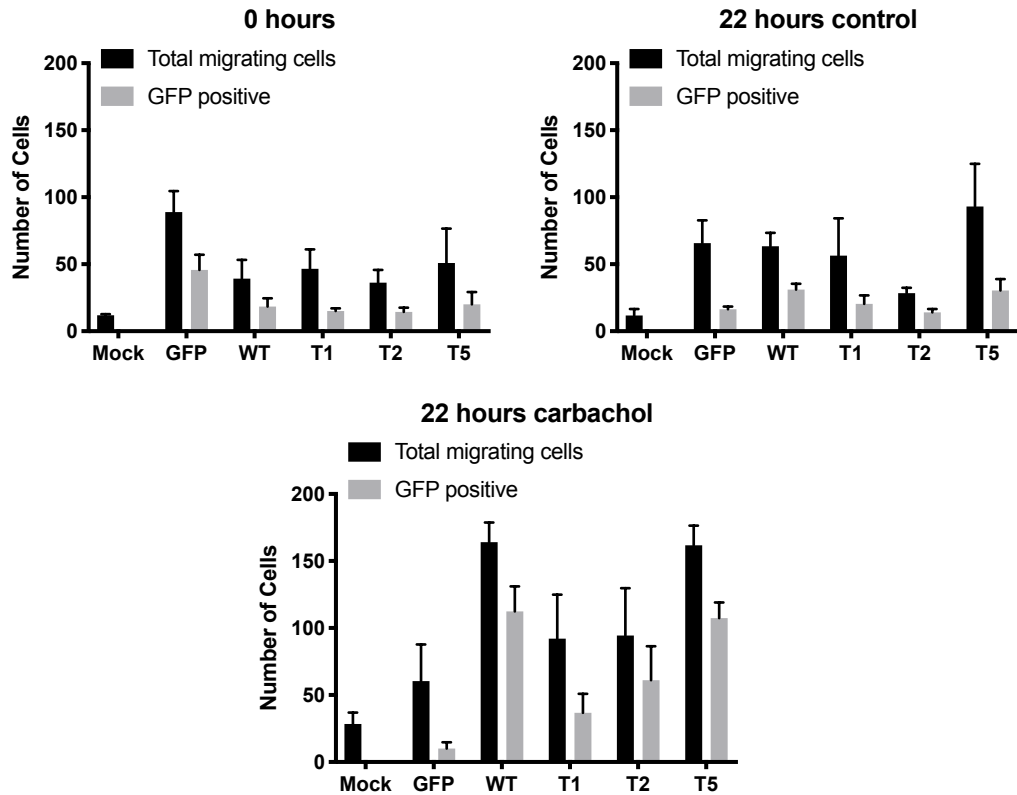


Figure 4.11 MCF-7L cells transiently overexpressing GFP, WTmGFP-SK1, mGFP-SK1-K49E or mGFP-SK1-I51C in response to S1P in the wound after 22 hours control or carbachol treatment or immediately after scoring

The bar graphs represent the total number of cells in the wound either immediately after wounding (0 hours), or after carbachol (100 μ M, 22 hours) or control (dH₂O, 1% (v/v), 22 hours) treatment (n=3).

Scratch assay

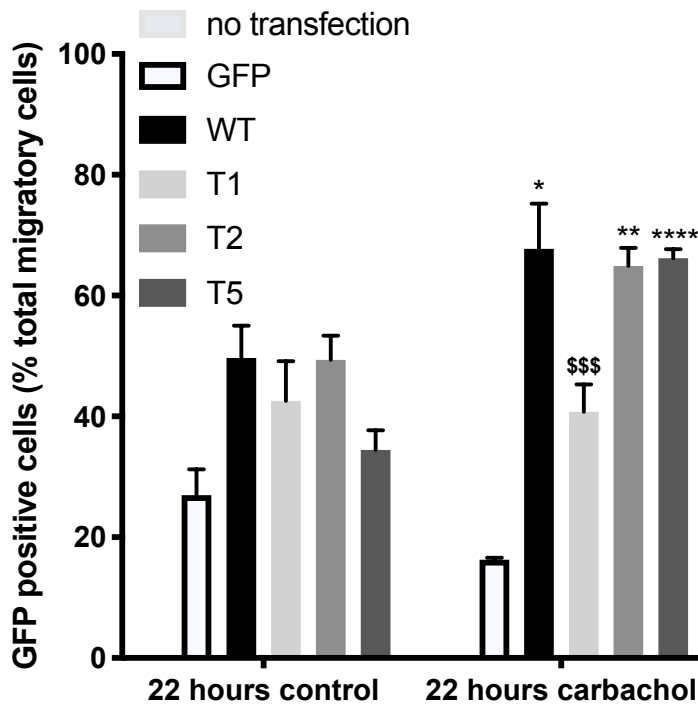


Figure 4.12 Quantification of the carbachol migration assay of MCF-7L cells transiently overexpressing GFP, WTmGFP-SK1 or mGFP-SK1 T1-5 in response to carbachol

The bar graph represents the % migration of GFP positive cells into the wound (n=3); *p<0.05, **p<0.01 and ****p<0.0001 for stimulated *versus* control for a given construct; \$\$\$p<0.001 for stimulated mGFP-SK1 T1 versus stimulated WTmGFP-SK1 (two-way ANOVA with Tukey post hoc test).

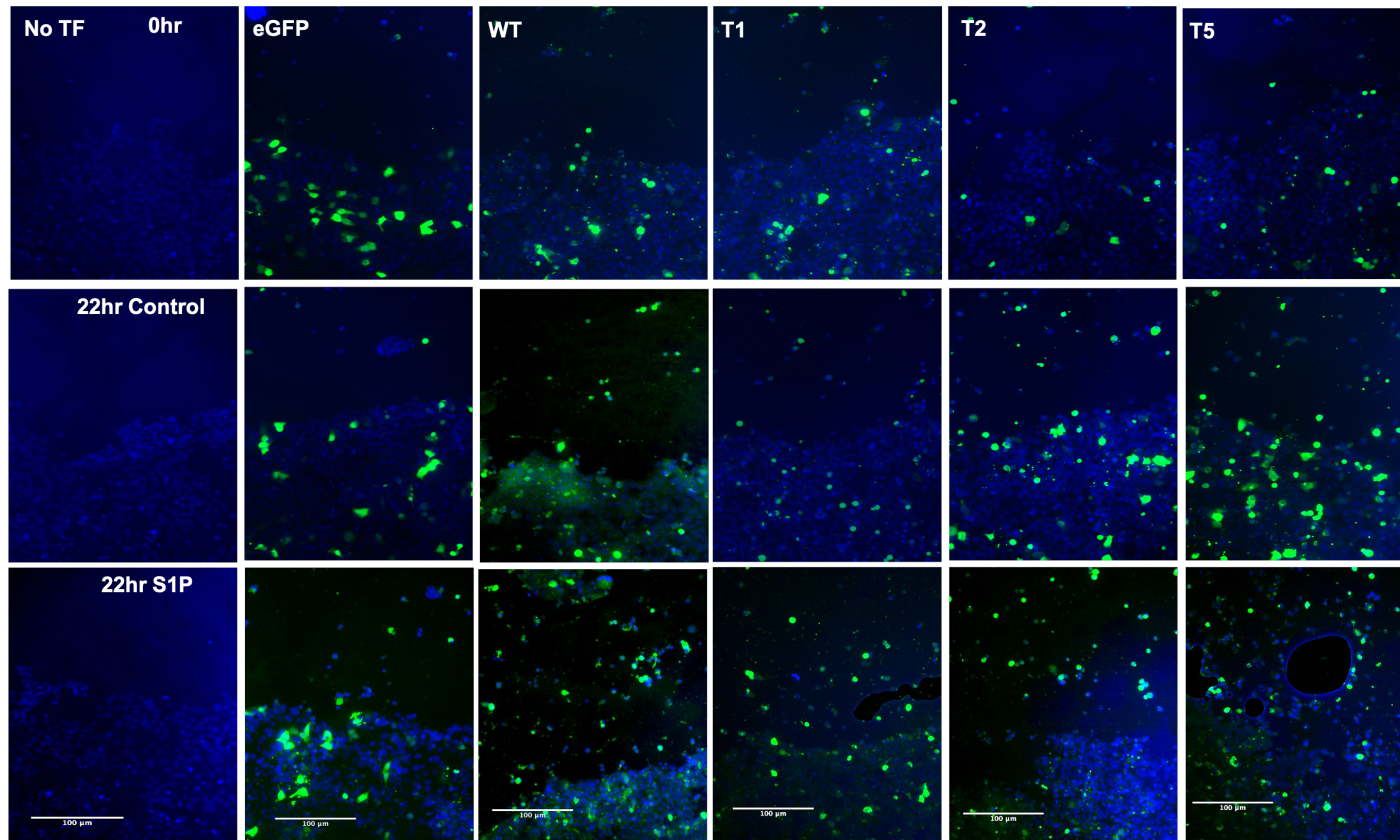


Figure 4.13 Migration assay of S1P stimulated MCF-7L cells transiently overexpressing GFP, WTmGFP-SK1 or mGFP-SK1 T1-5

MCF-7L cells transiently overexpressing GFP, WTmGFP-SK1 or mGFP-SK1 T1-5 were treated with carbachol (100 μ M, 22 hours) or as control (dH₂O, 1% (v/v), 22 hours) following the application of a wound to the cell monolayer. 10x oil magnification photomicrographs showing the migration of cells into the wounded area. Cells were processed and mounted with a DAPI-containing mount to stain DNA (blue). mGFP-SK1 forms were detected by GFP. Results are representative of 3 independent experiments.

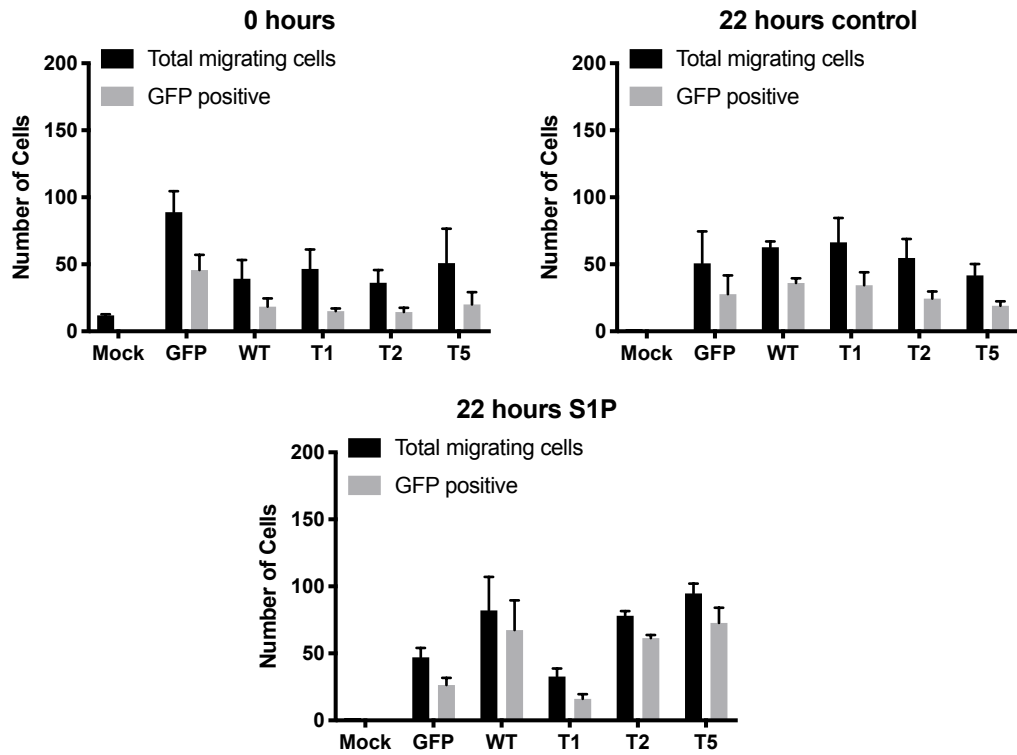


Figure 4.14 MCF-7L cells transiently overexpressing GFP, WTmGFP-SK1, mGFP-SK1-K49E or mGFP-SK1-I51C in response to S1P in the wound after 22 hours control or S1P treatment or immediately after scoring

The bar graphs represent the total number of cells in the wound either immediately after wounding (0 hours), or after S1P (5 μ M, 22 hours) or control (dH₂O, 1% (v/v), 22 hours) treatment (n=3).

Scratch assay

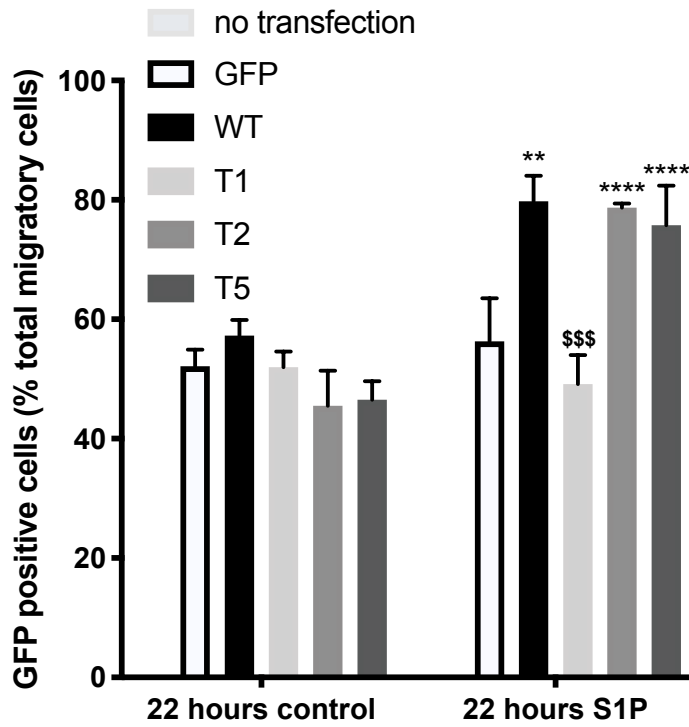


Figure 4.15 Quantification of the S1P migration assay of MCF-7L cells transiently overexpressing GFP, WTmGFP-SK1 or mGFP-SK1 T1-5 in response to S1P

The bar graph represents the % migration of GFP positive cells into the wound (n=3); **p<0.01 and ****p<0.0001 for stimulated *versus* control for a given construct; \$\$\$p<0.001 for stimulated *mGFP-SK1* T1 versus stimulated *WTmGFP-SK1* (two-way ANOVA with Tukey post hoc test).

4.2.5 Translocation of mGFP-SK1-T1/2/5 is not due to hyperphosphorylation

It is known that PP2A B'α subunit binds to the C-terminus of SK1, dephosphorylating Ser²²⁵ and hence inactivating the enzyme (Barr et al., 2008). Therefore, the possibility that *mGFP-SK1 T2-5* was translocating due to hyperphosphorylation through a lack of PP2A B'α binding was investigated. To test this, translocation of MCF-7L cells transiently overexpressing WT*mGFP-SK1* or *mGFP-SK1 T1/2/5* was observed in the presence of the MEK-1 inhibitor, PD98059, thereby preventing translocation by Ser²²⁵ phosphorylation.

In this case PD98059 blocked PMA-mediated SK1 translocation of cells transiently overexpressing WT*mGFP-SK1* and *mGFP-SK1 T1/2/5*, thereby confirming that *mGFP-SK1 T2/5* and importantly, *mGFP-SK1 T1* translocation was phosphorylation-dependent in response to PMA (Fig. 4.16). However, PD98059 was unable to block the translocation of WT*mGFP-SK1* and *mGFP-SK1 T2/5* in response to carbachol and S1P (Fig. 4.16), suggesting that PP2A binding and therefore, the phosphorylation state of the enzyme had no effect on the translocation of *mGFP-SK1 T2/5* in response to carbachol and S1P.

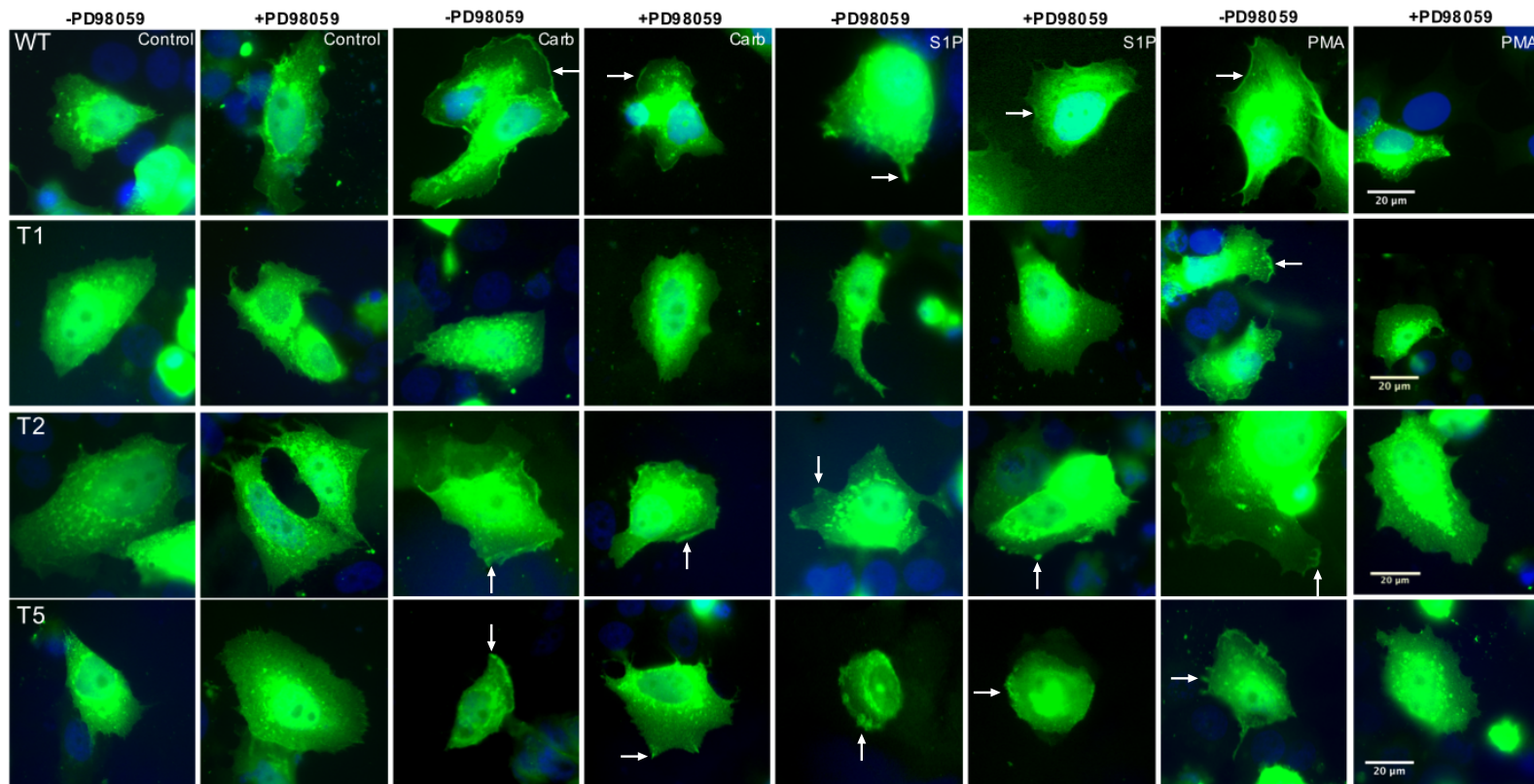


Figure 4.16 Stimulated MCF-7L cells transiently overexpressing WTmGFP-SK1 or mGFP-SK1 T1/2/5 pre-treated with PD98059

40x oil magnification photomicrographs of MCF-7L cells transiently overexpressing WTmGFP-SK1 or mGFP-SK1 T1/2/5, pre-treated with PD98059 (50 μ M, 1 hour) and stimulated with S1P (5 μ M, 10 mins), PMA (1 μ M, 10 mins) or carbachol (100 μ M, 10 mins) and compared to cells that were not pre-treated. Cells were processed and mounted with a DAPI-containing mount to stain DNA (blue). mGFP-SK1 forms were detected by GFP (arrows represent translocated SK1).. Representative result is of three independent experiments.

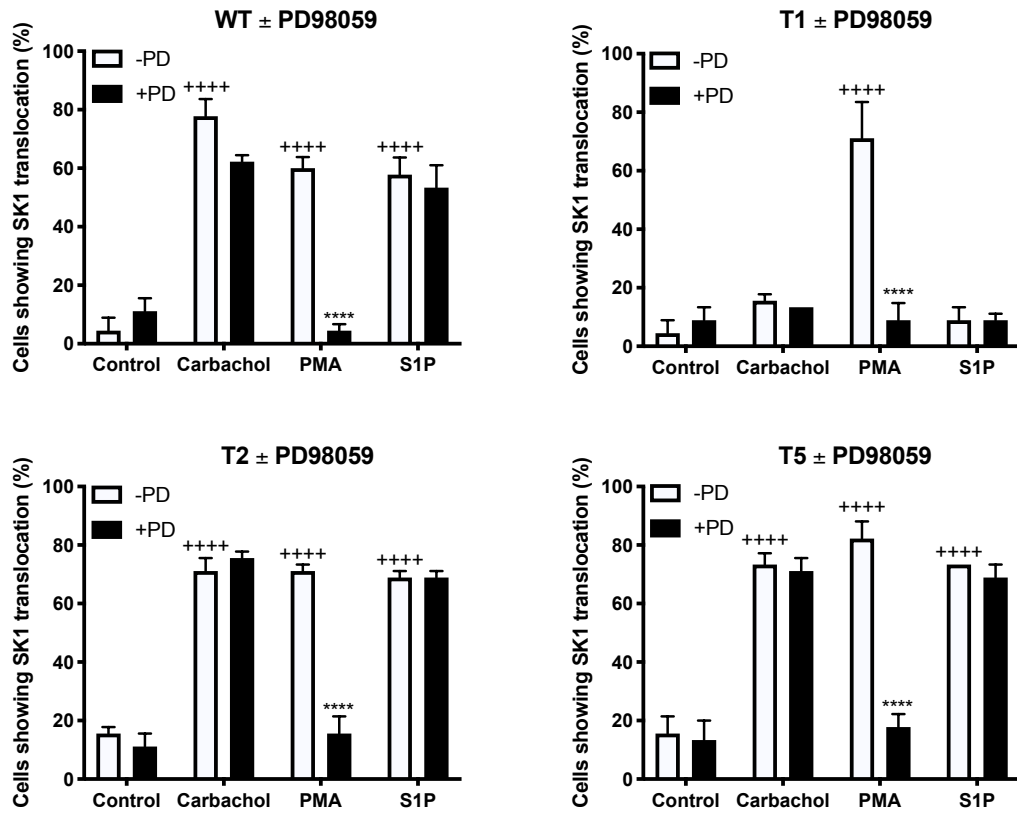


Figure 4.17 % of stimulated MCF-7L cells transiently overexpressing WTmGFP-SK1 or mGFP-SK1 T1/2/5 showing translocation when pre-treated with PD98059

The bar graph represents the % of MCF-7L cells transiently overexpressing WTmGFP-SK1 or mGFP-SK1 T1/2/5 showing translocated mGFP-SK1 in response to S1P (5 μ M, 10 mins), PMA (1 μ M, 10 mins), carbachol (100 μ M, 10 mins) or vehicle (Con, DMSO, 0.1% (v/v)), with and without pre-treatment of PD98059 (50 μ M, 1 hour). 15 random cells on 3 separate cover slips were analysed (n=3); ****p<0.0001 for PMA alone versus PMA with PD98059; +++++p<0.00001 for stimulus versus control (two-way ANOVA with Tukey's multiple comparison test).

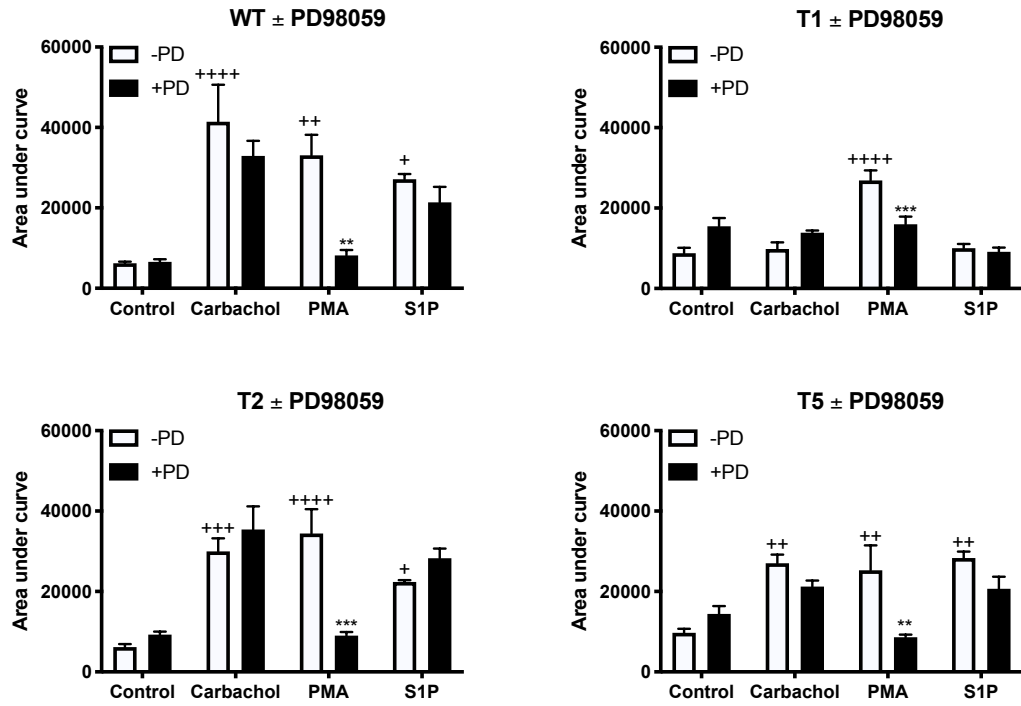


Figure 4.18 Area under curve analysis of MCF-7L transiently overexpressing WTmGFP-SK1 or mGFP-SK1 T1/2/5 pre-treated with PD98059

The bar graph represents the AUC of the total level of WTmGFP-SK1 translocation in response to S1P (5 μ M, 10 mins), PMA (1 μ M, 10 mins), carbachol (100 μ M, 10 mins) or vehicle (Con, DMSO, 0.1% (v/v)), with and without pre-treatment of PD98059 (50 μ M, 1 hour) (n=5); **p<0.01, ***p<0.001 for PMA alone versus PMA with PD98059; +p<0.05, ++p<0.01, +++p<0.001 and ++++p<0.0001 for stimulus versus control (two-way ANOVA with Tukey's multiple comparison test).

4.2.8 The effect of C-terminus length on phosphatidic acid interaction

Initial reports show that C-terminal fragments of SK1 interact with acidic PA (Delon et al., 2004). It is now believed however that the C-terminus acting is able to act in a capping manner (Adams et al., 2016), whereby we propose that uncapping leads to interdomain twisting to allow for a contiguous membrane engagement interface comprising of a hydrophobic patch and positively charged residues. We hence investigated the importance of the C-terminal length on the electrostatic interaction with PA. For this, MCF-7L cells transiently overexpressing truncated forms of *mGFP-SK1* were pre-treated with the PLD inhibitor FIPI, before being simulated with S1P, PMA or carbachol and tested for their ability to translocate.

Similarly to WT*mGFP-SK1*, FIPI pre-treatment blocked the translocation of *mGFP-SK1* T2-5 to the PM in response to carbachol (Fig. 4.19) or S1P (Fig. 4.21), which was also observed as a reduction in membrane pixel intensity (Fig. 4.19 & 4.21). These findings suggest that the formation of membrane-bound PA remains vital for the translocation of *mGFP-SK1* T2-5.

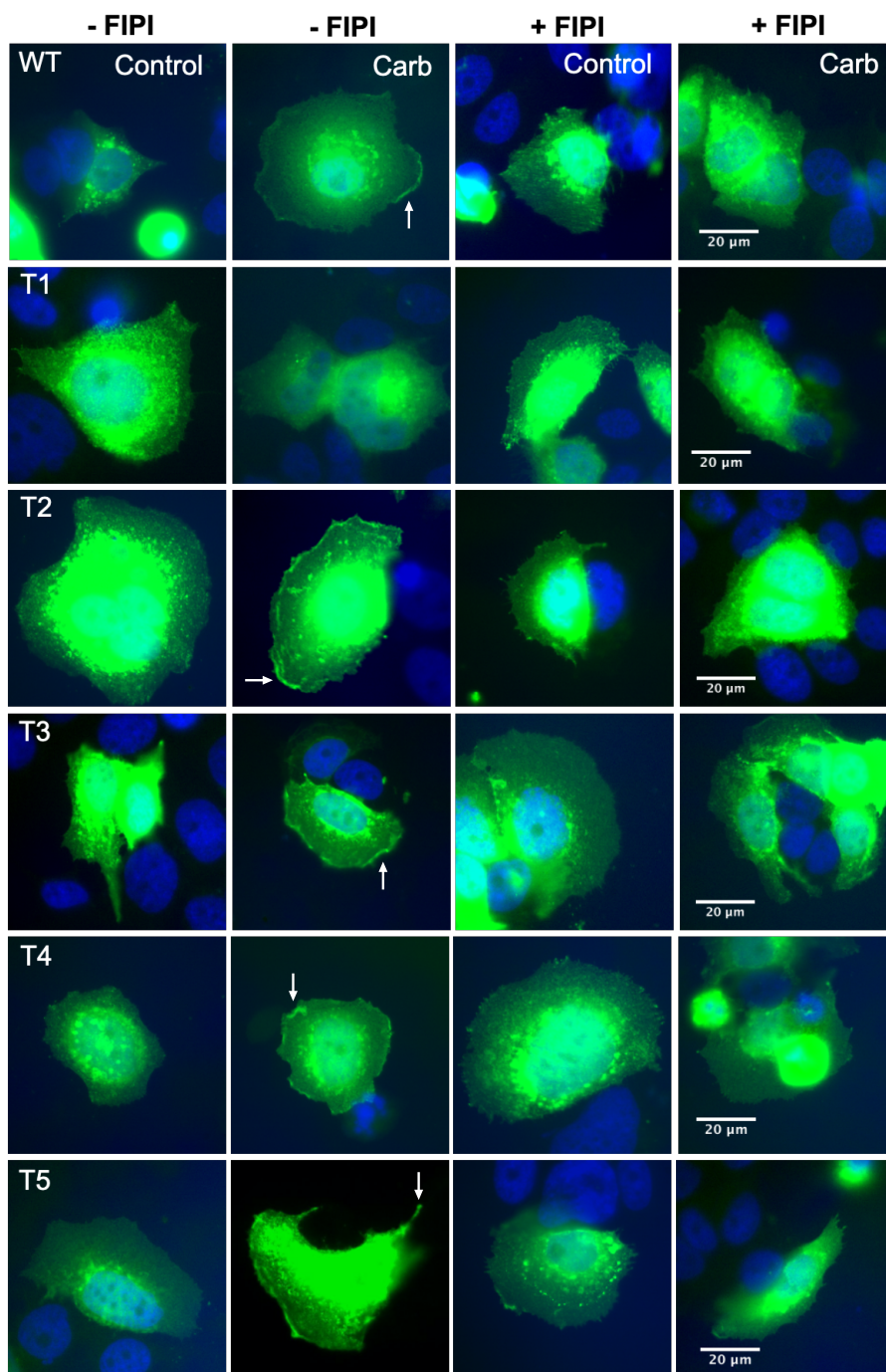


Figure 4.19 Carbachol stimulated MCF-7L cells transiently overexpressing WTmGFP-SK1 or mGFP-SK1 T1-5 pre-treated with FIPI

40x oil magnification photomicrographs of MCF-7L cells transiently overexpressing WTmGFP-SK1 or mGFP-SK1 T1-5 pre-treated with FIPI (PLD-1/2 inhibitor) (100 nM, 1 hour) and stimulated with carbachol (100 μ M, 10 minutes) or vehicle (Con, DMSO, 0.1% (v/v)) and compared to cells not re-treated. Cells were processed (see methods) and mounted with DAPI-containing mount to stain DNA (blue). SK1 was detected with by GFP (arrows represent translocated SK1). Representative results is of 3 independent experiments.

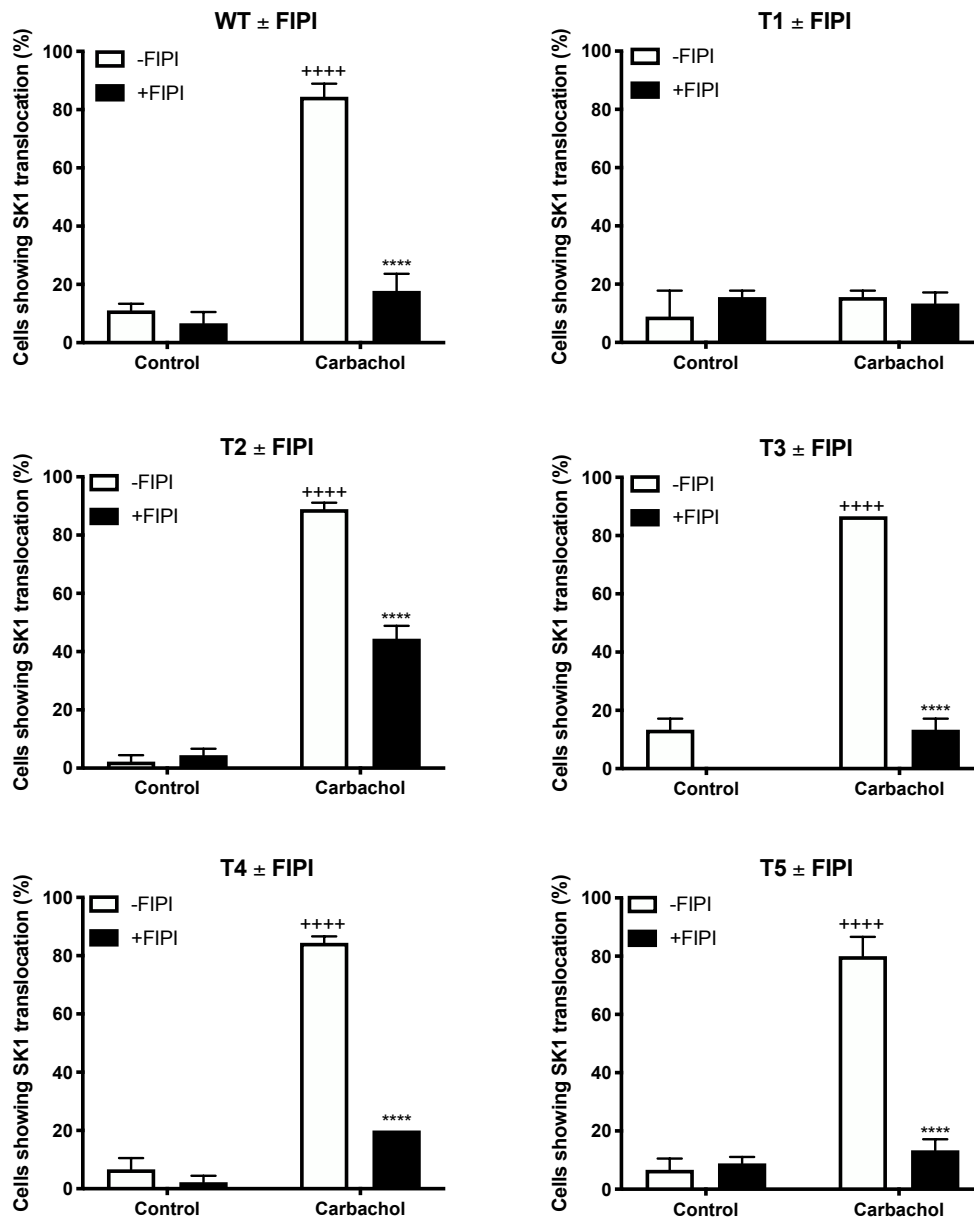


Figure 4.20 % of carbachol stimulated MCF-7L cells transiently overexpressing WTmGFP-SK1 or mGFP-SK1 T1-5 showing translocation when pre-treated with FIPI

The bar graph represents the % of MCF-7L cells transiently overexpressing WTmGFP-SK1 or mGFP-SK1 T1-5 showing translocated mGFP-SK1 in response to carbachol (100 μ M, 10 mins) or vehicle (Con, DMSO, 0.1% (v/v)), with and without pre-treatment of FIPI (100 nM, 1 hour). 15 random cells on 3 separate cover slips were analysed (n=3); ****p<0.0001 for stimulus alone versus stimulus with FIPI; ****p<0.0001 for stimulus versus control (two-way ANOVA with Tukey's multiple comparison test).

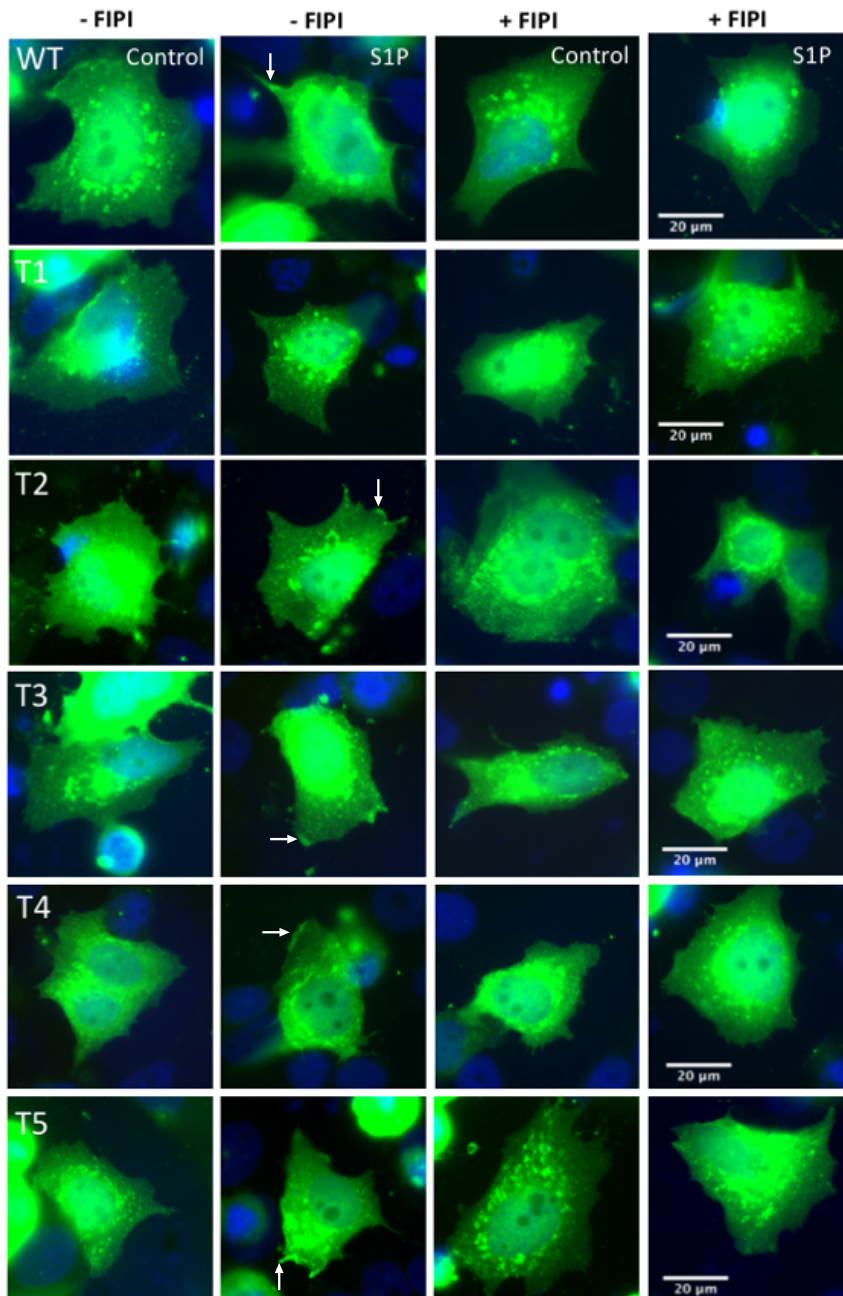


Figure 4.21 S1P stimulated MCF-7L cells transiently overexpressing WTmGFP-SK1 or mGFP-SK1 T1-5 pre-treated with FIPI

40x oil magnification photomicrographs of MCF-7L cells transiently overexpressing WTmGFP-SK1 or mGFP-SK1 T1-5 pre-treated with FIPI (PLD-1/2 inhibitor) (100 nM, 1 hour) and stimulated with S1P (5 μM, 10 minutes) or vehicle (Con, DMSO, 0.1% (v/v)) and compared to cells not re-treated. Cells were processed (see methods) and mounted with DAPI-containing mount to stain DNA (blue). SK1 was detected with by GFP (arrows represent translocated SK1).. Representative results is of 3 independent experiments.

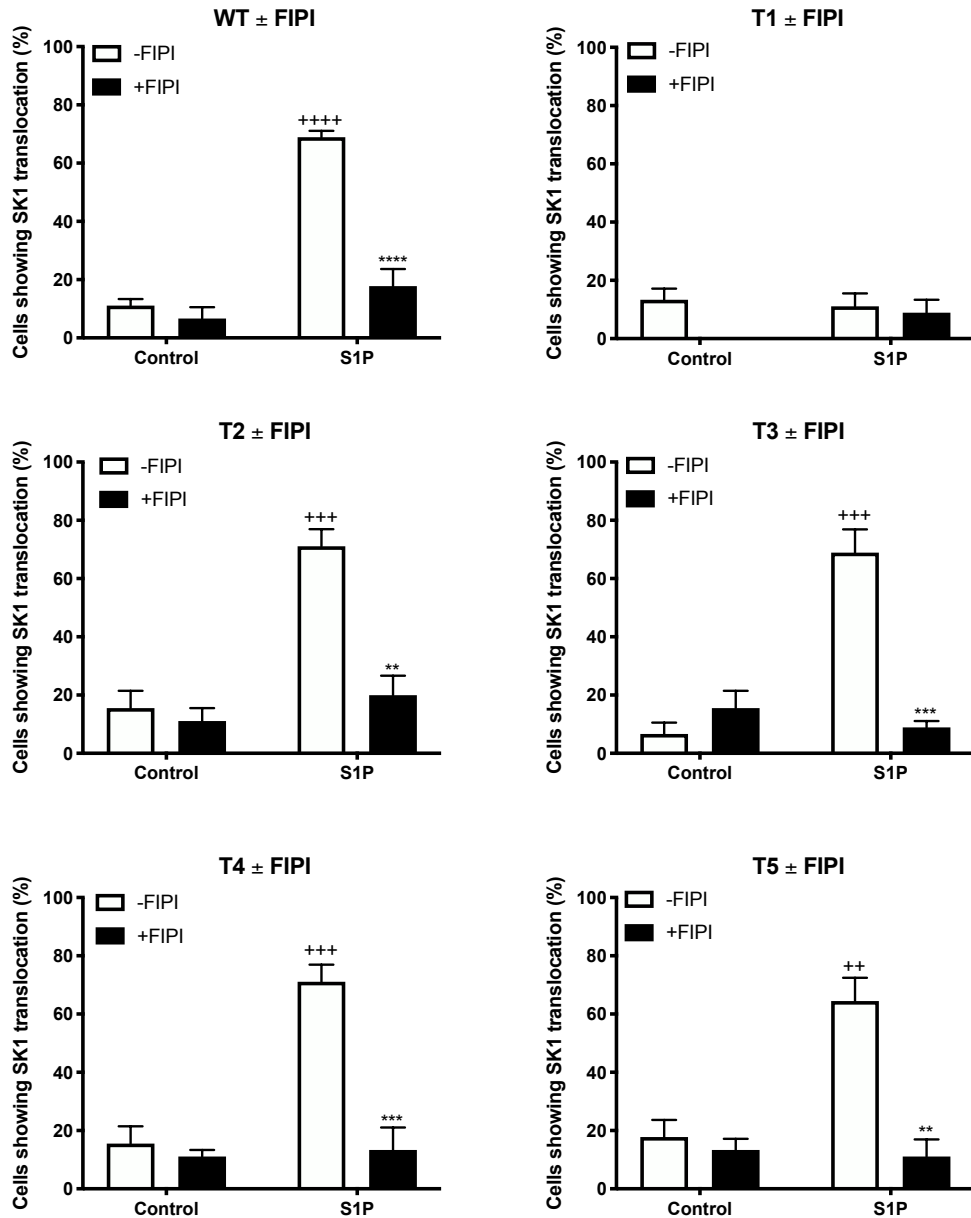


Figure 4.22 % of S1P stimulated MCF-7L cells transiently overexpressing WTmGFP-SK1 or mGFP-SK1 T1-5 showing translocation when pre-treated with FIPI

The bar graph represents the % of MCF-7L cells transiently overexpressing WTmGFP-SK1 or mGFP-SK1 T1-5 showing translocated mGFP-SK1 in response to S1P (5 μ M, 10 mins) or vehicle (Con, DMSO, 0.1% (v/v)), with and without pre-treatment of FIPI (100 nM, 1 hour). 15 random cells on 3 separate cover slips were analysed (n=3); **p<0.01, ***p<0.001 and ****p<0.0001 for stimulus alone versus stimulus with FIPI; ++p<0.01, +++p<0.001 and ****p<0.0001 for stimulus versus control (two-way ANOVA with Tukey's multiple comparison test).

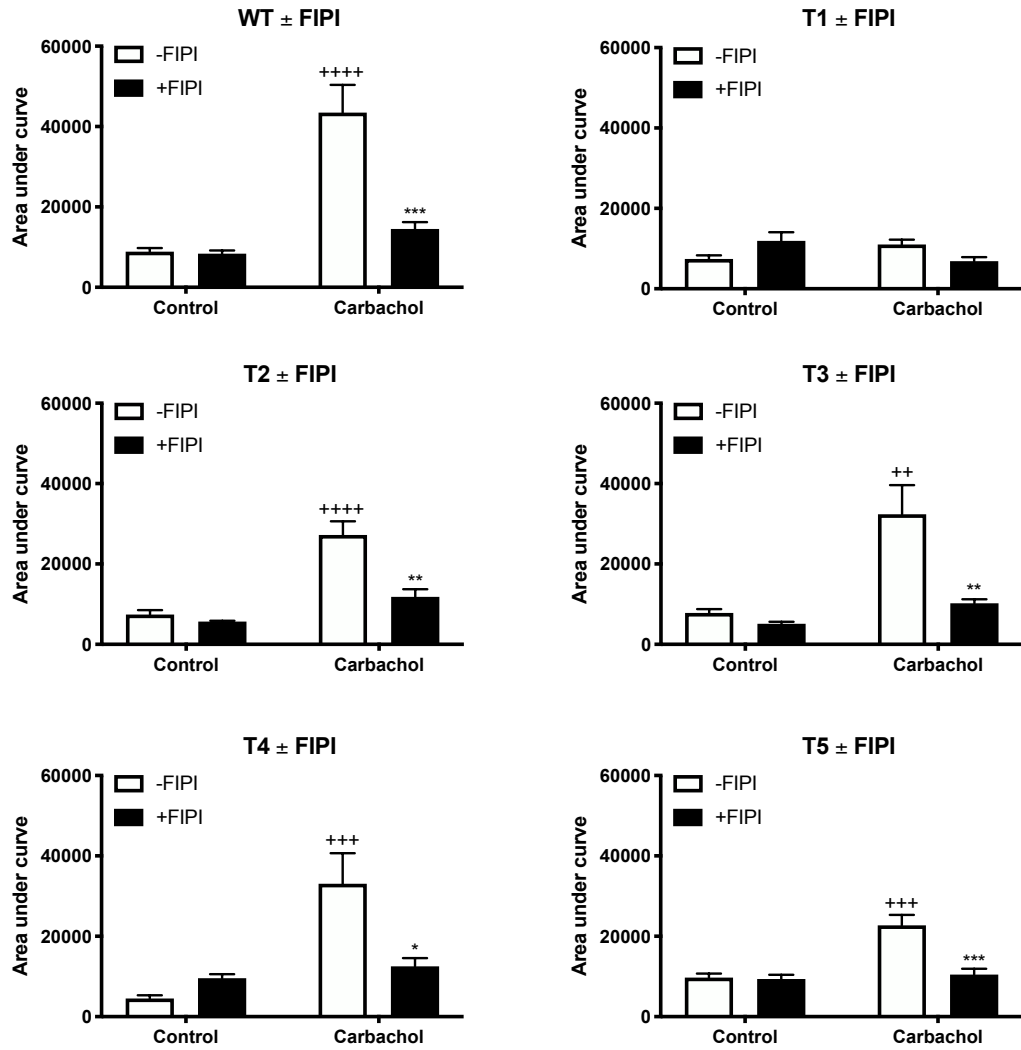


Figure 4.23 Area under curve analysis for carbachol stimulated cells transiently overexpressing WTmGFP-SK1 or mGFP-SK1 T1-5 pre-treated with FIPI

The bar graph represents the AUC of the total level of WTmGFP-SK1 or mGFP-SK1 T1-5 translocation in response to carbachol (100 μ M, 10 mins) or vehicle (Con, DMSO, 0.1% (v/v)), with and without pre-treatment of FIPI (100 nM, 1 hour) (n=5); *p<0.05, **p<0.01 and ***p<0.001 for stimulus alone versus stimulus with FIPI; **p<0.01, ***p<0.001 and ****p<0.0001 for stimulus versus control (two-way ANOVA with Tukey's multiple comparison test).

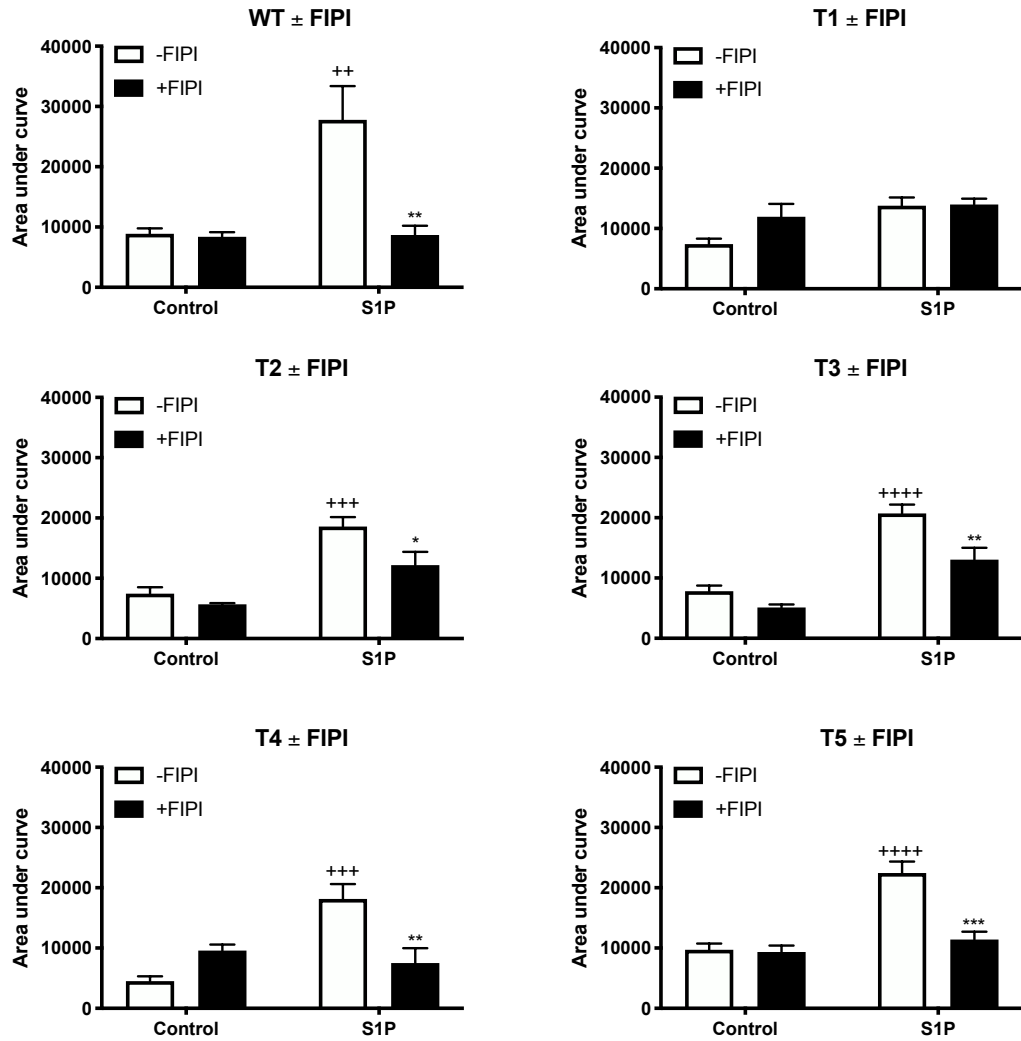


Figure 4.24 Area under curve analysis for S1P stimulated cells transiently overexpressing WTmGFP-SK1 or mGFP-SK1 T1-5 pre-treated with FIPI

The bar graph represents the AUC of the total level of WTmGFP-SK1 or mGFP-SK1 T1-5 translocation in response to S1P (5 μ M, 10 mins) or vehicle (Con, DMSO, 0.1% (v/v)), with and without pre-treatment of FIPI (100 nM, 1 hour) (n=5); *p<0.05, **p<0.01 and ***p<0.001 for stimulus alone versus stimulus with FIPI; **p<0.01, ***p<0.001 and ****p<0.0001 for stimulus versus control (two-way ANOVA with Tukey's multiple comparison test).

4.2.9 The effect of C-terminus length on G_q interaction

Previous reports and this study demonstrated the importance of G_q for the translocation of SK1 (ter Braak et al., 2009). The C-terminally truncated SK1 mutants were therefore tested for their dependence on G_q to translocate, whilst investigating possible C-terminus displacement via G_q.

MCF-7L cells transiently overexpressing truncated forms of mGFP-SK1 were examined for their ability to translocate in the presence of the G_q inhibitor, YM254890. YM254890 blocked carbachol- or S1P-mediated translocation of mGFP-SK1 T2-T5, similar to WTmGFP-SK1 (Fig. 4.25 & 4.27). This was also observed as a reduction in membrane intensity staining of mGFP-SK1 T2-T5 when cells were pre-treated with YM254890 and subsequently stimulated with carbachol or S1P (Fig. 4.25 & 4.27).

These findings indicate that G_q activation remains vital for the translocation of C-terminally truncated SK1. This also suggests that G_q is not responsible for displacing the last 10 amino-acids of the C-terminal region of SK1 and thus is not involved in regulating inter-domain movements within the enzyme. Further investigation is required to reveal whether G_q binds indirectly or directly and to which amino acid residues.

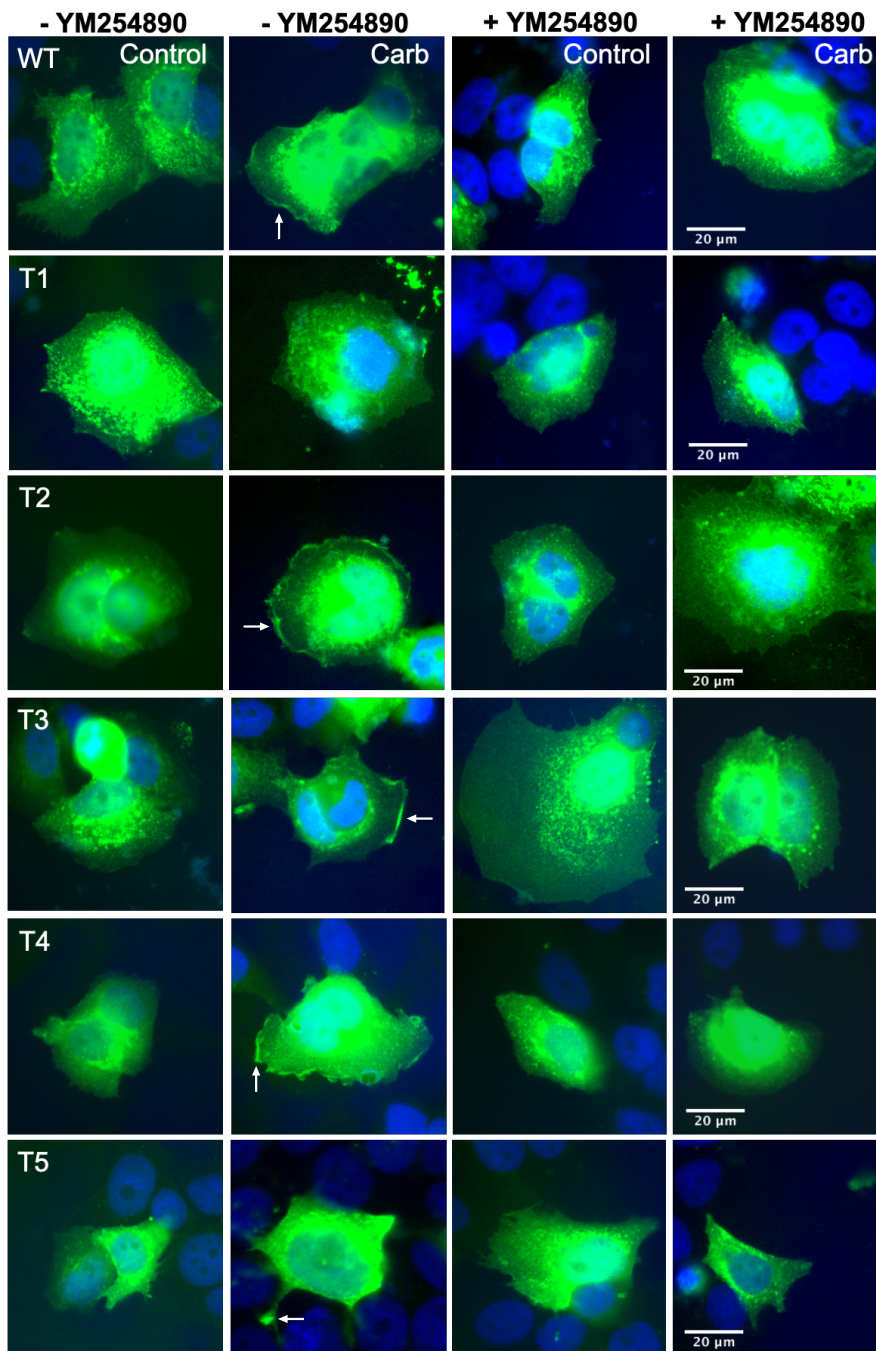


Figure 4.25 Carbachol stimulated MCF-7L cells transiently overexpressing WTmGFP-SK1 or mGFP-SK1 T1-5 pre-treated with YM254890

40x oil magnification photomicrographs of MCF-7L cells transiently overexpressing WTmGFP-SK1 or mGFP-SK1 T1-5 pre-treated with YM254890 (10 μ M, 30 minutes) and stimulated with carbachol (100 μ M, 10 minutes) or vehicle (Con, DMSO, 0.1% (v/v)) and compared to cells not re-treated. Cells were processed (see methods) and mounted with DAPI-containing mount to stain DNA (blue). SK1 was detected with by GFP (arrows represent translocated SK1). Representative results is of 3 independent experiments.

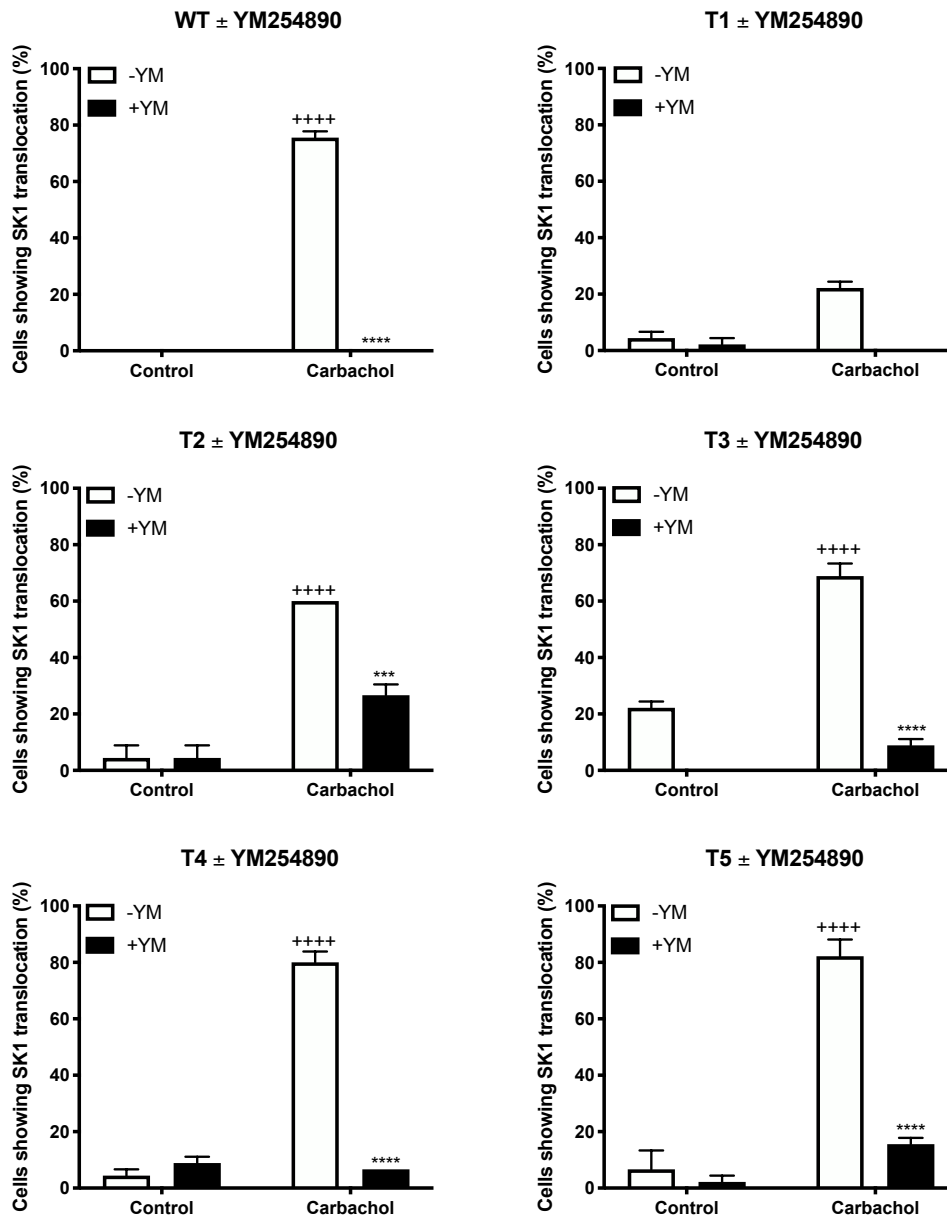


Figure 4.26 % of carbachol stimulated MCF-7L cells transiently overexpressing WTmGFP-SK1 or mGFP-SK1 T1-5 showing translocation when pre-treated with YM254890

The bar graph represents the % of MCF-7L cells transiently overexpressing WTmGFP-SK1 or mGFP-SK1 T1-5 showing translocated mGFP-SK1 in response to carbachol (100 μ M, 10 mins) or vehicle (Con, DMSO, 0.1% (v/v)), with and without pre-treatment of YM254890 (10 μ M, 30 minutes). 15 random cells on 3 separate cover slips were analysed (n=3); ***p<0.001 and ****p<0.0001 for stimulus alone versus stimulus with FIPI; ****p<0.0001 for stimulus versus control (two-way ANOVA with Tukey's multiple comparison test).

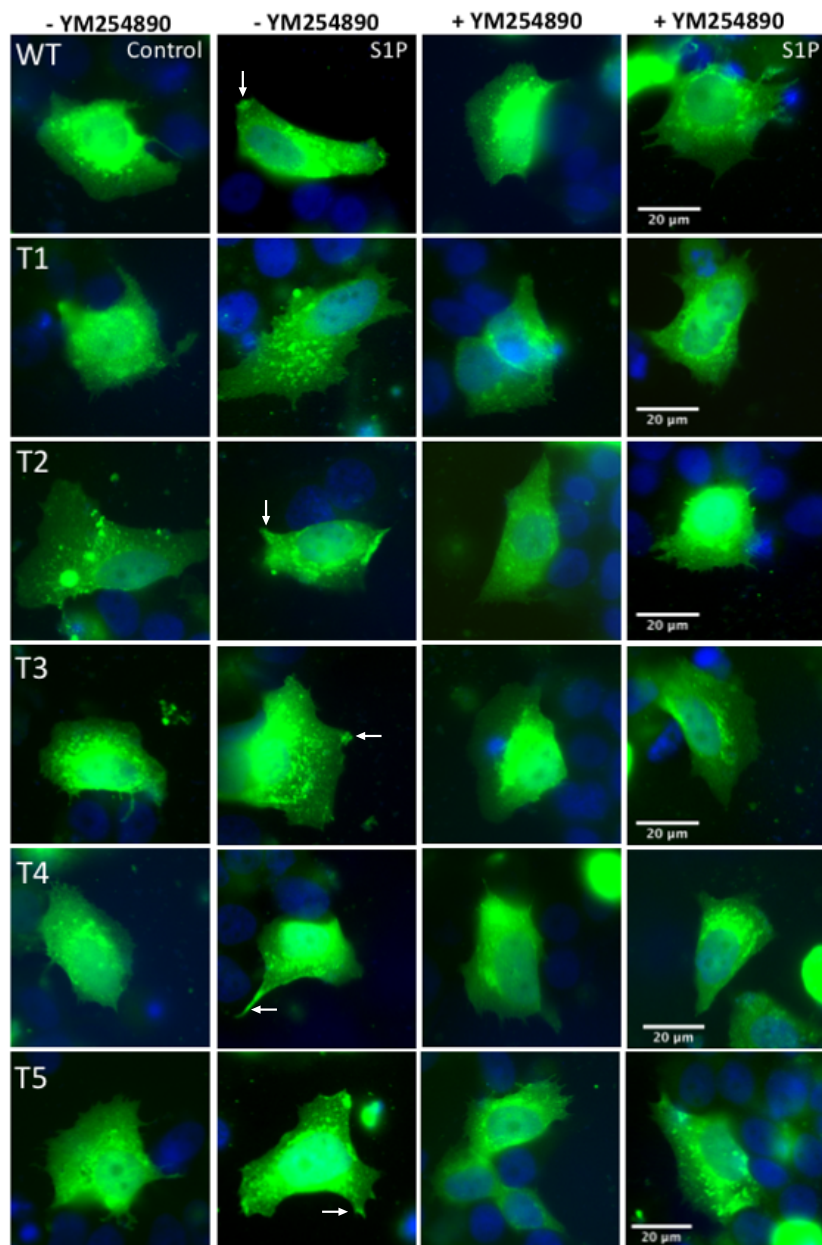


Figure 4.27 S1P stimulated MCF-7L cells transiently overexpressing WTmGFP-SK1 or mGFP-SK1 T1-5 pre-treated with YM254890

40x oil magnification photomicrographs of MCF-7L cells transiently overexpressing WTmGFP-SK1 or mGFP-SK1 T1-5 pre-treated with YM254890 (10 μM, 30 minutes) and stimulated with S1P (5 μM, 10 minutes) or vehicle (Con, DMSO, 0.1% (v/v)) and compared to cells not re-treated. Cells were processed (see methods) and mounted with DAPI-containing mount to stain DNA (blue). SK1 was detected with by GFP (arrows represent translocated SK1). Representative results is of 3 independent experiments.

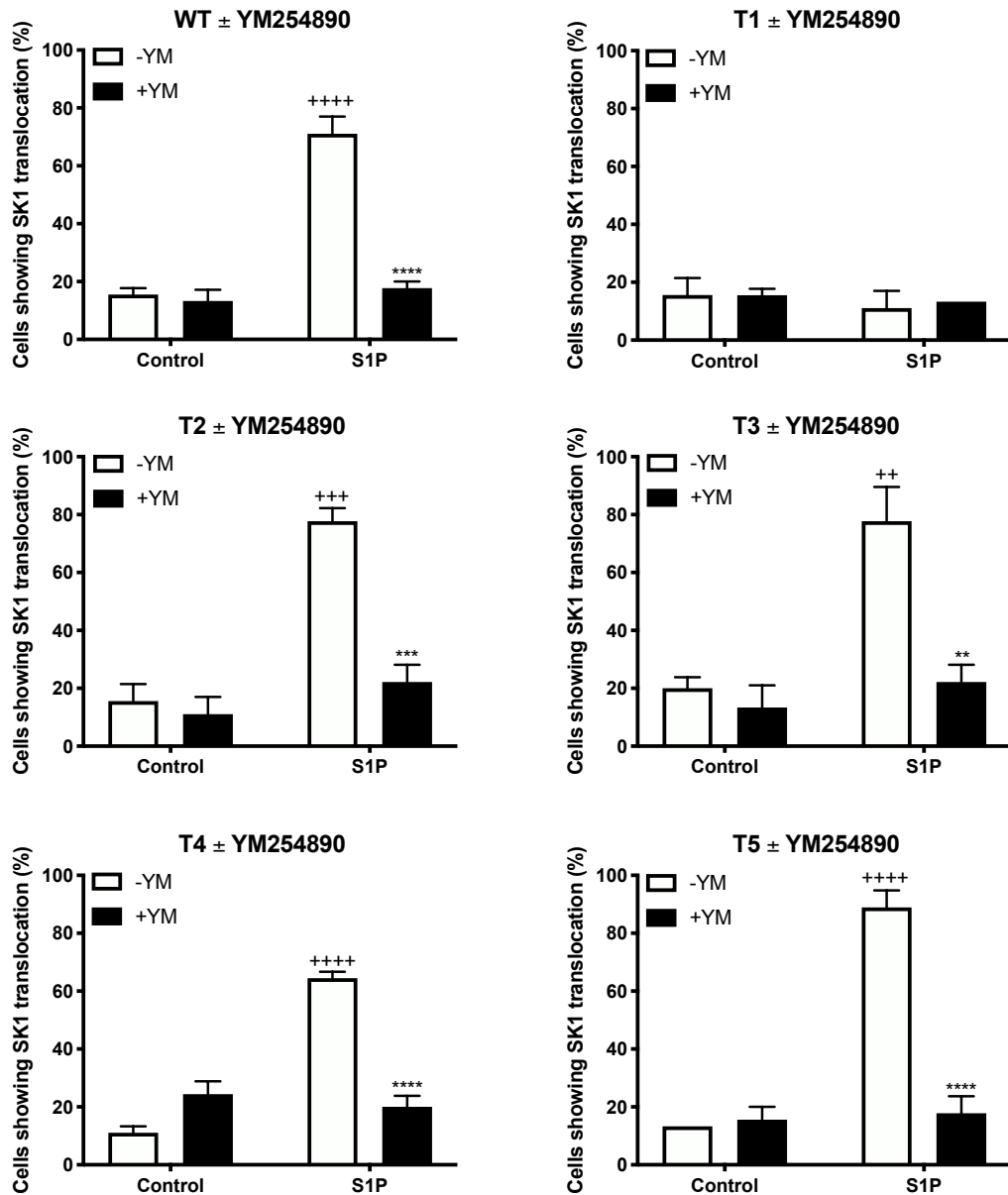


Figure 4.28 % of S1P stimulated MCF-7L cells transiently overexpressing WTmGFP-SK1 or mGFP-SK1 T1-5 showing translocation when pre-treated with YM254890

The bar graph represents the % of MCF-7L cells transiently overexpressing WTmGFP-SK1 or mGFP-SK1 T1-5 showing translocated mGFP-SK1 in response to S1P (5 μ M, 10 minutes) or vehicle (Con, DMSO, 0.1% (v/v)), with and without pre-treatment of YM254890 (10 μ M, 30 minutes). 15 random cells on 3 separate cover slips were analysed (n=3); **p<0.01, ***p<0.001 and ****p<0.0001 for stimulus alone versus stimulus with FIPI; **p<0.01, ***p<0.001 and ****p<0.0001 for stimulus versus control (two-way ANOVA with Tukey's multiple comparison test).

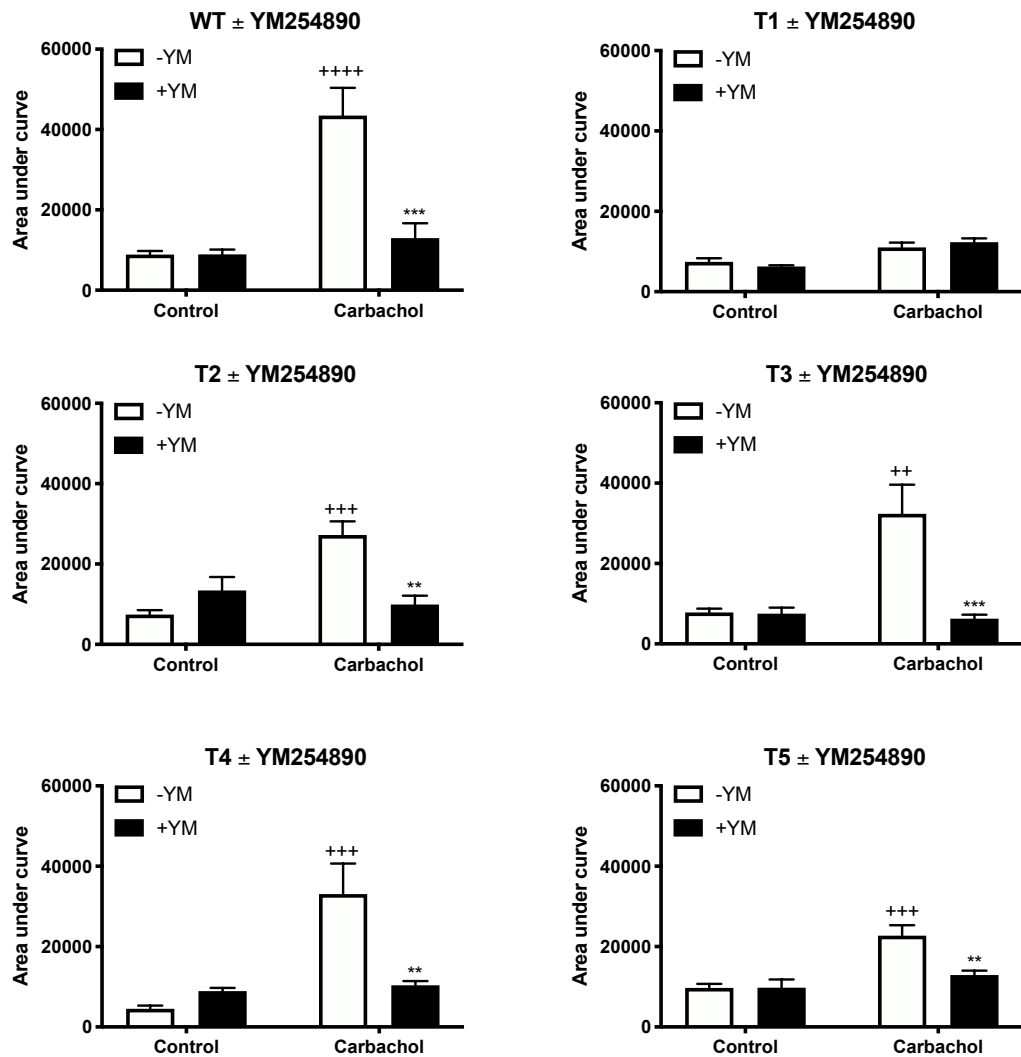


Figure 4.29 Area under curve analysis for carbachol stimulated cells transiently overexpressing WTmGFP-SK1 or mGFP-SK1 T1-5 pre-treated with YM254890

The bar graph represents the AUC of the total level of WTmGFP-SK1 or mGFP-SK1 T1-5 translocation in response to carbachol (100 μ M, 10 mins) or vehicle (Con, DMSO, 0.1% (v/v)), with and without pre-treatment of YM254890 (10 μ M, 30 mins) (n=5); **p<0.01 and ***p<0.001 for stimulus alone versus stimulus with FIPI; **p<0.01, ***p<0.001 and ****p<0.0001 for stimulus versus control (two-way ANOVA with Tukey's multiple comparison test).

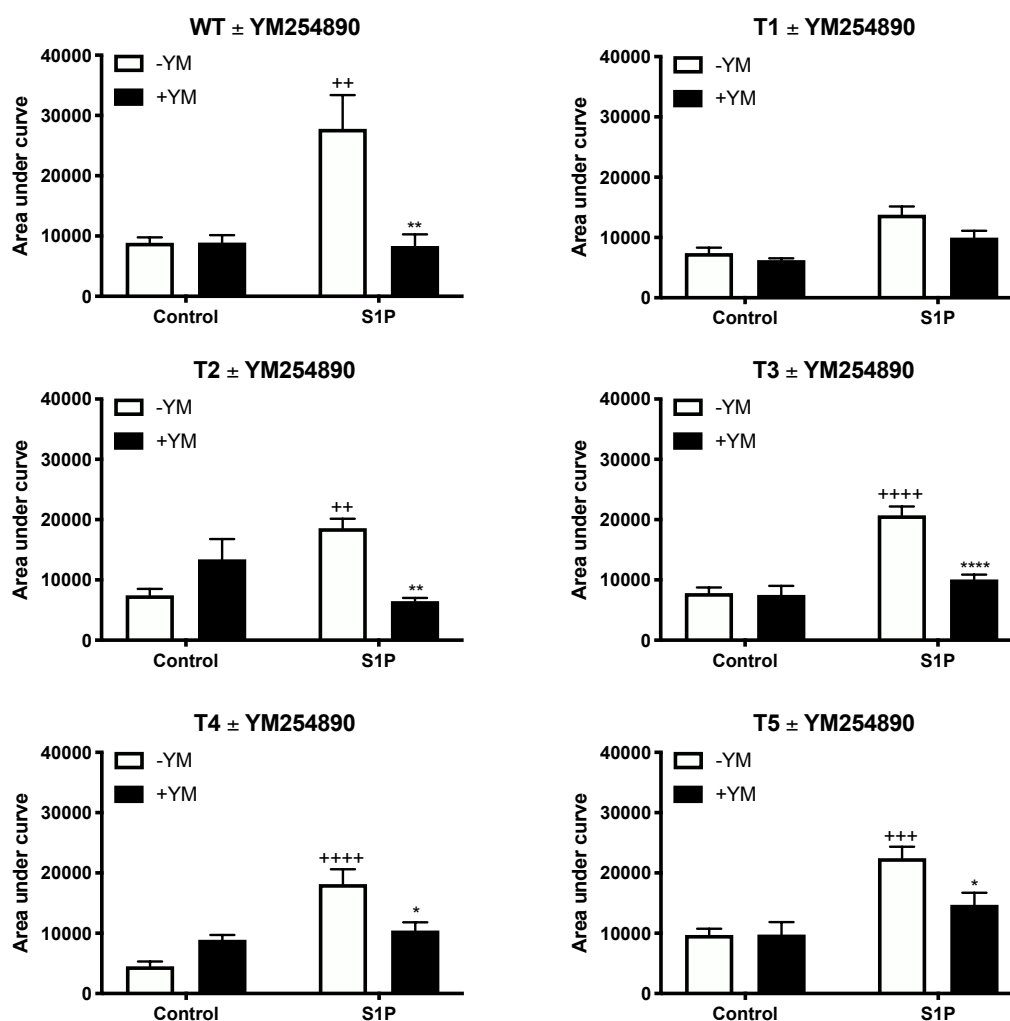


Figure 4.30 Area under curve analysis for S1P stimulated cells transiently overexpressing WTmGFP-SK1 or mGFP-SK1 T1-5 pre-treated with YM254890

The bar graph represents the AUC of the total level of WTmGFP-SK1 or mGFP-SK1 T1-5 translocation in response to S1P (5 μ M, 10 mins) or vehicle (Con, DMSO, 0.1% (v/v)), with and without pre-treatment of YM254890 (10 μ M, 30 mins) (n=5); *p<0.05, **p<0.01 and ****p<0.0001 for stimulus alone versus stimulus with FIPI; **p<0.01, ***p<0.001 and ****p<0.0001 for stimulus versus control (two-way ANOVA with Tukey's multiple comparison test).

4.2.10 Generation and characterization of mGFP-SK1 R-loop mutant

G_q binds PLC at Thr²⁵⁷ and Trp²⁶³, however crystallographic analysis suggests the C-terminus of SK1 could also bind to G_q at residues Thr²⁵⁷ and Trp²⁶³. Binding of G_q using these residues is therefore not feasible and in agreement with earlier observations (4.2.9) that demonstrate that mGFP-SK1 T2-5 retain a G_q requirement for their translocation, G_q is likely binding elsewhere on SK1.

One other potential binding site has been identified on the regulatory loop (R-loop), which resides on the reverse face of the SK1 C-terminal β -sandwich and is host to multiple phosphorylation sites, notably Ser²²⁵ (Pitson et al., 2003). It is thought that the R-loop is held in position by Asp²³⁵ inserting itself into the C-terminal β -sandwich, whereby Ser²²⁵ phosphorylation may displace Asp²³⁵ to disengage the R-loop, resulting in relaxation in the 93-ERDPW-97 sequence to allow for binding of acidic phospholipids. Therefore, the R-loop is suitably exposed to engage in protein-protein interactions and hence binding of G_q. One such sequence on the R-loop that is analogous to the site occupied by PLC is the 238-PLEEP-242 sequence. Site-directed mutagenesis was used to incorporate negative charge to the potential 238-PLEEP-242 binding site to investigate the potential of this site in SK1 to bind G_q at the R-loop (Fig. 4.31).

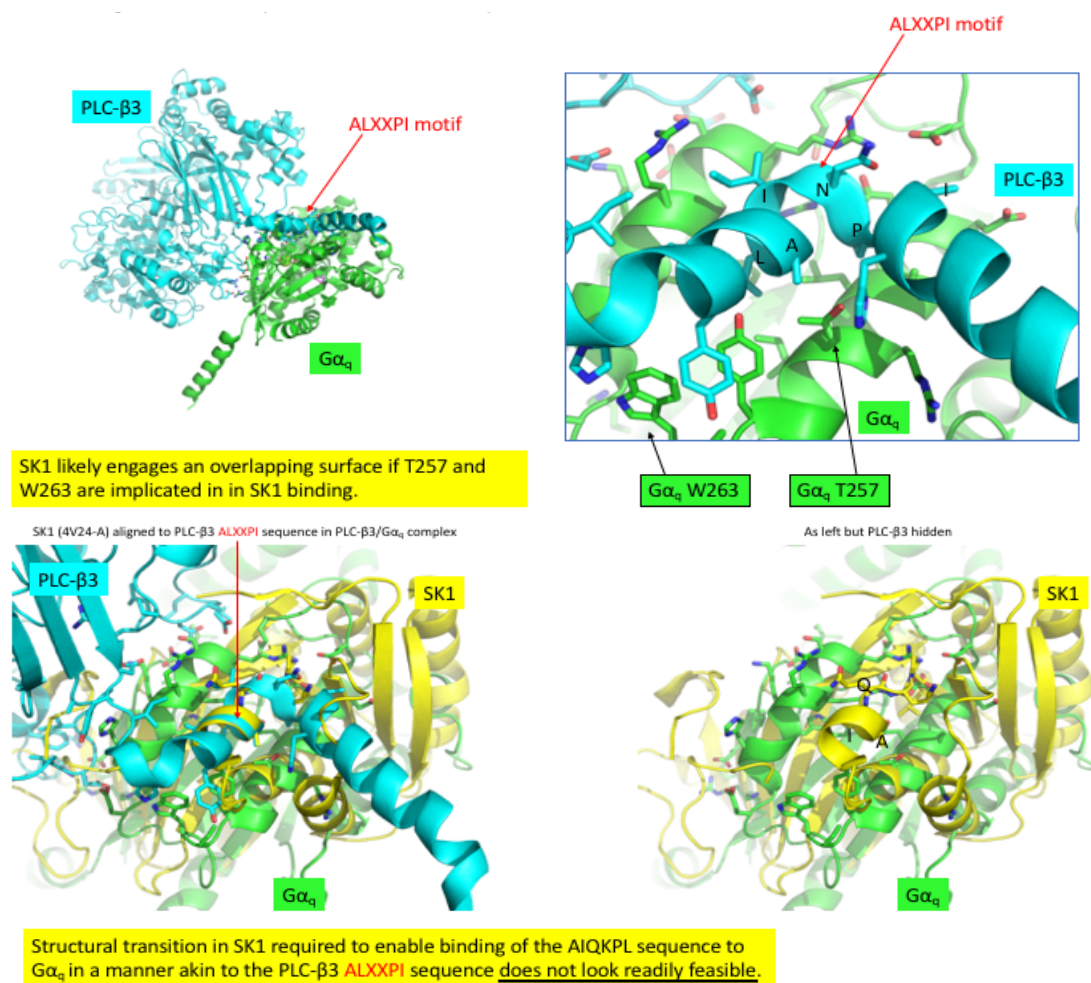


Figure 4.31 G_q binds to PLC using the same binding site required to bind the SK1 C-terminus

PLC binds to G_q at residues Thr²⁵⁷ and Trp²⁶³. Crystallographic analysis revealed that the putative C-terminus binding site for G_q is also Thr²⁵⁷ and Trp²⁶³ which is occupied by PLC; therefore, it is likely that G_q binds elsewhere on SK1.

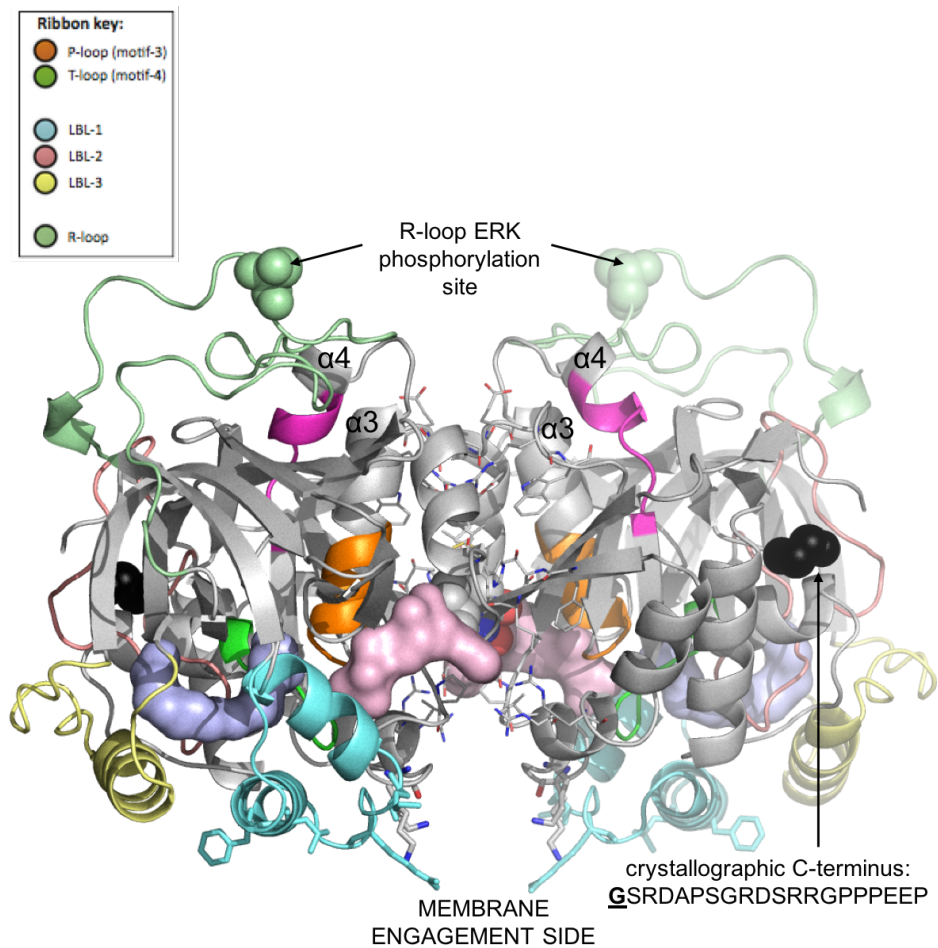


Figure 4.32 Crystal structure of dimeric SK1 depicting the solvent-exposed R-loop

Crystal structure of dimeric SK1 depicting the C-terminus in relation to the R-loop (adapted from (Adams et al., 2016)).

WTmGFP-SK1	451	LASLR IYQGQLAYLPVGT V ASKRPASTLVQ R GPVD TH LVPLEEPVPS HWT	500
mGFP-SK1-R	451	LASLR IYQGQLAYLPVGT V ASKRPASTLVQ R GPVD TH LVPLA A PVPS HWT	500

Figure 4.33 mGFP-SK1 R-loop mutant contains a double point mutation

A double base point mutation in WTmGFP-SK1 at the E240 and E241 position from GAG to GCG changed the amino acids at positions 240 and 241 to alanine, thereby incorporating negative charge to the potential G_q binding site.

4.2.11 mGFP-SK1-R loop mutant retains the ability to translocate

Previous observations indicated that translocation of SK1 was under G_q drive, albeit independent of the length of the C-terminus. We therefore proposed that the exposed SK1 R-loop, previously shown to be important for phosphorylation-dependent translocation (Pitson et al., 2003), is also important for G_q binding and hence G_q -mediated translocation.

MCF-7L cells transiently overexpressing *mGFP-SK1* R-loop mutant were tested for their ability to display translocation in response to S1P, PMA or carbachol. The successful overexpression of *mGFP-SK1* R-loop mutant was confirmed by western blot analysis using an anti-GFP antibody ($M_r=69$ kDa) (Fig. 4.34). Immunofluorescence microscopy revealed that S1P, PMA or carbachol promoted the translocation of *mGFP-SK1* R-loop mutant to the PM similarly to *WTmGFP-SK1* (Fig. 4.34). This observation was also evident when measuring membrane intensity of *mGFP-SK1* R-loop mutant and *WTmGFP-SK1* (Fig. 4.36). This suggests that the 238-PLEEP-242 R-loop sequence is not crucial for G_q interaction with SK1.

Further analysis into the phenotype of translocation indicated that similar to *WTmGFP-SK1*, carbachol and S1P promoted the translocation of *mGFP-SK1* R-loop mutant to lamellipodia and filopodia, respectively. Although PMA promoted the translocation of the *mGFP-SK1* R-loop mutant to lamellipodia, this was reduced compared the *WTmGFP-SK1* (Fig. 4.37). These data reinforce the notion that the R-loop might be important for phosphorylation-dependent translocation of SK1.

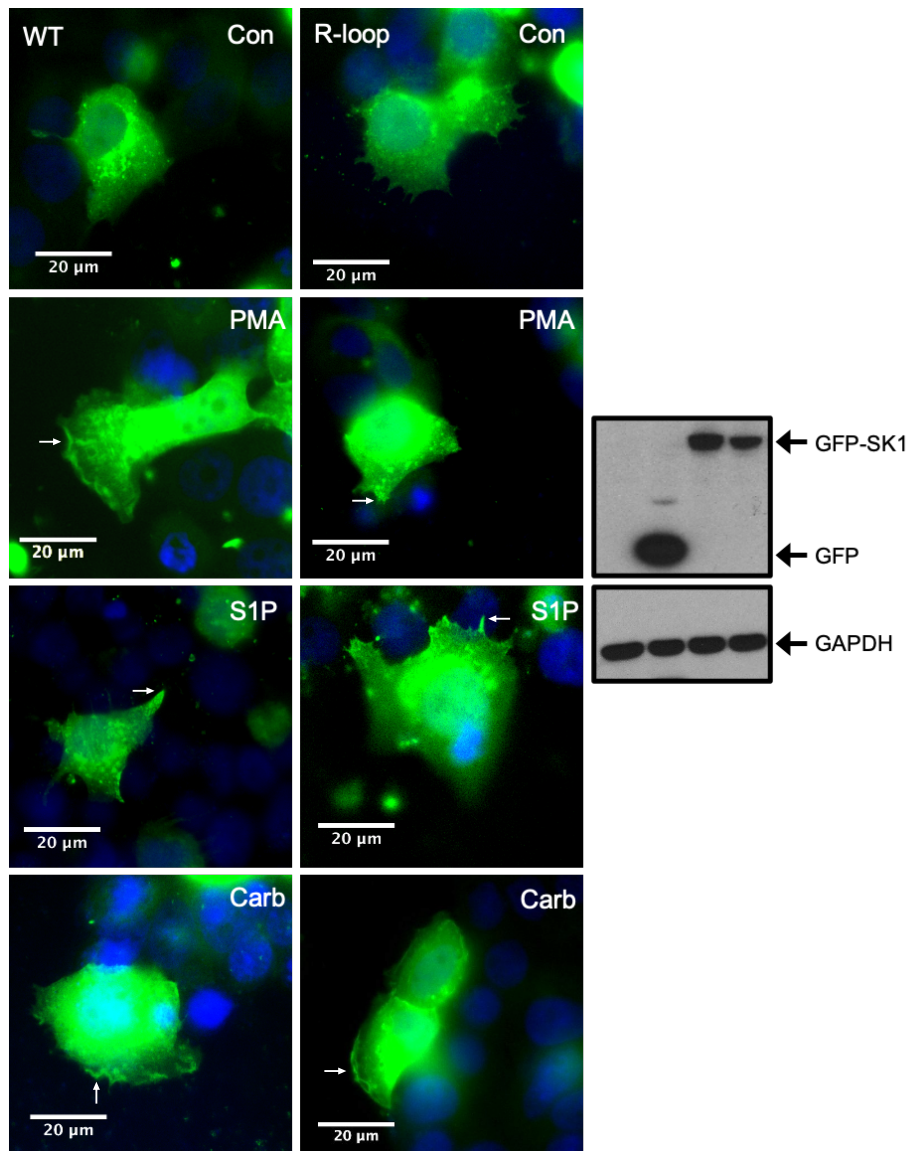


Figure 4.34 Stimulated MCF-7L cells transiently overexpressing WTmGFP-SK1 or mGFP-SK1 R-loop mutant

40x oil magnification photomicrographs of MCF-7L cells showing the translocation of WTmGFP-SK1 or mGFP-SK1 R-loop mutant in response to S1P (5 μ M, 10 minutes), PMA (1 μ M, 10 minutes), carbachol (100 μ M, 10 minutes) or vehicle (DMSO, 0.1% (v/v)). Cells were processed (see methods) and mounted with DAPI-containing mount to stain DNA (blue). mGFP-SK1 forms were detected by GFP. Representative results is of 3 independent experiments. Inset is a western blot confirming the successful expression of WTmGFP-SK1 or mGFP-SK1 R-loop mutant using an anti-GFP antibody (lane 1: mock transfected cells; lane 2: transiently transfected GFP cells (27 kDa); lane 3: transiently transfected WTmGFP-SK1 cells (Mr = 69 kDa); lane 4: transiently transfected mGFP-SK1 R-loop mutant cells (Mr = 69 kDa)).

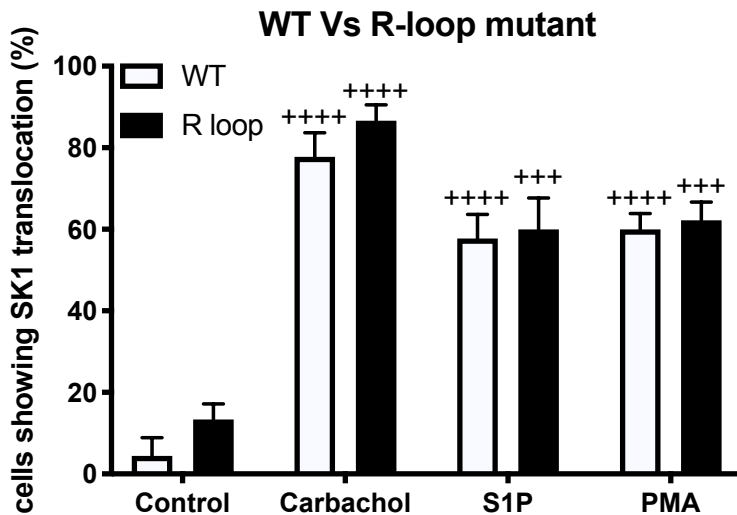


Figure 4.35 % of stimulated MCF-7L cells transiently overexpressing WTmGFP-SK1 or mGFP-SK1 R-loop mutant showing translocation

The bar graph represents the % of MCF-7L cells transiently overexpressing WTmGFP-SK1 or mGFP-SK1 R-loop mutant showing translocated mGFP-SK1 in response to S1P (5 μ M, 10 mins), PMA (1 μ M, 10 mins), carbachol (100 μ M, 10 mins) or vehicle (Con, DMSO, 0.1% (v/v)). 15 random cells on 3 separate cover slips were analysed (n=3); ***p<0.001 and ****p<0.0001 for stimulus versus control for WT or R-loop mutant (two-way ANOVA with Tukey's multiple comparison test).

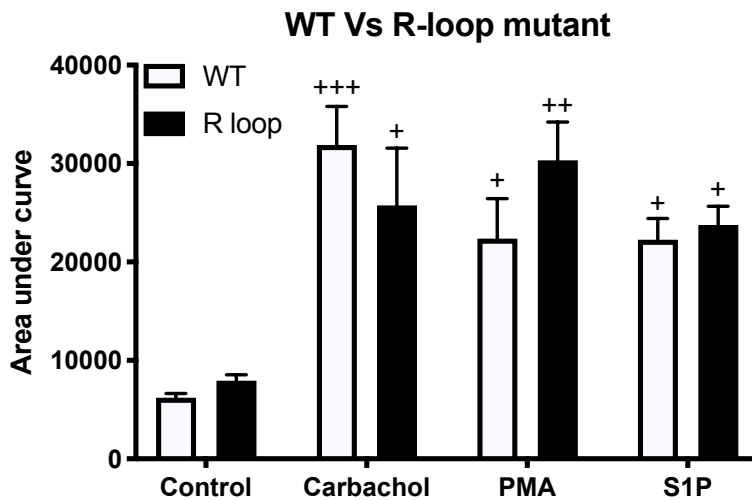


Figure 4.36 Area under curve analysis of stimulated MCF-7L cells transiently overexpressing WTmGFP-SK1 or mGFP-SK1 R-loop mutant

The bar graph represents the AUC of the total level of WTmGFP-SK1 or mGFP-SK1 R-loop mutant translocation in response to S1P (5 μ M, 10 mins), PMA (1 μ M, 10 mins), carbachol (100 μ M, 10 mins) or vehicle (Con, DMSO, 0.1% (v/v)) (n=5); *p<0.05, **p<0.01 and ***p<0.001 for stimulus versus control for WT or R-loop mutant (two-way ANOVA with Tukey's multiple comparison test).

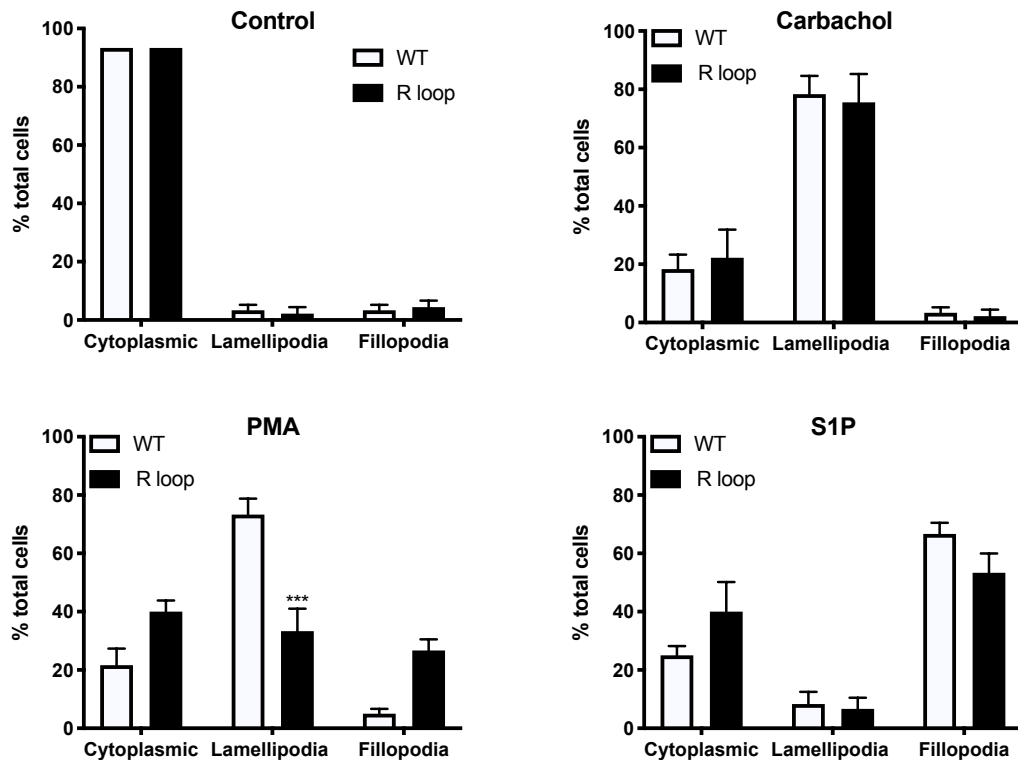


Figure 4.37 Phenotypic shift of stimulated MCF-7L cells transiently overexpressing mGFP-SK1 R-loop mutant compared to WTmGFP-SK1

The bar graphs represents the % of MCF-7L cells transiently overexpressing *mGFP-SK1* R-loop mutant showing *mGFP-SK1* in spread (lamellipodia) or filopodia micro-domains in response to S1P (5 μ M, 10 minutes), PMA (1 μ M, 10 minutes) or carbachol (100 μ M, 10 minutes) or vehicle (DMSO, 0.1% (v/v)) and compared to the phenotype displayed by WT*mGFP-SK1*. 15 random cells on 4 separate cover slips were analysed (n=4); ***p<0.001 for R-loop mutant *versus* WT for a given phenotype (two-way ANOVA with Tukey's multiple comparison test).

4.3 Discussion

SK1 is able to translocate to the PM in a phosphorylation-dependent (Pitson et al., 2003) or independent manner (ter Braak et al., 2009). Both mechanisms are thought to involve a hydrophobic patch on LBL-1 and positively charged residues that make up a contiguous membrane-binding interface when the CTD and NTD are able to freely twist following the uncapping of the C-terminal tail. Membrane engagement therefore involves hydrophobic and electrostatic interactions with membrane-bound acidic phospholipids (Delon et al., 2004; Stahelin et al., 2005).

Herein we show that the removal of 5 amino acids from the C-terminus (PPEEP) produces an enzyme that exhibits reduced translocation in response to carbachol or S1P, but not PMA. Therefore, the last 5 amino acids are important for

phosphorylation-independent translocation. Further truncation of the C-terminal restores sensitivity to carbachol and S1P to promote translocation of SK1. This provides evidence that amino acids 6-10 of the C-terminus acts as a locking motif to prevent translocation. Moreover, release of the locking motif is via binding of a putative adapter protein to the last 5 amino acids, perhaps to displace the C-terminal tail completely from the locking engagement site. This might increase twisting in a N-terminal domain:C-terminal domain (NTD:CTD) 'connecting rod' to allow for a contiguous hydrophobic and positively charged surface, used by SK1 to associate with the PM. In this regard, WT*mGFP-SK1* has both locking motif and binding site for the adapter protein, whereas *mGFP-SK1 T1* retains only the locking motif, rendering the enzyme less able to translocate without phosphorylation. Further truncation past amino acid 5 of the C-terminal removes the locking motif, bypassing the need for binding of the adapter protein and therefore the enzyme is capable of translocation upon G_q activation and the formation of PA. The inability of the T1 mutant to translocate to the PM in response to S1P or carbachol is translated into an impaired cellular response, as unlike the cells over-expressing WT*mGFP-SK1*, those cells over-expressing the T1 mutant exhibited reduced migration in response to carbachol or S1P. Therefore, residency on the PM by SK1 is essential for the migratory response.

4.3.1 Translocation is regulated by a locking motif and displacement motif that governs inter-domain twisting about a twisted strand pair and the alignment of the membrane-engagement interface

Removal of the last 5 amino acids of the C-terminus (PPEEP) produced an enzyme defective in GPCR-mediated translocation, but not phosphorylation-dependent translocation, which was rectified by further truncation. These findings suggest that the displacement motif is non-critical for phosphorylation-dependent translocation in response to ERK activation. Furthermore, analysis of available crystal structures indicate that the R-loop is well positioned to mediate similar interdomain movements. Therefore, Ser²²⁵ phosphorylation under PMA drive is likely to orchestrate similar release of the 'locking motif', bypassing the need for adapter protein binding to PPEEP. This would explain why T1, in which only the 'locking motif' is present, retains the ability to translocate in response to PMA. Both of these mechanisms therefore govern interdomain twisting and thus the alignment of a contiguous membrane-binding interface.

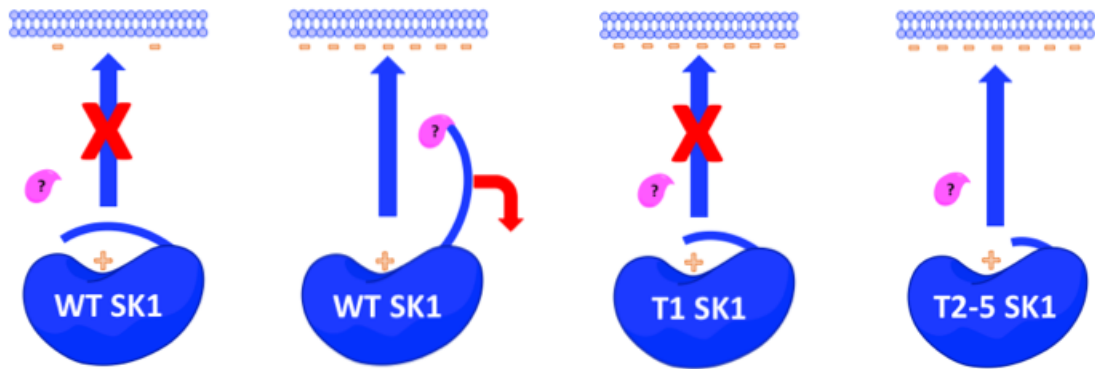


Figure 4.34 locking motif and the displacement motif in the C-terminal tail

At rest, the 'locking motif' of the C-terminus restricts inter-domain twisting and thus the membrane-engagement interface is misaligned. Ligand-induced activation leads to the recruitment of an adapter protein that binds to the 'displacement motif' at the last 5 amino acids; releasing the 'locking motif' and in turn enables inter-domain twisting and the alignment of a contiguous membrane-binding interface that is able to interact with anionic membrane-bound PA. T1 is unable to translocate as the 'locking motif' cannot be released as the enzyme lacks the 'displacement motif'. Translocation is restored upon further truncation where both motifs are removed, simply requiring G_q activation and PA formation.

Crystal structure analysis indicated a long, twisted strand pair (green ribbon) between the CTD (pink structure) and NTD (blue structure) (Fig. 4.35), which is conserved in *mSK1* and *hSK1* acting as a 'connecting rod'. In this regard, SK1 shares similar conformational movements with DAGK_cat lipid kinases such as YegS from *S. typhimurium* and *E. coli* and DgkB from *S. aureus* (Bakali et al., 2007; Nichols et al., 2007; Miller et al., 2008). Comparative structural analysis has revealed that prokaryotic relatives of SK1 similarly display interdomain twisting about a twisted strand pair (Nichols et al., 2007), analogous to the 'connecting rod' present in SK1, which may regulate membrane binding and activity. In this regard, it is thought that rotational freedom governs the topographical alignment/misalignment of the membrane engagement interface, comprised on hydrophobic patches on LBL-1 and a positively charged cluster of amino acids on the surface of the enzyme. For translocation to occur these membrane engagement sites must form a contiguous binding interface. In a cytoplasm we propose that the membrane engagement sites of SK1 are misaligned, with activation of the enzyme leading to twisting about the 'connecting rod' to form a contiguous membrane binding interface. Further investigation is required in order to establish the role of the LBL-1 and positive charged cluster topography for the monomer.

The C-terminal tail appears to thread through a cleft in the 'connecting rod' (Fig. 4.35). It is the displacement of which that would enable coiling of the domains about the 'connecting rod' and simultaneous optimal alignment of the NTD:CTD contiguous membrane binding interface for translocation and catalysis. Indeed, this mechanism has been shown to be important for the PM binding of prokaryotic relatives of SK1 (Jerga et al., 2009). Therefore, it is proposed that within the cytosolic/inactive state (blue dotted line), the C-terminus 'locking motif' features hydrogen bonds with the 'connecting rod' (His¹⁵⁶/His³⁵⁵) and remains lodged between the 'connecting rod' cleft to prevent inter-domain twisting (Fig. 4.35). In this case the membrane engagement determinants remain misaligned. Ligand-induced orientation in the C-terminus (red dotted line) from the cleft of the 'connecting rod' by carbachol/S1P or PMA enables the binding of an adaptor protein to the displacement motif/key (PPEEP) or displacement of the His¹⁵⁶/His³⁵⁵ hydrogen bonds by R-loop Asp²³⁵ (cyan loop), respectively. This is proposed to release of N89 and rotational freedom of the stranded pair to align membrane-engagement determinants. This mechanism provides regulation of SK1 translocation based on the rotational freedom about the twisted strand pair that governs the alignment of a contiguous membrane-binding interface. Moreover this model would explain why complete removal of the C-terminus leads to constitutive PM localisation in HEK293 cells (Hengst et al., 2010), whereby the 'connecting rod' is able to freely twist. A possible explanation for the lack of constitutive PM localisation in MCF-7L cells compared with HEK293 cells (Hengst et al., 2010) may be due different levels of PLD activity or diacylglycerol kinase that phosphorylates diacylglycerol to produce PA. In HEK293 cells this would negate the need for receptor-induced formation of PA. Differences in the PLD level/activity of MCF-7L cells and HEK293 cells remains to be investigated.

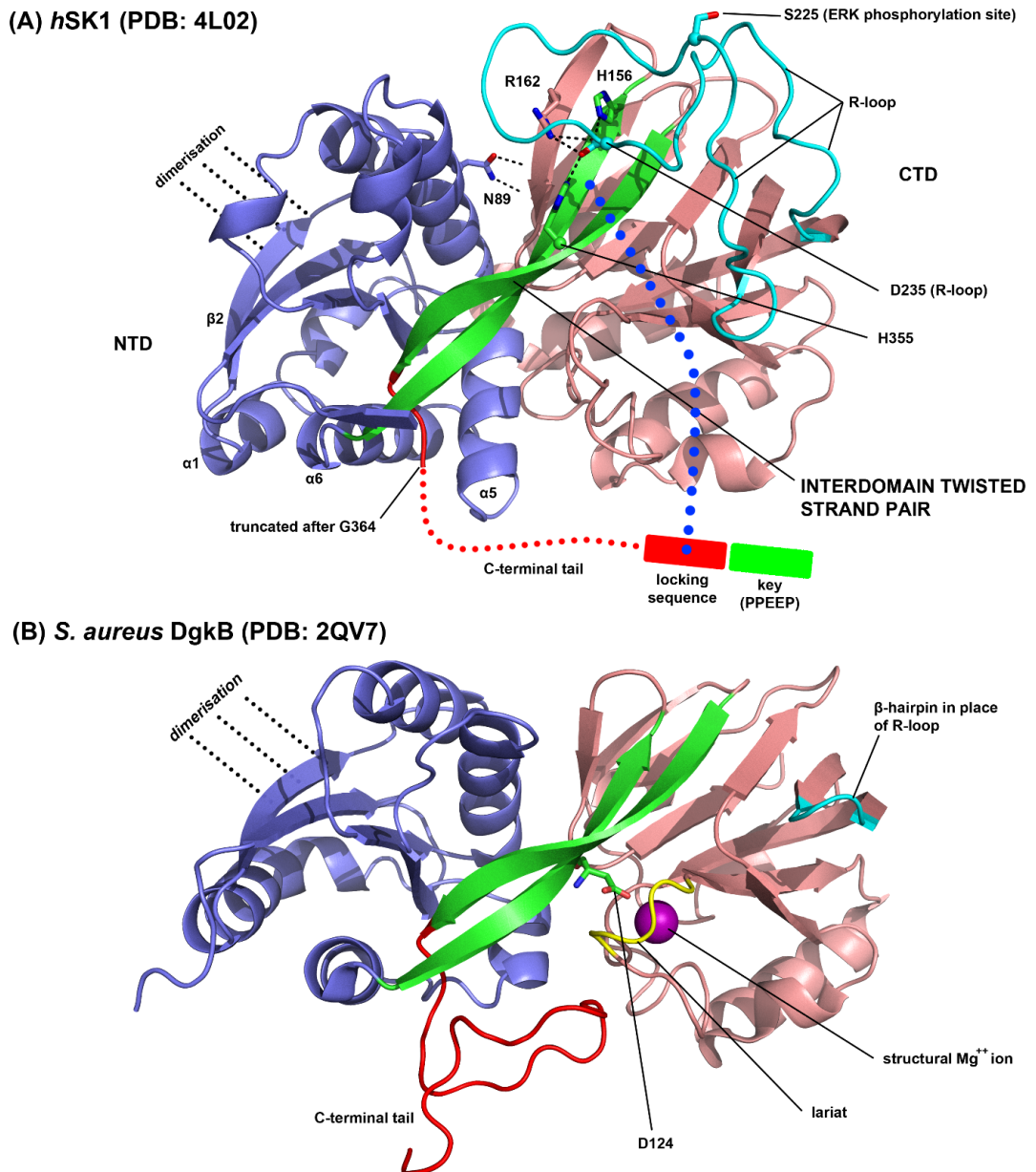


Figure 4.35 Structural rationale for alignment of membrane engagement determinants orchestrated by R-loop and C-terminal tail

(A) SK1 and other related DAGK_cat proteins have a long, twisted pair (green ribbon) between the NTD (blue structure) and CTD (pink structure) that acts as a ‘connecting rod’ whereby the domains can twist about. This inter-domain movement is thought to control the topographical alignment or misalignment of a contiguous membrane binding interface, composed of a positively charged cluster of residues and hydrophobic patches on LBL-1. (B) Prokaryotic DAGK_cat proteins, such as DgkB from *S. aureus* (PDB: 2QV7) shown here, display many of the same conformational properties to SK1 (same colour coding). The R-loop is replaced by a simple hairpin and an Mg^{2+} ion (purple sphere) is held in a lariat loop (yellow ribbon) which engages through Asp¹²⁴ on the twisted strand pair and has a similar role in controlling rotational freedom of the strand pair to that of the C-terminus/R-loop in SK1.

Further analysis of the phenotypes of translocation reveal that complete removal of the C-terminus (T5) promoted ligand-induced translocation to filopodia in response to ligands that have previously shown to promote translocation to lamellipodia. This implies a role for Gly³⁶⁴ and the 4 other amino acids further removed in *mGFP-SK1* T5 for either, preventing translocation to lamellipodia or promoting translocation to filopodia by perhaps 'stabilizing' the dimeric form of the enzyme. The key issue here might be the role of Gly³⁶⁴, whereby *mGFP-SK1* T5 retains no capping capability over helix- α 5 that is involved in ATP binding and T-loop plasticity, therefore the shift in phenotype may be due to changes in catalytic capability or dimerisation properties of the enzyme. It is possible that complete truncation of the C-terminus enables greater rotational freedom about the 'connecting rod' to align the NTD:CTD and allow for a more facile NTD:NTD dimerization. This assembly appears crucial for the formation of the densely packed positively charged residues at the dimer groove, which enables the dimer to translocate to filopodia (as previously discussed in 3.3.5). Furthermore, T1 is incapable of translocating to the PM in response to carbachol, previously indicated to shift the equilibrium in favour of the monomer, or S1P that favours the dimer. Therefore, this provides basis for the C-terminus regulating translocation of both monomeric and dimeric SK1 forms.

Truncation of the C-terminus does not lead to hyperphosphorylation of SK1, previously shown to bind PP2A (Barr et al., 2008), thereby demonstrating T2-T5 exhibits *bona fide* GPCR-mediated translocation that is phosphorylation independent. This is in corroboration with other studies reporting no change in the phosphorylation state of the enzyme after complete truncation of the C-terminus (Hengst et al., 2010). Furthermore, the translocation of T1 in response to PMA is blocked when ERK-1/2 activation is inhibited, indicating that T1 is able to translocate in a phosphorylation-dependent manner. Alternatively, the lack of PMA-induced translocation of T1-5 in the presence of PD98059 may also be explained by changes in PA levels. PLD is known to be activated downstream of PKC (Singer et al., 1996). Moreover, all 3 agonists stimulate PKC and hence PLD activity. However PMA is the only agonist that is dependent on ERK-1/2 in terms of promoting the translocation of SK1 and has been shown here to be the most powerful activator of ERK-1/2. Thus ERK-1/2 induced translocation of SK1 likely requires a threshold level of ERK-1/2 activation, in addition to PLD. Conversely, carbachol and S1P are dependent on PLD but not ERK-1/2.

4.3.2 G_q is not binding to the regulatory loop of SK1

G_q remains vital for the translocation of T2-T5 and therefore is facilitating translocation independently of the C-terminus. An alternative binding site would allow G_q to simultaneously bind SK1 as well as PLC and would explain why T2-5 remain unable to translocate when G_q activity was blocked. Analysis of the crystal structure revealed a potential binding site on the R-loop of SK1, which shared a similar sequence to the proposed binding site on the C-terminal tail. It is already known that Ser²²⁵ can be phosphorylated on the R-loop to induce phosphorylation-dependent translocation (Pitson et al., 2003), however it is not yet clear whether this is as a result of structural changes.

Mutagenesis to incorporate negative charge into the potential binding site (238-PLLEP-242 to 238-PLAAP-242) and thus disrupt potential G_q binding did not affect the ability of SK1 to translocate the PM. This infers that G_q is likely binding indirectly or elsewhere on SK1. Further investigation is required to identify if/where G_q binds, which may provide novel therapeutics for preventing the translocation of SK1. Further observations revealed that mutation to the R-loop resulted in reduced PMA-mediated translocation to lamellipodia. These observations infer a functional role for the R-loop in regulating translocation of SK1 to specific PM micro-domains, more specifically to lamellipodia in a phosphorylation-dependent manner.

4.4 Summary and future directions

To summarise, we show that the C-terminal tail of SK1 can regulate the translocation of SK1 to specific PM micro-domains in a ligand-specific manner. Furthermore, the G_q and PA dependency for translocation is independent of the C-terminus length. The C-terminus is, however, likely to provide regulation over inter-domain twisting about a twisted strand pair, known as the 'connecting rod', through the existence of a 'locking motif' and 'displacement motif'. Displacement of the C-terminus from the 'connecting rod' allows rotational freedom of the two domains and thus the ability to form a contiguous membrane binding interface composed of positively charged and hydrophobic residues necessary for translocation. Moreover, the data suggests that the 'locking motif' and 'displacement motif' are required for phosphorylation-independent translocation, with Ser²²⁵ phosphorylation potentially acting as the release mechanism.

Further investigation will focus on identifying the adapter protein responsible for binding to the 'displacement motif'. By using mass spectrometry, it may be possible

to investigate the differences in protein-protein interactions between WTmGFP-SK1 and the defective C-terminally truncated T1 mutant and thus identify the adapter protein. In addition we aim to confirm this interaction by siRNA knockdown of the adapter protein, that may provide a novel therapeutic approach for diseases such as cancer where SK1 translocation drives disease pathology (Cuvillier 2008). Unfortunately, laboratory work ceased due to the COVID-19 outbreak and thus further investigation was not permitted.

Chapter 6

General discussion and future directions

6.0 General discussion and future directions

6.1 General discussion

Sphingolipids are essential lipids involved in the structure of eukaryotic cell membranes, although more recently they have been acknowledged to have additional important roles as bioactive lipid mediators in signal transduction. Arguably the most important of these bioactive lipids are S1P and ceramide formed by sphingosine kinases (SK1 and SK2) and dihydroceramide desaturase, respectively, that control cell fate (Olivera et al., 1999) and are involved in cancer cell pathophysiology (Newton et al., 2015). SK1 has a crucial role in tumour growth (Olivera et al., 1999), tumour vascularisation (Licht et al., 2003) and metastasis (Visentin et al., 2006), ultimately driving oncogenic transformation (Xia et al., 2000). It is not surprising therefore that high levels of SK1 correlates with poorer prognosis (Pyne et al., 2012; Zhang et al., 2014). Hence SK1 has gained substantial interest of recent times, although there is still much to learn about translocation that governs activation of the enzyme. Previous studies demonstrate that SK1 is able to translocate in a manner that is dependent on phosphorylation of the Ser²²⁵ residue (Pitson et al., 2003; Pitman et al., 2015) and independently of Ser²²⁵ phosphorylation involving G_q activation (ter Braak et al., 2009). This has raised the question; what are the mechanisms of SK1 translocation via phosphorylation-dependent and -independent mechanism and what are the structural features of SK1 that enable this to occur? The primary aim of the current study was to uncover mechanisms governing the translocation of SK1, with a predominant focus on dimerization (chapter 3) and the C-terminal tail (chapter 4) that are thought to regulate alignment of the membrane binding interface. This is in response to a growing literature indicating that SK1 can act as dimer (Lim et al., 2011; Adams et al., 2016) as well as the originally characterised monomeric form (Olivera et al., 1998), with the C-terminus likely to regulate translocation of both forms (Adams et al., 2016). Moreover, SK1 recruitment to the PM has been shown to be required for endocytosis (Shen et al., 2014; Lima et al., 2017) that is implicated in cancer (Mosesson et al., 2008). Therefore, we additionally investigated the role of SK1 in endocytic processing (chapter 5).

Initial results substantiated reports that PA (Delon et al., 2004) and G_q (ter Braak et al., 2009) are important in facilitating the translocation of SK1 to the PM. SK1 is subject to a monomer/dimer equilibrium influenced in a ligand-specific manner that enables the translocation of SK1 to different PM micro-domains. Specifically, it was

identified that dimeric SK1 is able to translocate in a phosphorylation-independent manner to filopodia in response to S1P. However, as S1P promoted the migration of MCF-7L cells, this suggests that what is observed is most likely SK1 enriched filopodia. Co-localisation with markers of filopodia will be needed to confirm this. In contrast, the translocation of monomeric SK1 was to lamellipodia, which was phosphorylation-dependent in response to PMA and phosphorylation-independent in response to carbachol. Furthermore, results demonstrate that S1P or carbachol promote the migration of cells transiently over-expressing WT*mGFP-SK1*, therefore both monomeric and dimeric SK1 are able to drive migration. This notion is further substantiated by the fact that that T1 mutant over-expressing show reduced migration to S1P or carbachol. Moreover, restriction to solely monomeric SK1 resulted in a reduced ability of the enzyme to mobilise F-actin following stimulation, which coincided with a migrative inability. This suggests that a threshold level of translocation must be met (i.e. a certain level of S1P produced) in order to initiate migration. Furthermore, cells transiently overexpressing *mGFP-SK1-I51C* displayed constitutive migration that implies the process of dimerization alone results in pro-migratory signalling not dependent on PM localisation of the enzyme. The dimeric SK1 conformation is likely to provide curvature-sensitive binding to the PM (Adams et al., 2016), however it remains to be determined whether this is also the case for monomeric SK1. These novel findings are the first to show functional differences between monomeric and dimeric SK1, and that *mSK1* exist in a monomeric/dimeric equilibrium, which remains the subject of great debate. In order to perturb the monomer/dimer equilibrium and translocation to specific PM micro-domains, the precise mechanisms require further investigation.

Regulation of SK1 translocation has also been shown to involve the C-terminal (Hengst et al., 2010; Adams et al., 2016) and hence the regulatory role of the C-terminal tail was investigated. The findings illustrated that removal of 5 amino acids from the outermost region of the C-terminus produced an enzyme unable to translocate in a phosphorylation-independent manner, which was restored by further truncation. This indicated the presence of a 'locking motif' at amino acids 6-10 of the C-terminal tail, which can be released by the binding of an adapter protein to amino acids 1-5 of the C-terminal tail. In addition, previous crystallographic analysis has indicated that a contiguous membrane binding interface forms that allows simultaneous PM docking of SK1 and phosphorylation of SPH. Moreover, molecular modelling revealed that the C-terminal tail threads through a twisted strand pair that

connects the CTD and NTD, coined the 'connecting rod'. In this regard, it is thought that the alignment/misalignment of the membrane binding interface and hence translocation is determined by whether rotational freedom around the 'connecting rod' can be achieved, which is governed by orientation of the C-terminal tail. It is proposed that this mechanism governs the translocation of monomeric and dimeric SK1, presenting a unified mechanism for both phosphorylation-independent and -dependent translocation, whereby the C-terminal tail in latter case can be 'unlocked' by Ser²²⁵ phosphorylation.

These novel findings add to the current understanding of SK1 translocation and may provide therapeutic targets. Differential localisation of monomeric and dimeric SK1 may increase the spatial and temporal control over S1P production and thus provide the basis for pleiotropic S1P signalling. This might have implications in disease pathology in cases, for example, whereby dimeric SK1 may drive disease, whilst monomeric SK1 does not and *vice versa*. Indeed, previous studies have modelled putative allosteric SK1 inhibitors that target dimerization (Bayraktar et al., 2017), which is a therapeutic target for other kinases such as RAF (Hu et al., 2013), Ras (Nan et al., 2015) and epidermal growth factor receptor (Zhang et al., 2006).

Additionally, identification of the adapter protein responsible for binding to the 'displacement motif' remains unknown and will be the focus of future studies. Revealing its identity may provide a potential target to prevent the translocation of SK1 by developing locking peptides and small molecule drugs that mimic the locking peptide to maintain SK1 in a membrane engagement misaligned state in the cytoplasm. Such compounds could compete for binding of the 'displacement motif', thereby reducing the production of S1P, favourable in reducing the progression of cancer. Alternatively, in diseases where SK1 is thought to have reduced translocation/activity such as in Alzheimer's disease (Ceccom et al., 2014; Couttas et al., 2014), it may be possible to increase SK1 translocation/activity by enhancing C-terminal displacement through the creation of a peptide analogous to the adapter protein sequence or small molecules that mimic the peptide. Additional findings revealed that G_q was not binding to the R-loop of SK1 and thus further investigation is required to identify the G_q binding site. Constitutive G_q activation drives SK1 translocation (ter Braak et al., 2009). Therefore, identification of the binding site on SK1 may provide another target to modulate translocation without altering catalytic activity of the enzyme.

6.2 Conclusion and future directions

The current study presents evidence for a monomer/dimer SK1 equilibrium and adds knowledge to the phosphorylation-dependent and -independent mechanisms of SK1 translocation, additionally reinforcing the notion that SK1 is involved in endocytosis. Further investigation is required to identify how the 'locking motif' is able to hold the C-terminus in place and what protein-protein interactions are involved in displacement of the tail to ultimately regulate translocation. Additional investigation is also required to understand events involved in establishing dimerization of SK1 and subsequent translocation of monomeric/dimeric SK1 to different PM micro-domains. This may additionally reveal targets for cancer therapy whereby translocation of SK1 may be disrupted/targeted to certain PM micro-domains without altering the 'basal' catalytic activity of the enzyme, and thereby maintaining resting S1P levels. We also further investigated the role of SK1 in the endocytic process, although further research is needed to fully understand the role of SK1 in endosomal processing. Developing our understanding in this area may reveal how SK1 is involved in dysregulated autophagy and cell-surface presentation of receptors in cancer.

Chapter 7

References

7.0 References

- Acharya, S., J. Yao, P. Li, C. Zhang, F. J. Lowery, Q. Zhang, H. Guo, J. Qu, F. Yang, Wistuba, II, H. Piwnica-Worms, A. A. Sahin and D. Yu (2019). "Sphingosine Kinase 1 Signaling Promotes Metastasis of Triple-Negative Breast Cancer." *Cancer Res* **79**(16): 4211-4226.
- Adada, M. M., D. Canals, N. Jeong, A. D. Kelkar, M. Hernandez-Corbacho, M. J. Pulkoski-Gross, J. C. Donaldson, Y. A. Hannun and L. M. Obeid (2015). "Intracellular sphingosine kinase 2-derived sphingosine-1-phosphate mediates epidermal growth factor-induced ezrin-radixin-moesin phosphorylation and cancer cell invasion." *FASEB J* **29**(11): 4654-4669.
- Adams, D. R., S. Pyne and N. J. Pyne (2016). "Sphingosine Kinases: Emerging Structure-Function Insights." *Trends Biochem Sci* **41**(5): 395-409.
- Adams, D. R., S. Tawati, G. Berretta, P. L. Rivas, J. Baiget, Z. Jiang, A. Alsouk, S. P. Mackay, N. J. Pyne and S. Pyne (2019). "Topographical Mapping of Isoform-Selectivity Determinants for J-Channel-Binding Inhibitors of Sphingosine Kinases 1 and 2." *J Med Chem* **62**(7): 3658-3676.
- Akoglu, H. (2018). "User's guide to correlation coefficients." *Turk J Emerg Med* **18**(3): 91-93.
- Allende, M. L., T. Sasaki, H. Kawai, A. Olivera, Y. Mi, G. van Echten-Deckert, R. Hajdu, M. Rosenbach, C. A. Keohane, S. Mandala, S. Spiegel and R. L. Proia (2004). "Mice deficient in sphingosine kinase 1 are rendered lymphopenic by FTY720." *J Biol Chem* **279**(50): 52487-52492.
- Allende, M. L., G. Tuymetova, B. G. Lee, E. Bonifacio, Y. P. Wu and R. L. Proia (2010). "S1P1 receptor directs the release of immature B cells from bone marrow into blood." *J Exp Med* **207**(5): 1113-1124.
- Allende, M. L., T. Yamashita and R. L. Proia (2003). "G-protein-coupled receptor S1P1 acts within endothelial cells to regulate vascular maturation." *Blood* **102**(10): 3665-3667.
- Alsanafi, M., S. L. Kelly, K. Jubair, M. McNaughton, R. J. Tate, A. H. Merrill, Jr., S. Pyne and N. J. Pyne (2018). "Native and Polyubiquitinated Forms of Dihydroceramide Desaturase Are Differentially Linked to Human Embryonic Kidney Cell Survival." *Mol Cell Biol* **38**(23).
- Alvarez, S. E., K. B. Harikumar, N. C. Hait, J. Allegood, G. M. Strub, E. Y. Kim, M. Maceyka, H. Jiang, C. Luo, T. Kordula, S. Milstien and S. Spiegel (2010). "Sphingosine-1-phosphate is a missing cofactor for the E3 ubiquitin ligase TRAF2." *Nature* **465**(7301): 1084-1088.
- Alvarez, S. E., S. Milstien and S. Spiegel (2007). "Autocrine and paracrine roles of sphingosine-1-phosphate." *Trends Endocrinol Metab* **18**(8): 300-307.
- Ancellin, N., C. Colmont, J. Su, Q. Li, N. Mittereder, S. S. Chae, S. Stefansson, G. Liau and T. Hla (2002). "Extracellular export of sphingosine kinase-1 enzyme. Sphingosine 1-phosphate generation and the induction of angiogenic vascular maturation." *J Biol Chem* **277**(8): 6667-6675.
- Andrieu, G., A. Ledoux, S. Branka, M. Bocquet, J. Gilhodes, T. Walzer, K. Kasahara, M. Inagaki, R. A. Sabbadini, O. Cuvillier and A. Hatzoglou (2017). "Sphingosine 1-phosphate signaling through its receptor S1P5 promotes chromosome segregation and mitotic progression." *Sci Signal* **10**(472).
- Arikawa, K., N. Takuwa, H. Yamaguchi, N. Sugimoto, J. Kitayama, H. Nagawa, K. Takehara and Y. Takuwa (2003). "Ligand-dependent inhibition of B16 melanoma cell migration and invasion via endogenous S1P2 G protein-coupled receptor. Requirement of inhibition of cellular RAC activity." *J Biol Chem* **278**(35): 32841-32851.
- Badawy, S. M. M., T. Okada, T. Kajimoto, M. Hirase, S. A. Matovelo, S. Nakamura, D. Yoshida, T. Ijuin and S. I. Nakamura (2018). "Extracellular alpha-synuclein drives sphingosine 1-phosphate receptor subtype 1 out of lipid rafts, leading to impaired inhibitory G-protein signaling." *J Biol Chem* **293**(21): 8208-8216.
- Bagnjuk, K., J. B. Stockl, T. Frohlich, G. J. Arnold, R. Behr, U. Berg, D. Berg, L. Kunz, C. Bishop, J. Xu and A. Mayerhofer (2019). "Necroptosis in primate luteolysis: a role for ceramide." *Cell Death Discov* **5**: 67.
- Bailey, L. J., S. Alahari, A. Tagliaferro, M. Post and I. Caniggia (2017). "Augmented trophoblast cell death in preeclampsia can proceed via ceramide-mediated necroptosis." *Cell Death Dis* **8**(2): e2590.
- Bajjalieh, S. M., T. F. Martin and E. Floor (1989). "Synaptic vesicle ceramide kinase. A calcium-stimulated lipid kinase that co-purifies with brain synaptic vesicles." *J Biol Chem* **264**(24): 14354-14360.
- Bakali, H. M., M. D. Herman, K. A. Johnson, A. A. Kelly, A. Wieslander, B. M. Hallberg and P. Nordlund (2007). "Crystal structure of YegS, a homologue to the mammalian diacylglycerol kinases, reveals a novel regulatory metal binding site." *J Biol Chem* **282**(27): 19644-19652.
- Balaji Ragnathrao, V. A., M. Anwar, M. Z. Akhter, A. Chavez, Y. Mao, V. Natarajan, S. Lakshminathan, M. Chrzanoska-Wodnicka, A. Z. Dudek, L. Claesson-Welsh, J. K. Kitajewski, K. K. Wary, A. B. Malik and D. Mehta (2019). "Sphingosine-1-Phosphate Receptor 1 Activity Promotes Tumor Growth by Amplifying VEGF-VEGFR2 Angiogenic Signaling." *Cell Rep* **29**(11): 3472-3487 e3474.
- Banno, Y., Y. Takuwa, Y. Akao, H. Okamoto, Y. Osawa, T. Naganawa, S. Nakashima, P. G. Suh and Y. Nozawa (2001). "Involvement of phospholipase D in sphingosine 1-phosphate-induced activation of phosphatidylinositol 3-kinase and Akt in Chinese hamster ovary cells overexpressing EDG3." *J Biol Chem* **276**(38): 35622-35628.
- Barcelo-Coblijn, G., M. L. Martin, R. F. de Almeida, M. A. Noguera-Salva, A. Marcilla-Etxenike, F. Guardiola-Serrano, A. Luth, B. Kleuser, J. E. Halver and P. V. Escriba (2011). "Sphingomyelin and sphingomyelin synthase (SMS) in the malignant transformation of glioma cells and in 2-hydroxyoleic acid therapy." *Proc Natl Acad Sci U S A* **108**(49): 19569-19574.
- Barr, R. K., H. E. Lynn, P. A. Moretti, Y. Khew-Goodall and S. M. Pitson (2008). "Deactivation of sphingosine kinase 1 by protein phosphatase 2A." *J Biol Chem* **283**(50): 34994-35002.
- Bayraktar, O., E. Ozkirimli and K. Ulgen (2017). "Sphingosine kinase 1 (SK1) allosteric inhibitors that target the dimerization site." *Comput Biol Chem* **69**: 64-76.

Bergelin, N., T. Blom, J. Heikkila, C. Lof, C. Alam, S. Balthasar, J. P. Slotte, A. Hinkkanen and K. Tornquist (2009). "Sphingosine kinase as an oncogene: autocrine sphingosine 1-phosphate modulates ML-1 thyroid carcinoma cell migration by a mechanism dependent on protein kinase C-alpha and ERK1/2." *Endocrinology* **150**(5): 2055-2063.

Beyer, S., S. Schwalm, J. Pfeilschifter and A. Huwiler (2018). "Renal Mesangial Cells Isolated from Sphingosine Kinase 2 Transgenic Mice Show Reduced Proliferation and are More Sensitive to Stress-Induced Apoptosis." *Cell Physiol Biochem* **47**(6): 2522-2533.

Brachk, N., O. Dormond, S. Bekri, D. Golshayan, M. Correvon, L. Mazzolai, B. Steinmann and F. Barbey (2010). "Evidence for a role of sphingosine-1 phosphate in cardiovascular remodelling in Fabry disease." *Eur Heart J* **31**(1): 67-76.

Brinkmann, V., J. G. Cyster and T. Hla (2004). "FTY720: sphingosine 1-phosphate receptor-1 in the control of lymphocyte egress and endothelial barrier function." *Am J Transplant* **4**(7): 1019-1025.

Brizuela, L., I. Ader, C. Mazerolles, M. Bocquet, B. Malavaud and O. Cuvillier (2012). "First evidence of sphingosine 1-phosphate lyase protein expression and activity downregulation in human neoplasm: implication for resistance to therapeutics in prostate cancer." *Mol Cancer Ther* **11**(9): 1841-1851.

Brizuela, L., A. Dayon, N. Doumerc, I. Ader, M. Golzio, J. C. Izard, Y. Hara, B. Malavaud and O. Cuvillier (2010). "The sphingosine kinase-1 survival pathway is a molecular target for the tumor-suppressive tea and wine polyphenols in prostate cancer." *FASEB J* **24**(10): 3882-3894.

Brown, D. A. and E. London (2000). "Structure and function of sphingolipid- and cholesterol-rich membrane rafts." *J Biol Chem* **275**(23): 17221-17224.

Bryce, N. S., E. S. Clark, J. L. Leysath, J. D. Currie, D. J. Webb and A. M. Weaver (2005). "Cortactin promotes cell motility by enhancing lamellipodial persistence." *Curr Biol* **15**(14): 1276-1285.

Buehrer, B. M., E. S. Bardes and R. M. Bell (1996). "Protein kinase C-dependent regulation of human erythroleukemia (HEL) cell sphingosine kinase activity." *Biochim Biophys Acta* **1303**(3): 233-242.

Cartier, A., T. Leigh, C. H. Liu and T. Hla (2020). "Endothelial sphingosine 1-phosphate receptors promote vascular normalization and antitumor therapy." *Proc Natl Acad Sci U S A* **117**(6): 3157-3166.

Casasampere, M., Y. F. Ordonez, J. Casas and G. Fabrias (2017). "Dihydroceramide desaturase inhibitors induce autophagy via dihydroceramide-dependent and independent mechanisms." *Biochim Biophys Acta Gen Subj* **1861**(2): 264-275.

Cataldo, A. M., C. M. Peterhoff, J. C. Troncoso, T. Gomez-Isla, B. T. Hyman and R. A. Nixon (2000). "Endocytic pathway abnormalities precede amyloid beta deposition in sporadic Alzheimer's disease and Down syndrome: differential effects of APOE genotype and presenilin mutations." *Am J Pathol* **157**(1): 277-286.

Cattoretti, G., J. Mandelbaum, N. Lee, A. H. Chaves, A. M. Mahler, A. Chadburn, R. Dalla-Favera, L. Pasqualucci and A. J. MacLennan (2009). "Targeted disruption of the S1P2 sphingosine 1-phosphate receptor gene leads to diffuse large B-cell lymphoma formation." *Cancer Res* **69**(22): 8686-8692.

Coecoom, J., N. Loukh, V. Lauwers-Cances, C. Touriol, Y. Nicaise, C. Gentil, E. Uro-Coste, S. Pitson, C. A. Mauraage, C. Duyckaerts, O. Cuvillier and M. B. Delisle (2014). "Reduced sphingosine kinase-1 and enhanced sphingosine 1-phosphate lyase expression demonstrate deregulated sphingosine 1-phosphate signaling in Alzheimer's disease." *Acta Neuropathol Commun* **2**: 12.

Chae, S. S., J. H. Paik, H. Furneaux and T. Hla (2004). "Requirement for sphingosine 1-phosphate receptor-1 in tumor angiogenesis demonstrated by in vivo RNA interference." *J Clin Invest* **114**(8): 1082-1089.

Chalfant, C. E. and S. Spiegel (2005). "Sphingosine 1-phosphate and ceramide 1-phosphate: expanding roles in cell signaling." *J Cell Sci* **118**(Pt 20): 4605-4612.

Chan, J. P., Z. Hu and D. Sieburth (2012). "Recruitment of sphingosine kinase to presynaptic terminals by a conserved muscarinic signaling pathway promotes neurotransmitter release." *Genes Dev* **26**(10): 1070-1085.

Chang, C. L., M. C. Ho, P. H. Lee, C. Y. Hsu, W. P. Huang and H. Lee (2009). "S1P(5) is required for sphingosine 1-phosphate-induced autophagy in human prostate cancer PC-3 cells." *Am J Physiol Cell Physiol* **297**(2): C451-458.

Chatagnon, C. and P. Chatagnon (1958). "[Chemical research on brain tissue components during the 19th century: a British pioneer: John Lewis William Thudichum]." *Ann Med Psychol (Paris)* **116**(2): 267-282.

Chen, Y., P. Zhang, S. C. Xu, L. Yang, U. Voss, E. Ekblad, Y. Wu, Y. Min, E. Hertervig, A. Nilsson and R. D. Duan (2015). "Enhanced colonic tumorigenesis in alkaline sphingomyelinase (NPP7) knockout mice." *Mol Cancer Ther* **14**(1): 259-267.

Chipuk, J. E., G. P. McStay, A. Bharti, T. Kuwana, C. J. Clarke, L. J. Siskind, L. M. Obeid and D. R. Green (2012). "Sphingolipid metabolism cooperates with BAK and BAX to promote the mitochondrial pathway of apoptosis." *Cell* **148**(5): 988-1000.

Cho, Y. S., S. Challa, D. Moquin, R. Genga, T. D. Ray, M. Guildford and F. K. Chan (2009). "Phosphorylation-driven assembly of the RIP1-RIP3 complex regulates programmed necrosis and virus-induced inflammation." *Cell* **137**(6): 1112-1123.

Chun, J., T. Hla, K. R. Lynch, S. Spiegel and W. H. Moolenaar (2010). "International Union of Basic and Clinical Pharmacology. LXXVIII. Lysophospholipid receptor nomenclature." *Pharmacol Rev* **62**(4): 579-587.

Colie, S., P. P. Van Veldhoven, B. Kedjouar, C. Bedia, V. Albinet, S. C. Sorli, V. Garcia, M. Djavaheri-Mergny, C. Bauvy, P. Codogno, T. Levade and N. Andrieu-Abadie (2009). "Disruption of sphingosine 1-phosphate lyase confers resistance to chemotherapy and promotes oncogenesis through Bcl-2/Bcl-xL upregulation." *Cancer Res* **69**(24): 9346-9353.

Couttas, T. A., N. Kain, B. Daniels, X. Y. Lim, C. Shepherd, J. Kril, R. Pickford, H. Li, B. Garner and A. S. Don (2014). "Loss of the neuroprotective factor Sphingosine 1-phosphate early in Alzheimer's disease pathogenesis." *Acta Neuropathol Commun* **2**: 9.

Cuvillier, O. (2008). "Downregulating sphingosine kinase-1 for cancer therapy." *Expert Opin Ther Targets* **12**(8): 1009-1020.

Cuvillier, O., G. Pirianov, B. Kleuser, P. G. Vanek, O. A. Coso, S. Gutkind and S. Spiegel (1996). "Suppression of ceramide-mediated programmed cell death by sphingosine-1-phosphate." *Nature* **381**(6585): 800-803.

Dany, M., S. Gencer, R. Nganga, R. J. Thomas, N. Oleinik, K. D. Baron, Z. M. Szulc, P. Ruvolo, S. Kornblau, M. Andreeff and B. Ogretmen (2016). "Targeting FLT3-ITD signaling mediates ceramide-dependent mitophagy and attenuates drug resistance in AML." *Blood* **128**(15): 1944-1958.

Dayon, A., L. Brizuela, C. Martin, C. Mazerolles, N. Pirot, N. Doumerc, L. Nogueira, M. Golzio, J. Teissie, G. Serre, P. Rischmann, B. Malavaud and O. Cuvillier (2009). "Sphingosine kinase-1 is central to androgen-regulated prostate cancer growth and survival." *PLoS One* **4**(11): e8048.

De Luca, T., D. M. Morre and D. J. Morre (2010). "Reciprocal relationship between cytosolic NADH and ENOX2 inhibition triggers sphingolipid-induced apoptosis in HeLa cells." *J Cell Biochem* **110**(6): 1504-1511.

De Luca, T., D. M. Morre, H. Zhao and D. J. Morre (2005). "NAD⁺/NADH and/or CoQ/CoQH2 ratios from plasma membrane electron transport may determine ceramide and sphingosine-1-phosphate levels accompanying G1 arrest and apoptosis." *Biofactors* **25**(1-4): 43-60.

Delon, C., M. Manifava, E. Wood, D. Thompson, S. Krugmann, S. Pyne and N. T. Ktistakis (2004). "Sphingosine kinase 1 is an intracellular effector of phosphatidic acid." *J Biol Chem* **279**(43): 44763-44774.

Di Paolo, G. and T. W. Kim (2011). "Linking lipids to Alzheimer's disease: cholesterol and beyond." *Nat Rev Neurosci* **12**(5): 284-296.

Dickson, M. A., R. D. Carvajal, A. H. Merrill, Jr., M. Gonen, L. M. Cane and G. K. Schwartz (2011). "A phase I clinical trial of safinol in combination with cisplatin in advanced solid tumors." *Clin Cancer Res* **17**(8): 2484-2492.

Ding, G., H. Sonoda, H. Yu, T. Kajimoto, S. K. Goparaju, S. Jahangeer, T. Okada and S. Nakamura (2007). "Protein kinase D-mediated phosphorylation and nuclear export of sphingosine kinase 2." *J Biol Chem* **282**(37): 27493-27502.

Dolezalova, H., G. Shankar, M. C. Huang, D. D. Bikle and E. J. Goetzl (2003). "Biochemical regulation of breast cancer cell expression of S1P2 (Edg-5) and S1P3 (Edg-3) G protein-coupled receptors for sphingosine 1-phosphate." *J Cell Biochem* **88**(4): 732-743.

Doll, F., J. Pfeilschifter and A. Huwiler (2007). "Prolactin upregulates sphingosine kinase-1 expression and activity in the human breast cancer cell line MCF7 and triggers enhanced proliferation and migration." *Endocr Relat Cancer* **14**(2): 325-335.

Du, W., N. Takuwa, K. Yoshioka, Y. Okamoto, K. Gonda, K. Sugihara, A. Fukamizu, M. Asano and Y. Takuwa (2010). "S1P(2), the G protein-coupled receptor for sphingosine-1-phosphate, negatively regulates tumor angiogenesis and tumor growth in vivo in mice." *Cancer Res* **70**(2): 772-781.

El Buri, A., D. R. Adams, D. Smith, R. J. Tate, M. Mullin, S. Pyne and N. J. Pyne (2018). "The sphingosine 1-phosphate receptor 2 is shed in exosomes from breast cancer cells and is N-terminally processed to a short constitutively active form that promotes extracellular signal regulated kinase activation and DNA synthesis in fibroblasts." *Oncotarget* **9**(50): 29453-29467.

Elmore, S. (2007). "Apoptosis: a review of programmed cell death." *Toxicol Pathol* **35**(4): 495-516.

Endo, K., Y. Igarashi, M. Nisar, Q. H. Zhou and S. Hakomori (1991). "Cell membrane signaling as target in cancer therapy: inhibitory effect of N,N-dimethyl and N,N,N-trimethyl sphingosine derivatives on in vitro and in vivo growth of human tumor cells in nude mice." *Cancer Res* **51**(6): 1613-1618.

Feng, H., D. L. Stachura, R. M. White, A. Gutierrez, L. Zhang, T. Sanda, C. A. Jette, J. R. Testa, D. S. Neuberger, D. M. Langenau, J. L. Kutok, L. I. Zon, D. Traver, M. D. Fleming, J. P. Kanki and A. T. Look (2010). "T-lymphoblastic lymphoma cells express high levels of BCL2, S1P1, and ICAM1, leading to a blockade of tumor cell intravasation." *Cancer Cell* **18**(4): 353-366.

Filipenko, I., S. Schwalm, L. Reali, J. Pfeilschifter, D. Fabbro, A. Huwiler and U. Zangemeister-Wittke (2016). "Upregulation of the S1P3 receptor in metastatic breast cancer cells increases migration and invasion by induction of PGE2 and EP2/EP4 activation." *Biochim Biophys Acta* **1861**(11): 1840-1851.

French, K. J., R. S. Schrecengost, B. D. Lee, Y. Zhuang, S. N. Smith, J. L. Eberly, J. K. Yun and C. D. Smith (2003). "Discovery and evaluation of inhibitors of human sphingosine kinase." *Cancer Res* **63**(18): 5962-5969.

French, K. J., J. J. Upson, S. N. Keller, Y. Zhuang, J. K. Yun and C. D. Smith (2006). "Antitumor activity of sphingosine kinase inhibitors." *J Pharmacol Exp Ther* **318**(2): 596-603.

French, K. J., Y. Zhuang, L. W. Maines, P. Gao, W. Wang, V. Beljanski, J. J. Upson, C. L. Green, S. N. Keller and C. D. Smith (2010). "Pharmacology and antitumor activity of ABC294640, a selective inhibitor of sphingosine kinase-2." *J Pharmacol Exp Ther* **333**(1): 129-139.

Gamble, J. R., P. Xia, C. N. Hahn, J. J. Drew, C. J. Drogemuller, D. Brown and M. A. Vadas (2006). "Phenoxodiol, an experimental anticancer drug, shows potent antiangiogenic properties in addition to its antitumor effects." *Int J Cancer* **118**(10): 2412-2420.

Gandy, K. A., D. Canals, M. Adada, M. Wada, P. Roddy, A. J. Snider, Y. A. Hannun and L. M. Obeid (2013). "Sphingosine 1-phosphate induces filopodia formation through S1PR2 activation of ERM proteins." *Biochem J* **449**(3): 661-672.

Gao, P., Y. K. Peterson, R. A. Smith and C. D. Smith (2012). "Characterization of isoenzyme-selective inhibitors of human sphingosine kinases." *PLoS One* **7**(9): e44543.

Gao, P. and C. D. Smith (2011). "Ablation of sphingosine kinase-2 inhibits tumor cell proliferation and migration." *Mol Cancer Res* **9**(11): 1509-1519.

Gault, C. R., L. M. Obeid and Y. A. Hannun (2010). "An overview of sphingolipid metabolism: from synthesis to breakdown." *Adv Exp Med Biol* **688**: 1-23.

Goel, H. L. and A. M. Mercurio (2013). "VEGF targets the tumour cell." *Nat Rev Cancer* **13**(12): 871-882.

Goetzl, E. J., H. Dolezalova, Y. Kong and L. Zeng (1999). "Dual mechanisms for lysophospholipid induction of proliferation of human breast carcinoma cells." *Cancer Res* **59**(18): 4732-4737.

Golfier, S., S. Kondo, T. Schulze, T. Takeuchi, G. Vassileva, A. H. Achtman, M. H. Graler, S. J. Abbondanzo, M. Wiekowski, E. Kremmer, Y. Endo, S. A. Lira, K. B. Bacon and M. Lipp (2010). "Shaping of terminal megakaryocyte differentiation and proplatelet development by sphingosine-1-phosphate receptor S1P4." *FASEB J* **24**(12): 4701-4710.

Gomez-Brouchet, A., D. Pchejetski, L. Brizuela, V. Garcia, M. F. Altie, M. L. Maddelein, M. B. Delisle and O. Cuvillier (2007). "Critical role for sphingosine kinase-1 in regulating survival of neuroblastoma cells exposed to amyloid-beta peptide." *Mol Pharmacol* **72**(2): 341-349.

Gomez-Munoz, A., A. Martin, L. O'Brien and D. N. Brindley (1994). "Cell-permeable ceramides inhibit the stimulation of DNA synthesis and phospholipase D activity by phosphatidate and lysophosphatidate in rat fibroblasts." *J Biol Chem* **269**(12): 8937-8943.

Graeler, M. and E. J. Goetzl (2002). "Activation-regulated expression and chemotactic function of sphingosine 1-phosphate receptors in mouse splenic T cells." *FASEB J* **16**(14): 1874-1878.

Graler, M. H., R. Grosse, A. Kusch, E. Kremmer, T. Gudermann and M. Lipp (2003). "The sphingosine 1-phosphate receptor S1P4 regulates cell shape and motility via coupling to Gi and G12/13." *J Cell Biochem* **89**(3): 507-519.

Gril, B., A. N. Paranjape, S. Woditschka, E. Hua, E. L. Dolan, J. Hanson, X. Wu, W. Kloc, E. Izycka-Swieszewska, R. Duchnowska, R. Peksa, W. Biernat, J. Jassem, N. Nayar, P. K. Brastianos, O. M. Hall, C. J. Peer, W. D. Figg, G. T. Pauly, C. Robinson, S. Difiilippantonio, E. Bialecki, P. Metellus, J. P. Schneider and P. S. Steeg (2018). "Reactive astrocytic S1P3 signaling modulates the blood-tumor barrier in brain metastases." *Nat Commun* **9**(1): 2705.

Guo, X. Z., W. W. Zhang, L. S. Wang, Z. Z. Lu, H. Wang, J. H. Xu and H. Tian (2006). "[Adenovirus-mediated overexpression of KAI1 suppresses sphingosine kinase activation and metastasis of pancreatic carcinoma cells]." *Zhonghua Nei Ke Za Zhi* **45**(9): 752-754.

Hait, N. C., J. Allegood, M. Maceyka, G. M. Strub, K. B. Harikumar, S. K. Singh, C. Luo, R. Marmorstein, T. Kordula, S. Milstien and S. Spiegel (2009). "Regulation of histone acetylation in the nucleus by sphingosine-1-phosphate." *Science* **325**(5945): 1254-1257.

Han, L., M. B. Stope, M. L. de Jesus, P. A. Oude Weernink, M. Urban, T. Wieland, D. Roskopf, K. Mizuno, K. H. Jakobs and M. Schmidt (2007). "Direct stimulation of receptor-controlled phospholipase D1 by phospho-cofilin." *EMBO J* **26**(19): 4189-4202.

Hanada, K., K. Kumagai, S. Yasuda, Y. Miura, M. Kawano, M. Fukasawa and M. Nishijima (2003). "Molecular machinery for non-vesicular trafficking of ceramide." *Nature* **426**(6968): 803-809.

Hannun, Y. A. (1996). "Functions of ceramide in coordinating cellular responses to stress." *Science* **274**(5294): 1855-1859.

Hao, F., M. Tan, X. Xu, J. Han, D. D. Miller, G. Tigyi and M. Z. Cui (2007). "Lysophosphatidic acid induces prostate cancer PC3 cell migration via activation of LPA(1), p42 and p38alpha." *Biochim Biophys Acta* **1771**(7): 883-892.

Heffernan-Stroud, L. A. and L. M. Obeid (2013). "Sphingosine kinase 1 in cancer." *Adv Cancer Res* **117**: 201-235.

Hengst, J. A., J. M. Guilford, E. J. Conroy, X. Wang and J. K. Yun (2010). "Enhancement of sphingosine kinase 1 catalytic activity by deletion of 21 amino acids from the COOH-terminus." *Arch Biochem Biophys* **494**(1): 23-31.

Hengst, J. A., J. M. Guilford, T. E. Fox, X. Wang, E. J. Conroy and J. K. Yun (2009). "Sphingosine kinase 1 localized to the plasma membrane lipid raft microdomain overcomes serum deprivation induced growth inhibition." *Arch Biochem Biophys* **492**(1-2): 62-73.

Hernandez-Coronado, C. G., A. Guzman, H. Castillo-Juarez, D. Zamora-Gutierrez and A. M. Rosales-Torres (2019). "Sphingosine-1-phosphate (S1P) in ovarian physiology and disease." *Ann Endocrinol (Paris)* **80**(5-6): 263-272.

Hernandez-Tiedra, S., G. Fabrias, D. Davila, I. J. Salanueva, J. Casas, L. R. Montes, Z. Anton, E. Garcia-Taboada, M. Salazar-Roa, M. Lorente, J. Nylandsted, J. Armstrong, I. Lopez-Valero, C. S. McKee, A. Serrano-Puebla, R. Garcia-Lopez, J. Gonzalez-Martinez, J. L. Abad, K. Hanada, P. Boya, F. Goni, M. Guzman, P. Lovat, M. Jaattela, A. Alonso and G. Velasco (2016). "Dihydroceramide accumulation mediates cytotoxic autophagy of cancer cells via autolysosome destabilization." *Autophagy* **12**(11): 2213-2229.

Hisano, Y., N. Kobayashi, A. Kawahara, A. Yamaguchi and T. Nishi (2011). "The sphingosine 1-phosphate transporter, SPNS2, functions as a transporter of the phosphorylated form of the immunomodulating agent FTY720." *J Biol Chem* **286**(3): 1758-1766.

Hobson, J. P., H. M. Rosenfeldt, L. S. Barak, A. Olivera, S. Poulton, M. G. Caron, S. Milstien and S. Spiegel (2001). "Role of the sphingosine-1-phosphate receptor EDG-1 in PDGF-induced cell motility." *Science* **291**(5509): 1800-1803.

Hu, J., E. C. Stites, H. Yu, E. A. Germino, H. S. Meharena, P. J. S. Stork, A. P. Kornev, S. S. Taylor and A. S. Shaw (2013). "Allosteric activation of functionally asymmetric RAF kinase dimers." *Cell* **154**(5): 1036-1046.

Hu, T., Z. Liu and X. Shen (2011). "Roles of phospholipase D in phorbol myristate acetate-stimulated neutrophil respiratory burst." *J Cell Mol Med* **15**(3): 647-653.

Huang, Y. L., W. P. Huang and H. Lee (2011). "Roles of sphingosine 1-phosphate on tumorigenesis." *World J Biol Chem* **2**(2): 25-34.

Hubbard, J. B., V. Silin and A. L. Plant (1998). "Self assembly driven by hydrophobic interactions at alkanethiol monolayers: mechanisms of formation of hybrid bilayer membranes." *Biophys Chem* **75**(3): 163-176.

Huwiler, A., F. Doll, S. Ren, S. Klawitter, A. Greening, I. Romer, S. Bubnova, L. Reinsberg and J. Pfeilschifter (2006). "Histamine increases sphingosine kinase-1 expression and activity in the human arterial endothelial cell line EA.hy 926 by a PKC-alpha-dependent mechanism." *Biochim Biophys Acta* **1761**(3): 367-376.

- Igarashi, N., T. Okada, S. Hayashi, T. Fujita, S. Jahangeer and S. Nakamura (2003). "Sphingosine kinase 2 is a nuclear protein and inhibits DNA synthesis." *J Biol Chem* **278**(47): 46832-46839.
- Igarashi, Y., S. Hakomori, T. Toyokuni, B. Dean, S. Fujita, M. Sugimoto, T. Ogawa, K. el-Ghendy and E. Racker (1989). "Effect of chemically well-defined sphingosine and its N-methyl derivatives on protein kinase C and src kinase activities." *Biochemistry* **28**(17): 6796-6800.
- Im, D. S., C. E. Heise, N. Ancellin, B. F. O'Dowd, G. J. Shei, R. P. Heavens, M. R. Rigby, T. Hla, S. Mandala, G. McAllister, S. R. George and K. R. Lynch (2000). "Characterization of a novel sphingosine 1-phosphate receptor, Edg-8." *J Biol Chem* **275**(19): 14281-14286.
- Inagaki, Y., P. Y. Li, A. Wada, S. Mitsutake and Y. Igarashi (2003). "Identification of functional nuclear export sequences in human sphingosine kinase 1." *Biochem Biophys Res Commun* **311**(1): 168-173.
- Ishii, I., B. Friedman, X. Ye, S. Kawamura, C. McGiffert, J. J. Contos, M. A. Kingsbury, G. Zhang, J. H. Brown and J. Chun (2001). "Selective loss of sphingosine 1-phosphate signaling with no obvious phenotypic abnormality in mice lacking its G protein-coupled receptor, LP(B3)/EDG-3." *J Biol Chem* **276**(36): 33697-33704.
- Jaillard, C., S. Harrison, B. Stankoff, M. S. Aigrot, A. R. Calver, G. Duddy, F. S. Walsh, M. N. Pangalos, N. Arimura, K. Kaibuchi, B. Zalc and C. Lubetzki (2005). "Edg8/S1P5: an oligodendroglial receptor with dual function on process retraction and cell survival." *J Neurosci* **25**(6): 1459-1469.
- Jarman, K. E., P. A. Moretti, J. R. Zebol and S. M. Pitson (2010). "Translocation of sphingosine kinase 1 to the plasma membrane is mediated by calcium- and integrin-binding protein 1." *J Biol Chem* **285**(1): 483-492.
- Jeffery, D. R., C. E. Markowitz, A. T. Reder, B. Weinstock-Guttman and K. Tobias (2011). "Fingolimod for the treatment of relapsing multiple sclerosis." *Expert Rev Neurother* **11**(2): 165-183.
- Jerga, A., D. J. Miller, S. W. White and C. O. Rock (2009). "Molecular determinants for interfacial binding and conformational change in a soluble diacylglycerol kinase." *J Biol Chem* **284**(11): 7246-7254.
- Johnson, K. R., K. P. Becker, M. M. Facchinetti, Y. A. Hannun and L. M. Obeid (2002). "PKC-dependent activation of sphingosine kinase 1 and translocation to the plasma membrane. Extracellular release of sphingosine-1-phosphate induced by phorbol 12-myristate 13-acetate (PMA)." *J Biol Chem* **277**(38): 35257-35262.
- Johnson, K. R., K. Y. Johnson, H. G. Crellin, B. Ogretmen, A. M. Boylan, R. A. Harley and L. M. Obeid (2005). "Immunohistochemical distribution of sphingosine kinase 1 in normal and tumor lung tissue." *J Histochem Cytochem* **53**(9): 1159-1166.
- Jolly, P. S., M. Bektas, A. Olivera, C. Gonzalez-Espinosa, R. L. Proia, J. Rivera, S. Milstien and S. Spiegel (2004). "Transactivation of sphingosine-1-phosphate receptors by FcepsilonRI triggering is required for normal mast cell degranulation and chemotaxis." *J Exp Med* **199**(7): 959-970.
- Ju, T., D. Gao and Z. Y. Fang (2016). "Targeting colorectal cancer cells by a novel sphingosine kinase 1 inhibitor PF-543." *Biochem Biophys Res Commun* **470**(3): 728-734.
- Kachler, K., M. Bailer, L. Heim, F. Schumacher, M. Reichel, C. D. Holzinger, S. Trump, S. Mittler, J. Monti, D. I. Trufa, R. J. Rieker, A. Hartmann, H. Sirbu, B. Kleuser, J. Kornhuber and S. Finotto (2017). "Enhanced Acid Sphingomyelinase Activity Drives Immune Evasion and Tumor Growth in Non-Small Cell Lung Carcinoma." *Cancer Res* **77**(21): 5963-5976.
- Kajiwara, K., A. Ikeda, A. Aguilera-Romero, G. A. Castillon, S. Kagiwada, K. Hanada, H. Riezman, M. Muniz and K. Funato (2014). "Osh proteins regulate COPII-mediated vesicular transport of ceramide from the endoplasmic reticulum in budding yeast." *J Cell Sci* **127**(Pt 2): 376-387.
- Kapitonov, D., J. C. Allegood, C. Mitchell, N. C. Hait, J. A. Almenara, J. K. Adams, R. E. Zipkin, P. Dent, T. Kordula, S. Milstien and S. Spiegel (2009). "Targeting sphingosine kinase 1 inhibits Akt signaling, induces apoptosis, and suppresses growth of human glioblastoma cells and xenografts." *Cancer Res* **69**(17): 6915-6923.
- Kawahara, A., T. Nishi, Y. Hisano, H. Fukui, A. Yamaguchi and N. Mochizuki (2009). "The sphingolipid transporter spns2 functions in migration of zebrafish myocardial precursors." *Science* **323**(5913): 524-527.
- Kedderis, L. B., H. P. Bozgian, J. M. Kleeman, R. L. Hall, T. E. Palmer, S. D. Harrison, Jr. and R. L. Susick, Jr. (1995). "Toxicity of the protein kinase C inhibitor safingol administered alone and in combination with chemotherapeutic agents." *Fundam Appl Toxicol* **25**(2): 201-217.
- Kim, E. Y., B. Choi, J. E. Kim, S. O. Park, S. M. Kim and E. J. Chang (2020). "Interleukin-22 Mediates the Chemotactic Migration of Breast Cancer Cells and Macrophage Infiltration of the Bone Microenvironment by Potentiating S1P/S1PR Signaling." *Cells* **9**(1).
- Kim, K. B., J. S. Yi, N. Nguyen, J. H. Lee, Y. C. Kwon, B. Y. Ahn, H. Cho, Y. K. Kim, H. J. Yoo, J. S. Lee and Y. G. Ko (2011). "Cell-surface receptor for complement component C1q (gC1qR) is a key regulator for lamellipodia formation and cancer metastasis." *J Biol Chem* **286**(26): 23093-23101.
- Kim, S. J. and J. Li (2013). "Caspase blockade induces RIP3-mediated programmed necrosis in Toll-like receptor-activated microglia." *Cell Death Dis* **4**: e716.
- Kitatani, K., J. Idkowiak-Baldys and Y. A. Hannun (2008). "The sphingolipid salvage pathway in ceramide metabolism and signaling." *Cell Signal* **20**(6): 1010-1018.
- Kluk, M. J. and T. Hla (2002). "Signaling of sphingosine-1-phosphate via the S1P/EDG-family of G-protein-coupled receptors." *Biochim Biophys Acta* **1582**(1-3): 72-80.
- Kobayashi, N., S. Kawasaki-Nishi, M. Otsuka, Y. Hisano, A. Yamaguchi and T. Nishi (2018). "MFSD2B is a sphingosine 1-phosphate transporter in erythroid cells." *Sci Rep* **8**(1): 4969.
- Kohama, T., A. Olivera, L. Edsall, M. M. Nagiec, R. Dickson and S. Spiegel (1998). "Molecular cloning and functional characterization of murine sphingosine kinase." *J Biol Chem* **273**(37): 23722-23728.

Kohno, T. and Y. Igarashi (2008). "Attenuation of cell motility observed with high doses of sphingosine 1-phosphate or phosphorylated FTY720 involves RGS2 through its interactions with the receptor S1P." *Genes Cells* **13**(7): 747-757.

Konerding, M. A., W. Malkusch, B. Klapthor, C. van Ackern, E. Fait, S. A. Hill, C. Parkins, D. J. Chaplin, M. Presta and J. Denekamp (1999). "Evidence for characteristic vascular patterns in solid tumours: quantitative studies using corrosion casts." *Br J Cancer* **80**(5-6): 724-732.

Kono, M., Y. Mi, Y. Liu, T. Sasaki, M. L. Allende, Y. P. Wu, T. Yamashita and R. L. Proia (2004). "The sphingosine-1-phosphate receptors S1P1, S1P2, and S1P3 function coordinately during embryonic angiogenesis." *J Biol Chem* **279**(28): 29367-29373.

Korc, M. and R. E. Friesel (2009). "The role of fibroblast growth factors in tumor growth." *Curr Cancer Drug Targets* **9**(5): 639-651.

Kothapalli, R., I. Kusmartseva and T. P. Loughran (2002). "Characterization of a human sphingosine-1-phosphate receptor gene (S1P5) and its differential expression in LGL leukemia." *Biochim Biophys Acta* **1579**(2-3): 117-123.

Kraveka, J. M., L. Li, Z. M. Szulc, J. Bielawski, B. Ogretmen, Y. A. Hannun, L. M. Obeid and A. Bielawska (2007). "Involvement of dihydroceramide desaturase in cell cycle progression in human neuroblastoma cells." *J Biol Chem* **282**(23): 16718-16728.

Kupperman, E., S. An, N. Osborne, S. Waldron and D. Y. Stainier (2000). "A sphingosine-1-phosphate receptor regulates cell migration during vertebrate heart development." *Nature* **406**(6792): 192-195.

Kusner, D. J., C. R. Thompson, N. A. Melrose, S. M. Pitson, L. M. Obeid and S. S. Iyer (2007). "The localization and activity of sphingosine kinase 1 are coordinately regulated with actin cytoskeletal dynamics in macrophages." *J Biol Chem* **282**(32): 23147-23162.

LaMontagne, K., A. Littlewood-Evans, C. Schnell, T. O'Reilly, L. Wyder, T. Sanchez, B. Probst, J. Butler, A. Wood, G. Liao, E. Billy, A. Theuer, T. Hla and J. Wood (2006). "Antagonism of sphingosine-1-phosphate receptors by FTY720 inhibits angiogenesis and tumor vascularization." *Cancer Res* **66**(1): 221-231.

Lee, H., J. Deng, M. Kujawski, C. Yang, Y. Liu, A. Herrmann, M. Kortylewski, D. Horne, G. Somlo, S. Forman, R. Jove and H. Yu (2010). "STAT3-induced S1PR1 expression is crucial for persistent STAT3 activation in tumors." *Nat Med* **16**(12): 1421-1428.

Lee, Y. M., K. Venkataraman, S. I. Hwang, D. K. Han and T. Hla (2007). "A novel method to quantify sphingosine 1-phosphate by immobilized metal affinity chromatography (IMAC)." *Prostaglandins Other Lipid Mediat* **84**(3-4): 154-162.

Lepley, D., J. H. Paik, T. Hla and F. Ferrer (2005). "The G protein-coupled receptor S1P2 regulates Rho/Rho kinase pathway to inhibit tumor cell migration." *Cancer Res* **65**(9): 3788-3795.

Li, J., B. Zhang, Y. Bai, Y. Liu, B. Zhang and J. Jin (2019). "Upregulation of sphingosine kinase 1 is associated with recurrence and poor prognosis in papillary thyroid carcinoma." *Oncol Lett* **18**(5): 5374-5382.

Li, M. H., T. Sanchez, H. Yamase, T. Hla, M. L. Oo, A. Pappalardo, K. R. Lynch, C. Y. Lin and F. Ferrer (2009). "S1P/S1P1 signaling stimulates cell migration and invasion in Wilms tumor." *Cancer Lett* **276**(2): 171-179.

Li, Q. F., C. T. Wu, H. F. Duan, H. Y. Sun, H. Wang, Z. Z. Lu, Q. W. Zhang, H. J. Liu and L. S. Wang (2007). "Activation of sphingosine kinase mediates suppressive effect of interleukin-6 on human multiple myeloma cell apoptosis." *Br J Haematol* **138**(5): 632-639.

Li, S., H. Tanaka, H. H. Wang, S. Yoshiyama, H. Kumagai, A. Nakamura, D. L. Brown, S. E. Thatcher, G. L. Wright and K. Kohama (2006). "Intracellular signal transduction for migration and actin remodeling in vascular smooth muscle cells after sphingosylphosphorylcholine stimulation." *Am J Physiol Heart Circ Physiol* **291**(3): H1262-1272.

Liang, J., M. Nagahashi, E. Y. Kim, K. B. Harikumar, A. Yamada, W. C. Huang, N. C. Hait, J. C. Allegood, M. M. Price, D. Avni, K. Takabe, T. Kordula, S. Milstien and S. Spiegel (2013). "Sphingosine-1-phosphate links persistent STAT3 activation, chronic intestinal inflammation, and development of colitis-associated cancer." *Cancer Cell* **23**(1): 107-120.

Licht, T., L. Tsurunikov, H. Reuveni, T. Yarnitzky and S. A. Ben-Sasson (2003). "Induction of pro-angiogenic signaling by a synthetic peptide derived from the second intracellular loop of S1P3 (EDG3)." *Blood* **102**(6): 2099-2107.

Lim, K. G., F. Tonelli, Z. Li, X. Lu, R. Bittman, S. Pyne and N. J. Pyne (2011). "FTY720 analogues as sphingosine kinase 1 inhibitors: enzyme inhibition kinetics, allosterism, proteasomal degradation, and actin rearrangement in MCF-7 breast cancer cells." *J Biol Chem* **286**(21): 18633-18640.

Lima, S., S. Milstien and S. Spiegel (2017). "Sphingosine and Sphingosine Kinase 1 Involvement in Endocytic Membrane Trafficking." *J Biol Chem* **292**(8): 3074-3088.

Lin, M., W. Liao, M. Dong, R. Zhu, J. Xiao, T. Sun, Z. Chen, B. Wu and J. Jin (2018). "Exosomal neutral sphingomyelinase 1 suppresses hepatocellular carcinoma via decreasing the ratio of sphingomyelin/ceramide." *FEBS J* **285**(20): 3835-3848.

Linardic, C. M. and Y. A. Hannun (1994). "Identification of a distinct pool of sphingomyelin involved in the sphingomyelin cycle." *J Biol Chem* **269**(38): 23530-23537.

Liu, H., Y. Ma, H. W. He, W. L. Zhao and R. G. Shao (2017). "SPHK1 (sphingosine kinase 1) induces epithelial-mesenchymal transition by promoting the autophagy-linked lysosomal degradation of CDH1/E-cadherin in hepatoma cells." *Autophagy* **13**(5): 900-913.

Liu, H., M. Sugiura, V. E. Nava, L. C. Edsall, K. Kono, S. Poulton, S. Milstien, T. Kohama and S. Spiegel (2000). "Molecular cloning and functional characterization of a novel mammalian sphingosine kinase type 2 isoform." *J Biol Chem* **275**(26): 19513-19520.

Liu, H., R. E. Toman, S. K. Goparaju, M. Maceyka, V. E. Nava, H. Sankala, S. G. Payne, M. Bektas, I. Ishii, J. Chun, S. Milstien and S. Spiegel (2003). "Sphingosine kinase type 2 is a putative BH3-only protein that induces apoptosis." *J Biol Chem* **278**(41): 40330-40336.

Liu, S. Q., Y. J. Su, M. B. Qin, Y. B. Mao, J. A. Huang and G. D. Tang (2013). "Sphingosine kinase 1 promotes tumor progression and confers malignancy phenotypes of colon cancer by regulating the focal adhesion kinase pathway and adhesion molecules." *Int J Oncol* **42**(2): 617-626.

Liu, Y., R. Wada, T. Yamashita, Y. Mi, C. X. Deng, J. P. Hobson, H. M. Rosenfeldt, V. E. Nava, S. S. Chae, M. J. Lee, C. H. Liu, T. Hla, S. Spiegel and R. L. Proia (2000). "Edg-1, the G protein-coupled receptor for sphingosine-1-phosphate, is essential for vascular maturation." *J Clin Invest* **106**(8): 951-961.

Liu, Y. Y., V. Gupta, G. A. Patwardhan, K. Bhinge, Y. Zhao, J. Bao, H. Mehendale, M. C. Cabot, Y. T. Li and S. M. Jazwinski (2010). "Glucosylceramide synthase upregulates MDR1 expression in the regulation of cancer drug resistance through cSrc and beta-catenin signaling." *Mol Cancer* **9**: 145.

Liu, Z., N. MacRitchie, S. Pyne, N. J. Pyne and R. Bittman (2013). "Synthesis of (S)-FTY720 vinylphosphonate analogues and evaluation of their potential as sphingosine kinase 1 inhibitors and activators." *Bioorg Med Chem* **21**(9): 2503-2510.

Long, J. S., J. Edwards, C. Watson, S. Tovey, K. M. Mair, R. Schiff, V. Natarajan, N. J. Pyne and S. Pyne (2010). "Sphingosine kinase 1 induces tolerance to human epidermal growth factor receptor 2 and prevents formation of a migratory phenotype in response to sphingosine 1-phosphate in estrogen receptor-positive breast cancer cells." *Mol Cell Biol* **30**(15): 3827-3841.

Long, J. S., Y. Fujiwara, J. Edwards, C. L. Tannahill, G. Tigyi, S. Pyne and N. J. Pyne (2010). "Sphingosine 1-phosphate receptor 4 uses HER2 (ERBB2) to regulate extracellular signal regulated kinase-1/2 in MDA-MB-453 breast cancer cells." *J Biol Chem* **285**(46): 35957-35966.

Loveridge, C., F. Tonelli, T. Leclercq, K. G. Lim, J. S. Long, E. Berdyshev, R. J. Tate, V. Natarajan, S. M. Pitson, N. J. Pyne and S. Pyne (2010). "The sphingosine kinase 1 inhibitor 2-(p-hydroxyanilino)-4-(p-chlorophenyl)thiazole induces proteasomal degradation of sphingosine kinase 1 in mammalian cells." *J Biol Chem* **285**(50): 38841-38852.

Maceyka, M., T. Rohrbach, S. Milstien and S. Spiegel (2020). "Role of Sphingosine Kinase 1 and Sphingosine-1-Phosphate Axis in Hepatocellular Carcinoma." *Handb Exp Pharmacol* **259**: 3-17.

Maceyka, M., H. Sankala, N. C. Hait, H. Le Stunff, H. Liu, R. Toman, C. Collier, M. Zhang, L. S. Satin, A. H. Merrill, Jr., S. Milstien and S. Spiegel (2005). "SphK1 and SphK2, sphingosine kinase isoenzymes with opposing functions in sphingolipid metabolism." *J Biol Chem* **280**(44): 37118-37129.

MacLennan, A. J., S. J. Benner, A. Andringa, A. H. Chaves, J. L. Rosing, R. Vesey, A. M. Karpman, S. A. Cronier, N. Lee, L. C. Erway and M. L. Miller (2006). "The S1P2 sphingosine 1-phosphate receptor is essential for auditory and vestibular function." *Hear Res* **220**(1-2): 38-48.

Magrassi, L., N. Marziliano, F. Inzani, P. Cassini, I. Chiaranda, M. Skrap, S. Pizzolito, C. Arienta and E. Arbustini (2010). "EDG3 and SHC3 on chromosome 9q22 are co-amplified in human ependymomas." *Cancer Lett* **290**(1): 36-42.

Maines, L. W., L. R. Fitzpatrick, K. J. French, Y. Zhuang, Z. Xia, S. N. Keller, J. J. Upson and C. D. Smith (2008). "Suppression of ulcerative colitis in mice by orally available inhibitors of sphingosine kinase." *Dig Dis Sci* **53**(4): 997-1012.

Malchinkhuu, E., K. Sato, T. Maehama, C. Mogi, H. Tomura, S. Ishiuchi, Y. Yoshimoto, H. Kurose and F. Okajima (2008). "S1P(2) receptors mediate inhibition of glioma cell migration through Rho signaling pathways independent of PTEN." *Biochem Biophys Res Commun* **366**(4): 963-968.

Marchesini, N. and Y. A. Hannun (2004). "Acid and neutral sphingomyelinases: roles and mechanisms of regulation." *Biochem Cell Biol* **82**(1): 27-44.

Marfe, G., C. Di Stefano, A. Gambacurta, T. Ottone, V. Martini, E. Abruzzese, L. Mologni, P. Sinibaldi-Salimei, P. de Fabritis, C. Gambacorti-Passerini, S. Amadori and R. B. Birge (2011). "Sphingosine kinase 1 overexpression is regulated by signaling through PI3K, AKT2, and mTOR in imatinib-resistant chronic myeloid leukemia cells." *Exp Hematol* **39**(6): 653-665 e656.

Marquardt, B., D. Frith and S. Stabel (1994). "Signalling from TPA to MAP kinase requires protein kinase C, raf and MEK: reconstitution of the signalling pathway in vitro." *Oncogene* **9**(11): 3213-3218.

Matsushima-Nishiwaki, R., N. Yamada, K. Fukuchi and O. Kozawa (2018). "Sphingosine 1-phosphate (S1P) reduces hepatocyte growth factor-induced migration of hepatocellular carcinoma cells via S1P receptor 2." *PLoS One* **13**(12): e0209050.

McNaughton, M., M. Pitman, S. M. Pitson, N. J. Pyne and S. Pyne (2016). "Proteasomal degradation of sphingosine kinase 1 and inhibition of dihydroceramide desaturase by the sphingosine kinase inhibitors, SKI or ABC294640, induces growth arrest in androgen-independent LNCaP-AI prostate cancer cells." *Oncotarget* **7**(13): 16663-16675.

Means, C. K. and J. H. Brown (2009). "Sphingosine-1-phosphate receptor signalling in the heart." *Cardiovasc Res* **82**(2): 193-200.

Merrill, A. H., Jr. (2002). "De novo sphingolipid biosynthesis: a necessary, but dangerous, pathway." *J Biol Chem* **277**(29): 25843-25846.

Messias, C. V., E. Santana-Van-Vliet, J. P. Lemos, O. C. Moreira, V. Cotta-de-Almeida, W. Savino and D. A. Mendes-da-Cruz (2016). "Sphingosine-1-Phosphate Induces Dose-Dependent Chemotaxis or Fugetaxis of T-ALL Blasts through S1P1 Activation." *PLoS One* **11**(1): e0148137.

Miller, D. J., A. Jerga, C. O. Rock and S. W. White (2008). "Analysis of the *Staphylococcus aureus* DgkB structure reveals a common catalytic mechanism for the soluble diacylglycerol kinases." *Structure* **16**(7): 1036-1046.

Mitra, P., C. A. Oskertizian, S. G. Payne, M. A. Beaven, S. Milstien and S. Spiegel (2006). "Role of ABCC1 in export of sphingosine-1-phosphate from mast cells." *Proc Natl Acad Sci U S A* **103**(44): 16394-16399.

Mizugishi, K., T. Yamashita, A. Olivera, G. F. Miller, S. Spiegel and R. L. Proia (2005). "Essential role for sphingosine kinases in neural and vascular development." *Mol Cell Biol* **25**(24): 11113-11121.

Mizumura, K., M. J. Justice, K. S. Schweitzer, S. Krishnan, I. Bronova, E. V. Berdyshev, W. C. Hubbard, Y. Pewzner-Jung, A. H. Futerman, A. M. K. Choi and I. Petrache (2018). "Sphingolipid regulation of lung epithelial cell mitophagy and necroptosis during cigarette smoke exposure." *FASEB J* **32**(4): 1880-1890.

Mosesson, Y., G. B. Mills and Y. Yarden (2008). "Derailed endocytosis: an emerging feature of cancer." *Nat Rev Cancer* **8**(11): 835-850.

Muz, B., P. de la Puente, F. Azab and A. K. Azab (2015). "The role of hypoxia in cancer progression, angiogenesis, metastasis, and resistance to therapy." *Hypoxia (Auckl)* **3**: 83-92.

- Nagahashi, M., K. Takabe, K. P. Terracina, D. Soma, Y. Hirose, T. Kobayashi, Y. Matsuda and T. Wakai (2014). "Sphingosine-1-phosphate transporters as targets for cancer therapy." *Biomed Res Int* **2014**: 651727.
- Nakade, Y., Y. Banno, T. K. K. K. K. Hagiwara, S. Sobue, M. Koda, M. Suzuki, T. Kojima, A. Takagi, H. Asano, Y. Nozawa and T. Murate (2003). "Regulation of sphingosine kinase 1 gene expression by protein kinase C in a human leukemia cell line, MEG-O1." *Biochim Biophys Acta* **1635**(2-3): 104-116.
- Nan, X., T. M. Tamguney, E. A. Collisson, L. J. Lin, C. Pitt, J. Galeas, S. Lewis, J. W. Gray, F. McCormick and S. Chu (2015). "Ras-GTP dimers activate the Mitogen-Activated Protein Kinase (MAPK) pathway." *Proc Natl Acad Sci U S A* **112**(26): 7996-8001.
- Nemoto, S., M. Nakamura, Y. Osawa, S. Kono, Y. Itoh, Y. Okano, T. Murate, A. Hara, H. Ueda, Y. Nozawa and Y. Banno (2009). "Sphingosine kinase isoforms regulate oxaliplatin sensitivity of human colon cancer cells through ceramide accumulation and Akt activation." *J Biol Chem* **284**(16): 10422-10432.
- Neubauer, H. A., D. H. Pham, J. R. Zebol, P. A. Moretti, A. L. Peterson, T. M. Leclercq, H. Chan, J. A. Powell, M. R. Pitman, M. S. Samuel, C. S. Bonder, D. J. Creek, B. L. Gliddon and S. M. Pitson (2016). "An oncogenic role for sphingosine kinase 2." *Oncotarget* **7**(40): 64886-64899.
- Neubauer, H. A., M. N. Tea, J. R. Zebol, B. L. Gliddon, C. Stefanidis, P. A. B. Moretti, M. R. Pitman, M. Costabile, J. Kular, B. W. Stringer, B. W. Day, M. S. Samuel, C. S. Bonder, J. A. Powell and S. M. Pitson (2019). "Cytoplasmic dynein regulates the subcellular localization of sphingosine kinase 2 to elicit tumor-suppressive functions in glioblastoma." *Oncogene* **38**(8): 1151-1165.
- Newton, J., S. Lima, M. Maceyka and S. Spiegel (2015). "Revisiting the sphingolipid rheostat: Evolving concepts in cancer therapy." *Exp Cell Res* **333**(2): 195-200.
- Nganga, R., N. Oleinik, J. Kim, S. P. Selvam, R. De Palma, K. A. Johnson, R. Y. Parikh, V. Gangaraju, Y. Peterson, M. Dany, R. V. Stahelin, C. Voelkel-Johnson, Z. M. Szulc, E. Bieberich and B. Ogretmen (2019). "Receptor-interacting Ser/Thr kinase 1 (RIPK1) and myosin IIA-dependent ceramidosomes form membrane pores that mediate blebbing and necroptosis." *J Biol Chem* **294**(2): 502-519.
- Nguyen-Tran, D. H., N. C. Hait, H. Sperber, J. Qi, K. Fischer, N. Ieronimakis, M. Pantoja, A. Hays, J. Allegood, M. Reyes, S. Spiegel and H. Ruohola-Baker (2014). "Molecular mechanism of sphingosine-1-phosphate action in Duchenne muscular dystrophy." *Dis Model Mech* **7**(1): 41-54.
- Nichols, C. E., H. K. Lamb, M. Lockyer, I. G. Charles, S. Pyne, A. R. Hawkins and D. K. Stammers (2007). "Characterization of Salmonella typhimurium YegS, a putative lipid kinase homologous to eukaryotic sphingosine and diacylglycerol kinases." *Proteins* **68**(1): 13-25.
- Nishimura, A., K. Kitano, J. Takasaki, M. Taniguchi, N. Mizuno, K. Tago, T. Hakoshima and H. Itoh (2010). "Structural basis for the specific inhibition of heterotrimeric Gq protein by a small molecule." *Proc Natl Acad Sci U S A* **107**(31): 13666-13671.
- Novgorodov, A. S., M. El-Alwani, J. Bielawski, L. M. Obeid and T. I. Gudz (2007). "Activation of sphingosine-1-phosphate receptor S1P5 inhibits oligodendrocyte progenitor migration." *FASEB J* **21**(7): 1503-1514.
- Nyberg, L., R. D. Duan, J. Axelson and A. Nilsson (1996). "Identification of an alkaline sphingomyelinase activity in human bile." *Biochim Biophys Acta* **1300**(1): 42-48.
- Obeid, L. M., C. M. Linardic, L. A. Karolak and Y. A. Hannun (1993). "Programmed cell death induced by ceramide." *Science* **259**(5102): 1769-1771.
- Offermanns, S., T. Wieland, D. Homann, J. Sandmann, E. Bombien, K. Spicher, G. Schultz and K. H. Jakobs (1994). "Transfected muscarinic acetylcholine receptors selectively couple to Gi-type G proteins and Gq/11." *Mol Pharmacol* **45**(5): 890-898.
- Ogretmen, B. (2018). "Sphingolipid metabolism in cancer signalling and therapy." *Nat Rev Cancer* **18**(1): 33-50.
- Ogretmen, B. and Y. A. Hannun (2004). "Biologically active sphingolipids in cancer pathogenesis and treatment." *Nat Rev Cancer* **4**(8): 604-616.
- Ogretmen, B., B. J. Pettus, M. J. Rossi, R. Wood, J. Usta, Z. Szulc, A. Bielawska, L. M. Obeid and Y. A. Hannun (2002). "Biochemical mechanisms of the generation of endogenous long chain ceramide in response to exogenous short chain ceramide in the A549 human lung adenocarcinoma cell line. Role for endogenous ceramide in mediating the action of exogenous ceramide." *J Biol Chem* **277**(15): 12960-12969.
- Ohkura, S. I., S. Usui, S. I. Takashima, N. Takuwa, K. Yoshioka, Y. Okamoto, Y. Inagaki, N. Sugimoto, T. Kitano, M. Takamura, T. Wada, S. Kaneko and Y. Takuwa (2017). "Augmented sphingosine 1 phosphate receptor-1 signaling in cardiac fibroblasts induces cardiac hypertrophy and fibrosis through angiotensin II and interleukin-6." *PLoS One* **12**(8): e0182329.
- Ohotski, J., J. Edwards, B. Elsberger, C. Watson, C. Orange, E. Mallon, S. Pyne and N. J. Pyne (2013). "Identification of novel functional and spatial associations between sphingosine kinase 1, sphingosine 1-phosphate receptors and other signaling proteins that affect prognostic outcome in estrogen receptor-positive breast cancer." *Int J Cancer* **132**(3): 605-616.
- Ohotski, J., J. S. Long, C. Orange, B. Elsberger, E. Mallon, J. Doughty, S. Pyne, N. J. Pyne and J. Edwards (2012). "Expression of sphingosine 1-phosphate receptor 4 and sphingosine kinase 1 is associated with outcome in oestrogen receptor-negative breast cancer." *Br J Cancer* **106**(8): 1453-1459.
- Okada, T., G. Ding, H. Sonoda, T. Kajimoto, Y. Haga, A. Khosrowbeygi, S. Gao, N. Miwa, S. Jahangeer and S. Nakamura (2005). "Involvement of N-terminal-extended form of sphingosine kinase 2 in serum-dependent regulation of cell proliferation and apoptosis." *J Biol Chem* **280**(43): 36318-36325.
- Okoshi, H., S. Hakomori, M. Nisar, Q. H. Zhou, S. Kimura, K. Tashiro and Y. Igarashi (1991). "Cell membrane signaling as target in cancer therapy. II: Inhibitory effect of N,N,N-trimethylsphingosine on metastatic potential of murine B16 melanoma cell line through blocking of tumor cell-dependent platelet aggregation." *Cancer Res* **51**(22): 6019-6024.
- Olesch, C., E. Siraït-Fischer, M. Berkefeld, A. F. Fink, R. M. Susen, B. Ritter, B. E. Michels, D. Steinhilber, F. R. Greten, R. Savai, K. Takeda, B. Brune and A. Weigert (2020). "S1PR4 ablation reduces tumor growth and improves chemotherapy via CD8+ T cell expansion." *J Clin Invest*.
- Olivera, A., T. Kohama, L. Edsall, V. Nava, O. Cuvillier, S. Poulton and S. Spiegel (1999). "Sphingosine kinase expression increases intracellular sphingosine-1-phosphate and promotes cell growth and survival." *J Cell Biol* **147**(3): 545-558.

Olivera, A., T. Kohama, Z. Tu, S. Milstien and S. Spiegel (1998). "Purification and characterization of rat kidney sphingosine kinase." *J Biol Chem* **273**(20): 12576-12583.

Olivera, A. and S. Spiegel (1993). "Sphingosine-1-phosphate as second messenger in cell proliferation induced by PDGF and FCS mitogens." *Nature* **365**(6446): 557-560.

Osborne, N., K. Brand-Arzamendi, E. A. Ober, S. W. Jin, H. Verkade, N. G. Holtzman, D. Yelon and D. Y. Stainier (2008). "The spinster homolog, two of hearts, is required for sphingosine 1-phosphate signaling in zebrafish." *Curr Biol* **18**(23): 1882-1888.

Pan, J., Y. F. Tao, Z. Zhou, B. R. Cao, S. Y. Wu, Y. L. Zhang, S. Y. Hu, W. L. Zhao, J. Wang, G. L. Lou, Z. Li, X. Feng and J. Ni (2011). "An novel role of sphingosine kinase-1 (SPHK1) in the invasion and metastasis of esophageal carcinoma." *J Transl Med* **9**: 157.

Panneer Selvam, S., R. M. De Palma, J. J. Oaks, N. Oleinik, Y. K. Peterson, R. V. Stahelin, E. Skordalakes, S. Ponnusamy, E. Garrett-Mayer, C. D. Smith and B. Ogretmen (2015). "Binding of the sphingolipid S1P to hTERT stabilizes telomerase at the nuclear periphery by allosterically mimicking protein phosphorylation." *Sci Signal* **8**(381): ra58.

Parham, K. A., J. R. Zebol, K. L. Tooley, W. Y. Sun, L. M. Moldenhauer, M. P. Cockshell, B. L. Gliddon, P. A. Moretti, G. Tigyi, S. M. Pitson and C. S. Bonder (2015). "Sphingosine 1-phosphate is a ligand for peroxisome proliferator-activated receptor-gamma that regulates neoangiogenesis." *FASEB J* **29**(9): 3638-3653.

Park, K., H. Ikushiro, H. S. Seo, K. O. Shin, Y. I. Kim, J. Y. Kim, Y. M. Lee, T. Yano, W. M. Holleran, P. Elias and Y. Uchida (2016). "ER stress stimulates production of the key antimicrobial peptide, cathelicidin, by forming a previously unidentified intracellular S1P signaling complex." *Proc Natl Acad Sci U S A* **113**(10): E1334-1342.

Pastukhov, O., S. Schwalm, U. Zangemeister-Wittke, D. Fabbro, F. Bornancin, L. Japtok, B. Kleuser, J. Pfeilschifter and A. Huwiler (2014). "The ceramide kinase inhibitor NVP-231 inhibits breast and lung cancer cell proliferation by inducing M phase arrest and subsequent cell death." *Br J Pharmacol* **171**(24): 5829-5844.

Paugh, S. W., B. S. Paugh, M. Rahmani, D. Kapitonov, J. A. Almenara, T. Kordula, S. Milstien, J. K. Adams, R. E. Zipkin, S. Grant and S. Spiegel (2008). "A selective sphingosine kinase 1 inhibitor integrates multiple molecular therapeutic targets in human leukemia." *Blood* **112**(4): 1382-1391.

Payne, A. W., D. K. Pant, T. C. Pan and L. A. Chodosh (2014). "Ceramide kinase promotes tumor cell survival and mammary tumor recurrence." *Cancer Res* **74**(21): 6352-6363.

Pettus, B. J., A. Bielawska, S. Spiegel, P. Roddy, Y. A. Hannun and C. E. Chalfant (2003). "Ceramide kinase mediates cytokine- and calcium ionophore-induced arachidonic acid release." *J Biol Chem* **278**(40): 38206-38213.

Pfisterer, K., J. Levitt, C. D. Lawson, R. J. Marsh, J. M. Heddlestone, E. Wait, S. M. Ameer-Beg, S. Cox and M. Parsons (2020). "FMNL2 regulates dynamics of fascin in filopodia." *J Cell Biol* **219**(5).

Pham, D. H., J. A. Powell, B. L. Gliddon, P. A. Moretti, A. Tsykin, M. Van der Hoek, R. Kenyon, G. J. Goodall and S. M. Pitson (2014). "Enhanced expression of transferrin receptor 1 contributes to oncogenic signalling by sphingosine kinase 1." *Oncogene* **33**(48): 5559-5568.

Pitman, M. R., R. K. Barr, B. L. Gliddon, A. M. Magarey, P. A. Moretti and S. M. Pitson (2011). "A critical role for the protein phosphatase 2A B'alpha regulatory subunit in dephosphorylation of sphingosine kinase 1." *Int J Biochem Cell Biol* **43**(3): 342-347.

Pitman, M. R., M. Costabile and S. M. Pitson (2016). "Recent advances in the development of sphingosine kinase inhibitors." *Cell Signal* **28**(9): 1349-1363.

Pitman, M. R. and S. M. Pitson (2010). "Inhibitors of the sphingosine kinase pathway as potential therapeutics." *Curr Cancer Drug Targets* **10**(4): 354-367.

Pitman, M. R., J. A. Powell, C. Coolen, P. A. Moretti, J. R. Zebol, D. H. Pham, J. W. Finnie, A. S. Don, L. M. Ebert, C. S. Bonder, B. L. Gliddon and S. M. Pitson (2015). "A selective ATP-competitive sphingosine kinase inhibitor demonstrates anti-cancer properties." *Oncotarget* **6**(9): 7065-7083.

Pitson, S. M. (2011). "Regulation of sphingosine kinase and sphingolipid signaling." *Trends Biochem Sci* **36**(2): 97-107.

Pitson, S. M., P. A. Moretti, J. R. Zebol, H. E. Lynn, P. Xia, M. A. Vadas and B. W. Wattenberg (2003). "Activation of sphingosine kinase 1 by ERK1/2-mediated phosphorylation." *EMBO J* **22**(20): 5491-5500.

Pitson, S. M., P. Xia, T. M. Leclercq, P. A. Moretti, J. R. Zebol, H. E. Lynn, B. W. Wattenberg and M. A. Vadas (2005). "Phosphorylation-dependent translocation of sphingosine kinase to the plasma membrane drives its oncogenic signalling." *J Exp Med* **201**(1): 49-54.

Platt, F. M. (2014). "Sphingolipid lysosomal storage disorders." *Nature* **510**(7503): 68-75.

Pulkoski-Gross, M. J., M. L. Jenkins, J. P. Truman, M. F. Salama, C. J. Clarke, J. E. Burke, Y. A. Hannun and L. M. Obeid (2018). "An intrinsic lipid-binding interface controls sphingosine kinase 1 function." *J Lipid Res* **59**(3): 462-474.

Pyne, N. J., A. El Buri, D. R. Adams and S. Pyne (2018). "Sphingosine 1-phosphate and cancer." *Adv Biol Regul* **68**: 97-106.

Pyne, N. J. and S. Pyne (2010). "Sphingosine 1-phosphate and cancer." *Nat Rev Cancer* **10**(7): 489-503.

Pyne, S., D. R. Adams and N. J. Pyne (2016). "Sphingosine 1-phosphate and sphingosine kinases in health and disease: Recent advances." *Prog Lipid Res* **62**: 93-106.

Pyne, S., D. R. Adams and N. J. Pyne (2018). "Sphingosine Kinases as Druggable Targets." *Handb Exp Pharmacol*.

Pyne, S., J. Chapman, L. Steele and N. J. Pyne (1996). "Sphingomyelin-derived lipids differentially regulate the extracellular signal-regulated kinase 2 (ERK-2) and c-Jun N-terminal kinase (JNK) signal cascades in airway smooth muscle." *Eur J Biochem* **237**(3): 819-826.

Pyne, S., J. Edwards, J. Ohotski and N. J. Pyne (2012). "Sphingosine 1-phosphate receptors and sphingosine kinase 1: novel biomarkers for clinical prognosis in breast, prostate, and hematological cancers." *Front Oncol* **2**: 168.

Rahmaniyan, M., R. W. Curley, Jr., L. M. Obeid, Y. A. Hannun and J. M. Kravka (2011). "Identification of dihydroceramide desaturase as a direct in vitro target for fenretinide." *J Biol Chem* **286**(28): 24754-24764.

Ren, S., C. Xin, J. Pfeilschifter and A. Huwiler (2010). "A novel mode of action of the putative sphingosine kinase inhibitor 2-(p-hydroxyanilino)-4-(p-chlorophenyl) thiazole (SKI II): induction of lysosomal sphingosine kinase 1 degradation." *Cell Physiol Biochem* **26**(1): 97-104.

Riboni, L., A. Prinetti, R. Bassi and G. Tettamanti (1994). "Formation of bioactive sphingoid molecules from exogenous sphingomyelin in primary cultures of neurons and astrocytes." *FEBS Lett* **352**(3): 323-326.

Ridley, A. J., H. F. Paterson, C. L. Johnston, D. Diekmann and A. Hall (1992). "The small GTP-binding protein rac regulates growth factor-induced membrane ruffling." *Cell* **70**(3): 401-410.

Rius, R. A., L. C. Edsall and S. Spiegel (1997). "Activation of sphingosine kinase in pheochromocytoma PC12 neuronal cells in response to trophic factors." *FEBS Lett* **417**(2): 173-176.

Romer, W., L. L. Pontani, B. Sorre, C. Rentero, L. Berland, V. Chambon, C. Lamaze, P. Bassereau, C. Sykes, K. Gaus and L. Johannes (2010). "Actin dynamics drive membrane reorganization and scission in clathrin-independent endocytosis." *Cell* **140**(4): 540-553.

Roviezzo, F., F. Del Galdo, G. Abbate, M. Bucci, D. D'Agostino, E. Antunes, G. De Dominicis, L. Parente, F. Rossi, G. Cirino and R. De Palma (2004). "Human eosinophil chemotaxis and selective in vivo recruitment by sphingosine 1-phosphate." *Proc Natl Acad Sci U S A* **101**(30): 11170-11175.

Ruckhaberle, E., A. Rody, K. Engels, R. Gaetje, G. von Minckwitz, S. Schiffmann, S. Grosch, G. Geisslinger, U. Holtrich, T. Karn and M. Kaufmann (2008). "Microarray analysis of altered sphingolipid metabolism reveals prognostic significance of sphingosine kinase 1 in breast cancer." *Breast Cancer Res Treat* **112**(1): 41-52.

Sadahira, Y., F. Ruan, S. Hakomori and Y. Igarashi (1992). "Sphingosine 1-phosphate, a specific endogenous signaling molecule controlling cell motility and tumor cell invasiveness." *Proc Natl Acad Sci U S A* **89**(20): 9686-9690.

Saddoughi, S. A., S. Gencer, Y. K. Peterson, K. E. Ward, A. Mukhopadhyay, J. Oaks, J. Bielawski, Z. M. Szulc, R. J. Thomas, S. P. Selvam, C. E. Senkal, E. Garrett-Mayer, R. M. De Palma, D. Fedarovich, A. Liu, A. A. Habib, R. V. Stahelin, D. Perrotti and B. Ogretmen (2013). "Sphingosine analogue drug FTY720 targets I2PP2A/SET and mediates lung tumour suppression via activation of PP2A-RIPK1-dependent necroptosis." *EMBO Mol Med* **5**(1): 105-121.

Salazar, M., A. Carracedo, I. J. Salanueva, S. Hernandez-Tiedra, M. Lorente, A. Egia, P. Vazquez, C. Blazquez, S. Torres, S. Garcia, J. Nowak, G. M. Fimia, M. Piacentini, F. Cecconi, P. P. Pandolfi, L. Gonzalez-Feria, J. L. Iovanna, M. Guzman, P. Boya and G. Velasco (2009). "Cannabinoid action induces autophagy-mediated cell death through stimulation of ER stress in human glioma cells." *J Clin Invest* **119**(5): 1359-1372.

Sanchez, T., A. Skoura, M. T. Wu, B. Casserty, E. O. Harrington and T. Hla (2007). "Induction of vascular permeability by the sphingosine-1-phosphate receptor-2 (S1P2R) and its downstream effectors ROCK and PTEN." *Arterioscler Thromb Vasc Biol* **27**(6): 1312-1318.

Sanna, M. G., J. Liao, E. Jo, C. Alfonso, M. Y. Ahn, M. S. Peterson, B. Webb, S. Lefebvre, J. Chun, N. Gray and H. Rosen (2004). "Sphingosine 1-phosphate (S1P) receptor subtypes S1P1 and S1P3, respectively, regulate lymphocyte recirculation and heart rate." *J Biol Chem* **279**(14): 13839-13848.

Santana, P., L. A. Pena, A. Haimovitz-Friedman, S. Martin, D. Green, M. McLoughlin, C. Cordon-Cardo, E. H. Schuchman, Z. Fuks and R. Kolesnick (1996). "Acid sphingomyelinase-deficient human lymphoblasts and mice are defective in radiation-induced apoptosis." *Cell* **86**(2): 189-199.

Sarkar, S., M. Maceyka, N. C. Hait, S. W. Paugh, H. Sankala, S. Milstien and S. Spiegel (2005). "Sphingosine kinase 1 is required for migration, proliferation and survival of MCF-7 human breast cancer cells." *FEBS Lett* **579**(24): 5313-5317.

Sato, K., E. Malchinkhuu, Y. Horiuchi, C. Mogi, H. Tomura, M. Tosaka, Y. Yoshimoto, A. Kuwabara and F. Okajima (2007). "Critical role of ABCA1 transporter in sphingosine 1-phosphate release from astrocytes." *J Neurochem* **103**(6): 2610-2619.

Schnitzer, S. E., A. Weigert, J. Zhou and B. Brune (2009). "Hypoxia enhances sphingosine kinase 2 activity and provokes sphingosine-1-phosphate-mediated chemoresistance in A549 lung cancer cells." *Mol Cancer Res* **7**(3): 393-401.

Schnute, M. E., M. D. McReynolds, T. Kasten, M. Yates, G. Jerome, J. W. Rains, T. Hall, J. Chrencik, M. Kraus, C. N. Cronin, M. Saabye, M. K. Highkin, R. Broadus, S. Ogawa, K. Cukyne, L. E. Zawadzke, V. Peterkin, K. Iyanar, J. A. Scholten, J. Wendling, H. Fujiwara, O. Nemirovskiy, A. J. Wittwer and M. M. Nagiec (2012). "Modulation of cellular S1P levels with a novel, potent and specific inhibitor of sphingosine kinase-1." *Biochem J* **444**(1): 79-88.

Schwalm, S., M. Erhardt, I. Romer, J. Pfeilschifter, U. Zangemeister-Witke and A. Huwiler (2020). "Ceramide Kinase Is Upregulated in Metastatic Breast Cancer Cells and Contributes to Migration and Invasion by Activation of PI 3-Kinase and Akt." *Int J Mol Sci* **21**(4).

Sensen, S. C., C. Stauber, P. Keul, B. Levkau, T. Schoneberg and M. H. Graler (2008). "Selective activation of G alpha i mediated signalling of S1P3 by FTY720-phosphate." *Cell Signal* **20**(6): 1125-1133.

Sentelle, R. D., C. E. Senkal, W. Jiang, S. Ponnusamy, S. Gencer, S. P. Selvam, V. K. Ramshesh, Y. K. Peterson, J. J. Lemasters, Z. M. Szulc, J. Bielawski and B. Ogretmen (2012). "Ceramide targets autophagosomes to mitochondria and induces lethal mitophagy." *Nat Chem Biol* **8**(10): 831-838.

Serra, M. and J. D. Saba (2010). "Sphingosine 1-phosphate lyase, a key regulator of sphingosine 1-phosphate signaling and function." *Adv Enzyme Regul* **50**(1): 349-362.

Shah, M. V., R. Zhang, R. Irby, R. Kothapalli, X. Liu, T. Arrington, B. Frank, N. H. Lee and T. P. Loughran, Jr. (2008). "Molecular profiling of LGL leukemia reveals role of sphingolipid signaling in survival of cytotoxic lymphocytes." *Blood* **112**(3): 770-781.

Shen, H., F. Giordano, Y. Wu, J. Chan, C. Zhu, I. Milosevic, X. Wu, K. Yao, B. Chen, T. Baumgart, D. Sieburth and P. De Camilli (2014). "Coupling between endocytosis and sphingosine kinase 1 recruitment." *Nat Cell Biol* **16**(7): 652-662.

Shimo, T., S. Matsumura, S. Ibaragi, S. Isowa, K. Kishimoto, H. Mese, A. Nishiyama and A. Sasaki (2007). "Specific inhibitor of MEK-mediated cross-talk between ERK and p38 MAPK during differentiation of human osteosarcoma cells." *J Cell Commun Signal* **1**(2): 103-111.

Siddique, M. M., Y. Li, L. Wang, J. Ching, M. Mal, O. Ilkayeva, Y. J. Wu, B. H. Bay and S. A. Summers (2013). "Ablation of dihydroceramide desaturase 1, a therapeutic target for the treatment of metabolic diseases, simultaneously stimulates anabolic and catabolic signaling." *Mol Cell Biol* **33**(11): 2353-2369.

Simons, K. and E. Ikonen (1997). "Functional rafts in cell membranes." *Nature* **387**(6633): 569-572.

Singer, S. J. and G. L. Nicolson (1972). "The fluid mosaic model of the structure of cell membranes." *Science* **175**(4023): 720-731.

Singer, W. D., H. A. Brown, X. Jiang and P. C. Sternweis (1996). "Regulation of phospholipase D by protein kinase C is synergistic with ADP-ribosylation factor and independent of protein kinase activity." *J Biol Chem* **271**(8): 4504-4510.

Singh, S. K. and S. Spiegel (2020). "Sphingosine-1-phosphate signaling: A novel target for simultaneous adjuvant treatment of triple negative breast cancer and chemotherapy-induced neuropathic pain." *Adv Biol Regul* **75**: 100670.

Singleton, P. A., S. M. Dudek, E. T. Chiang and J. G. Garcia (2005). "Regulation of sphingosine 1-phosphate-induced endothelial cytoskeletal rearrangement and barrier enhancement by S1P1 receptor, PI3 kinase, Tiam1/Rac1, and alpha-actinin." *FASEB J* **19**(12): 1646-1656.

Skoura, A., T. Sanchez, K. Claffey, S. M. Mandala, R. L. Proia and T. Hla (2007). "Essential role of sphingosine 1-phosphate receptor 2 in pathological angiogenesis of the mouse retina." *J Clin Invest* **117**(9): 2506-2516.

Sobue, S., T. Iwasaki, C. Sugisaki, K. Nagata, R. Kikuchi, M. Murakami, A. Takagi, T. Kojima, Y. Banno, Y. Akao, Y. Nozawa, R. Kannagi, M. Suzuki, A. Abe, T. Naoe and T. Murate (2006). "Quantitative RT-PCR analysis of sphingolipid metabolic enzymes in acute leukemia and myelodysplastic syndromes." *Leukemia* **20**(11): 2042-2046.

Song, L., H. Xiong, J. Li, W. Liao, L. Wang, J. Wu and M. Li (2011). "Sphingosine kinase-1 enhances resistance to apoptosis through activation of PI3K/Akt/NF-kappaB pathway in human non-small cell lung cancer." *Clin Cancer Res* **17**(7): 1839-1849.

Sordillo, L. A., P. P. Sordillo and L. Helson (2016). "Sphingosine Kinase Inhibitors as Maintenance Therapy of Glioblastoma After Ceramide-Induced Response." *Anticancer Res* **36**(5): 2085-2095.

Spiegel, S., M. A. Maccis, M. Maceyka and S. Milstien (2019). "New insights into functions of the sphingosine-1-phosphate transporter SPNS2." *J Lipid Res* **60**(3): 484-489.

Stahelin, R. V., J. H. Hwang, J. H. Kim, Z. Y. Park, K. R. Johnson, L. M. Obeid and W. Cho (2005). "The mechanism of membrane targeting of human sphingosine kinase 1." *J Biol Chem* **280**(52): 43030-43038.

Stanislaus, D., J. A. Janovick, S. Brothers and P. M. Conn (1997). "Regulation of G(q/11)alpha by the gonadotropin-releasing hormone receptor." *Mol Endocrinol* **11**(6): 738-746.

Strelow, A., K. Bernardo, S. Adam-Klages, T. Linke, K. Sandhoff, M. Kronke and D. Adam (2000). "Overexpression of acid ceramidase protects from tumor necrosis factor-induced cell death." *J Exp Med* **192**(5): 601-612.

Strub, G. M., M. Paillard, J. Liang, L. Gomez, J. C. Allegood, N. C. Hait, M. Maceyka, M. M. Price, Q. Chen, D. C. Simpson, T. Kordula, S. Milstien, E. J. Lesnfsky and S. Spiegel (2011). "Sphingosine-1-phosphate produced by sphingosine kinase 2 in mitochondria interacts with prohibitin 2 to regulate complex IV assembly and respiration." *FASEB J* **25**(2): 600-612.

Su, W., O. Yeku, S. Olepu, A. Genna, J. S. Park, H. Ren, G. Du, M. H. Gelb, A. J. Morris and M. A. Frohman (2009). "5-Fluoro-2-indolyl des-chlorohalopemide (FIPI), a phospholipase D pharmacological inhibitor that alters cell spreading and inhibits chemotaxis." *Mol Pharmacol* **75**(3): 437-446.

Sugimoto, N., N. Takuwa, H. Okamoto, S. Sakurada and Y. Takuwa (2003). "Inhibitory and stimulatory regulation of Rac and cell motility by the G12/13-Rho and Gi pathways integrated downstream of a single G protein-coupled sphingosine-1-phosphate receptor isoform." *Mol Cell Biol* **23**(5): 1534-1545.

Sugiura, M., K. Kono, H. Liu, T. Shimizugawa, H. Minekura, S. Spiegel and T. Kohama (2002). "Ceramide kinase, a novel lipid kinase. Molecular cloning and functional characterization." *J Biol Chem* **277**(26): 23294-23300.

Sun, L., H. Wang, Z. Wang, S. He, S. Chen, D. Liao, L. Wang, J. Yan, W. Liu, X. Lei and X. Wang (2012). "Mixed lineage kinase domain-like protein mediates necrosis signaling downstream of RIP3 kinase." *Cell* **148**(1-2): 213-227.

Sutherland, C. M., P. A. Moretti, N. M. Hewitt, C. J. Bagley, M. A. Vadas and S. M. Pitson (2006). "The calmodulin-binding site of sphingosine kinase and its role in agonist-dependent translocation of sphingosine kinase 1 to the plasma membrane." *J Biol Chem* **281**(17): 11693-11701.

Taha, T. A., K. Kitatani, J. Bielawski, W. Cho, Y. A. Hannun and L. M. Obeid (2005). "Tumor necrosis factor induces the loss of sphingosine kinase-1 by a cathepsin B-dependent mechanism." *J Biol Chem* **280**(17): 17196-17202.

Takabe, K., R. H. Kim, J. C. Allegood, P. Mitra, S. Ramachandran, M. Nagahashi, K. B. Harikumar, N. C. Hait, S. Milstien and S. Spiegel (2010). "Estradiol induces export of sphingosine 1-phosphate from breast cancer cells via ABCG1 and ABCG2." *J Biol Chem* **285**(14): 10477-10486.

Takabe, K. and S. Spiegel (2014). "Export of sphingosine-1-phosphate and cancer progression." *J Lipid Res* **55**(9): 1839-1846.

Takasaki, J., T. Saito, M. Taniguchi, T. Kawasaki, Y. Moritani, K. Hayashi and M. Kobori (2004). "A novel Galphq/11-selective inhibitor." *J Biol Chem* **279**(46): 47438-47445.

Takasugi, N., T. Sasaki, K. Suzuki, S. Osawa, H. Isshiki, Y. Hori, N. Shimada, T. Higo, S. Yokoshima, T. Fukuyama, V. M. Lee, J. Q. Trojanowski, T. Tomita and T. Iwatsubo (2011). "BACE1 activity is modulated by cell-associated sphingosine-1-phosphate." *J Neurosci* **31**(18): 6850-6857.

- Takuwa, Y., W. Du, X. Qi, Y. Okamoto, N. Takuwa and K. Yoshioka (2010). "Roles of sphingosine-1-phosphate signaling in angiogenesis." *World J Biol Chem* **1**(10): 298-306.
- Tea, M. N., S. I. Poonnoose and S. M. Pitson (2020). "Targeting the Sphingolipid System as a Therapeutic Direction for Glioblastoma." *Cancers (Basel)* **12**(1).
- ter Braak, M., K. Danneberg, K. Lichte, K. Liphardt, N. T. Ktistakis, S. M. Pitson, T. Hla, K. H. Jakobs and D. Meyer zu Heringdorf (2009). "Galpha(q)-mediated plasma membrane translocation of sphingosine kinase-1 and cross-activation of S1P receptors." *Biochim Biophys Acta* **1791**(5): 357-370.
- Tonelli, F., K. G. Lim, C. Loveridge, J. Long, S. M. Pitson, G. Tigyi, R. Bittman, S. Pyne and N. J. Pyne (2010). "FTY720 and (S)-FTY720 vinylphosphonate inhibit sphingosine kinase 1 and promote its proteasomal degradation in human pulmonary artery smooth muscle, breast cancer and androgen-independent prostate cancer cells." *Cell Signal* **22**(10): 1536-1542.
- Trajkovic, K., C. Hsu, S. Chiantia, L. Rajendran, D. Wenzel, F. Wieland, P. Schwillie, B. Brugger and M. Simons (2008). "Ceramide triggers budding of exosome vesicles into multivesicular endosomes." *Science* **319**(5867): 1244-1247.
- Tsai, H. C., Y. Huang, C. S. Garriss, M. A. Moreno, C. W. Griffin and M. H. Han (2016). "Effects of sphingosine-1-phosphate receptor 1 phosphorylation in response to FTY720 during neuroinflammation." *JCI Insight* **1**(9): e86462.
- Vadas, M., P. Xia, G. McCaughan and J. Gamble (2008). "The role of sphingosine kinase 1 in cancer: oncogene or non-oncogene addiction?" *Biochim Biophys Acta* **1781**(9): 442-447.
- Van Brocklyn, J. R., C. A. Jackson, D. K. Pearl, M. S. Kotur, P. J. Snyder and T. W. Prior (2005). "Sphingosine kinase-1 expression correlates with poor survival of patients with glioblastoma multiforme: roles of sphingosine kinase isoforms in growth of glioblastoma cell lines." *J Neuropathol Exp Neurol* **64**(8): 695-705.
- Van Brocklyn, J. R., N. Young and R. Roof (2003). "Sphingosine-1-phosphate stimulates motility and invasiveness of human glioblastoma multiforme cells." *Cancer Lett* **199**(1): 53-60.
- Vandenabeele, P., L. Galluzzi, T. Vanden Berghe and G. Kroemer (2010). "Molecular mechanisms of necroptosis: an ordered cellular explosion." *Nat Rev Mol Cell Biol* **11**(10): 700-714.
- Vanlangenakker, N., M. J. Bertrand, P. Bogaert, P. Vandenabeele and T. Vanden Berghe (2011). "TNF-induced necroptosis in L929 cells is tightly regulated by multiple TNFR1 complex I and II members." *Cell Death Dis* **2**: e230.
- Veale, K. J., C. Offenhauser and R. Z. Murray (2011). "The role of the recycling endosome in regulating lamellipodia formation and macrophage migration." *Commun Integr Biol* **4**(1): 44-47.
- Venkata, J. K., N. An, R. Stuart, L. J. Costa, H. Cai, W. Coker, J. H. Song, K. Gibbs, T. Matson, E. Garrett-Mayer, Z. Wan, B. Ogrtmen, C. Smith and Y. Kang (2014). "Inhibition of sphingosine kinase 2 downregulates the expression of c-Myc and Mcl-1 and induces apoptosis in multiple myeloma." *Blood* **124**(12): 1915-1925.
- Vesper, H., E. M. Schmelz, M. N. Nikolova-Karakashian, D. L. Dillehay, D. V. Lynch and A. H. Merrill, Jr. (1999). "Sphingolipids in food and the emerging importance of sphingolipids to nutrition." *J Nutr* **129**(7): 1239-1250.
- Visentin, B., J. A. Vekich, B. J. Sibbald, A. L. Cavalli, K. M. Moreno, R. G. Matteo, W. A. Garland, Y. Lu, S. Yu, H. S. Hall, V. Kundra, G. B. Mills and R. A. Sabbadini (2006). "Validation of an anti-sphingosine-1-phosphate antibody as a potential therapeutic in reducing growth, invasion, and angiogenesis in multiple tumor lineages." *Cancer Cell* **9**(3): 225-238.
- Vu, T. M., A. N. Ishizu, J. C. Foo, X. R. Toh, F. Zhang, D. M. Whee, F. Torta, A. Cazenave-Gassiot, T. Matsumura, S. Kim, S. E. S. Toh, T. Suda, D. L. Silver, M. R. Wenk and L. N. Nguyen (2017). "Mfsd2b is essential for the sphingosine-1-phosphate export in erythrocytes and platelets." *Nature* **550**(7677): 524-528.
- Walzer, T., L. Chiossone, J. Chaix, A. Calver, C. Carozzo, L. Garrigue-Antar, Y. Jacques, M. Baratin, E. Tomasello and E. Vivier (2007). "Natural killer cell trafficking in vivo requires a dedicated sphingosine 1-phosphate receptor." *Nat Immunol* **8**(12): 1337-1344.
- Wang, F., J. R. Van Brocklyn, L. Edsall, V. E. Nava and S. Spiegel (1999). "Sphingosine-1-phosphate inhibits motility of human breast cancer cells independently of cell surface receptors." *Cancer Res* **59**(24): 6185-6191.
- Wang, F., J. R. Van Brocklyn, J. P. Hobson, S. Movafagh, Z. Zukowska-Grojec, S. Milstien and S. Spiegel (1999). "Sphingosine 1-phosphate stimulates cell migration through a G(i)-coupled cell surface receptor. Potential involvement in angiogenesis." *J Biol Chem* **274**(50): 35343-35350.
- Wang, F. and Z. Wu (2018). "Sphingosine kinase 1 overexpression is associated with poor prognosis and oxaliplatin resistance in hepatocellular carcinoma." *Exp Ther Med* **15**(6): 5371-5376.
- Wang, J., S. Knapp, N. J. Pyne, S. Pyne and J. M. Elkins (2014). "Crystal Structure of Sphingosine Kinase 1 with PF-543." *ACS Med Chem Lett* **5**(12): 1329-1333.
- Wang, L., R. Bittman, J. G. Garcia and S. M. Dudek (2015). "Junctional complex and focal adhesion rearrangement mediates pulmonary endothelial barrier enhancement by FTY720 S-phosphonate." *Microvasc Res* **99**: 102-109.
- Wang, Q., J. Li, G. Li, Y. Li, C. Xu, M. Li, G. Xu and S. Fu (2014). "Prognostic significance of sphingosine kinase 2 expression in non-small cell lung cancer." *Tumour Biol* **35**(1): 363-368.
- Wang, S., Y. Liang, W. Chang, B. Hu and Y. Zhang (2018). "Triple Negative Breast Cancer Depends on Sphingosine Kinase 1 (SphK1)/Sphingosine-1-Phosphate (S1P)/Sphingosine 1-Phosphate Receptor 3 (S1PR3)/Notch Signaling for Metastasis." *Med Sci Monit* **24**: 1912-1923.
- Wang, W., M. H. Graeler and E. J. Goetzl (2005). "Type 4 sphingosine 1-phosphate G protein-coupled receptor (S1P4) transduces S1P effects on T cell proliferation and cytokine secretion without signaling migration." *FASEB J* **19**(12): 1731-1733.

Wang, Z., X. Min, S. H. Xiao, S. Johnstone, W. Romanow, D. Meininger, H. Xu, J. Liu, J. Dai, S. An, S. Thibault and N. Walker (2013). "Molecular basis of sphingosine kinase 1 substrate recognition and catalysis." *Structure* **21**(5): 798-809.

Warren, B. A., P. Shubik, R. Wilson, H. Garcia and R. Feldman (1978). "The microcirculation in two transplantable melanomas of the hamster. I. In vivo observations in transparent chambers." *Cancer Lett* **4**(2): 109-116.

Watson, C., J. S. Long, C. Orange, C. L. Tannahill, E. Mallon, L. M. McGlynn, S. Pyne, N. J. Pyne and J. Edwards (2010). "High expression of sphingosine 1-phosphate receptors, S1P1 and S1P3, sphingosine kinase 1, and extracellular signal-regulated kinase-1/2 is associated with development of tamoxifen resistance in estrogen receptor-positive breast cancer patients." *Am J Pathol* **177**(5): 2205-2215.

Watson, P. and D. J. Stephens (2005). "ER-to-Golgi transport: form and formation of vesicular and tubular carriers." *Biochim Biophys Acta* **1744**(3): 304-315.

Weber, K., R. Roelandt, I. Bruggeman, Y. Estornes and P. Vandenabeele (2018). "Nuclear RIPK3 and MLKL contribute to cytosolic necrosome formation and necroptosis." *Commun Biol* **1**: 6.

Wedegaertner, P. B., D. H. Chu, P. T. Wilson, M. J. Levis and H. R. Bourne (1993). "Palmitoylation is required for signaling functions and membrane attachment of Gq alpha and Gs alpha." *J Biol Chem* **268**(33): 25001-25008.

Wehrle-Haller, B. (2012). "Structure and function of focal adhesions." *Curr Opin Cell Biol* **24**(1): 116-124.

Windh, R. T., M. J. Lee, T. Hla, S. An, A. J. Barr and D. R. Manning (1999). "Differential coupling of the sphingosine 1-phosphate receptors Edg-1, Edg-3, and H218/Edg-5 to the G(i), G(q), and G(12) families of heterotrimeric G proteins." *J Biol Chem* **274**(39): 27351-27358.

Xia, P., J. R. Gamble, L. Wang, S. M. Pitson, P. A. Moretti, B. W. Wattenberg, R. J. D'Andrea and M. A. Vadas (2000). "An oncogenic role of sphingosine kinase." *Curr Biol* **10**(23): 1527-1530.

Xia, P., L. Wang, P. A. Moretti, N. Albanese, F. Chai, S. M. Pitson, R. J. D'Andrea, J. R. Gamble and M. A. Vadas (2002). "Sphingosine kinase interacts with TRAF2 and dissects tumor necrosis factor-alpha signaling." *J Biol Chem* **277**(10): 7996-8003.

Yamada, A., M. Nagahashi, T. Aoyagi, W. C. Huang, S. Lima, N. C. Hait, A. Maiti, K. Kida, K. P. Terracina, H. Miyazaki, T. Ishikawa, I. Endo, M. R. Waters, Q. Qi, L. Yan, S. Milstien, S. Spiegel and K. Takabe (2018). "ABCC1-Exported Sphingosine-1-phosphate, Produced by Sphingosine Kinase 1, Shortens Survival of Mice and Patients with Breast Cancer." *Mol Cancer Res* **16**(6): 1059-1070.

Yamamoto, S., Y. Yako, Y. Fujioka, M. Kajita, T. Kameyama, S. Kon, S. Ishikawa, Y. Ohba, Y. Ohno, A. Kihara and Y. Fujita (2016). "A role of the sphingosine-1-phosphate (S1P)-S1P receptor 2 pathway in epithelial defense against cancer (EDAC)." *Mol Biol Cell* **27**(3): 491-499.

Yamamura, S., Y. Yatomi, F. Ruan, E. A. Sweeney, S. Hakomori and Y. Igarashi (1997). "Sphingosine 1-phosphate regulates melanoma cell motility through a receptor-coupled extracellular action and in a pertussis toxin-insensitive manner." *Biochemistry* **36**(35): 10751-10759.

Yamanaka, M., D. Shegogue, H. Pei, S. Bu, A. Bielawska, J. Bielawski, B. Pettus, Y. A. Hannun, L. Obeid and M. Trojanowska (2004). "Sphingosine kinase 1 (SPHK1) is induced by transforming growth factor-beta and mediates TIMP-1 up-regulation." *J Biol Chem* **279**(52): 53994-54001.

Yamashita, H., J. Kitayama, D. Shida, H. Yamaguchi, K. Mori, M. Osada, S. Aoki, Y. Yatomi, Y. Takuwa and H. Nagawa (2006). "Sphingosine 1-phosphate receptor expression profile in human gastric cancer cells: differential regulation on the migration and proliferation." *J Surg Res* **130**(1): 80-87.

Yoshida, Y., M. Nakada, T. Harada, S. Tanaka, T. Furuta, Y. Hayashi, D. Kita, N. Uchiyama, Y. Hayashi and J. Hamada (2010). "The expression level of sphingosine-1-phosphate receptor type 1 is related to MIB-1 labeling index and predicts survival of glioblastoma patients." *J Neurooncol* **98**(1): 41-47.

Yoshihara, M., Y. Yamakita, H. Kajiyama, T. Senga, Y. Koya, M. Yamashita, A. Nawa and F. Kikkawa (2020). "Filopodia play an important role in the trans-endothelial migration of ovarian cancer cells." *Exp Cell Res*: 112011.

Young, M. M. and H. G. Wang (2018). "Sphingolipids as Regulators of Autophagy and Endocytic Trafficking." *Adv Cancer Res* **140**: 27-60.

Zanet, J., A. Jayo, S. Plaza, T. Millard, M. Parsons and B. Stramer (2012). "Fascin promotes filopodia formation independent of its role in actin bundling." *J Cell Biol* **197**(4): 477-486.

Zhang, J., N. Honbo, E. J. Goetzl, K. Chatterjee, J. S. Karliner and M. O. Gray (2007). "Signals from type 1 sphingosine 1-phosphate receptors enhance adult mouse cardiac myocyte survival during hypoxia." *Am J Physiol Heart Circ Physiol* **293**(5): H3150-3158.

Zhang, T., H. C. Sun, Y. Xu, K. Z. Zhang, L. Wang, L. X. Qin, W. Z. Wu, Y. K. Liu, S. L. Ye and Z. Y. Tang (2005). "Overexpression of platelet-derived growth factor receptor alpha in endothelial cells of hepatocellular carcinoma associated with high metastatic potential." *Clin Cancer Res* **11**(24 Pt 1): 8557-8563.

Zhang, X., J. Gureasko, K. Shen, P. A. Cole and J. Kuriyan (2006). "An allosteric mechanism for activation of the kinase domain of epidermal growth factor receptor." *Cell* **125**(6): 1137-1149.

Zhang, X., K. Kitatani, M. Toyoshima, M. Ishibashi, T. Usui, J. Minato, M. Egiz, S. Shigeta, T. Fox, T. Deering, M. Kester and N. Yaegashi (2018). "Ceramide Nanoliposomes as a MLKL-Dependent, Necroptosis-Inducing, Chemotherapeutic Reagent in Ovarian Cancer." *Mol Cancer Ther* **17**(1): 50-59.

Zhang, Y., Y. Wang, Z. Wan, S. Liu, Y. Cao and Z. Zeng (2014). "Sphingosine kinase 1 and cancer: a systematic review and meta-analysis." *PLoS One* **9**(2): e90362.

Zhao, J., J. Liu, J. F. Lee, W. Zhang, M. Kandouz, G. C. VanHecke, S. Chen, Y. H. Ahn, F. Lonardo and M. J. Lee (2016). "TGF-beta/SMAD3 Pathway Stimulates Sphingosine-1 Phosphate Receptor 3 Expression: IMPLICATION OF SPHINGOSINE-1 PHOSPHATE RECEPTOR 3 IN LUNG ADENOCARCINOMA PROGRESSION." *J Biol Chem* **291**(53): 27343-27353.

Zhao, Z., J. Ma, B. Hu, Y. Zhang and S. Wang (2018). "SPHK1 promotes metastasis of thyroid carcinoma through activation of the S1P/S1PR3/Notch signaling pathway." *Exp Ther Med* **15**(6): 5007-5016.

Zhou, H., X. Yin, F. Bai, W. Liu, S. Jiang and J. Zhao (2020). "The Role and Mechanism of S1PR5 in Colon Cancer." *Cancer Manag Res* **12**: 4759-4775.

Zhu, W., B. L. Gliddon, K. E. Jarman, P. A. B. Moretti, T. Tin, L. V. Parise, J. M. Woodcock, J. A. Powell, A. Ruskiewicz, M. R. Pitman and S. M. Pitson (2017). "CIB1 contributes to oncogenic signalling by Ras via modulating the subcellular localisation of sphingosine kinase 1." *Oncogene* **36**(18): 2619-2627.

Zhu, W., K. E. Jarman, N. A. Lokman, H. A. Neubauer, L. T. Davies, B. L. Gliddon, H. Taing, P. A. B. Moretti, M. K. Oehler, M. R. Pitman and S. M. Pitson (2017). "CIB2 Negatively Regulates Oncogenic Signaling in Ovarian Cancer via Sphingosine Kinase 1." *Cancer Res* **77**(18): 4823-4834.